Under-ice communities structured by sea-ice habitats in changing Arctic and Antarctic ecosystems

Dissertation
with the Aim of Achieving a Doctoral Degree in Natural Science
at the Faculty of Mathematics, Informatics and Natural Sciences
Department of Biology of the University of Hamburg

submitted by

Carmen Lucia David

M.Sc. Oceanography and Marine Environments
M.Sc. Environmental Sciences
B.Sc. Ecology and Environmental Protection/Biology

Hamburg 2015

Day of oral defence: 13th of November, 2015

The following evaluators recommend the admission of the dissertation:

1. Evaluator **Prof. Dr. Angelika Brandt**
Universität Hamburg, Biozentrum Grindel und Zoologisches Museum, Martin-Luther King-Platz 3, 20146 Hamburg

2. Evaluator **Dr. Hauke Flores**
Alfred-Wegner-Institut Helmholtz-Zentrum für Polar- und Meeresforschung, Am Handelshafen 12, 27570 Bremerhaven

Table of contents

SUMMARY

Over the past decades, the effects of global-climate change have been observed in the polar oceans, disproportionally higher in the Arctic Ocean and to a lesser degree in some regions of the Southern Ocean. The dramatic reduction in the Arctic sea-ice extent, cover and thickness is believed to lead to an ice-free ocean in summer and a winter sea-ice cover consisting mainly of first-year ice. Atmospheric anomalies around the Antarctic continent are expected to amplify the divergent pattern of sea-ice drift, which may lead to a looser pack-ice with reduced ridges and rafted structures. Changes in sea-ice habitat structure and biogeochemical conditions in the surface water and, hence, in primary production, will have dramatic effects on sea-ice associated fauna.

Our knowledge about how changes in sea-ice dynamics affect the associated fauna is limited, especially in the ice-covered central Arctic and the seasonal ice zone of the Southern Ocean. Ice-associated fauna is difficult to evaluate due to a lack of quantitative reports of species abundances and distribution. Moreover, understanding the factors that control ice-associated fauna distribution is crucial to predict how the ice-associated ecosystems in the polar oceans will react to further sea-ice decline.

The **overall aim** of this thesis is to improve our understanding of the distribution and association of meso- and macrofauna communities with sea-ice habitat properties in central Arctic Ocean and northern Weddell Sea. Specific goals are to i) quantify the under-ice fauna distribution at large spatial scales, and identify under-ice community structures and their key species, ii) investigate how different community structures relate to environmental gradients and iii) analyse the relationships of the key species with environmental variables of the under-ice habitat. The innovative approach of this study is the use of the Surface and Under Ice Trawl (SUIT). The SUIT is equipped with an array of sensors to measure environmental parameters like sea-ice thickness and coverage, water temperature, salinity and chlorophyll *a* concentration; whilst collecting fauna.

Chapter I and **III** address the first two goals by relating the under-ice faunal distribution with the variability of sea-ice and underlying water-column properties. Our results show that in summer, in the central Arctic Ocean, nutrient concentration, surface salinity and sea-ice coverage define two distinct environmental regimes (**Chapter I**). The under-ice community structure mirrors the environmental patterns at the basin scale. On small-scale patterns, abrupt changes in the dominance

of ice-associated amphipods at ice-covered stations versus pelagic amphipods at nearby ice-free stations emphasise the influence of sea-ice. The autotrophic resources were not sufficient to satisfy the demand of dominant grazers of the under-ice community, suggesting a high degree of heterotrophy in the system. During winter, the under-ice community in the northern Weddell Sea is heterogeneous at the basin scale. (**Chapter III**). The balance between numerically dominant species, i.e. Antarctic krill and copepods, defines different community types driven by biogeographic distribution patterns, sea-ice coverage and seasonal progression.

Chapter II addresses my third goal by investigating the drivers of under-ice polar cod, *Boreogadus saida,* distribution in the central Arctic Ocean. The results show that polar cod was omnipresent with a median abundance of 5000 ind. km^{-2}. Higher abundance is associated with thicker ice, higher ice coverage and lower surface salinity or with higher abundance of the ice-amphipod, *Apherusa glacialis*. I hypothesise that under-ice fish arrive in the central Arctic by drifting with sea-ice formed in coastal areas. This implies that fish sampled in the Amundsen Basin originated from the Laptev Sea coast, while fish sampled in the Nansen Basin originated from the Kara Sea.

Chapter IV goes one step further by investigating the carbon demand of dominant ice-associated and pelagic species during winter, in relation to food availability and predation pressure. Spatial variability of grazing and predation pressure is unequally distributed between the ice-water interface layer and the water column. The value of the under-ice environment as a winter habitat for Antarctic krill larvae and certain zooplankton species seemed to be given primarily by ice algae as an additional abundant carbon source and low predation pressure compared to the water column.

In **conclusion**, the under-ice habitat supports a diverse and rich fauna, composed by a mixture of ice-associated and pelagic organisms. The under-ice community is largely structured by the seasonal dynamics of sea-ice and regional patterns. The low availability of autotrophic resources in the oligotrophic Arctic Ocean and the low light regime in Weddell Sea during the wintertime, indicate that ice algae constitute a crucial additional food source. Switching to a dominantly heterotrophic food web (**Chapter I, IV**) might be an adaptation to reduced sea-ice algal production as a result of sea-ice decline. The loss of sea-ice habitat, a sheltered environment for krill larvae, polar cod and other ice-associated species, however, would need to be investigated further to understand the consequences for the affected populations.

ZUSAMMENFASSUNG

Die Auswirkungen des globalen Klimawandels sind seit einigen Jahrzehnten in den Polarmeeren deutlich zu beobachten, besonders stark im Arktischen Ozean, aber auch in einigen Regionen des Südpolarmeeres. Im Arktischen Ozean könnte die dramatische Abnahme der Ausdehnung und Dicke des Meereises schon bald zu eisfreien Sommermonaten und dünnerem einjährigem Meereis während der Wintermonate führen. Im Südpolarmeer geht man davon aus, dass atmosphärische Anomalien die bereits divergente Meereisdrift verstärken und so zu einer Abnahme des Packeises und deutlich reduzierter Bildung von Presseisrücken führen. Diese Änderungen des Meereishabitats sowie der Biogeochemie im Oberflächenwasser – und damit der Primärproduktion – haben dramatische Auswirkungen auf die Meereis-assoziierte Fauna.

Unser Verständnis dieses Wandels im Meereis und der daraus resultierenden Auswirkungen auf die assoziierte Fauna ist noch begrenzt, insbesondere in der zentralen Arktis und der saisonalen Meereiszone des Südpolarmeeres. Der akute Mangel an quantitativen Studien zu Abundanz und Verteilung der entsprechenden Arten erschwert eine Evaluierung der Meereis-assoziierten Fauna. Dieses Verständnis ist jedoch essentiell um Vorhersagen darüber zu treffen, wie Artengemeinschaften im Ökosystem Meereis auf eine weitere Abnahme der Meereisausdehnung reagieren werden.

Das Ziel dieser Arbeit ist es, unser Verständnis der Verteilung und Habitatsabhängigkeit von Meso- und Makrofauna im arktischen Ozean und dem nördlichen Weddellmeer zu erweitern. Schwerpunkte sind dabei insbesondere i) die großflächige Quantifizierung der Fauna unter dem Eis sowie die Identifizierung von Artengemeinschaften und ihrer Schlüsselarten, ii) die Relation der unterschiedlichen Gemeinschaften zu Gradienten in ihrer Umwelt und iii) der Einfluss ökologischer Kenngrößen auf Schüsselarten unter dem Eis. Eine Innovation dieser Studie ist die nutzen des *Surface and Under Ice Trawl* (SUIT), welches zur Datengewinnung benutzt wurde. Das SUIT enthält eine Reihe von Sensoren zur Messung der Meereisdicke, Wassertemperatur, Salinität und Chlorophyll *a* Konzentration. Gleichzeitig wird es zur Beprobung der Fauna genutzt.

Kapitel I und **III** behandeln die ersten zwei Zielsetzungen und setzen die Fauna unter dem Eis in Relation zu Eigenschaften des Meereises und der Wassersäule. Unsere Ergebnisse zeigen, dass im Sommer zwei unterschiedliche Regime bezüglich Nährstoffkonzentration, Salinität des Oberflächenwassers und Meereisbedeckung in der Arktis existieren (**Kapitel I**). Die

Artengemeinschaft unter dem Eis spiegelt diese ökologischen Muster auf der Ebene des gesamten Meeresbeckens wider. Abrupte Änderungen der Artenzusammensetzung von Meereis-assoziierten Amphipoden hin zu pelagischen Amphipoden in eisfreien Regionen verdeutlichen diesen Einfluss des Meereises. In eisbedeckten Regionen war die Anzahl autotropher Organismen nicht ausreichend, um den Bedarf dominierender Primärkonsumenten zu decken, was auf einen hohen Grad an Heterotrophie hindeutet. Im Winter war die Artenzusammensetzung im nördlichen Weddellmeer heterogen (**Kapitel III**). Das Wechselspiel von zahlenmäßig überlegenen Arten wie Antarktischem Krill und Copepoden reflektiert dabei biogeographische Verteilungsmuster, Meereisbedeckung und den saisonalen Jahresverlauf.

Kapitel II behandelt die dritte Zielsetzung und beleuchtet Einflüsse auf die Verteilung des Polardorschs *Boreogadus saida* in der zentralen Arktis. Die Ergebnisse zeigen eine omnipräsente Abundanz des Polardorschs von 5000 ind. pro km^2 (Median). Höhere Abundanzen korrelieren mit dickerem Eis, größerer Meereisbedeckung und niedrigerer Salinität des Oberflächenwassers bzw. stärkerem Vorkommen des Eisamphipoden *Apherusa glacialis*. Wir vermuten, dass Fische unter dem Eis die zentrale Arktis durch Meereisdrift aus küstennahen Regionen erreichen. Folglich müsste der beprobte Fisch in der Amundsenbucht ursprünglich aus der Laptewsee stammen, im Nansenbecken beprobter Fisch dagegen aus der Karasee.

In **Kapitel IV** gehen wir einen Schritt weiter und untersuchen den Kohlenstoffbedarf dominanter Arten unter dem Eis und im Pelagial während des Winters, insbesondere im Verhältnis zu Nahrungsverfügbarkeit und Fraßdruck. Räumliche Unterschiede von *Grazing* und Fraßdruck sind ungleich zwischen dem Untereishabitat und der Wassersäule verteilt. Der hohe Nutzen des Untereishabitats für die Überwinterung Antarktischer Krilllarven und anderer Zooplanktonarten scheint insbesondere durch das Vorkommen von Eisalgen als Kohlenstoffquelle und den Schutz vor Fraßfeinden gegeben.

Zusammenfassend stellen wir fest, dass das Untereishabitat eine diverse Fauna beheimatet, die sowohl Meereis-assoziierte, als auch pelagiale Arten einschließt. Die Artengemeinschaft wird vornehmlich durch saisonale Meereisdynamik und regionale Strukturen charakterisiert. Die niedrige Verfügbarkeit autotropher Ressourcen im oligotrophen Arktischen Ozean und das Lichtregime des Antarktischen Winters im Weddellmeer weisen auf die entscheidende Bedeutung von Eisalgen als zusätzliche Nahrungsquelle hin. Ein Wechsel hin zu einem vornehmlich heterotrophen

Nahrungsnetz (**Kapitel I, IV**) stellt möglicherweise eine Anpassung an verminderte Produktionsraten von Eisalgen infolge der Meereisabnahme dar. Weitere Studien sind nötig, um den Effekt des Meereisrückgangs auf larvalen Krill, Polardorsch und andere Eis-assoziierte Arten vorherzusagen.

ABBREVIATION LIST

Chl *a*	Chlorophyll *a*
FYI	First-year ice
MYI	Multi-year ice
MIZ	Marginal ice zone
SIZ	Seasonal ice zone
SUIT	Surface and Under Ice Trawl
RMT	Rectangular Midwater Trawl

1. *Introduction*

1.1. Polar Oceans

The polar oceans are unique environments characterised by low exposure of solar energy and extreme seasonality in radiation budget due to the spherical shape of the Earth and its inclination axis. These particularities result in high seasonality in light conditions, low temperatures and a sea-ice cover. The Arctic marine realm has a polar regime, being positioned directly at the North Pole (66°N - 90°N), while the Antarctic marine realm has a subpolar regime, positioned much further away from the pole (55°S - 78°S).

Partially due to these geographical differences, environmental changes, caused primarily by climate warming, are disproportionate in the two polar oceans. Climate changes have been most evident in the Arctic Ocean, where summer sea ice extent has been declining considerably over the past decades. In the Antarctic region, circumpolar sea-ice decline is expected to commence during the present century.

1.1.1.Arctic Ocean

The Arctic Ocean is located in the Northern hemisphere north of the Arctic Circle (66° 34´N). It is the smallest and shallowest of the world's oceans. It is surrounded by land and has limited exchange with the Atlantic and Pacific Oceans. It is formed by a deep central basin surrounded by shallow shelves. These shelves receive over 10% of the global river runoff and, thus, can sustain high productivity (Carmack and Wassmann 2006; Tremblay and Gagnon 2009). In contrast, the offshore deep central basins are permanently ice-covered and are believed to be less productive (Sakshaug 2004).

The central Arctic Ocean is divided into two basins by the Lomonosov Ridge: the Amerasian and Eurasian Basins (Fig. 1) (Jakobsson et al. 2004). The Eurasian Basin is permanently ice-covered with bottom depths >4000 m. The Gakkel Ridge subdivides this basin into the nearly equally sized Nansen and Amundsen Basins. They receive the inflow of warm, saline, phosphate- and nitrate-rich Atlantic waters through the Fram Strait. The Fram Strait branch of the Atlantic Water is largely recirculated within the Nansen Basin. The Barents Sea branch flows eastwards along the Siberian shelves until it reaches the Laptev Sea (Rudels et al. 2013) before flowing into the Amundsen Basin with the Transpolar Drift. This major ocean surface current transports sea ice from Laptev and East Siberian Sea across central Arctic Ocean towards the Fram Strait (Mysak 2001).

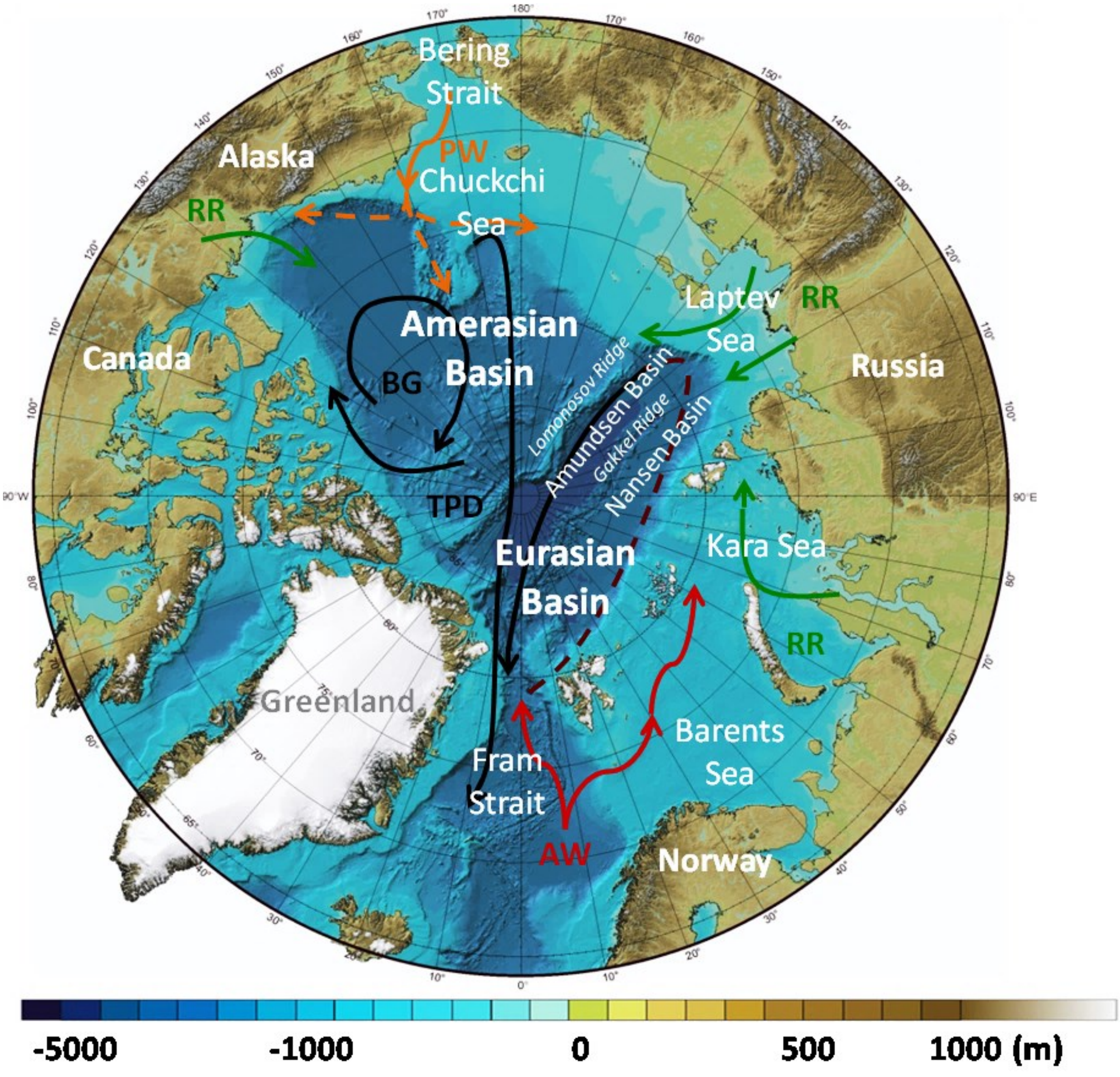

Figure 1. Major Arctic Ocean basins and adjacent seas with surface circulation features (reproduced with permission from Fernández-Méndez 2014; adapted from Jakobsson et al. 2004, Rudels 2013) showing the inflow of Pacific Water (PW) in orange and Atlantic Water (AW) in red, river runoff in greed (RR) and polar waters currents such as Beaufort Gyre (BG) and Transpolar Drift (TPD). Background colors show bathymetry.

The main characteristic of the Arctic Ocean is the permanent sea-ice cover in its centre and the seasonal ice-covered surrounding marginal seas (Horner et al. 1992). The sea ice forms in winter along the shelves and is transported by wind and surface currents over the deep basins (Pfirman et al. 1997). A portion of the sea ice is recirculated within the anti-cyclonic Beaufort Gyre in the central and western Arctic Ocean, contributing to the formation of multi-year ice (MYI) (Rigor and Wallace 2004). The Transpolar Drift advects a considerable portion of the marginal sea ice out of the Arctic Ocean through the Fram Strait (Kwok et al. 2004). Sea ice drifting with the wind and currents is often referred to as 'pack-ice'. Conversely, the sea ice that is 'fastened' to the coastline, to the sea floor along shores or to grounded icebergs is defined as '(land-)fast ice'.

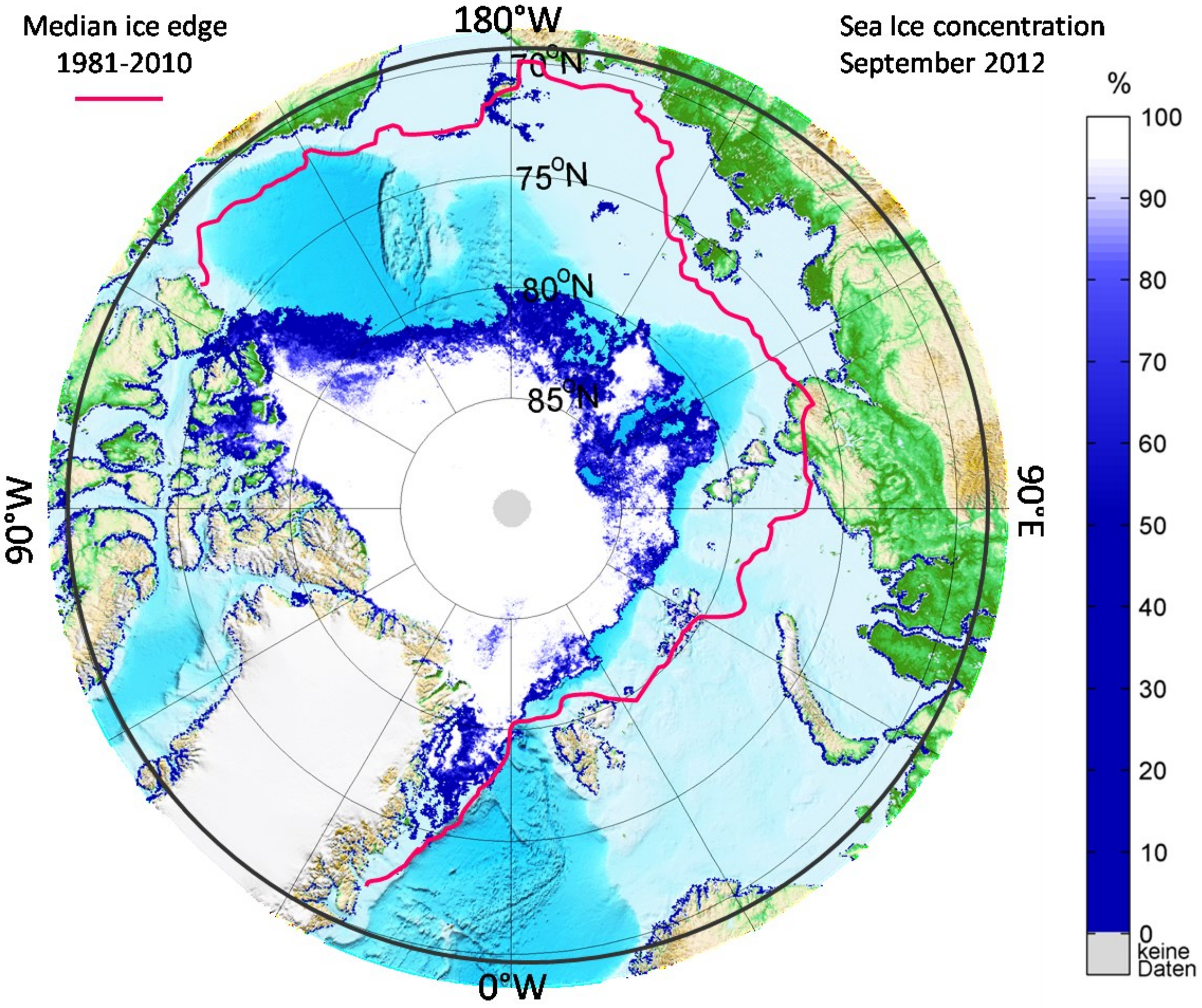

Figure 2. Sea-ice concentration in September 2012 (Data source: meereisportal.de University of Bremen and Alfred Wegener Institute). Red line represents the median sea-ice edge in September from 1981-2010 (Data source: http://nsidc.org National Snow and Ice Data Centre).

Over the past three decades, the Arctic sea-ice extent (defined as the ice-covered area with sea-ice concentration >15%) was about 15 million km^2 in winter and about 6 million km^2 in summer (Data source: www.meereisportal.de University of Bremen and Alfred Wegener Institute). Sea-ice extent, however, has been decreasing since the age of satellite observations (Comiso and Hall 2014). In summer 2012 a historical sea-ice minimum extent of 3.4 million km^2 was recorded. The long-term averaged modal ice thickness is about 2.5 m, decreasing at a rate of 0.3 m yr^{-1} (Renner et al. 2014).

1.1.2.The Southern Ocean

The Southern Ocean is located in the Southern Hemisphere, surrounding the Antarctic continent. It is the largest and deepest of the world oceans, circumpolar and free of land in the north, except a number of subantarctic islands. The Antarctic continental shelves are mostly narrow and unusually deep (450 m) (Post et al. 2014); broader shelves, such as in the Weddell and Ross Sea, contain large glacial embayments. The Southern Ocean is considered the central link in the global thermohaline circulation by connecting all the major oceans. Accordingly, it is divided into three sectors: Pacific, Atlantic and Indian Oceans (De Broyer et al. 2014).

The main hydrographical feature of the Southern Ocean is the Antarctic Circumpolar Current (ACC). The ACC flows from west to east around the Southern Ocean and it is the most powerful current on Earth (134-164 Sv; (Griesel et al. 2012). The eastward flow of the ACC and the overlying westerly winds create a series of fronts that separate the warmer subtropical regime from the subpolar regime, the latter consisting of the Weddell and Ross Sea gyres and Antarctic coastal and shelf waters. Two of the most distinct and continuous circumpolar fronts are the Sub-Antarctic Front (SAF) and the Polar Front (PF) (Fig. 3). The Sub-Antarctic Zone exists north of the SAF, between the SAF and the PF is the Polar Frontal Zone, and the Antarctic Zone exists south of the PF (Whitworth III 1980).

The Antarctic Zone of the Southern Ocean is seasonally ice covered. The extent of sea ice ranges from 19 million km^2 in winter to 4 million km^2 in summer (Fig. 4), making it one of the largest physical changes in water surface conditions anywhere on the planet (De Broyer et al. 2014). Most of the Antarctic pack-ice is annual, with a mean thickness of less than 1 m (Worby et al. 2008). In some regions, particularly in the Weddell Sea, the pack-ice can be perennial, reaching a thickness of 3 to 4 m, with ridged and rafted surfaces. The Weddell Sea has the largest latitudinal extent of sea ice, whereas the East Antarctic sector has a relatively narrow extent of sea ice.

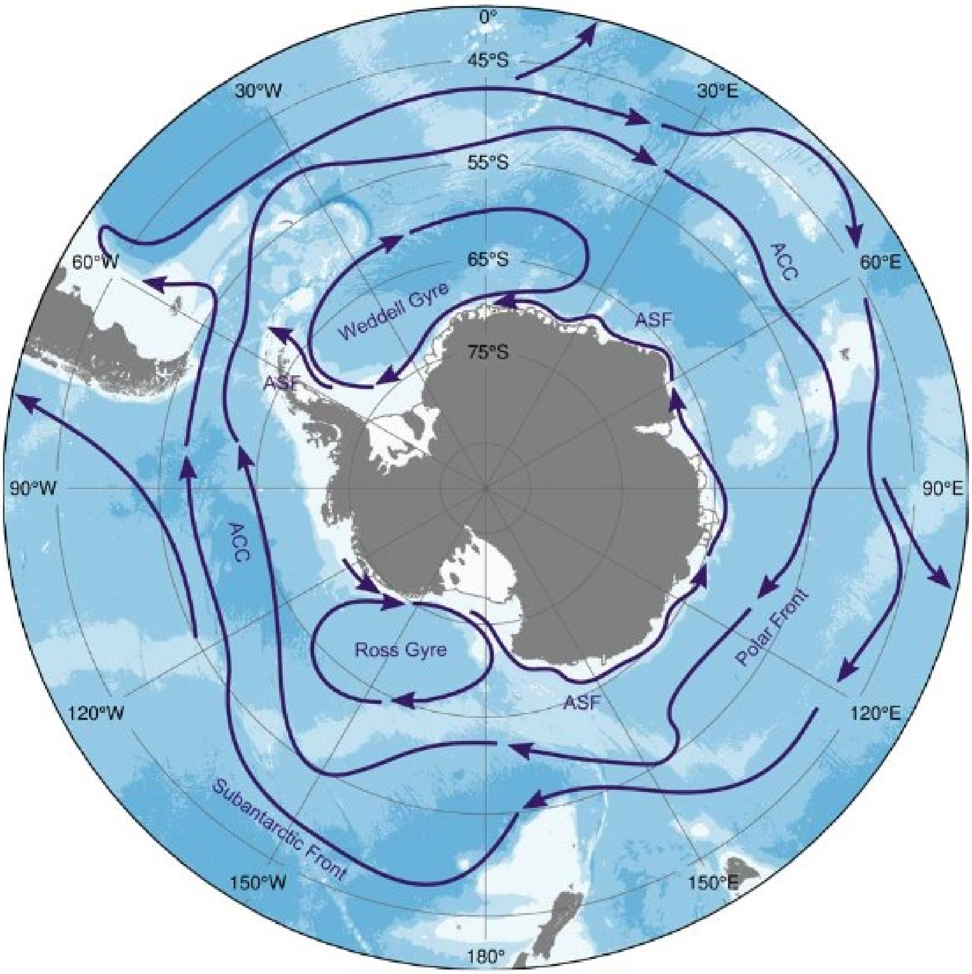

Figure 3. Major Southern Ocean circulation features (reproduced from Post et al. 2014; Rintoul et al. 2001) showing the Polar and Sub-Antarctic Fronts of the Antarctic Circumpolar Current, subpolar gyres and Antarctic Slope Front (ASF). Background colors show bathymetry.

1.1.1.The Arctic and Southern Ocean: changing systems

The Arctic Ocean is experiencing some of the most pronounced effects of global-climate change (ACIA 2004). During the past decades, a substantial reduction in sea ice concentration, thickness and duration was recorded in the Arctic Ocean (Kwok and Rothrock 2009; Rigor and Wallace 2004; Shimada et al. 2006; Stroeve et al. 2012). Sea-ice extent is decreasing at an average rate of 10% per decade (Polyakov2010); in the next decades this will lead to a largely ice-free ocean in late summer and a winter cover consisting mainly of first-year ice (Wassmann and Reigstad 2011). Along with the steady decrease in ice thickness, the Arctic Ocean may have already lost over 50% of its sea-ice volume during the past four decades (Kwok and Rothrock 2009; Tilling et al. 2015).

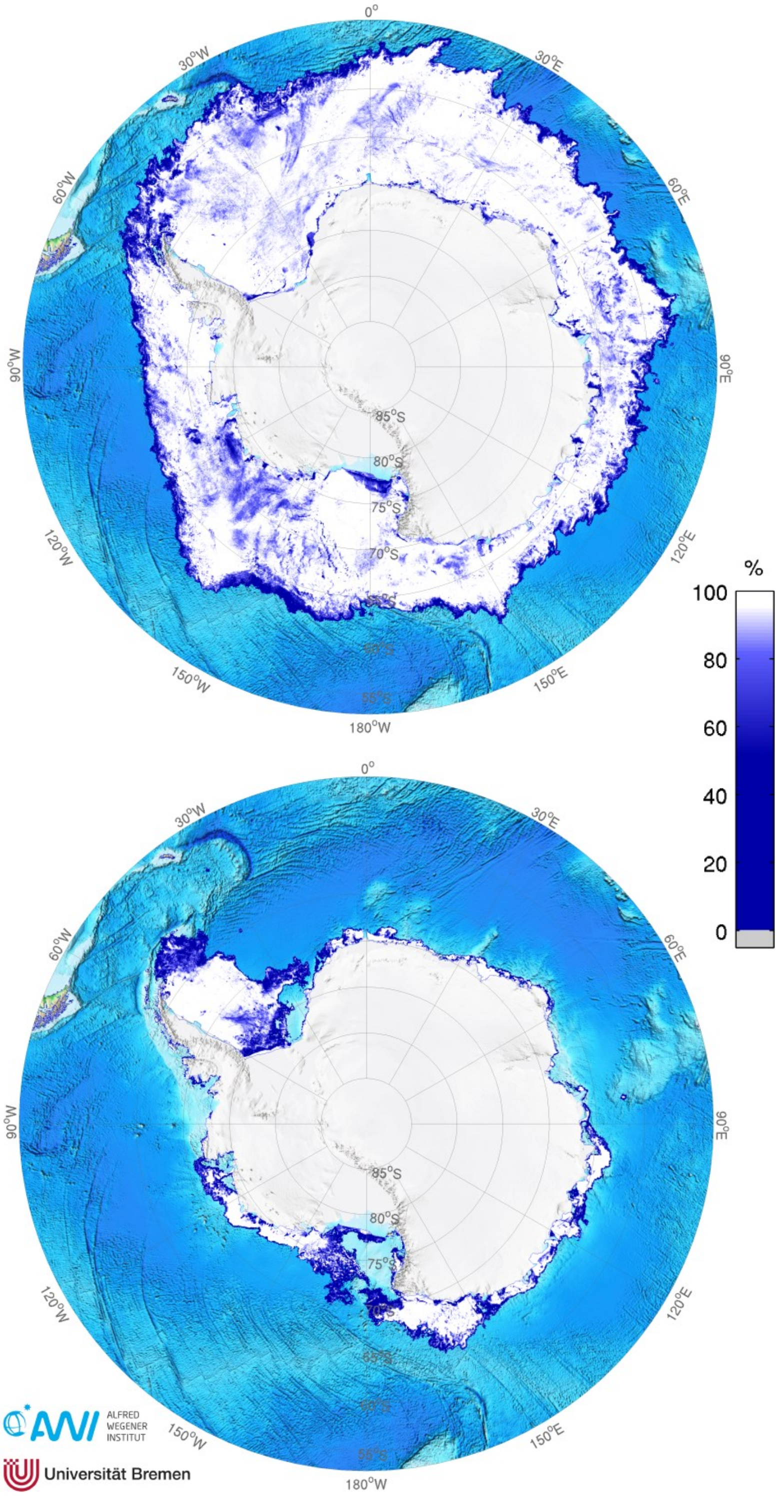

Figure 4. Sea ice concentration in September 2013 (upper) and February 2013 (lower) (Maps downloaded from meereisportal.de, hosted by University of Bremen and Alfred Wegener Institute). Background colours show bathymetry. Legend shows sea-ice concentration (%).

In the Southern Ocean the patterns of change have been more complex. The sea-ice extent decreased in the Ross Sea, the Western Pacific sector, and the Bellingshausen/Amundsen Seas, but increased in the Weddell Sea and Indian sector, leading to a slight rise in the overall winter sea-ice extent (Dong and Zou 2014). The ice anomalies are considered to be a result of wind variations associated with changes in atmospheric-pressure patterns around the Antarctic (King 2014). Stronger cyclonic systems are believed to advect sea ice northwards and, thus, expand the sea-ice extent (Turner et al. 2013). This divergent pattern of sea-ice drift may lead to a looser pack-ice with reduced ridges and rafted structures.

The changes mentioned above are expected to result in modifications of the biological systems in the ice-covered regions. In the Arctic Ocean, reduction in the extent and thickness of sea ice leads to more light availability in the water column, which may induce an increase in the net primary production (Arrigo et al. 2008; Arrigo and van Dijken 2011). This may be true on the shelves where nutrient supply by advection or vertical mixing can be extensive. Over the deep basins, however, primary production can be nutrient-limited due to strengthened stratification by ice melt (Tremblay and Gagnon 2009). Accordingly, sea-ice loss will lead to a decrease of the ice algal production. Under a climate-change warming scenario, an expected 25% loss of sea ice over the next century would increase primary production in the Southern Ocean by approximately 10%, resulting in a slight negative feedback on climate warming (Arrigo and Thomas 2004). Wassmann and Reigstad (2011) suggested that reduction of primary production in the seasonal ice zone will result in lower food supply for the pelagic heterotrophs. This will be mostly recycled in the pelagic zone; therefore, resulting in reduced quality and less variable vertical export of biogenic matter.

To what extent these changes in sea ice and primary production will impact marine fauna is an open question. The number of documented changes in ice-covered waters from the central Arctic Ocean and the Southern Ocean remains low. Few studies have compiled available historical data to identify changing patterns in polar marine ecosystems (Darnis et al. 2012; Flores et al. 2012; Grebmeier 2012; McBride et al. 2014; Nicol et al. 2008). Reviewing changes in the Antarctic sea-ice ecosystems, however, Nicol et al. (2008) pointed out that most conclusions on population change come from inferences drawn from a variety of isolated sources, with considerable uncertainties regarding data collection. Ice algae and associated communities remain especially difficult to evaluate due to lack of quantitative reports of their abundance and distribution (Wassmann et al. 2011).

1.2. Sea-ice habitats

1.2.1. Sea-ice algae contribution to primary production

The Arctic and Southern Oceans are distinct from the other oceans through the huge annual variability in sea-ice extent and their extreme seasonality in light regime. In the Arctic region, the ice cover doubles in size from summer to winter, while in the Antarctic the ice cover in summer is five times lower than in winter. The presence of sea ice influences how much light penetrates the water column and the depth of mixing processes, which in turn determines the replenishment of nutrients in the surface. Thus, sea-ice properties, like concentration, thickness and snow cover, largely regulate the intensity of primary production over the ice-covered areas (Arrigo 2008).

The most important primary producers are microscopic unicellular algae, mainly diatoms, phototrophic dinoflagellates, and other small eukaryotic protists (Kilias et al. 2014; Lizotte 2001). The autotrophic community living in the sea ice is referred to as ice algae, and the autotrophs living in the water column are called phytoplankton. The algal community in land-fast ice is mainly composed of diatoms, while in pack-ice, flagellates can also contribute to the community (Gradinger 1999), with relatively low biomass levels however (Dieckmann et al. 1990).

Over the deep basins of the Southern Ocean, ice algae growth is primarily limited by light. The lower light level, caused by deeper snow cover in the drifting pack-ice compared to the snow-free and more productive fast ice zones, is the primary factor in producing differences in algal production between the two systems (Ackley and Sullivan 1994). In the Arctic Ocean, ice algae are light limited at the beginning of the bloom (Horner and Schrader 1982), then fluctuate between light and nutrient limitation, finally remaining nutrient limited towards the end of the bloom (Lavoie et al. 2005). Algae released from melting sea ice are prone to form aggregates and sink. Some of these aggregates are consumed while sinking and some reach the sea floor and feed the organisms living at the sea bottom, accelerating the energy transfer between realms, a process known as cryo-pelagic and cryo-benthic couplings, respectively.

In general, Antarctic sea ice supports higher biomass than Arctic sea ice. The mean algal biomass reported in Antarctic studies was, on average, 133 mg Chl *a* m^{-2}, about 50% more than in the Arctic (Arrigo 2008; Meiners et al. 2012). There is, however, high spatial variability in biomass distribution. Land-fast ice accumulates more biomass than pack-ice. Within the pack-ice, the marginal ice zone (MIZ) is known to be a region of high primary productivity in the Southern Ocean (Arrigo and

Thomas 2004; Saenz and Arrigo 2014), while the Arctic MIZ is rather moderate (Carmack and Wassmann 2006). The relative contribution of ice algae to the total primary production is generally low but increases with increasing latitude (Carmack and Wassmann 2006). In the central Arctic Ocean ice algae can contribute with more than 50% to total primary production (Fernández-Méndez et al. 2015; Gosselin et al. 1997). In contrast, in the ice-covered regions of the Southern Ocean, ice algae only account for up to 25% of total annual primary production (Arrigo and Thomas 2004). On the Antarctic shelves, however, ice algae contribution can increase up to 50% (McMinn et al. 2010).

1.2.2. Sea-ice associated fauna

Sea-ice habitats represent a feeding and reproduction ground, nursery or refuge, for a number of organisms, which are associated with the sea ice to different degrees. Smaller species live within the sea-ice matrix, and are referred to as sea-ice meiofauna. Larger animals like euphausiids and amphipods, are found either occasionally, seasonally or permanently at the underside of sea ice (Schnack-Schiel 2003) and are referred to as ice-associated fauna. Until today, information is lacking to what extent many of these species are associated with the sea ice.

The herbivorous organisms found in close association with the under-ice habitat are observed directly scraping the ice algae from the bottom of the sea ice or filtering the underlying water ice algae expulsed from the ice. Ice algae are considered a critical carbon source in sea-ice related food webs (O'Brien et al. 2011; Søreide et al. 2013; Søreide et al. 2006). Besides ice algae, other resources provided by sea-ice habitats like protozoans, small copepods and detritus may offer an alternative food source for omnivorous species, especially during winter when resources are scarce (Daly 1990; Gannefors et al. 2005; Meyer 2012; Schmidt et al. 2014).

The species living within or under ice can spend their entire life cycle associated with sea ice or only a part of their life cycle (Arndt and Swadling 2006). The former depend on year-round sea ice as substrate, the latter have to adapt their cycles to seasonal dynamics of melting and growth of sea-ice. Most of the species found associated with the Antarctic sea-ice have a short life span of ≤1 year, comprising mostly small copepods. The Arctic ice-associated fauna is dominated by amphipods and comprise species with a longer life span, e.g. the gammarid amphipod *Gammarus wilkitzkii* Birula, 1897 living up to 6 years (Poltermann 2000).

The topographic features of the underside of ice are important for colonization, as their variety provides a wide range of microhabitats (Krembs et al. 2002). Comparable with a reverse benthic habitat, the underside of ice draws inhabitants with a particular attraction for substrate, like benthic gammarid amphipods or harpacticoid copepods. Organisms feeding under ice have the advantage of expending little energy encountering prey because they merely have to scan a plane rather than a volume. Sea-ice structures provide resting grounds, reducing the energetic demands of organisms that need to maintain their vertical position in the water column. Polar cod (*Boreogadus saida* Lepechin, 1774), the most abundant fish in the Arctic pack-ice, were observed resting in wedges at the edge of ice floes (Gradinger and Bluhm 2004). By resting in these wedges, polar cod also avoid visual predators as the narrow sea-ice structures make it impossible for larger top predators to reach them. Similarly, swarms of Antarctic krill (*Euphausia superba* Dana, 1850) larvae were reported within rafted sea-ice structures, where they find shelter from currents and predators while resting or feeding (Meyer et al. 2009).

1.2.3.Ecological importance of under-ice fauna

Climate change related alterations of Arctic and Antarctic sea-ice habitats are expected to significantly impact on the interaction of ice-associated organisms with the environment, with repercussions on ecosystem functioning. The nature of this interaction remains poorly understood.

The energy flow through an ecosystem is represented by an interconnection of food chains, characterized by many weak interactions and a few strong interactions between species either at the same or at a different trophic level (McCann et al. 1998). Both compartments, denoting one or more species grouped according to trophic guilds, and the strengths of interactions have significant roles in the efficiency and persistence of ecosystems facing environmental disturbances (Rooney et al. 2006).

In the Arctic Ocean, calanoid copepods dominate the biomass (Kosobokova and Hirche 2009; Kosobokova and Hopcroft 2010), feed on ice algae and have excellent conversion rates, which result in high lipid content (Falk-Petersen et al. 1987). The Arctic fish, polar cod, feeds extensively on calanoid copepods (Falardeau et al. 2014; Lønne and Gulliksen 1989; Scott et al. 1999) and itself represents a preferential prey for top predators like seabirds and marine mammals (Haug et al. 2007; Matley et al. 2012; Welch et al. 1992). Ice algae – calanoid copepods – polar cod – top predators, represents what is probably one of the strongest and most efficient pathways in the energy flux through the Arctic food web (Welch et al. 1992). Yet all components of this flux are closely related with sea ice. Decline in sea-ice coverage may result in low food availability and quality for calanoid copepods with a bottom-up effect in the food chain (Leu et al. 2006). For upper trophic levels, besides food availability or quality, the spawning and foraging areas will also be affected. For polar cod, reduced spawning season will have tremendous consequences on the entire system, as this species is believed to affect up to 75% of energy transfer between zooplankton and vertebrate predators (Darnis et al. 2012).

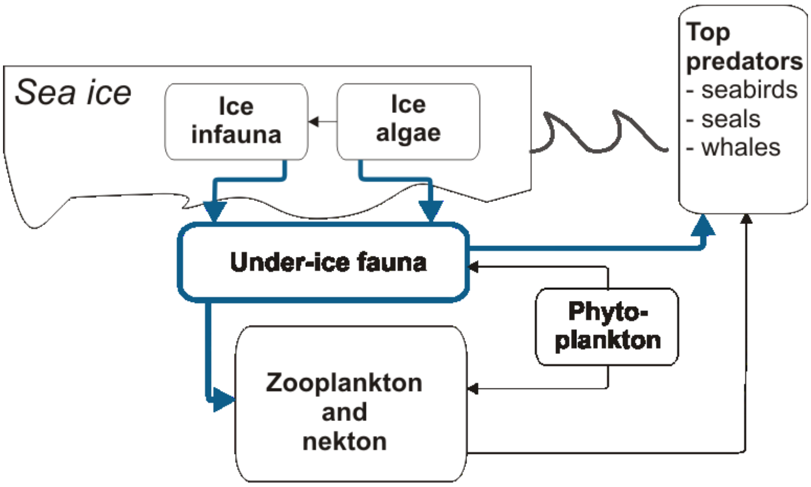

Figure 5. Schematic overview of the under-ice fauna compartment; the flux of energy is represented by arrows (reproduced from Flores 2009).

An early view of the entire Southern Ocean was that it consisted of a simple system with diatoms feeding a vast Antarctic krill population, which in turn was consumed by large, and mostly migratory, populations of seals, seabirds and whales (Hempel 1985). Nowadays, it has been shown that, at least over the shelves, the role of ice krill (*Euphausia crystallorophias* Holt & Tattersall, 1906) and midwater fish (*Pleuragramma antarcticum* Boulenger, 1902) as grazers of lower levels and food for higher trophic levels, e.g. seals, penguins, pelagic birds, whales, can be just as critical (Smith et al. 2007). For now, the role of *E. superba* in Antarctic food web remains important due to their large standing stock still existent (Atkinson et al. 2009). To a large extent, the Antarctic krill-based ecosystem is spatially coincident with the sea-ice zone (Atkinson et al. 2008; Nicol et al. 2008). Successful recruitment of krill was proven to be dependent on sea-ice conditions from the previous winter, i.e. lower krill abundance followed winters with reduced sea-ice cover (Atkinson et al. 2004; Fisher et al. 2004; Loeb et al. 1997); as during winter, the resources in the water column are scarce and Antarctic krill larvae agglomerate under ice, feeding on ice algae (Meyer et al. 2009). Their overwintering success, therefore, depends on ice algae availability (Daly 1990). A decline in sea-ice will strongly impact this key Antarctic species with, as yet, unknown consequences and magnitude of the cascade effects in the functionality of this efficient food chain.

With on-going climate change and decline of sea-ice habitats, ice-associated fauna will probably need new strategies to compensate for habitat loss (Berge et al. 2012; Poltermann et al. 2000). Changes in the marine polar food webs through alteration of the sea-ice environment and primary production, or decline of key species' populations will likely reflect in the redistribution of the trophic-energy transfer through the entire ecosystem via different pathways. Before we are able to predict the expected changes, we must first understand how the present sea-ice associated ecosystem is functioning. Thus, the immediate need is to investigate the mechanisms controlling the 'key species – sea-ice' interaction. To achieve this aim, an adequate quantification of the ice-associated fauna's distribution is required since any modification in the abundances and distribution of these species will be reflected in the entire ecosystem functionality. Secondly, the primary environmental factors, inducing any modifications in ice-associated species abundances and distribution, need to be recognised and their potential for predicting future change assessed.

1.3. Objectives

Ice-covered areas are difficult to access as, sampling is time-consuming and expensive. Despite increased efforts in collecting and classifying ice-associated fauna, there are still many gaps in our understanding of their distributional patterns. They can be influenced by a wide range of environmental factors, including the physical and biogeochemical properties of sea-ice and the underlying water column.

The **overall aim** of this thesis is to improve the understanding of the distribution and association of meso- and macrofauna communities in the surface layer (0-2 m) under the ice and in open water with the habitat properties of the sea ice and underlying water column.

Specifically, I address the following **objectives**: i) evaluate the most important environmental variables defining the under-ice habitats, ii) quantify the under-ice fauna distribution at large spatial scales, identifying under-ice community structures and their key species, iii) investigate how different community structures relate to environmental gradients and iv) analyse the relationships of the key species with environmental variables of the under-ice habitat.

The main **research questions** addressed in this thesis are:

1. How is the **under-ice community** structured by habitat properties? What are the dominating species? Which environmental variables have the highest impact on community structure?
2. Which of the **dominant species** are highly relevant for ecosystem dynamics? How do the environmental variables relate to these species?

The innovative approach of this study is the use of a relatively new trawling device, the Surface and Under Ice Trawl (SUIT; van Franeker et al. 2009). Sampling the underside of sea ice over an average 1.5 km profile, considerably improves the coverage of the spatial variability of a patchy-distributed fauna (Schnack-Schiel 2003). The increased sampling effort compared to other methods like under-ice pumps, hand nets or remotely operated vehicles, captures a considerably greater part of the under-ice species diversity. The SUIT was developed to estimate the available under-ice resources for top predators. It was previously tested and used in the Lazarev Sea, Southern Ocean (Flores et al. 2011). Here, we used an improved version of the SUIT equipped with a new array of sensors which measure environmental parameters, such as ice thickness, concentration, temperature, salinity, chlorophyll *a* concentration; whilst collecting fauna. Our results will increase our understanding of the way in which environmental parameters impact under-ice species distribution, abundance and diversity. These new findings create a baseline with the potential to lead to large-scale extrapolations of distribution patterns and to future predictions on the effects of climate change.

1.4. Methods

1.4.1. The Surface and Under Ice Trawl

Data was collected during two expeditions: 1) RV Polarstern expedition PS80 (ARK XXVII/3), between 2nd August – 29th September 2012, across the ice-covered Eurasian part of the Arctic Ocean deep-sea basin, between 82° and 89°N, and 30° to 130°E; 2) RV Polarstern expedition PS81 (ANT XXIX/7), between 31st August – 2nd October 2013, across the ice-covered northern Weddell Sea, between 61°S 42°W and 58°S 25°W.

Sampling was performed with the SUIT, which consisted of a steel frame with a 2 m x 2 m opening and 2 parallel 15 m long nets attached: (1) a 7 mm half-mesh commercial shrimp net, lined with 0.3 mm mesh in the rear 3 m of the net, covered 1.5 m of the opening width and (2) a 0.3 mm mesh zooplankton net covered 0.5 m of the opening width. Floats attached to the top of the frame kept the net at the surface or the sea-ice underside. To enable sampling under undisturbed ice, an asymmetric bridle forces the net to tow at an angle of approximately 60° starboard of the ship's track, at a cable length of 150 m.

1.4.2. Environmental data collection

A sensor array was mounted in the SUIT frame, consisting of an Acoustic Doppler Current Profiler (ADCP), a Conductivity Temperature Depth probe (CTD) with built-in fluorometer, an altimeter, 2 spectral radiometers, and a video camera. Water inflow speed was estimated using a Nortek Aquadopp® Acoustic Doppler Current Profiler (ADCP). Temperature and salinity profiles were obtained with a Sea and Sun CTD75M probe. A built-in Turner Cyclops fluorometer was used to estimate under-ice chlorophyll concentration. Calibration of fluorometric chlorophyll *a* concentrations was done from water samples obtained during stationary sea-ice work. The calibration coefficients were derived from the relationship between chlorophyll *a* concentrations of water samples (measured with High Pressure Liquid Chromatography) with fluorometric chlorophyll *a* concentrations of the corresponding depth range. Data gaps in the CTD measurements caused by low battery voltage were filled using complementary datasets from the ADCP data (pressure) and the shipboard sensors (temperature and salinity), using correction factors determined by linear regression. An altimeter Tritech PA500/6-E connected to the CTD probe measured the distance between the net and the underside of the sea-ice. Sea-ice draft was calculated as the difference between the depth of the net relative to the water level, measured by the CTD pressure sensor, and the distance to the sea-ice underside, measured by the altimeter, and corrected for pitch and roll angles. Draft was then converted into ice thickness by using a sea-ice density value of 834 kg m^{-3} for the Arctic Ocean, determined from sea-ice core samples, and 900 kg m^{-3} theoretically assumed for Weddell Sea (B. Lange pers. comm.).

During each haul, changes in ship speed, ice concentration [%] and irregularities were estimated visually by an observer on deck. GPS waypoints were recorded by the observer when the SUIT was deployed and hauled in, when it behaved abnormally, or when the environment changed, e.g. when the SUIT entered or exited the sea ice. The distance sampled over ground was estimated by multiplying the amount of time the SUIT was in the water (s) with the average speed in water (m s^{-1}). The distance sampled under ice was estimated in the analogue way for the period while the SUIT was under ice. The distance sampled under ice was then expressed as percentage ice coverage of the total distance sampled over ground.

Gridded daily sea-ice concentrations for the Arctic Ocean derived from SSMIS and for the Southern Ocean derived from AMSR2 satellite data, using the algorithm specified by Spreen et al. (2008), were downloaded from the sea-ice portal hosted by the University of Bremen (www.meereisportal.de).

1.4.3. Biological data

The catch was partially sorted on board. Fish and ctenophores were immediately extracted from samples. Several species were sampled for biochemical analysis and stored at -20°C and -80°C. The remaining material was immediately preserved in 4% formaldehyde/seawater solution for quantitative analysis. After the cruise, the quantitative samples were analysed for species composition and abundance at the Alfred Wegener Institute. Macrofauna (> 0.5 cm) abundances were derived from the analysis of the shrimp net samples. Copepod and ostracod abundances were derived from the analysis of the zooplankton net samples. With few exceptions, all animals were identified to the species level and to the developmental stage and sex (copepod species). Abundances were calculated by dividing the total number of animals per haul by the trawled area. The trawled area was calculated by multiplying the distance sampled in water, estimated from ADCP data, with the net width (0.5 m for the zooplankton net, and 1.5 m for the shrimp net respectively).

1.5. Publications outline

This cumulative dissertation summarizes the research findings of my PhD project, which was conducted from July 2012 to August 2015. This work was part of the Helmholtz Association Young Investigators Group *Iceflux*: Ice-ecosystem carbon flux in polar oceans (VH-NG-800) developed by H. Flores. The *Iceflux* project intends to produce a concise quantitative evaluation of the contribution of sea-ice-derived carbon to Arctic and Antarctic marine food webs, considering changing sea-ice environments.

The main focus of my work was to investigate the distribution and association of the under-ice meso- and macrofauna communities with sea-ice habitat properties in central Arctic Ocean and northern Weddell Sea, Southern Ocean. The thesis includes a general introduction and a synoptic discussion and is composed of four publications (Chapters I – IV) presented as manuscripts listed below.

Chapter I and **III** answer my first research question by investigating the distribution of under-ice fauna sampled with the SUIT for the first time in the central Arctic Ocean and in the northern Weddell Sea. In these chapters, I relate the variability of sea-ice and underlying water-column properties with faunal distribution by showing how environmental patters reflect on community structure.

Chapter I focuses on under-ice fauna sampled in the central Arctic Ocean during summer 2012, when a historical minimum sea-ice extent was recorded. I describe how sea-ice and water-column parameters, such as nutrients concentrations, surface salinity and sea-ice coverage, define two, distinct environmental regimes. I show that under-ice community structure mirrors the environmental patterns at basin scale. I further emphasise the influence of sea-ice on small-scale patterns by abrupt changes in the dominance of ice-associated amphipods at ice-covered stations versus pelagic amphipods at nearby ice-free stations.

Chapter I: Community structure of under-ice fauna in the Eurasian central Arctic Ocean in relation to environmental properties of sea-ice habitats.

Carmen David, Benjamin Lange, Benjamin Rabe, Hauke Flores

This study was designed by myself and discussed with H. Flores. Field sampling was performed by C. David, H. Flores and B. Lange. Species identification and counting was performed by C. David. Sensor data were processed by B. Lange. Oceanographic data were provided by B. Rabe. The analysis of data was performed by C. David with support from H. Flores. Writing of the manuscript was realized by C. David with contribution from all authors. This paper was published in Marine Ecology Progress Series (2015) 522:15-32.

In **Chapter II**, I investigate the drivers of under-ice polar cod distribution in the high Arctic and develop a new hypothesis regarding their potential origin. This study provides the first abundance estimates of polar cod over the vast area of central Arctic pack-ice. Using statistical modelling, I relate fish abundance with environmental variables, such as ice thickness and surface water salinity. I hypothesise that under-ice fish arrive in the central Arctic by drifting with sea ice formed in coastal areas. I analyse their potential area of origin by back-tracking the areas of sampled sea-ice.

Chapter II – Under-ice distribution of polar cod *Boreogadus saida* in the central Arctic Ocean and their association with sea-ice habitat properties.

Carmen David, Benjamin Lange, Thomas Krumpen, Fokje Schaafsma, Jan Andries van Franeker, Hauke Flores

This study concept was developed by myself with advice from H. Flores. Field sampling was performed by C. David, H. Flores and B. Lange. Fish measurements and dissection was performed by C. David and H. Flores. Energy content measurement was performed by F. Schaafsma. Sensor data were processed by B. Lange. Sea-ice back-tracking data were provided by T. Krumpen. The analysis of data was performed by C. David. Writing of the manuscript was realized by C. David with contribution from all authors. This paper was published in Polar Biology (2015) in a special issue on the "Ecology of Arctic Gadids":1-14, doi:10.1007/s00300-015-1774-0

Chapter III focuses on under-ice fauna sampled in the northern Weddell Sea, one of the most productive areas of this polar environment. Sampling was performed during late winter/early spring 2013, when the largest extent of sea ice over the past three decades was recorded in the Southern Ocean. I show that the under-ice community is heterogeneous, probably driven by biogeographic distribution patterns, sea-ice habitat properties, and seasonal progression. I demonstrate how the balance between numerically dominant species, i.e. Antarctic krill and copepods, defines different community types in relation to environmental variability.

Chapter III – Community structure of under-ice fauna in relation to winter sea-ice habitat properties from the Weddell Sea.

Carmen David, Fokje Schaafsma, Jan Andries van Franeker, Benjamin Lange, Angelika Brandt, Hauke Flores

This study was designed by myself and discussed with H. Flores. Field sampling was performed by C. David, F. Schaafsma and J. A. van Franeker. Species identification and counting was performed by C. David and F. Schaafsma. Sensor data were processed by C. David and B. Lange. The analysis of data was performed by C. David. Writing of the manuscript was realized by C. David with contribution from all authors. This paper is under review in Polar Biology (submission date: 21.08.2015; manuscript number: POBI-S-15-00239)

In **Chapter IV**, I investigate the carbon demand of dominant ice-associated and pelagic species during winter in response to autotrophic food availability, grazing and predation pressure. I show that spatial variability of grazing and predation pressure is unequally distributed between the ice-water interface layer and the water column. I further discuss how the three factors impacting the main bulk of carbon demand make the under-ice habitat attractive for some species, including the Antarctic krill larvae.

Chapter IV – What makes the under-ice habitat attractive during winter: carbon demand of Antarctic krill larvae and ice-associated copepods in relation to food availability and predation pressure in the northern Weddell Sea.

Carmen David, Fokje Schaafsma, Jan Andries van Franeker, Evgeny Pakhomov, Brian Hunt, Angelika Brandt, Hauke Flores

The scientific concept of this study was developed by C. David with advice from H. Flores. Under-ice sampling was performed by C. David, F. Schaafsma, J. A. van Franeker. Species identification and counting was performed by C. David and F. Schaafsma. Zooplankton data from water column was provided by E. Pakhomov and B. Hunt. The analysis of data was performed by C. David. Writing of the manuscript was realized by C. David with contribution from all authors. This paper is in preparation for publication.

2.1. Chapter I

Community structure of under-ice fauna in the Eurasian central Arctic Ocean in relation to environmental properties of sea-ice habitats

Carmen David[1,2*], Benjamin Lange[1,2], Benjamin Rabe[1], Hauke Flores[1,2]

[1] Alfred Wegener Institut Helmholtz-Zentrum für Polar- und Meeresforschung, Am Handelshafen 12, 27570, Bremerhaven, Germany; [2] University Hamburg, Centre for Natural History (CeNak), Zoological Museum, Biocenter Grindel, Martin-Luther-King Platz 3, 20146, Hamburg, Germany

Published in Marine Ecology Progress Series
522:15-32 doi: 10.3354/meps11156

ABSTRACT

Arctic sea-ice decline is expected to have a significant impact on Arctic marine ecosystems. Ice-associated fauna play a key role in this context because they constitute a unique part of Arctic biodiversity and transmit carbon from sea-ice algae into pelagic and benthic food webs. Our study presents the first regional-scale record of under-ice faunal distribution and the environmental characteristics of under-ice habitats throughout the Eurasian Basin. Sampling was conducted with a Surface and Under Ice Trawl, equipped with a sensor array recording ice thickness and other physical parameters during trawling. We identified 2 environmental regimes, broadly coherent with the Nansen and Amundsen Basins. The Nansen Basin regime was distinguished from the Amundsen Basin regime by heavier sea-ice conditions, higher surface salinities and higher nitrate + nitrite concentrations. We found a diverse (28 species) under-ice community throughout the Eurasian Basin. Change in community structure reflected differences in the relative contribution of abundant species. Copepods (*Calanus hyperboreus* and *C. glacialis*) dominated in the Nansen Basin regime. In the Amundsen Basin regime, amphipods (*Apherusa glacialis*, *Themisto libellula*) dominated. Polar cod *Boreogadus saida* was present throughout the sampling area. Abrupt changes from a dominance of ice-associated amphipods at ice-covered stations to a dominance of pelagic amphipods (*T. libellula*) at nearby ice-free stations emphasised the decisive influence of sea ice on small-scale patterns in the surface-layer community. The observed response in community composition to different environmental regimes indicates potential long-term alterations in Arctic marine ecosystems as the Arctic Ocean continues to change.

INTRODUCTION

The Arctic Ocean is experiencing some of the most pronounced effects of global climate change (Arctic Climate Impact Assessment 2004). During the past 4 decades, reductions in sea-ice concentration and thickness and in the duration of the melting season have been recorded in the Arctic Ocean (Kwok and Rothrock 2009; Markus et al. 2009; Overland and Wang 2013; Rigor and Wallace 2004; Shimada et al. 2006; Stroeve et al. 2012) and are predicted to continue in the future (Johannessen et al. 2004; Polyakov et al. 2005; Stroeve et al. 2007). The Arctic Ocean is changing from a perennial multi-year ice (MYI)-dominated system to a seasonal first-year ice (FYI) system (Maslanik et al. 2011). In 2012, the sea-ice extent was reduced to approximately half of the mean for the past four decades, resulting in large open-water areas (Parkinson and Comiso 2013).

These changes are expected to result in modifications of the biological systems in the Arctic Ocean. Reduction in the extent and thickness of sea ice leads to more light availability in the water column, which has been hypothesised to induce a net increase in primary production (Arrigo et al. 2008; Arrigo and van Dijken 2011). This may be true on the shelves where nutrient supply by advection or vertical mixing can be extensive. Over the basins, however, primary production can be nutrient-limited due to strengthened stratification by ice melt (Tremblay and Gagnon 2009). Sea-ice loss will lead to a decrease in ice algal production, which can account for up to 50% of the primary production in the central Arctic Ocean (Gosselin et al. 1997). Ice algae are considered a high-quality food source for Arctic marine food webs (Søreide et al. 2013; Søreide et al. 2006). How these changes in primary production will impact marine fauna is an open question. The number of documented changes in Arctic planktonic systems is low, and the number reported from the central Arctic Ocean even lower is (Wassmann et al. 2011). Lack of biological baseline data makes it impossible to estimate the effect of recent environmental changes on the biological system (Kosobokova and Hirche 2000). Increasing efforts have been made in recent years to investigate zooplankton distribution at different scales (Hopcroft et al. 2005; Hunt et al. 2014; Matsuno et al. 2012; Pomerleau et al. 2014). Only recently, have zooplankton data from different Arctic cruises been compiled into a large-scale analysis, providing a first baseline to monitor the influence of environmental change on the Arctic pelagic system (Kosobokova and Hirche 2009). It should be born in mind, however, that this dataset dates from the 1990s, a period when environmental change in the Arctic Ocean was already on-going.

Most affected by environmental changes are the organisms living in association with sea ice. Ice-associated fauna have been described as those species that complete their entire life cycle within the sea ice or spend only part of their life cycle associated with sea ice (Melnikov and Kulikov 1980). Many uncertainties still remain in understanding the association of these organisms with sea-ice habitats. Community structure of ice-associated fauna is assumed to be related to ice age, density and under-ice topography (Hop and Pavlova 2008; Hop et al. 2000). Ice-associated species may prefer a certain type of ice, e.g. MYI or FYI (Hop et al. 2000). Some, such as the large amphipod *Gammarus wilkitzkii*, are found associated with ridges, which provide shelter during the melting season (Gradinger et al. 2010; Hop and Pavlova 2008). The widely distributed amphipod *Apherusa glacialis* prefers flat ice floes (Hop and Pavlova 2008), or ice edges (Beuchel and Lønne 2002; Hop et al. 2000).

Crucial for the functioning of the Arctic ecosystem is the role of ice-associated fauna in the energy transfer to higher trophic levels (Budge et al. 2008). The dominance of diatom fatty acid trophic markers in the lipids of calanoid copepods and ice-associated amphipods underpins the importance of sea-ice algae as a critical carbon source in Arctic food webs (Budge et al. 2008; Falk-Petersen et al. 2009). Feeding extensively on calanoid copepods (Benoit et al. 2010; Scott et al. 1999) and amphipods (Matley et al. 2013), polar cod *Boreogadus saida* in turn represents a preferential prey for seabirds and marine mammals (Bradstreet and Cross 1982; Finley and Gibb 1982; Welch et al. 1992). As a key species of the Arctic system, the polar cod is believed to account for up to 75% of the energy transfer between zooplankton and vertebrate predators (Welch et al. 1992). Ice algae–copepods/amphipods–polar cod–top predators represents probably one of the most efficient pathways in energy flux through the Arctic food web, yet all its components are closely related with sea ice (Harter et al. 2013; Hop and Gjøsæter 2013; Scott et al. 1999). Changes in composition, abundance, size and energy content of ice-associated communities will influence the energy flux through the Arctic marine ecosystem and, hence, the growth and survival of top predators (Laidre and Heide-Jørgensen 2005; Mehlum and Gabrielsen 1993). Therefore, an accurate quantification of ice-associated fauna on large spatial scales is crucial to understand the functioning of Arctic sea-ice-dependent ecosystems and their future fate. The sea-ice-covered Arctic Ocean, however, is difficult to access. In particular, sampling under the sea ice is challenging. Most commonly, ice-associated macrofauna have been sampled by divers (Arndt and Pavlova 2005; Hop et al. 2011). This method is excellent in describing the small-scale structure of ice habitats during sampling, yet the spatial variability of the organism distributions may not be covered representatively. Ice floes which appear biologically poor are not sampled due to limited time at ice stations, while it is impossible to obtain all organisms from ice floes with rich fauna (Hop and Pavlova 2008). A new sampling gear used in the Southern Ocean for the first time, the Surface and Under Ice Trawl (SUIT) (van Franeker et al. 2009), overcomes the spatial limitation of observations by divers (Flores et al. 2012). SUIT enables large-scale horizontal sampling of the 0–2 m surface layer both under sea ice and in open water.

The aim of the present study is to describe the association of macrofaunal communities in the surface layer (0–2 m) under ice and in open water, with habitat properties of the sea ice and the underlying water column. In particular we address the following objectives:

(1) We identify key environmental variables of sea ice and water column that structure under-ice habitats.
(2) We provide a basin-wide inventory of under-ice fauna in the Eurasian central Arctic Ocean and to highlight key species defining the under-ice communities.
(3) We investigate the role of under-ice habitat properties in structuring the under-ice community.

MATERIALS AND METHODS

Study area and sampling technique

Sampling was performed during RV *Polarstern* expedition ARK XXVII/3, between 2 August to 29 September 2012, across the ice-covered Eurasian part of the Arctic Ocean deep-sea basin, from 82° to 89°N, and 30° to 130°E (Fig. 1). Thirteen horizontal hauls were performed under different ice types (MYI, FYI), and in open water. Sampling was performed with an improved version of the Surface and Under Ice Trawl (SUIT) (van Franeker et al. 2009). The improved SUIT consisted of a steel frame with a 2 x 2 m opening and 2 parallel 15 m long nets attached: (1) a 7 mm half-mesh commercial shrimp net, lined with 0.3 mm mesh in the rear 3 m of the net, covered 1.5 m of the opening width and (2) a 0.3 mm mesh zooplankton net covered 0.5 m of the opening width. Floats attached to the top of the frame kept the net at the surface or the sea-ice underside. To enable sampling under undisturbed ice, an asymmetric bridle forces the net to tow off at an angle of approximately 60° to starboard of the ship's track, at a cable length of 150 m. A detailed description of the SUIT sampling performance is provided as supplementary material by Flores et al. (2012). Depending on the ice conditions, SUIT haul durations varied between 3 and 38 min, with a mean of 24 min.

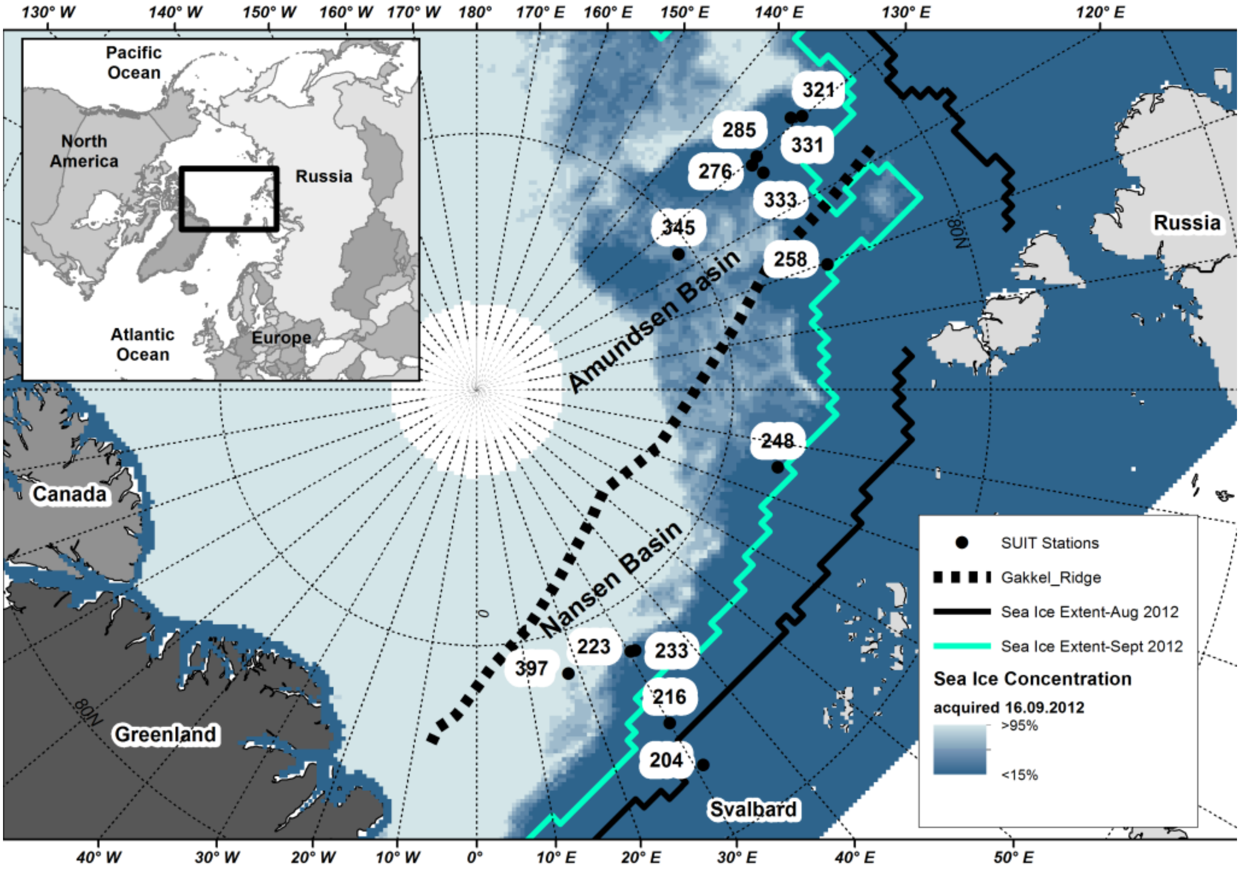

Figure 1. SUIT (Surface and Under Ice Trawl) station map during RV 'Polarstern' expedition IceARC (ARK XXVII/3). Sea-ice concentration on 16 September 2012 (data acquired from Bremen University; www.iup.uni-bremen.de:8084/amsr/) and mean sea-ice extent for August and September 2012 are represented on the map (data acquired from NSIDC Fetterer et al. 2002, updated daily). Number codes next to sampling locations indicate station numbers

Environmental data

A sensor array was mounted in the SUIT frame, consisting of an Acoustic Doppler Current Profiler (ADCP), a Conductivity Temperature Depth probe (CTD) with built-in fluorometer, an altimeter, 2 spectral radiometers, and a video camera. Water inflow speed was estimated using a Nortek Aquadopp® ADCP. Three acoustic beams operating at a frequency of 2 MHZ allowed constructing 3-dimensional profiles of the currents in the net opening. The ADCP measured the current velocity at 3 locations across the SUIT opening. The ADCP was also equipped with sensors for pressure, pitch, role, and heading. These data were used to reconstruct the position of the SUIT in the water during each haul as an indicator of the catch performance. Temperature and salinity profiles were obtained with a Sea and Sun CTD75M probe. The Practical Salinity Scale (PSS-78) was used for salinity values (Fofonoff 1985). A built-in Turner Cyclops fluorometer was used to estimate under-ice chlorophyll concentration. Calibration of fluorometric chlorophyll *a* concentrations was done from water samples obtained during stationary sea ice work. The calibration coefficients were derived from the linear relationship between chlorophyll *a* concentrations of water samples (measured with High Pressure Liquid Chromatography) with fluorometric chlorophyll *a* concentrations of the corresponding 1 m depth range ($n = 2484$; adj. $r^2 = 0.63$; $p < 0.001$). Data gaps in the CTD measurements caused by low battery voltage were filled using complementary datasets from the ADCP data (pressure) and the shipboard sensors (temperature and salinity), using correction factors determined by linear regression. An altimeter Tritech PA500/6-E connected to the CTD probe measured the distance between the net and the sea-ice underside. Sea-ice draft was calculated as the difference between the depth of the net relative to the water level, measured by the CTD pressure sensor, and the distance to the sea-ice underside, measured by the altimeter, and corrected for pitch and roll angles. Draft was then converted into ice thickness by using a sea ice density value of 834 kg m^{-3}, determined from sea-ice core samples.

During each haul, changes in ship speed, ice concentration (%) and irregularities were estimated visually by an observer on deck. GPS waypoints were recorded by the observer when the SUIT was deployed and hauled in, when it behaved abnormally, or when the environment changed, e.g. when the SUIT entered or exited the sea ice. The distance sampled over ground was estimated by multiplying the amount of time the SUIT was in the water (s) with the average speed in water (m s^{-1}). The distance sampled under ice was estimated in an analogue way for the period during which the SUIT was under ice. The distance sampled under ice was then expressed as percentage ice coverage of the total distance sampled over ground.

Gridded daily sea-ice concentrations for the Arctic Ocean derived from SSMIS satellite data using the algorithm specified by Spreen et al. (2008), were downloaded from the sea-ice portal of the University of Bremen (www.meereisportal.de).

A CTD probe with a carousel water sampler was used to collect environmental parameters from the water column near SUIT stations. The CTD (Seabird SBE9+) was equipped with a seafloor altimeter (Benthos), a fluorometer (Wetlabs FLRTD), a dissolved oxygen sensor (SBE 43) and a transmissiometer (Wetlabs C-Star). Details of the CTD sampling procedure were provided in Boetius et al. (2013). Data are available online in the PANGEA database (Rabe et al. 2012). Among all CTD stations, the closest in time and space to the SUIT stations were chosen (Table 1). Nutrients were analysed in an air-conditioned laboratory container with a continuous flow auto analyser (Technicon TRAACS 800) following the procedure described in Boetius et al. (2013). Measurements were made simultaneously on 4 channels: PO_4, Si, NO_2 + NO_3 together and NO_2 separately.

The depth of the upper mixed-layer was calculated from the ship CTD profiles after Shaw et al. (2009), who define the depth of the mixed layer as the depth of the profile where the density difference to the surface exceeds 20% of the density difference between 100 m and the surface.

The relative light intensity was calculated by dividing the solar elevation angle during the SUIT haul by the solar elevation angle at solar maximum for the corresponding location. Solar elevation angles were calculated using the National Oceanic and Atmospheric Administration's (NOAA) online solar calculator with latitude, longitude, date and time as inputs (www.esrl.noaa.gov/gmd/grad/solcalc/).

Table 1. Station table of Surface and Under Ice Trawls (SUITs) and the corresponding conductivity-temperature-depth (CTD) stations; NB is Nansen Basin and AB is Amundsen Basin

		SUIT					CTD			
Haul	Basin	Station code	Station date (mo/d/yr)	Latitude (°N)	Longitude (°E)	Bottom depth [m]	Station code	Station date	Latitude (°N)	Longitude (°E)
1	NB	204	8/5/2012	81.45	31.10	423	208	8/6/2012	81.46	31.04
2	NB	216	8/7/2012	82.48	30.03	3610	215	8/7/2012	82.49	30.00
3	NB	223	8/9/2012	84.07	30.43	4016	227	8/9/2012	84.02	31.22
4	NB	233	8/11/201	84.04	31.30	4011	227	8/9/2012	84.02	31.22
5	NB	248	8/16/201	83.93	75.50	3424	242	8/16/2012	83.90	76.07
6	NB	258	8/20/201	82.74	109.63	3575	254	8/20/2012	82.69	109.12
7	AB	276	8/25/201	83.07	129.12	4188	281	8/26/2012	82.89	129.82
8	AB	285	8/26/201	82.89	129.78	4174	281	8/26/2012	82.89	129.82
9	AB	321	9/4/2012	81.71	130.03	4011	324	9/4/2012	81.92	131.12
10	AB	331	9/5/2012	81.90	130.86	4036	324	9/4/2012	81.92	131.12
11	AB	333	9/6/2012	82.99	127.10	4187	333	9/6/2012	83.00	127.18
12	AB	345	9/9/2012	85.25	123.84	4354	342	9/9/2012	85.16	123.35
13	NB	397	9/29/201	84.17	17.92	4028	387	9/28/2012	84.37	17.52

Biological data

The catch was partially sorted on board. Polar cod and ctenophores were immediately extracted from samples. The remaining samples from the shrimp and the zooplankton nets were then each equally divided into 2 parts with a plankton splitter (Motoda 1959). From each sample, part of the material was immediately preserved in 4% formaldehyde/seawater solution for quantitative analysis. After the cruise, the quantitative samples were analysed for species composition and density at the Alfred Wegener Institute in Bremerhaven, Germany. Macrofauna (> 0.5 cm) densities were derived from the analysis of the shrimp net samples. Copepod densities were derived from analysis of the zooplankton net samples. With few exceptions, all animals were identified to the species level and, in copepod species, to developmental stage and sex. The adult copepods and their larger juvenile stages (the copepodites CV and CIV) were both considered in density calculations. Densities were calculated dividing the total number of animals per haul by the trawled area. The trawled area was calculated by multiplying the distance sampled in water, estimated from ADCP data (Flores et al. 2011), with the net width (0.5 m for the zooplankton net and 1.5 m for the shrimp net).

Data analysis

Scatter plots between each possible combination of 2 environmental variables were used to identify pairs of datasets with high colinearity (Zuur et al. 2007). In pairs with Spearman's rank correlation coefficients >0.7, only one variable was chosen for subsequent analysis based on the ecological relevance to the scientific objectives of this study and the comparability with other studies. From a total of 30 variables analysed, 12 were retained for further statistical analysis (Table 2). A Principal Component Analysis (PCA) (Mardia et al. 1979) was applied on the environmental dataset to reveal patterns in habitat typologies according to properties of the sea ice and the underlying water column.

In order to investigate patterns of diversity over the sampling area, 3 diversity indices were calculated for the whole biological dataset, as well as for sub-groupings derived from environmental data analysis: (1) species richness (the number of species observed at each station) (S); (2) the Shannon index (H) (Shannon 1948); and (3) Pielou's evenness index (J). Species accumulation curves were plotted to assess the impact of sampling effort on species diversity. To assess the statistical difference between sub-groupings, the Mann-Whitney-Wilcoxon test was performed on diversity indices and on cumulated species densities at stations (Mann and Whitney 1947).

Species density data were analysed using Non Metric Multidimensional Scaling (NMDS) (Kruskal 1964) based on a Bray-Curtis similarity matrix (Bray and Curtis 1957). NMDS is commonly regarded as the most robust unconstrained ordination method in community ecology (Minchin 1987). Square-root transformations and Wisconsin double standardization were applied to the data to gradually down-weight the dominant taxa. The performance of the NMDS was assessed with Shepard plots and stress values (Clarke and Warwick 2001; Legendre and Legendre 2012). ANOSIM (Clarke & Ainsworth 1993) was used to test for significant differences in the community structure between *a priori* defined groupings, e.g. ocean basins and sea-ice regimes.

Table 2. Environmental variables characterising sea-ice habitats

Variable (abbreviation)	Unit	Value range
Sampled ice coverage during SUIT hauls (Coverage)	%	0 to 100
Modal ice thickness (Thickness)	m	0 to 1.25
Standard deviation of ice thickness (SD)	m	0 to 0.88
Surface-water temperature (Temperature)	°C	-1.76 to -1.06
Surface-water salinity (Salinity)		29.38 to 32.87
Chlorophyll *a* concentration at the surface (Chla-surface)	mg m^{-3}	0.06 to 0.24
Chlorophyll *a* concentration at the depth of the chlorophyll *a* maximum (Chla)	mg m^{-3}	0.15 to 0.63
Silicate concentration at the depth of the chlorophyll *a* maximum (Si)	µmol l^{-1}	1.17 to 4.80
Combined nitrate + nitrite concentration at the depth of the chlorophyll *a* maximum	µmol l^{-1}	0.12 to 6.84
Phosphate concentration at the depth of the chlorophyll *a* maximum (PO_4)	µmol l^{-1}	0.20 to 0.55
Relative daylight intensity (Relative light)	-	0 to 0.91
Mixed layer depth (MLD)	m	9 to 25

The association of the community structure with the physical environment was evaluated with a Mantel test (Mantel 1967). The Mantel test relates 2 distance matrices, one from the biological and one from the environmental dataset, using Pearson correlation (Smouse et al. 1986). The bootstrapping procedure was applied with 999 iterations. Afterwards, the association of the community structure with all possible combinations of environmental variables was evaluated with the BioEnv analysis (Clarke and Ainsworth 1993). The BioEnv analysis estimates the subset of environmental variables that has the highest correlation with the biological data. The best subset was found using the Spearman's rank correlation coefficient between a Bray-Curtis similarity matrix of the species density data and a Euclidean dissimilarity matrix of the environmental variables.

For all analyses, R software Version 3.1.2 was used with the libraries vegan, FactoMineR, plyr and MASS (R Core Team 2015).

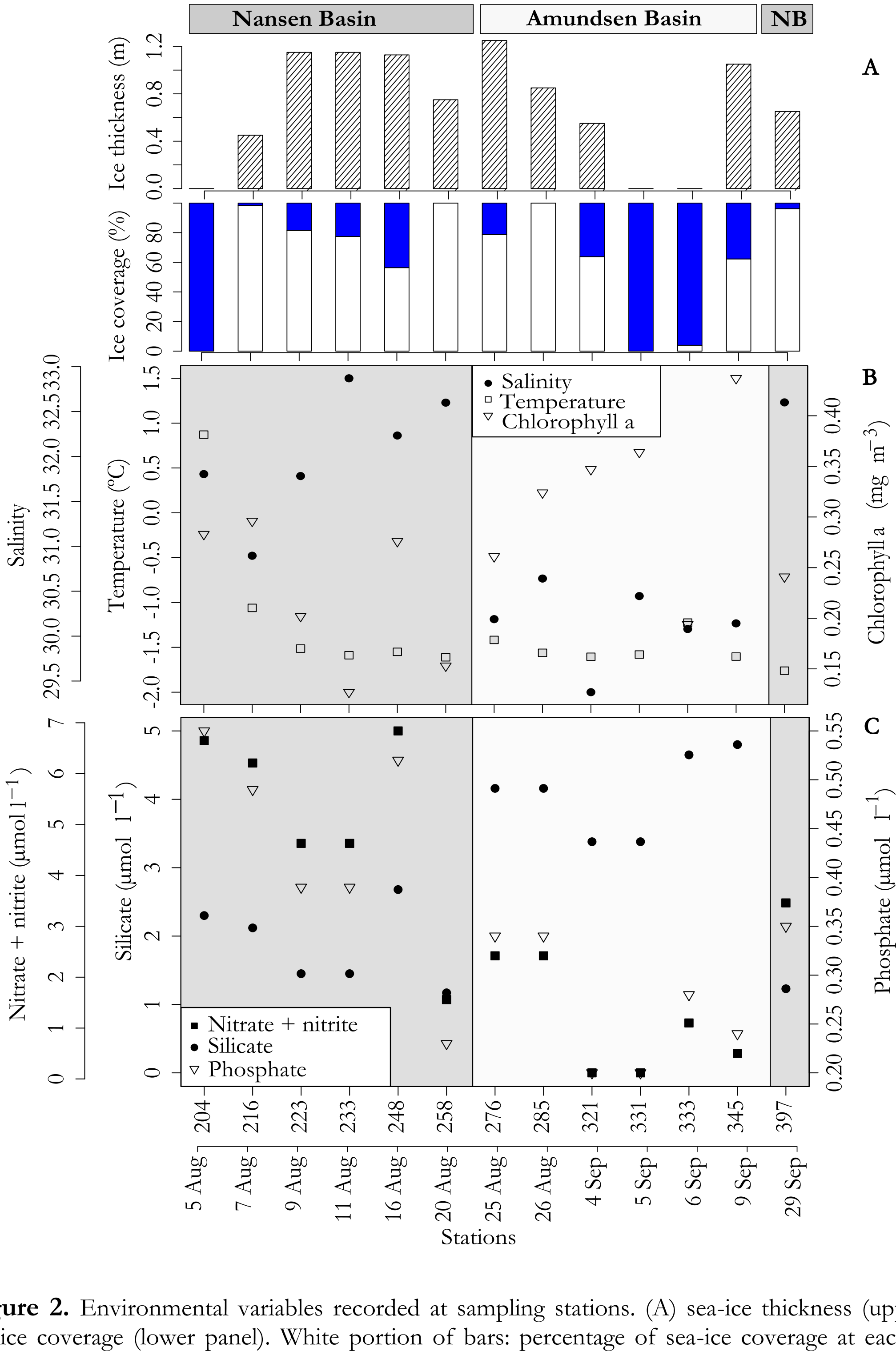

Figure 2. Environmental variables recorded at sampling stations. (A) sea-ice thickness (upper panel) and sea-ice coverage (lower panel). White portion of bars: percentage of sea-ice coverage at each station; grey portion of bars: remaining percentage of open water at each station. (B) Temperature, salinity and chlorophyll a concentration in the 0–2 m surface layer. (C) Nutrient concentrations at the depth of the chlorophyll *a* maximum. Nansen Basin stations are shown on dark grey background and Amundsen Basin stations on light grey background

RESULTS

Environmental conditions

Across the Eurasian Basin 13 stations were sampled. Seven stations were located in the Nansen Basin, and 6 stations in the Amundsen Basin. Six of the Nansen Basin stations were sampled during the first half of August, and the Amundsen Basin stations during late August to mid-September.

The last station was sampled in the Nansen Basin on 29 September 2012 at the onset of winter (Table 1). All stations had water depths > 3400 m, except Stn 204 in the Nansen Basin, which was located in open waters over the continental slope at a depth of 423 m. Because oceanographic conditions at the slope station differed markedly from those in the rest of the sampling area, it was not included in the multivariate analysis, but is discussed separately. Besides Stn 204 in the Nansen Basin, 2 of the Amundsen Basin stations were nearly ice-free. At all other stations sea ice was present, ice concentrations ranging from 56 to 100% (Fig. 2A). Modal ice thickness ranged from 0.45 to 1.25 m. Within the deep-sea basins, surface temperatures ranged between –1.8 and –1°C. The surface temperature at the slope station 204 was 0.8°C (Fig. 2A).

In the PCA of physical variables, 63.6% of the variance in the dataset was explained on the first 2 axes (Fig. 3). The first axis explained 36.6% of the variance and was mainly driven by gradients of nutrients, salinity and sea-ice properties. Along this axis a clear distinction was evident between 2 environmental clusters that corresponded to the stations situated in the Nansen Basin and the Amundsen Basin, respectively.

Because the environmental gradients in our dataset represent not only spatial patterns, but also an often inseparable temporal signal over the 2 month sampling period, the clusters are referred to as spatio-temporal ‘regimes’, roughly corresponding to the 2 ocean basins. Sea-ice concentration and thickness gradients increased towards the Nansen Basin regime. The 2 open-water stations in the Amundsen Basin were clearly distinguished from all other stations, and were associated with the lowest sea-ice concentration and thickness values. Furthermore, the Nansen Basin regime was associated with high values of salinity and nitrate + nitrite, and low values of silicate and chlorophyll *a* concentrations in the 0–2 m surface layer. Conversely, the Amundsen Basin regime was associated with high chlorophyll *a* concentrations, high silicate concentrations, and low values of salinity and nitrate + nitrite. The second axis explained 26.94% of the variance and was mainly associated with gradients of temperature, chlorophyll *a* concentration at the chlorophyll maximum depth and relative light intensity. Along this axis, 2 stations were distinguished from the Nansen Basin regime cluster. Stn 216 had 100% ice coverage, high surface water temperatures and high chlorophyll *a* concentrations at the chlorophyll maximum depth (Fig. 2). Stn 397 had the lowest surface-water temperatures and lowest relative light intensity. The open-water station (Stn 333) was distinguished along the second axis from the cluster of the Amundsen Basin regime by high surface-water temperatures and high chlorophyll *a* concentrations at the chlorophyll maximum depth.

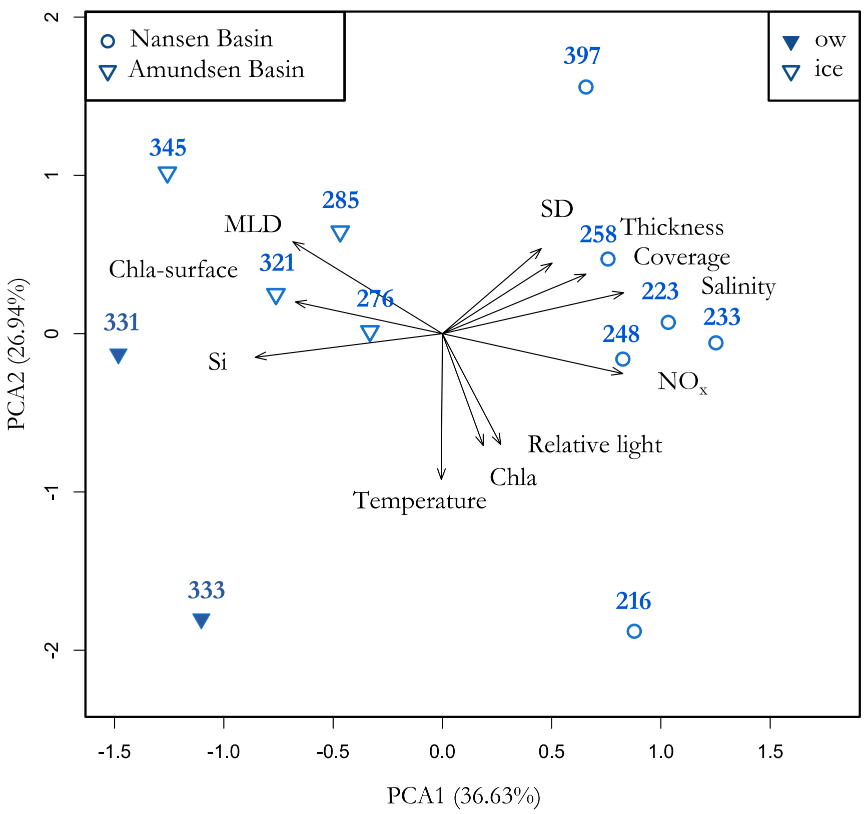

Figure 3. Principal Component Analysis of environmental variables at the sampling stations. Variable labels as defined in Table 2. Nansen Basin stations are represented by circles; Amundsen Basin stations are represented by triangles; ice: under-ice stations; ow: open-water stations. Percentage values on the axes represent the explained variance on the first (PCA 1) and second (PCA 2) dimensions.

When single environmental parameters were compared between the 2 regimes, surface salinity was significantly higher in the Nansen Basin regime (30–33) than in the Amundsen Basin regime (29–31) (Wilcoxon test: W = 0, *p*-value < 0.01) (Fig. 2B). The mixed layer depth (MLD) was shallowest at the first ice station (Stn 216; 9 m), which was situated at the ice edge. At the beginning of the cruise in the Nansen Basin regime, the MLD was around 15 m deep and increased with time, reaching up to 30 m in the Amundsen Basin regime. At the last station sampled in the Nansen Basin regime (Stn 397), the MLD was again shallower. High average values of nitrate + nitrite (4.8 µmol l^{-1}), and phosphate (0.4 µmol l^{-1}), and low values of silicate (1.7 µmol l^{-1}) characterised surface waters of the Nansen Basin regime (Fig. 2C). The opposite conditions were encountered in the Amundsen Basin regime, with low values of nitrate + nitrite (1.4 µmol l^{-1}), and phosphate (0.2 µmol l^{-1}), and high values of silicate (3.5 µmol l^{-1}). The differences between the 2 regimes in nutrient concentration were statistically significant (Wilcoxon test NO_x: W = 2, *p*-value < 0.01; PO_4: *W* = 4, *p*-value < 0.05; Si: *W* = 36, *p*-value < 0.01). At the station positioned over the Gakkel Ridge (Stn 258), all nutrients had very low concentrations. In the 2 open-water stations in the Amundsen Basin regime (Stns 331 and 333), nitrate + nitrite and phosphate were depleted in the surface waters. The averaged surface chlorophyll *a* concentration over the entire sampling area was 0.27 mg m^{-3}, ranging between 0.12 and 0.43 mg m^{-3}. The surface chlorophyll *a* concentrations were slightly higher in the Amundsen Basin regime than in the Nansen Basin regime (Wilcoxon test: *W*=30, *p*-value < 0.1). The highest value was found at Stn 345 in the Amundsen Basin regime (Fig. 2B).

Taxonomic composition

In total, 28 species belonging to 10 phyla were identified in our samples (Table 3). Copepods had the highest densities, accounting for 69% of the mean relative density over all stations, followed by amphipods with 28% (Fig. 4). The balance between copepods and amphipods, however, was markedly different between the 2 environmental regimes: in the Nansen Basin regime, copepods accounted for >82% of the mean density, whereas, in the Amundsen Basin regime, copepods contributed only 53%. Here the amphipods co-dominated the species composition, accounting for 43% of the mean density (Fig. 4). Appendicularians contributed 1.3% to the overall density, but this value was driven by extremely high densities at only 2 stations. Ctenophores had a high frequency of occurrence over the entire sampling area, but with highly variable densities. At 2 stations ctenophores heavily dominated the biomass of the samples. The other taxonomic groups accounted for <1% of the density.

Table 3. List of species with mean densities and frequency of occurrence over the sampling area; SD: standard deviation

Taxon	Mean density (ind. 100 m^{-2})	SD	Range	Frequency of occurrence
CTENOPHORA				
Beroe spp. Fabricius, 1780	2.11	4.75	0 – 15.79	0.85
Mertensia ovum Fabricius, 1780	0.19	0.38	0 – 1.35	0.85
MOLLUSCA				
Clione limacina Phipps, 1774	0.69	0.87	0 – 2.76	0.69
Limacina helicina Phipps, 1774	1.13	2.89	0 – 10.64	0.62
ANNELIDA				
Unidentified polychaete	<0.01	0.02		0.23
ARTHROPODA				
Apherusa glacialis Hansen, 1888	58.19	70.48	0.33 – 221.84	1.00
Eusirus holmi Hansen, 1887	0.19	0.22	0 – 0.62	0.69
Gammaracanthus loricatus Sabine, 1821	<0.01	0.01	0 – 0.04	0.15
Gammarus wilkitzkii Birula, 1897	0.10	0.18	0 – 0.71	0.92
Onisimus glacialis Sars, 1900	1.12	1.34	0 – 3.97	0.85
Onisimus nanseni Sars, 1900	0.35	0.57	0 – 1.66	0.46
Themisto abyssorum Boeck, 1871	0.75	1.07	0 – 3.13	0.69
Themisto libellula Lichtenstein, 1822	20.14	25.69	0.11 – 85.36	1
Euphausiacea				
Thysanoessa inermis Kroyer, 1861	0.03	0.07	0 – 0.25	0.31
Unidentified euphausid	<0.01	0.01	0 – 0.04	0.08
Copepoda				
Calanus finmarchicus Gunnerus, 1765	52.40	187.39	0 – 676.04	0.23
Calanus glacialis Jaschnov, 1955	641.27	1078.52	3.78 – 3052.83	1
Calanus hyperboreus Kroyer, 1838	104.08	174.46	0 – 494.62	0.85
**Pseudocalanus* spp. Boeck, 1872	24.60	33.29	0 – 109.22	0.92
Metridia longa Lubbock, 1854	172.47	619.49	0 – 2234.26	0.31
Paraeuchaeta glacialis Hansen, 1886	0.08	0.17	0 – 0.44	0.23
*Unidentified harpacticoid	0.32	0.69	0 – 1.96	0.31
**Tisbe spp.*	20.13	20.26	0 – 68.26	0.92
Ostracoda				
Boroecia borealis Sars, 1866	<0.01	0.01	0 – 0.04	0.08
CHAETOGNATHA				
Eukrohnia hamata Möbius, 1875	11.01	36.3	0 – 131.76	0.69
Parasagitta elegans Verrill, 1873	0.15	0.28	0 – 1.01	0.54
CHORDATA				
Oikopleura vanhoeffeni Lohmann, 1896	47.37	145.39	0 – 526.54	0.31
VERTEBRATA				
Boreogadus saida Lepechin, 1774	0.41	0.42	0 – 1.2	0.77

*values might be underestimated due to small size of the organisms relative to the mesh size used

Variability in species diversity, density and distribution

The highest number of species (20) was encountered at Stn 285 in the Amundsen Basin regime. Three other stations, 2 situated in the Nansen Basin regime and one in the Amundsen Basin regime, had 19 species each. The lowest species richness (*S*), Shannon diversity (*H*) and evenness (*J*) were encountered at the slope Stn (204), where only 8 species were found (Table 4.). The highest Shannon and evenness indices were encountered at an open-water station (Stn 331) in the Amundsen Basin regime. Species richness and Shannon diversity showed no significant difference between the 2 environmental regimes (Wilcoxon test S: $W = 29$, p-value > 0.1; H: $W = 32$, p-value < 0.1), while species evenness (*J*) was significantly higher in the Amundsen Basin than in the Nansen Basin (Wilcoxon test: $W = 34$, p-value < 0.05).

Table 4. Diversity indices calculated at each sampling station

Station code	Richness	Shannon	Evenness
204	8	0.04	0.02
216	13	1.30	0.51
223	17	1.68	0.59
233	13	0.74	0.29
248	19	1.21	0.41
258	19	1.16	0.40
276	18	1.61	0.56
285	20	1.43	0.48
321	16	1.78	0.64
331	19	2.02	0.69
333	18	1.52	0.53
345	18	1.76	0.61
397	17	0.45	0.16
Nansen Basin	24	0.94	0.34
Amundsen Basin	24	1.69	0.58
Total	28	1.28	0.45

Cumulated densities of all species ranged from 0.3 ind. m^{-2} at Stn 216 to 69 ind. m^{-2} at Stn 248 (Fig. 5). Overall densities were significantly higher in the Nansen Basin regime than in the Amundsen Basin regime (Wilcoxon test: $W = 6$, p-value < 0.05) (Fig. 5). This difference between the 2 environmental regimes remained relevant even when Stn 248, which had the highest abundance, was excluded from statistical analysis (Wilcoxon test: $W = 6$, p-value < 0.05). The most abundant species were the copepods *Calanus hyperboreus* and *C. glacialis*. The low density exception at Stn 216 was

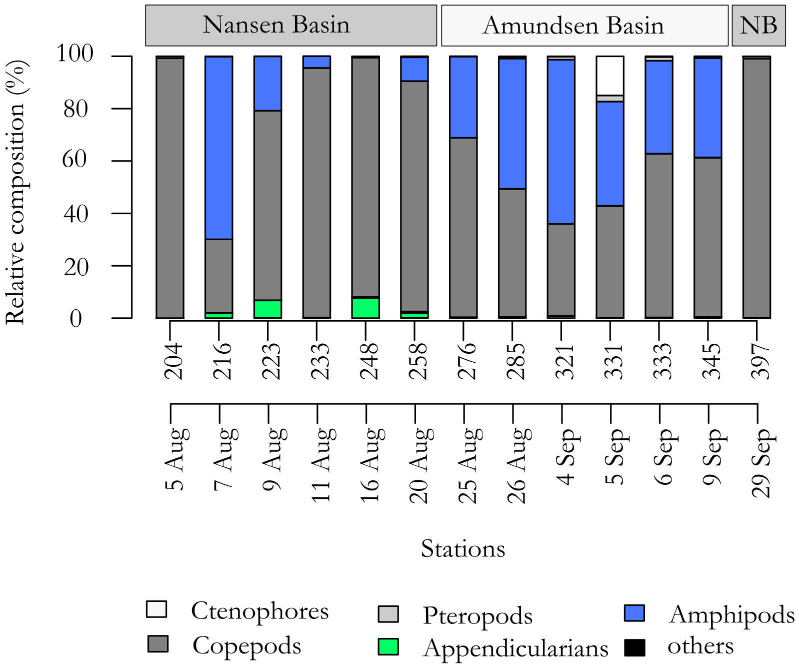

Figure 4. Relative density of taxonomic groups at the sampling stations (numbers on the x-axis). NB: Nansen Basin

caused by exceptionally low numbers of copepods. Stn 248 was unique in its species composition. Only at this station, did *C. finmarchichus* dominate numerically, and high densities of the appendicularian *Oikopleura vanhoeffeni* and the chaetognats *Eukrohnia hamata* and *Parasagitta elegans* were encountered. The biomass composition at this station was heavily dominated by ctenophores and tunicates. The last station (Stn 397) in the Nansen Basin regime differed from all other stations by a dominance of *Metridia longa* over all other copepod species. Among the amphipods, the ice-associated species *A. glacialis* was numerically dominant at all stations, except the 2 open-water stations (Stn 331 and 333) in the Amundsen Basin. Here, the amphipod *Themisto libellula* was most abundant, though also present throughout the sampling area. Polar cod was present over the survey area with few exceptions: the open water slope-station (Stn 204), a station (Stn 233) at which technical trawling problems probably affected the catch efficiency of the net for fast-swimming fish, and the early winter station (Stn 397). The density of polar cod ranged from 0.3 to 1.2 ind. 100 m^{-2}, with highest densities at Stn 285 and 345 in the Amundsen Basin regime. In contrast to nearby under-ice stations, polar cod densities at the 2 open-water stations in the Amundsen Basin (331 and 333) were close to zero.

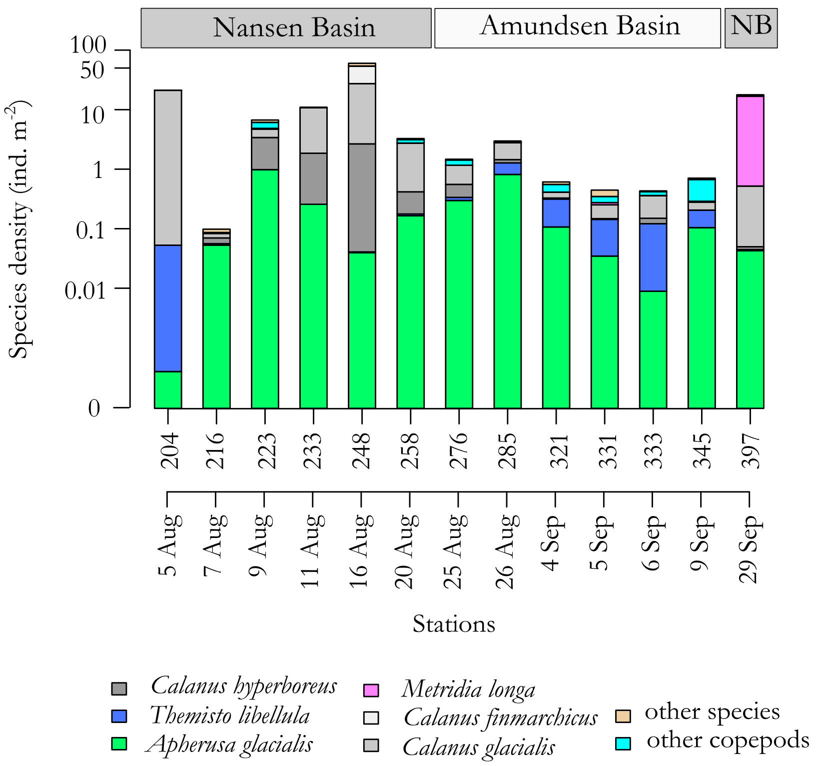

Figure 5. Species' cumulated density at the sampling stations (numbers on the x-axis). Densities are shown in log scale. Only dominant taxa are represented in the legend. NB: Nansen Basin

The association of environment and biota

The NMDS ordination of the community resembled the gradients of environmental variables of the PCA. In the NMDS ordination, stations grouped mainly according to the 2 environmental regimes of the Nansen and Amundsen Basins (ANOSIM: R = 0.38, p-value = 0.016) (Fig. 6). The copepods *C. hyperboreus* and *C. glacialis* and the amphipod *Eusirus holmii* were associated with the Nansen Basin regime. Polar cod and the amphipods *Onisimus nanseni* and *T. libellula* were associated with the Amundsen Basin regime. Stn 216 in the Nansen Basin grouped closer to the Amundsen Basin regime due to its high density of polar cod and *O. nanseni* and low copepod density. The amphipods *A. glacialis*, *G. wilkitzkii* and *Onisimus glacialis* grouped in the centre of the NMDS plot, indicating equal association with Nansen Basin regime and Amundsen Basin regime stations. The stations from the Amundsen Basin regime were more homogenous, presenting smaller distances between stations' positions in the NMDS ordination than those in the Nansen Basin regime. The 2 open-water stations, however, grouped clearly apart from the other stations in the Amundsen Basin regime. They were associated with the pelagic amphipod *T. libellula*.

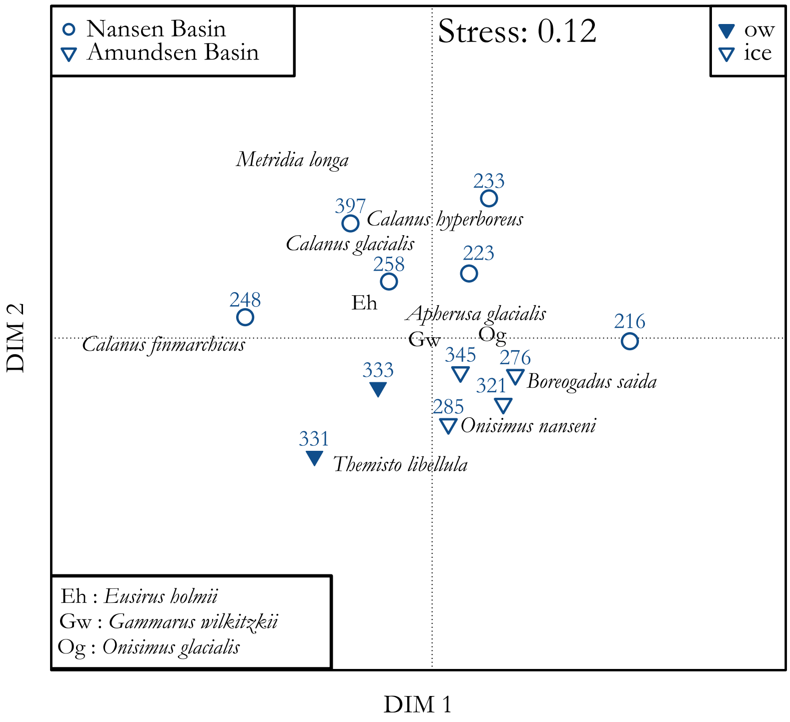

Figure 6. Non-Parametric Multi-Dimensional Scaling (NMDS) plot of the under-ice community structure. Station symbols (circles: Nansen Basin; triangles: Amundsen Basin; ow: open water; ice: under-ice) indicate the relative position of the community composition at each sampling location in the NMDS ordination. Species names indicate the relative position of polar cod and numerically dominant species in the NMDS ordination. DIM 1 & 2: NMDS dimension axes

The Mantel test and BioEnv analysis both showed a strong positive correlation between the environmental and biological datasets (Mantel test: Pearson correlation coefficient = 0.65, $p < 0.001$). In the BioEnv, nitrate + nitrite concentration in the surface layer had the highest correlation of a single environmental variable (0.60) with the variability of density-based species distribution (Table 5). The highest correlation (0.75) with the variability of density-based species distribution was achieved by a combination of nitrate + nitrite concentration, surface-water temperature and salinity, ice thickness, mixed-layer depth and surface chlorophyll *a* concentration (Table 5).

DISCUSSION

Under-ice habitat properties

During summer 2012 the Arctic Ocean experienced a historical minimum sea-ice extent (Parkinson and Comiso 2013). Polarstern cruise ARK XXVII/3 sampled in the high central Arctic during that time, first across the Nansen Basin during early August, and then across the Amundsen Basin during late August–early September, almost reaching the North Pole at 87.87°N, 59.65°E. Daily sea-ice concentration data, from passive microwave satellite measurements, were >90% in the Nansen Basin during August and approximately 70% in the Amundsen Basin during September (data source: www.meereisportal.de University of Bremen). These values were in good agreement with the range of sea-ice concentrations determined from SUIT sensors. At only one station (Stn 216) did these observations differ from the SUIT sensor-derived ice coverage of 100%, whereas satellite-derived ice coverage was 40%, averaged over 350 km^2, placing this station in the marginal ice zone. Our sampling area was mainly covered with FYI (>95%), with only small fractions of MYI (Boetius et al. 2013). In our ice-thickness profiles, modal ice thicknesses ranged from 0.45 to 1.25 m. In general, modal ice thickness was higher and more variable in the Nansen Basin regime than in the Amundsen Basin regime. Modal ice thicknesses from our SUIT hauls resembled the general pattern of airborne ice thickness measurements carried out in the survey area during ARK XXVII/3 (Lange & Hendricks pers. comm.). Electromagnetic airborne sea-ice thickness measurements confirm this range as mainly FYI (Haas et al. 2008). Therefore, our local sampling profiles largely resembled the general regional-scale situation in terms of sea ice concentration, age class and thickness.

Apart from sea-ice properties, our PCA results indicated that a variety of other environmental parameters structured our sampling stations into 2 regimes, which were broadly coherent with the 2 ocean basins sampled. These differences could in part be explained by seasonal processes, such as the melting of sea ice or the deepening of the mixed layer in the Amundsen Basin in late summer. We acknowledge the difficulty of disentangling spatial from temporal trends over our sampling area. We sampled within the pack ice, first in the Nansen Basin during early August, when a more compact sea-ice cover was present. At the end of August, while sampling in the Amundsen Basin, the pack ice began to loosen and ice was thinning, leaving locally large open-water areas, for example at Stns 331 and 333. Therefore, gradients of sea-ice properties were highly associated with the seasonal progression towards the end of summer, until the minimum sea-ice extent occurred on 16

September (Parkinson and Comiso 2013). Break-up of sea ice by early September likely allowed more light to penetrate into the water column. This favoured the increased chlorophyll *a* concentration we observed in the Amundsen Basin regime, locally depleting nutrients in the surface layer. This was demonstrated by the association of the open water stations with higher chlorophyll *a* concentrations (Fig. 2). Our last station sampled at the onset of winter in the Nansen Basin (Stn 397), however, had typical 'Nansen regime' values again, i.e. high salinity and low silicate concentrations at the depth of the chlorophyll *a* maximum (Fig. 2). This indicates that there was a strong regional component structuring the 2 regimes, besides some undoubtedly present seasonal trends.

The regional differences between the 2 regimes can largely be explained by water mass properties and circulation patterns. The Eurasian Basin is a permanently ice-covered basin with depths >4000 m. The Gakkel Ridge subdivides this basin into the nearly equally sized Nansen and Amundsen Basins. The Transpolar Drift current crosses both basins, transporting Polar Surface Water and sea ice from the Siberian shelf through the central Arctic Ocean towards the Fram Strait. A portion of the sea ice cover is recirculated within the anti-cyclonic Beaufort Gyre in the central and western Arctic Ocean, contributing to the formation of MYI (Rigor and Wallace 2004). A considerable portion of the marginal sea ice, however, is advected out of the Arctic Ocean through the Fram Strait (Kwok et al. 2004).

Nutrient-rich Atlantic Water is advected into the Eurasian Basin by 2 main branches: the Fram Strait branch and the Barents Sea branch. The Fram Strait branch of warm Atlantic Water is largely recirculated within the Nansen Basin, whereas the remaining Arctic Ocean basins, including the Amundsen Basin, are dominated by the Barents Sea branch (Rudels et al. 2013). This branch experiences water exchange by advection from the Laptev Sea continental margin, which is enriched in silicate (Bauch et al. 2014). Consequently, we found high silica and low nitrate + nitrite and phosphate concentrations in the Amundsen Basin regime, and the opposite situation in the Nansen Basin regime. Generally, Eurasian Basin regions with higher salinity indicate a higher Atlantic influence and can have surface nitrate concentrations in excess of 5 μmol l^{-1} even in summer (Codispoti et al. 2013). During our sampling, high salinities, high nitrate + nitrite, and high phosphate concentrations were present in the surface water of the Nansen Basin regime. Two stations, Stns 204 and 248, were exceptionally rich in nitrate + nitrite, with values at the chlorophyll maximum depth reaching up to 6.8 μmol l^{-1}. Stn 204 was situated on the Svalbard slope, near the inflow of Atlantic Water into the Arctic Ocean. Stn 248 was located near a convergent front formed by the Atlantic Water boundary current (Lalande et al. 2014). Nearby surface salinity and temperature profiles suggest freezing occurred prior to our arrival. The mixing due to haline convection during freezing could have added nutrients to the mixed layer from below, explaining the higher nitrate + nitrite and chlorophyll *a* concentrations.

Table 5. Combinations of environmental variables selected by BioEnv analysis. Variables were ranked according to their correlation coefficients with the biological dataset. *r*: Spearman correlation coefficient; other abbreviations see Table 2

No of variables	Environmental variables	*r*
1	NO_x	0.60
11	NO_x + Temperature + Salinity + Thickness + SD + Coverage + MLD + Chla-surface + Chla + Relative light + Si	0.67
2	NO_x + Temperature	0.69
3	NO_x + Temperature + Salinity	0.69
10	NO_x + Temperature + Salinity + Thickness + SD + MLD + Chla-surface + Chla + Relative light + Si	0.69
5	NO_x + Temperature + Salinity + Thickness + MLD	0.72
9	NO_x + Temperature + Salinity + Thickness + SD + MLD + Chla-surface + Chla + Relative light	0.72
4	NO_x + Temperature + Salinity + Thickness	0.73
6	NO_x + Temperature + Salinity + Thickness + Chla-surface + Chla	0.73
7	NO_x + Temperature + Salinity + Thickness + SD + MLD + Chla	0.75
8	NO_x + Temperature + Salinity + Thickness + SD + MLD + Chla-surface + Chla	0.75

Under-ice community composition

We identified a total of 28 species in the upper 2 m of the mostly ice-covered water column. In terms of species numbers, amphipods and copepods equally dominated the community with 8 species each (Table 3). Our overall species richness was low compared to previous, geographically more extended studies on Arctic epipelagic fauna (Auel and Hagen 2002; Kosobokova and Hirche 2000; Kosobokova et al. 2011; Kosobokova and Hopcroft 2010). Such comparisons are, however, complicated by differences in net type, mesh sizes and sampled depth interval. Most Arctic zooplankton studies integrated the epipelagic community over at least the upper 50 m. The species composition from those studies is thus much more influenced by pelagic fauna, mostly dominated by the often deeper dwelling copepods (Kosobokova and Hirche 2000). Considering ice-associated species reported from the northern Barents Sea, Svalbard, Laptev Sea, or Greenland Sea (Hop et al. 2000; Werner and Arbizu 1999; Werner and Auel 2005; Werner and Gradinger 2002), our study found the highest species richness compared to any individual study. This might be due to a larger under-ice surface area of approximately 4 km^2 sampled per station in our study. Sampling effort in previous under-ice studies was spatially limited to single ice floes and was mainly performed by divers with pumps or estimates made from video surveys (Hop et al. 2011; Hop and Pavlova 2008; Werner and Gradinger 2002). These studies described ice-associated species related to ice concentration and topography (Hop et al. 2000; Werner and Gradinger 2002). But sea-ice properties vary greatly from one ice floe to another, as does the ice-associated fauna. Using the SUIT enabled us to integrate both floes with low faunal densities and floes with high faunal densities. This approach can representatively capture the meso-scale variability of the under-ice environment and facilitate large-scale density estimates if other error sources are minimal. Such error sources may be the low efficiency of the SUIT to sample animals from crevices and wedges in the ice, or the ability of polar cod to avoid or escape the net. Reported habitat preferences and behaviour of the species sampled in this study indicate that underestimation due to preference of crevices may apply to single predatory species (e.g. *G. wilkitzkiii*), but not to those species clearly dominant in density in our and other under-ice studies, such as *A. glacialis* or *O. glacialis* (Gradinger et al. 2010; Gradinger and Bluhm 2004; Hop and Pavlova 2008). Videos from the SUIT camera show no indication of escape or avoidance of the net by polar cod, but the loss of fish through behavioural response cannot be assessed with certainty. The omnipresence of Polar cod in under-ice catches rather indicated that the sluggish lifestyle of this species (Gradinger and Bluhm 2004) may have worked in favour of sampling this species with a net that is relatively ineffective for catching fast-swimming fish.

We found higher densities of under-ice fauna in the Nansen Basin regime than in the Amundsen Basin regime. This pattern was mainly driven by high densities of large calanoid copepods. In the central Arctic Ocean, the mesozooplankton community in the surface 50 m is known to be dominated by *Calanus spp.* (Auel and Hagen 2002). The big herbivorous *C. hyperboreus* and *C. glacialis* dominated in our samples, contributing on average 9 and 38%, respectively, to the total density of the surface-layer community. *C. glacialis* largely dominated the surface community at the slope station

(Stn 204), with 99%. The Atlantic water species *C. finmarchichus* appeared in high numbers at only one station in the Nansen Basin (Stn 248). Situated near a convergence front, a freezing event prior to our arrival is believed to have caused convective mixing and entrainment of nutrients from the subsurface Atlantic Water at that station (Lalande et al. 2014). More nutrients added to the euphotic layer could have favoured increased productivity and subsequent immigration of grazers from the deeper Atlantic Water layer.

Besides the 3 *Calanus* species, *M. longa* and the smaller copepods *Pseudocalanus* spp. are important contributors to the surface community, in both the eastern (Kosobokova et al. 2011) and the western Arctic Ocean (Matsuno et al. 2012). A switch in dominance occurred at our last station, at the onset of freezing. Coincident with the migration of *Calanus spp.* into deeper layers (Darnis and Fortier 2014; Fortier et al. 2001; Hirche 1997; Madsen et al. 2001), *M. longa* largely dominated the surface community (Fig. 5). This species is known to remain active year-round (Ashjian et al. 2003), but seldom occurs above depths <25 m (Fortier et al. 2001) (Table 3). Low competition, avoidance of visual predators, and food availability at the ice underside might explain their rise to the ice-water interface at Stn 397. Also active year-around are the small copepods of the genus *Pseudocalanus* (Fortier et al. 2001). They were widespread across the 2 basins without any seasonal or regional patterns. The year-round active copepods might represent a nutritious food source for polar cod and other predatory members of the under-ice community during Arctic winter.

Six species of ice-associated amphipods were found in our study area. Our results are in agreement with numerous under-ice studies in finding that *A. glacialis* dominates the ice-amphipod community in FYI-dominated environments (Werner and Auel 2005). Where MYI and ridges are more prevalent, *G. wilkitzkii* occurs in higher abundances (Beuchel and Lønne 2002; Lønne and Gulliksen 1991). Whereas *A. glacialis* is found mainly in the water just below the ice, *G. wilkitzkii* stays mainly attached to the under-side of ice and hides in ice cracks (Hop and Pavlova 2008; Hop et al. 2000). We found only few *G. wilkitzkii* individuals at each station, but consistently over both basins. Ice thickness was highly variable, with ridges at all ice-covered stations, even though we sampled mainly under FYI. Interestingly, we found young *G. wilkitzkii* juveniles just released from the brood pouch in September, whereas the release period was previously documented to occur between April and May in the northern Barents Sea (Poltermann et al. 2000). One female of the rare ice-amphipod *Gammaracanthus loricatus* and a few *Onisimus spp.* females were also observed carrying juveniles in their pouches. Such a difference in the timing of juvenile release could be related to sea-ice seasonal dynamics and consequently food availability. Near Svalbard and in the Barents Sea, ice melting starts earlier. The spring bloom usually occurs in April, followed by high abundances of *Calanus* spp. This spring to summer succession in the food chain is regarded as an important factor for releasing the amphipods' young (Dalpadado 2002).

Swarms of the pelagic amphipod *T. libellula* have been reported to rise under landfast-ice (Gulliksen 1984). We noticed high numbers of *T. libellula* juveniles under the ice in the Amundsen Basin regime. At 2 locations, we observed a distinct change in community structure between nearby open-water and under-ice sampling locations. The difference in ice coverage was accurately mirrored by a clear dominance of the ice-associated amphipod *A. glacialis* in ice-covered waters, versus a dominance of the pelagic amphipod *T. libellula* in the surface community of ice-free waters. This pattern suggests that habitat partitioning between sympagic and pelagic species is abrupt, creating a small-scale pattern in the surface-layer community according to sea-ice conditions.

Two environmental regimes

In terms of species' presence, we found similar under-ice community compositions in the Nansen Basin and Amundsen Basin regimes. When the relative community structure was considered, however, gradual changes in community composition were ordered according to the 2 environmental regimes (Fig. 6). The Nansen regime was characterised by heavier sea ice, which can be considered as a compact, stable habitat. Both ice thickness and its standard deviation (an expression of sea-ice underside roughness) were correlated with the under-ice community structure. Around Svalbard, ice thickness was found to be the key variable impacting ice-associated faunal variability (Hop and Pavlova 2008).

Copepods (*Calanus* spp.) and the large ice-associated amphipod *E. holmii* were associated with the Nansen Basin regime (Fig. 6). In the water column, low chlorophyll *a* concentrations under a compact ice cover may indicate limited food availability due to light limitation, attracting copepods capable of under-ice grazing to the ice-water interface layer (Runge and Ingram 1991). In the more open Amundsen Basin regime, under-ice feeding was probably less important for *Calanus* spp., causing them to disperse in the water column. The Amundsen Basin was sampled 2 weeks after the Nansen Basin and was characterised by autumn conditions with loose sea-ice coverage, indicating a decaying sea-ice habitat with low nutrient concentrations but with higher chlorophyll *a* concentrations in the water column. Under-ice faunal densities in the Amundsen Basin regime were lower, but had higher diversity than in the Nansen Basin regime (Table 4). The density of adult copepods in the surface layer was considerably lower than in the Nansen Basin regime. There were, however, high numbers of *Calanus* spp., stages CI to CIII, present. These stages were not included in our density calculations, because the numbers caught did not represent true abundances due to our 0.3 mm mesh zooplankton net. These findings agree with the general patterns of seasonal vertical migration of *Calanus* spp. (Darnis and Fortier 2014). Migration of *Calanus* spp. starts in August in the Amundsen Gulf (Beauford Sea) (Darnis and Fortier 2014) and Fram Strait (Auel et al. 2003). At the end of summer, most copepods and their smaller stages have stored lipids, accounting for up to 50% of their body weight (Scott et al. 1999), to prepare for diapause (Auel et al. 2003). Only the juvenile stages CI to CIII of C. hyperboreus were noted to remain in the surface layer (Darnis and Fortier 2014). The progressive reduction of copepod numbers in our samples suggests that emigration from the surface layer might have gradually started at the end of August. With the decreased copepod density in the Amundsen Basin regime, the amphipods numerically co-dominated the under-ice community. Particularly, the carnivorous amphipod *T. libellula* was more abundant in the Amundsen Basin regime than in the Nansen Basin regime (Fig. 5). As a preferred prey of *T. libellula* (Auel et al. 2002; Noyon et al. 2009), the small copepodites could have attracted *T. libellula* to the surface layer. Overall, the Amundsen Basin regime appeared to support more carnivorous fauna, with a higher proportion of larger animals, such as *T. libellula, O. nanseni,* and polar cod. Higher sinking fluxes of detritus in the Amundsen Basin caused by melting sea ice (Lalande et al. 2014) indicate that additional food became available in the ice-water interface layer for opportunistic feeders, such as the amphipods *O. glacialis*, *O. nanseni* and *G. wilkitzkii* (Werner 1997).

A high degree of heterotrophy in the food web is supported for the entire Eurasian Basin by a tentative comparison of primary production versus food demand of the dominant grazers during our sampling period. In ice-covered waters of the Eurasian Basin, the integrated (median) primary production rate measured at the time of our sampling was 0.7 mg C m^{-2} d^{-1} in sea ice, and 18 mg C m^{-2} d^{-1} in the water column (Fernández-Méndez 2014). Experimentally derived mean ingestion rates range between 2.8 and 8.4 µg C $ind.^{-1}$ d^{-1} for *C. hyperboreus*, and between 6.0 and 18.0 µg C $ind.^{-1}$ d^{-1} for *C. glacialis* (Olli et al. 2007). For the herbivorous amphipod *A. glacialis*, the mean ingestion rate is about 13 µg C $ind.^{-1}$ d^{-1} (Werner 1997). Based on the mean densities of these species found in the ice-water interface layer (Table 3), their cumulative mean carbon demand ranged from about 0.1 to 0.2 mg C m^{-2} d^{-1}. Only a fraction of the carbon produced by ice algae, however, is available for grazers at the ice underside. This implies that the production of ice algae could have barely matched the food demand of under-ice grazers during the sampling period. Locally, however, they may have benefited from feeding on biomass-rich algal aggregates floating under the sea ice (Fernández-Méndez et al. 2014). In the water column, 0-200 m integrated densities of *C. hyperboreus* and *C. glacialis* derived from multinet sampling during the same cruise (B. Niehoff & J. Ehrlich unpubl. data) imply a mean carbon demand range of 9.5 to 28.4 mg C m^{-2} d^{-1} based on copepod ingestion rates according to Olli et al. (2007). In sea ice and the water column combined, a nearly 1:1 ratio of primary production versus grazer food demand could have contributed significantly to the low overall chlorophyll *a* concentrations in sea ice and water during our sampling period. It further indicates that peak production levels generating zooplankton growth had passed at most sampling locations before our sampling. This scenario agrees well with the mass export of algal biomass to the sea floor observed by Boetius et al. (2013) at several ice-sampling stations during our cruise, suggesting a major production peak in the investigation area prior to our sampling. At the time of sampling, the increased populations of zooplankton and under-ice fauna resulting from this bloom relied more on heterotrophic carbon sources than on autotrophic production.

CONCLUSIONS

This first large-scale survey of under-ice fauna in the Arctic deep-sea shows that a variety of species, including amphipods and polar cod, are present virtually everywhere in the Eurasian Basin, in spite of its presumed low productivity. Although under-ice faunal densities were relatively low compared to sea-ice habitats on the shelf, the omnipresence of animals in the vast deep-sea basins highlights the large-scale importance of the under-ice habitat in the Arctic Ocean.

Differences in sea-ice properties and nutrient concentrations were the key factors separating the sampled environments into the Nansen and Amundsen Basin regimes. The separation of these 2 regimes had both a seasonal and a strong regional component related to water-mass distribution, ice drift and current patterns. The under-ice community structure followed this environmental gradient, indicating a decisive role of both sea-ice and water-column characteristics for the distribution of species in the surface layer. Abrupt changes in the dominance of ice-associated amphipods at ice-covered stations versus pelagic amphipods at nearby ice-free stations emphasised a distinct influence of sea ice on small-scale patterns in the surface-layer community.

With respect to the decades of sea-ice decline before 2012, it is likely that the situation encountered in our study reflected a snapshot of a system in transition. Whether the past central Arctic under-ice community was more or less abundant, or differed in diversity and composition, is impossible to assess in the absence of appropriate baseline data. In the future, the central Arctic under-ice community will be exposed to continuing changes, including a further shortening of the ice-covered season, the complete disappearance of multi-year ice and changes in stratification and nutrient regimes. Due to their position around the North Pole, the central Arctic basins may constitute a critical refuge for the specifically ice-adapted biota of the Arctic Ocean for several decades. Whether or not the central Arctic Ocean can fulfil this function will depend on the many direct and indirect changes affecting the Arctic pack-ice and the resilience of individual ice-associated species. The subtle response of the under-ice community to many of these changing parameters suggests that changes already have impacted Arctic under-ice communities and will continue to do so in the future. Monitoring the course of changes in Arctic biodiversity and ecosystem structure will be key requirements for successful resource and conservation management in an Arctic Ocean in transition.

Acknowledgements

We thank Captain Uwe Pahl and the crew of RV Polarstern expedition IceArc (ARK XXVII-3) for their excellent support with work at sea. We thank Jan Andries van Franeker (IMARES) for kindly providing the Surface and Under Ice Trawl (SUIT) and Michiel van Dorssen for technical support with work at sea. We thank Karel Bakker for kindly providing the nutrient data. We thank Ilka Peeken for chlorophyll *a* measurements used for the calibration of under-ice fluorescence data. SUIT was developed by IMARES with support from the Netherlands Ministry of EZ (project WOT-04-009-036) and the Netherlands Polar Program (project ALW 866.13.009). This study is part of the Helmholtz Association Young Investigators Group *Iceflux*: Ice-ecosystem carbon flux in polar oceans (VH-NG-800). We thank the three anonymous reviewers for their helpful suggestions and comments that contributed significantly to the improvement of the manuscript.

References

Arctic Climate Impact Assessment, ACIA (2004) Impacts of a Warming Arctic. Cambridge University Press, Cambridge, UK

Arndt CE, Pavlova O (2005) Origin and fate of ice fauna in the Fram Strait and Svalbard area. Mar Ecol Progr Ser 301:55-66. doi:10.3354/meps301055

Arrigo KR, van Dijken G, Pabi S (2008) Impact of a shrinking Arctic ice cover on marine primary production. Geophys Res Lett 35. doi:10.1029/2008GL035028

Arrigo KR, van Dijken GL (2011) Secular trends in Arctic Ocean net primary production. J Geophys Res-Oceans 116. doi:10.1029/2011JC007151

Ashjian CJ, Campbell RG, Welch HE, Butler M, Van Keuren D (2003) Annual cycle in abundance, distribution, and size in relation to hydrography of important copepod species in the western Arctic Ocean. Deep-Sea Res Pt I 50:1235-1261. doi:10.1016/S0967-0637(03)00129-8

Auel H, Hagen W (2002) Mesozooplankton community structure, abundance and biomass in the central Arctic Ocean. Mar Biol 140:1013-1021. doi:10.1007/s00227-001-0775-4

Auel H, Harjes M, da Rocha R, Stübing D, Hagen W (2002) Lipid biomarkers indicate different ecological niches and trophic relationships of the Arctic hyperiid amphipods *Themisto abyssorum* and *T. libellula*. Polar Biol 25:374-383. doi:10.1007/s00300-001-0354-7

Auel H, Klages M, Werner I (2003) Respiration and lipid content of the Arctic copepod *Calanus hyperboreus* overwintering 1 m above the seafloor at 2,300 m water depth in the Fram Strait. Mar Biol 143:275-282. doi:10.1007/s00227-003-1061-4

Bauch D, Torres-Valdes S, Polyakov I, Novikhin A, Dmitrenko I, McKay J, Mix A (2014) Halocline water modification and along slope advection at the Laptev Sea continental margin. Ocean Science 10:141-154

Benoit D, Simard Y, Gagné J, Geoffroy M, Fortier L (2010) From polar night to midnight sun: photoperiod, seal predation, and the diel vertical migrations of polar cod (*Boreogadus saida*) under landfast ice in the Arctic Ocean. Polar Biol 33:1505-1520. doi:10.1007/s00300-010-0840-x

Beuchel F, Lønne OJ (2002) Population dynamics of the sympagic amphipods *Gammarus wilkitzkii* and *Apherusa glacialis* in sea ice north of Svalbard. Polar Biol 25:241-250. doi:10.1007/s00300-001-0329-8

Boetius A et al. (2013) Export of Algal Biomass from the Melting Arctic Sea Ice. Science 339:1430-1432. doi:10.1126/science.1231346

Bradstreet MSW, Cross WE (1982) Trophic Relationships At High Arctic Ice Edges. Arctic 35:1-12

Bray JR, Curtis JT (1957) An ordination of the upland forest communities of southern Wisconsin. Ecol Monogr 27:325-349

Budge SM, Wooller MJ, Springer AM, Iverson SJ, McRoy CP, Divoky GJ (2008) Tracing carbon flow in an arctic marine food web using fatty acid-stable isotope analysis. Oecologia 157:117-129. doi:10.1007/s00442-008-1053-7

Clarke K, Ainsworth M (1993) A method of linking multivariate community structure to environmental variables. Mar Ecol Progr Ser 92:205-205

Clarke KR, Warwick RM (2001) Change in marine communities: an approach to statistical analysis and interpretation, 2nd edition. PRIMER-E Limited, Plymouth Marine Laboratory, UK

Codispoti LA et al. (2013) Synthesis of primary production in the Arctic Ocean: III. Nitrate and phosphate based estimates of net community production. Prog Oceanogr 110:126-150. doi:10.1016/j.pocean.2012.11.006

Dalpadado P (2002) Inter-specific variations in distribution, abundance and possible life-cycle patterns of *Themisto spp.* (Amphipoda) in the Barents Sea. Polar Biol 25:656-666. doi:DOI 10.1007/s00300-002-0390-y

Darnis G, Fortier L (2014) Temperature, food and the seasonal vertical migration of key arctic copepods in the thermally stratified Amundsen Gulf (Beaufort Sea, Arctic Ocean). J Plankton Res 36:1092-1108. doi:10.1093/plankt/fbu035

Falk-Petersen S, Mayzaud P, Kattner G, Sargent J (2009) Lipids and life strategy of Arctic Calanus. Mar Biol Res 5:18-39. doi:10.1080/17451000802512267

Fernández-Méndez M (2014) Primary productivity in Arctic sea ice and ocean. PhD dissertation. University of Bremen, Bremen, Germany

Fernández-Méndez M, Wenzhöfer F, Peeken I, Sørensen HL, Glud RN, Boetius A (2014) Composition, Buoyancy Regulation and Fate of Ice Algal Aggregates in the Central Arctic Ocean. Plos One 9:e107452

Fetterer F, Knowles K, Meier W, Savoie M (2002, updated daily) Sea Ice Index. Monthly Mean Sea Ice Extent. Boulder, Colorado USA: National Snow and Ice Data Center. doi:10.7265/N5QJ7F7W

Finley KJ, Gibb EJ (1982) Summer diet of the narwhal (*Monodon monoceros*) in Pond Inlet, northern Baffin Island. Canadian Journal of Zoology 60:3353-3363. doi:10.1139/z82-424

Flores H et al. (2011) Macrofauna under sea ice and in the open surface layer of the Lazarev Sea, Southern Ocean. Deep-Sea Res Pt II 58:1948-1961

Flores H et al. (2012) The Association of Antarctic Krill *Euphausia superba* with the Under-Ice Habitat. PLoS ONE 7. doi:10.1371/journal.pone.0031775

Fofonoff N (1985) Physical properties of seawater: A new salinity scale and equation of state for seawater. J Geophys Res-Oceans 90:3332-3342

Fortier M, Fortier L, Hattori H, Saito H, Legendre L (2001) Visual predators and the diel vertical migration of copepods under Arctic sea ice during the midnight sun. J Plankton Res 23:1263-1278. doi:10.1093/plankt/23.11.1263

Gosselin M, Levasseur M, Wheeler PA, Horner RA, Booth BC (1997) New measurements of phytoplankton and ice algal production in the Arctic Ocean. Deep-Sea Res Pt II 44:1623-1644. doi:10.1016/S0967-0645(97)00054-4

Gradinger R, Bluhm B, Iken K (2010) Arctic sea-ice ridges—Safe heavens for sea-ice fauna during periods of extreme ice melt? Deep-Sea Res Pt II 57:86-95. doi:10.1016/j.dsr2.2009.08.008

Gradinger RR, Bluhm BA (2004) In-situ observations on the distribution and behavior of amphipods and Arctic cod (*Boreogadus saida*) under the sea ice of the High Arctic Canada Basin. Polar Biol 27:595-603. doi:10.1007/s00300-004-0630-4

Gulliksen B (1984) Under-ice fauna from Svalbard waters. Sarsia 69:17-23. doi:10.1080/00364827.1984.10420585

Haas C, Pfaffling A, Hendricks S, Rabenstein L, Etienne J-L, Rigor I (2008) Reduced ice thickness in Arctic Transpolar Drift favors rapid ice retreat. Geophys Res Lett 35:L17501. doi:10.1029/2008GL034457

Harter BB, Elliott KH, Divoky GJ, Davoren GK (2013) Arctic Cod (*Boreogadus saida*) as Prey: Fish Length-Energetics Relationships in the Beaufort Sea and Hudson Bay. Arctic 66:191–196

Hirche HJ (1997) Life cycle of the copepod *Calanus hyperboreus* in the Greenland Sea. Mar Biol 128:607-618. doi:10.1007/s002270050127

Hop H, Gjøsæter H (2013) Polar cod (*Boreogadus saida*) and capelin (*Mallotus villosus*) as key species in marine food webs of the Arctic and the Barents Sea. Mar Biol Res 9:878-894. doi:10.1080/17451000.2013.775458

Hop H, Mundy C, Gosselin M, Rossnagel A, Barber D (2011) Zooplankton boom and ice amphipod bust below melting sea ice in the Amundsen Gulf, Arctic Canada. Polar Biol 34:1947-1958. doi:10.1007/s00300-011-0991-4

Hop H, Pavlova O (2008) Distribution and biomass transport of ice amphipods in drifting sea ice around Svalbard. Deep-Sea Res Pt II 55:2292-2307. doi:10.1016/j.dsr2.2008.05.023

Hop H, Poltermann M, Lonne OJ, Falk-Petersen S, Korsnes R, Budgell WP (2000) Ice amphipod distribution relative to ice density and under-ice topography in the northern Barents Sea. Polar Biol 23:357-367. doi:10.1007/s003000050456

Hopcroft RR, Clarke C, Nelson RJ, Raskoff KA (2005) Zooplankton communities of the Arctic's Canada Basin: the contribution by smaller taxa. Polar Biol 28:198-206. doi:10.1007/s00300-004-0680-7

Hunt BPV et al. (2014) Zooplankton community structure and dynamics in the Arctic Canada Basin during a period of intense environmental change (2004 to 2009). J Geophys Res-Oceans 119:2518-2538. doi:10.1002/2013jc009156

Johannessen OM et al. (2004) Arctic climate change: observed and modelled temperature and sea-ice variability. Tellus A 56:328-341. doi:10.1111/j.1600-0870.2004.00060.x

Kosobokova K, Hirche H-J (2009) Biomass of zooplankton in the eastern Arctic Ocean – A base line study. Prog Oceanogr 82:265-280. doi:10.1016/j.pocean.2009.07.006

Kosobokova K, Hirche HJ (2000) Zooplankton distribution across the Lomonosov Ridge, Arctic Ocean: species inventory, biomass and vertical structure. Deep-Sea Res Pt I 47:2029-2060. doi:10.1016/S0967-0637(00)00015-7

Kosobokova K, Hopcroft R, Hirche H-J (2011) Patterns of zooplankton diversity through the depths of the Arctic's central basins. Mar Biodiv 41:29-50. doi:10.1007/s12526-010-0057-9

Kosobokova KN, Hopcroft RR (2010) Diversity and vertical distribution of mesozooplankton in the Arctic's Canada Basin. Deep-Sea Res Pt II 57:96-110. doi:10.1016/j.dsr2.2009.08.009

Kruskal JB (1964) Nonmetric multidimensional scaling: A numerical method. Psychometrika 29:115-129. doi:10.1007/bf02289694

Kwok R, Cunningham GF, Pang SS (2004) Fram Strait sea ice outflow. J Geophys Res-Oceans 109:C01009. doi:10.1029/2003jc001785

Kwok R, Rothrock DA (2009) Decline in Arctic sea ice thickness from submarine and ICESat records: 1958-2008. Geophys Res Lett 36:L15501. doi:10.1029/2009gl039035

Laidre KL, Heide-Jørgensen MP (2005) Arctic sea ice trends and narwhal vulnerability. Biological Conservation 121:509-517

Lalande C, Nöthig EM, Somavilla R, Bauerfeind E, Shevchenko V, Okolodkov Y (2014) Variability in under-ice export fluxes of biogenic matter in the Arctic Ocean. Global Biogeochem Cy 28:571-583. doi:10.1002/2013GB004735

Legendre P, Legendre L (2012) Numerical ecology. vol 24. Third edition edn. Elsevier

Lønne OJ, Gulliksen B (1991) Sympagic macro-fauna from multiyear sea-ice near Svalbard. Polar Biol 11:471-477. doi:10.1007/bf00233082

Madsen SD, Nielsen TG, Hansen BW (2001) Annual population development and production by *Calanus finmarchicus*, *C. glacialis* and *C. hyperboreus* in Disko Bay, western Greenland. Mar Biol 139:75-93. doi:10.1007/s002270100552

Mann HB, Whitney DR (1947) On a test of whether one of two random variables is stochastically larger than the other. Ann Math Stat:50-60

Mantel N (1967) The detection of disease clustering and a generalized regression approach. Cancer research 27:209-220

Mardia KV, Kent J, Bibby J (1979) Multivariate analysis (probability and mathematical statistics). London: Academic

Markus T, Stroeve JC, Miller J (2009) Recent changes in Arctic sea ice melt onset, freezeup, and melt season length. J Geophys Res-Oceans 114:C12024. doi:10.1029/2009jc005436

Maslanik J, Stroeve J, Fowler C, Emery W (2011) Distribution and trends in Arctic sea ice age through spring 2011. Geophys Res Lett 38:L13502. doi:10.1029/2011gl047735

Matley J, Fisk A, Dick T (2013) The foraging ecology of Arctic cod (*Boreogadus saida*) during open water (July–August) in Allen Bay, Arctic Canada. Mar Biol 160:2993-3004. doi:10.1007/s00227-013-2289-2

Matsuno K, Yamaguchi A, Shimada K, Imai I (2012) Horizontal distribution of calanoid copepods in the western Arctic Ocean during the summer of 2008. Polar Science 6:105-119. doi:10.1016/j.polar.2012.01.002

Mehlum F, Gabrielsen GW (1993) The diet of high-arctic seabirds in coastal and ice-covered, pelagic areas near the Svalbard archipelago. Polar Res 12:1-20. doi:10.1111/j.1751-8369.1993.tb00417.x

Melnikov I, Kulikov A (1980) The cryopelagic fauna of the central Arctic basin. Biology of the central Arctic Basin Nauka, Moscow:97-111

Minchin PR (1987) An evaluation of the relative robustness of techniques for ecological ordination. In: Prentice IC, van der Maarel E (eds) Theory and models in vegetation science. Springer, pp 89-107

Motoda S (1959) Devices of simple plankton apparatus. Memoirs of the Faculty of Fisheries Hokkaido University 7:73-94

Noyon M, Gasparini S, Mayzaud P (2009) Feeding of *Themisto libellula* (Amphipoda Crustacea) on natural copepods assemblages in an Arctic fjord (Kongsfjorden, Svalbard). Polar Biol 32:1559-1570. doi:10.1007/s00300-009-0655-9

Olli K et al. (2007) The fate of production in the central Arctic Ocean – top–down regulation by zooplankton expatriates? Prog Oceanogr 72:84-113. doi:10.1016/j.pocean.2006.08.002

Overland JE, Wang M (2013) When will the summer Arctic be nearly sea ice free? Geophys Res Lett 40:2097-2101

Parkinson CL, Comiso JC (2013) On the 2012 record low Arctic sea ice cover: Combined impact of preconditioning and an August storm. Geophys Res Lett 40:1356-1361. doi:10.1002/grl.50349

Poltermann M, Hop H, Falk-Petersen S (2000) Life under Arctic sea ice - reproduction strategies of two sympagic (ice-associated) amphipod species, *Gammarus wilkitzkii* and *Apherusa glacialis*. Mar Biol 136:913-920. doi:10.1007/s002270000307

Polyakov IV et al. (2005) One more step toward a warmer Arctic. Geophys Res Lett 32:L17605. doi:10.1029/2005gl023740

Pomerleau C, Nelson RJ, Hunt BPV, Sastri AR, Williams WJ (2014) Spatial patterns in zooplankton communities and stable isotope ratios (δ13C and δ15N) in relation to oceanographic conditions in the sub-Arctic Pacific and western Arctic regions during the summer of 2008. J Plankton Res 36:757-775. doi:10.1093/plankt/fbt129

R Core Team (2015) R: A language and environment for statistical computing. R Foundation for Statistical Computing, Vienna, Austria URL http://www.R-project.org/

Rabe B, Wisotzki A, Rettig S, Somavilla Cabrillo R, Sander H (2012) Physical oceanography during POLARSTERN cruise ARK-XXVII/3 (IceArc). *Alfred Wegener Institute, Helmholtz Center for Polar and Marine Research, Bremerhaven*. doi:10.1594/PANGAEA.802904

Rigor IG, Wallace JM (2004) Variations in the age of Arctic sea-ice and summer sea-ice extent. Geophys Res Lett 31. doi:10.1029/2004gl019492

Rudels B, Schauer U, Björk G, Korhonen M, Pisarev S, Rabe B, Wisotzki A (2013) Observations of water masses and circulation in the Eurasian Basin of the Arctic Ocean from the 1990s to the late 2000s. Ocean Science Discussions 9:147-169. doi:10.5194/os-9-147-2013

Runge JA, Ingram RG (1991) Under-ice feeding and diel migration by the planktonic copepods *Calanus glacialis* and *Pseudocalanus minutus* in relation to the ice algal production cycle in southeastern Hudson Bay, Canada. Mar Biol 108:217-225. doi:10.1007/bf01344336

Scott CL, Falk-Petersen S, Sargent JR, Hop H, Lønne OJ, Poltermann M (1999) Lipids and trophic interactions of ice fauna and pelagic zooplankton in the marginal ice zone of the Barents Sea. Polar Biol 21:65-70. doi:10.1007/s003000050335

Shannon C (1948) A mathematical theory of communication. Bell Sys Tech J 27:379-423

Shaw W, Stanton T, McPhee M, Morison J, Martinson D (2009) Role of the upper ocean in the energy budget of Arctic sea ice during SHEBA. J Geophys Res-Oceans 114. doi:10.1029/2008JC004991

Shimada K et al. (2006) Pacific Ocean inflow: Influence on catastrophic reduction of sea ice cover in the Arctic Ocean. Geophys Res Lett 33. doi:10.1029/2005gl025624

Smouse PE, Long JC, Sokal RR (1986) Multiple Regression and Correlation Extensions of the Mantel Test of Matrix Correspondence. Systematic Zoology 35:627-632. doi:10.2307/2413122

Søreide JE, Carroll ML, Hop H, Ambrose WG, Hegseth EN, Falk-Petersen S (2013) Sympagic-pelagic-benthic coupling in Arctic and Atlantic waters around Svalbard revealed by stable isotopic and fatty acid tracers. Mar Biol Res 9:831-850. doi:10.1080/17451000.2013.775457

Søreide JE, Hop H, Carroll ML, Falk-Petersen S, Hegseth EN (2006) Seasonal food web structures and sympagic–pelagic coupling in the European Arctic revealed by stable isotopes and a two-source food web model. Prog Oceanogr 71:59-87. doi:10.1016/j.pocean.2006.06.001

Spreen G, Kaleschke L, Heygster G (2008) Sea ice remote sensing using AMSR-E 89-GHz channels. J Geophys Res-Oceans 113:C02S03. doi:10.1029/2005jc003384

Stroeve J, Holland MM, Meier W, Scambos T, Serreze M (2007) Arctic sea ice decline: Faster than forecast. Geophys Res Lett 34:L09501. doi:10.1029/2007gl029703

Stroeve J, Serreze M, Holland M, Kay J, Malanik J, Barrett A (2012) The Arctic's rapidly shrinking sea ice cover: a research synthesis. Climatic Change 110:1005-1027. doi:10.1007/s10584-011-0101-1

Tremblay J-É, Gagnon J (2009) The effects of irradiance and nutrient supply on the productivity of Arctic waters: a perspective on climate change. In: Nihoul JJ, Kostianoy A (eds) Influence of Climate Change on the Changing Arctic and Sub-Arctic Conditions. NATO Science for Peace and Security Series C: Environmental Security. Springer Netherlands, pp 73-93. doi:10.1007/978-1-4020-9460-6_7

van Franeker JA, Flores H, Van Dorssen M (2009) Surface and Under Ice Trawl (SUIT). In: Flores H (2009) Frozen Desert Alive -The role of sea ice for pelagic macrofauna and its predators: implications for the Antarctic pack-ice food web. Dissertation, University of Groningen, Groningen, Netherlands

Wassmann P, Duarte CM, AgustÍ S, Sejr MK (2011) Footprints of climate change in the Arctic marine ecosystem. Global Change Biology 17:1235-1249. doi:10.1111/j.1365-2486.2010.02311.x

Welch HE et al. (1992) Energy Flow through the Marine Ecosystem of the Lancaster Sound Region, Arctic Canada. Arctic 45:343-357

Werner I (1997) Grazing of Arctic under-ice amphipods on sea-ice algae. Mar Ecol Progr Ser 160:93-99

Werner I, Arbizu MP (1999) The sub-ice fauna of the Laptev Sea and the adjacent Arctic Ocean in summer 1995. Polar Biol 21:71-79. doi:10.1007/s003000050336

Werner I, Auel H (2005) Seasonal variability in abundance, respiration and lipid composition of Arctic under-ice amphipods. Mar Ecol Progr Ser 292:251-262. doi:10.3354/meps292251

Werner I, Gradinger R (2002) Under-ice amphipods in the Greenland Sea and Fram Strait (Arctic): environmental controls and seasonal patterns below the pack ice. Mar Biol 140:317-326

Zuur AF, Ieno EN, Smith GM (2007) Analysing ecological data. vol 680. Springer New York, United States of America

2.2. Chapter II

Under-ice distribution of polar cod *Boreogadus saida* in the central Arctic Ocean and their association with sea-ice habitat properties

Carmen David[1,2*], Benjamin Lange[1,2], Thomas Krumpen[1], Fokje Schaafsma[3],
Jan Andries van Franeker[3], Hauke Flores[1,2]

[1] Alfred Wegener Institut Helmholtz-Zentrum für Polar- und Meeresforschung, Am Handelshafen 12, 27570, Bremerhaven, Germany; [2] University of Hamburg, Centre for Natural History (CeNak), Zoological Museum, Martin-Luther-King Platz 3, 20146, Hamburg, Germany; [3] Institute for Marine Research and Ecosystem Studies Wageningen UR (IMARES), PO Box 57, 1781 AG Den Helder, The Netherlands

Published in the special issue "Ecology of Arctic Gadids" of Polar Biology
doi: 10.1007/s00300-015-1774-0

ABSTRACT

In the Arctic Ocean, sea-ice habitats are undergoing rapid environmental change. Polar cod (*Boreogadus saida*) is the most abundant fish known to reside under the pack-ice. The under-ice distribution, association with sea-ice habitat properties and origins of polar cod in the central Arctic Ocean, however, are largely unknown. During the RV *Polarstern* expedition ARK XXVII/3 in the Eurasian Basin in 2012, we used for the first time in Arctic waters a Surface and Under Ice Trawl (SUIT) with an integrated bio-environmental sensor array. Polar cod was ubiquitous throughout the Eurasian Basin with a median abundance of 5000 ind. km^{-2}. The under-ice population consisted of young specimens with a total length between 52 and 140 mm, dominated by one-year old fish. Higher fish abundance was associated with thicker ice, higher ice coverage and lower surface salinity, or with higher densities of the ice-amphipod *Apherusa glacialis*. The fish were in good condition and well-fed according to various indices. Back-tracking of the sea ice indicated that sea ice sampled in the Amundsen Basin originated from the Laptev Sea coast, while sea ice sampled in the Nansen Basin originated from the Kara Sea. Assuming that fish were following the ice drift, this suggests that under-ice polar cod distribution in the Eurasian Basin is dependent on the coastal populations where the sea ice originates. The omnipresence of polar cod in the Eurasian Basin, in a good body condition, suggests that the central Arctic under-ice habitats may constitute a favourable environment for this species survival, a potential vector of genetic exchange and a recruitment source for coastal populations around the Arctic Ocean.

INTRODUCTION

The Arctic Ocean is facing some of the most pronounced effects of global climate change (IPCC 2014). During the past four decades, the Arctic Ocean has experienced lengthening of the melt season and a progressive reduction in sea ice extent and thickness (Kwok and Rothrock 2009; Markus et al. 2009; Rigor and Wallace 2004; Shimada et al. 2006; Stroeve et al. 2012). Sea ice decline is expected to have a direct impact on organisms living in association with the sea ice.

Polar cod (*Boreogadus saida*) is the most abundant Arctic fish that resides under the pack-ice (Gradinger and Bluhm 2004; Lønne and Gulliksen 1989). The pack-ice serves as habitat for an unknown part of the first- and second-year polar cod population (Lønne and Gulliksen 1989), while large populations are widespread around the Arctic shelves. Polar cod is considered an ecological key species in the Arctic Ocean due to its pan-Arctic distribution (Bouchard and Fortier 2011), large standing stocks (Geoffroy et al. 2011; Hop and Gjøsæter 2013) and its role as an energy transmitter to higher trophic levels (Harter et al. 2013; Hop et al. 1997a; Welch et al. 1992), Along the Arctic shelves, polar cod are often recorded below sea ice in autumn and winter (Benoit et al. 2008; Geoffroy et al. 2011). According to Welch et al. (1993) the sea ice may offer protection against marine mammals and predatory sea birds for which polar cod is known to be an important food source (Bradstreet and Cross 1982; Haug et al. 2007; Lønne and Gabrielsen 1992; Welch et al. 1992). When the ice melts, they become part of the bentho-pelagic stock (Falk-Petersen et al. 1986; Hop and Gjøsæter 2013; Hop et al. 1997b). High polar cod aggregations were reported in the presence of ice cover during winter in the Amundsen Gulf (Geoffroy et al. 2011), where estimated fish biomass reached 250 kt (Benoit et al. 2014). During the open water season, large schools of polar cod were reported from the Barrow Strait reaching up to 12000 t per school and Lancaster Region up to 75000 t per school (Welch et al. 1992). The only population regularly monitored persits in the Barents Sea, where the largest known standing stock of polar cod, up to 1.5 million t, exists (Hop and Gjøsæter 2013).

These high fish stock areas are believed to be important reproduction grounds for the polar cod. Reproduction success is related to sea ice extent and duration, i.e. timing of ice break-up and freezing, and the formation of early polynyas (Bouchard and Fortier 2008; Bouchard and Fortier 2011; Fortier et al. 2006). At the onset of winter, older polar cod follow the downward migration of zooplankton (Geoffroy et al. 2011), while larvae and young juveniles aggregate in the surface layer

(Benoit et al. 2014; Geoffroy et al. 2015). A part of the young polar cod remaining in the surface layer probably associates with the drifting sea ice and is carried away from the shelves, as young polar cod were frequently observed and sampled in drifting sea ice by divers (Lønne and Gulliksen 1989; Søreide et al. 2006). Many uncertainties regarding this behaviour remain to be elucidated. Observations by divers provided great insights into the under-ice behaviour of young polar cod. It was reported that narrow wedges of seawater along the edges of ice floes provide micro-habitats for polar cod inhabiting sea ice over the deep-basins (Gradinger and Bluhm 2004). Sea-ice habitat structure might therefore have a big impact on young polar cod survival. Yet no detailed studies have quantified the association of young polar cod with sea-ice habitat properties on large spatial scales. The few existing estimates are based on localised under-ice observations which do not reflect continuous environmental gradients, but rather exceptional events, e.g. calm weather conditions vs storms (Melnikov and Chernova 2013) or contrasting sea ice structure, e.g. flat vs rafted ice (Gradinger and Bluhm 2004; Lønne and Gulliksen 1989). This demonstrates a strong need for extended information regarding larger scale distribution patterns of under-ice polar cod and the condition of these fish in order to better understand this trait of polar cod's life history and implications for ecosystem functioning. A new sampling gear previously deployed in the Southern Ocean, the Surface and Under Ice Trawl (SUIT) (van Franeker et al. 2009), can overcome the spatial limitation of observations by divers (Flores et al. 2012) by enabling large-scale horizontal sampling of the 0-2 m surface layer both under sea ice and in open water.

This study focuses on polar cod sampled with SUIT during summer 2012 under pack-ice within the Eurasian sector of the central Arctic Ocean. The specific objectives are: (1) to investigate the under-ice distribution, population structure and physiological condition of polar cod in the Eurasian Basin, (2) to analyse the association of polar cod abundance with sea-ice habitat properties, and (3) to identify regions of origin where young polar cod found in the central Arctic Ocean might have entered the under-ice habitat.

METHODS

Sampling technique and data collection

Polar cod were sampled during the RV *Polarstern* expedition "IceArc" (ARK XXVII/3). Sampling was performed between 2 August and 29 September 2012 across the Eurasian sector of the central Arctic Ocean (Fig. 1). Thirteen horizontal hauls were performed under different sea ice types (multi-year ice, first-year ice) and degrees of ice coverage. Nine stations were positioned nearby representatively selected multi-disciplinary sea-ice stations (Boetius et al. 2013) to ensure comparability of parameters. The remaining four stations were completed at intermediate positions to maximise the coverage of the investigation area. Sampling was performed by horizontal trawling with a Surface and Under Ice Trawl (SUIT) (van Franeker et al. 2009). The SUIT consisted of a steel frame with a 2 m x 2 m opening and 2 parallel 15 m long nets attached: 1) A 7 mm half-mesh commercial shrimp net, lined with 0.3 mm mesh in the rear 3 m of the net, covered 1.5 m of the opening width. 2) A 0.3 mm mesh zooplankton net covered 0.5 m of the opening width. Floats attached to the top of the frame kept the net at the surface or the sea-ice underside. To enable sampling under undisturbed ice, an asymmetric bridle forces the net to tow off at an angle of approximately 60° to starboard of the ship's track, at a cable length of 150 m. A detailed description of the SUIT construction and sampling performance was provided as supplementary material in Flores et al. (2012). Depending on the ice conditions, SUIT haul durations varied between 3 and 38 min with a mean of 24 min, over a mean sampled distance of about 1.3 km (Table 2). A bio-environmental sensor array was mounted in the SUIT frame, consisting of an Acoustic Doppler Current Profiler, a conductivity-temperature-depth (CTD) probe with built-in fluorometer and altimeter, two spectral radiometers, and a video camera. A detailed description of environmental data acquisition was provided in David et al. (2015).

A CTD probe with a carousel water sampler was used to collect environmental parameters from the water column near SUIT stations (David et al. 2015). The depth of the upper mixed-layer was calculated from the ship CTD profiles after Shaw et al. (2009). Details of the CTD sampling procedure and nutrients analysis were provided in Boetius et al. (2013). Data are available online in the PANGAEA database (Rabe et al. 2012).

Sea ice back-tracking

To determine the pathways and formation areas of sampled sea ice we back-tracked the sampled sea ice areas over a period of two years using sea ice drift and concentration data from passive microwave satellite sensors. Passive microwave-based ice drift products were provided by different institutions and have been widely used in sea-ice studies and for model assimilation. The motion fields provided by the Centre for Satellite Exploitation and Research (CERSAT) at the Institut Francais de Recherche pour d'Exploitation de la Mer (IFREMER), France (hereafter referred to as CERSAT) are based on a combination of drift vectors estimated from scatterometer (SeaWinds/QuikSCAT and ASCAT/MetOp) and radiometer (SSM/I) data. They are available with a grid size of 62.5 km, using time lags of 3 days for the period between September and May. Hence, during the winter month the ice drift data provided by CERSAT was used in the tracking approach. Because of its year-round availability, Polar Pathfinder Sea Ice Motion Vectors (Version 2) provided by the National Snow and Ice Data Centre (NSIDC, Boulder, USA) were used for the calculation of ice pathways and sources during summer months. The product contains daily gridded fields of sea ice motion on a 25 km Equal Area Scalable Earth grid (EASE) (Fowler et al. 2013). The motion vectors are obtained from a variety of satellite-based sensors such as the SMMR, SSM/I, AMSR-E and Advanced Very High Resolution Radiometer (AVHRR), and buoy observations from the International Arctic Buoy Program (IABP). A description of the data set and the sea ice motions retrieval algorithm can be found in Fowler et al. (2013). Sea ice concentration data used in this study were also provided by the NSIDC. Data is calculated based on the Advanced Microwave Scanning (AMSR-E) Bootstrap Algorithm and available on a daily basis, with a 25 x 25 km spatial resolution (Fowler et al. 2013). Eurasian Basin sea ice covered area as monthly means for August and September 2012 were estimated in ArcGIS 10.1 using sea ice extent data provided by the NSIDC (Fetterer et al. 2002, updated daily), defining a sea ice concentration of 15% as the boundary between sea ice and open water. Lambert Azimuthal equal-area was used as projection system because it realistically preserves the area (Snyder 1992). During back-tracking, a specific particle is followed backward in time until: a) the ice particle approaches land, b) the sea ice concentration at the position of the particle reaches a critical value (< 15 %) and the ice is assumed to be melted, or c) the tracking time of two years is exceeded.

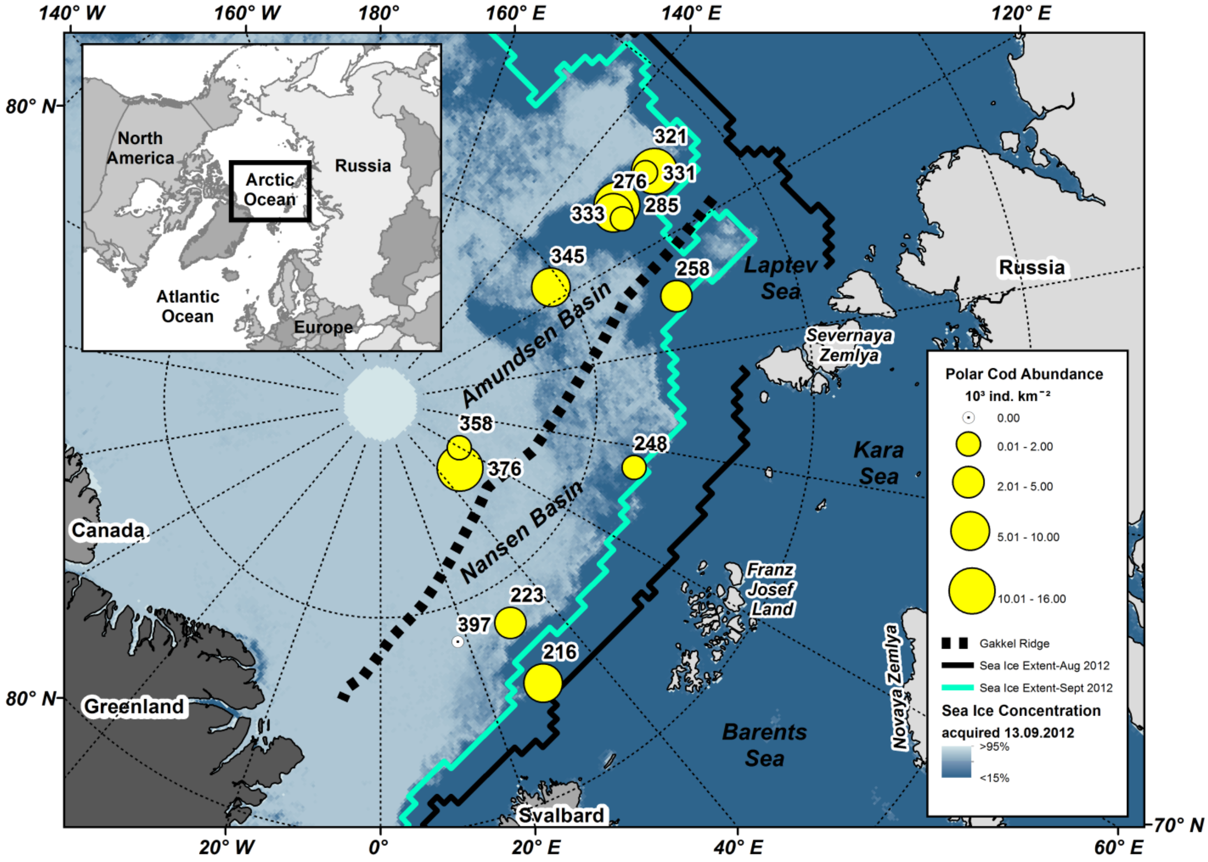

Figure 1. Station map during RV Polarstern expedition IceARC (ARK XXVII/3) and polar cod abundance. Sea ice concentration on 13 September 2012 (data acquired from Bremen University, http://www.iup.uni-bremen.de:8084/amsr/) and monthly mean sea ice extent for August and September 2012 are represented on the map (data acquired from NSIDC, Fetterer et al. 2002, daily updated). Number codes next to sampling locations indicate station numbers.

Fish processing

Immediately after sampling, fish were frozen at -20 °C. Before freezing, several fish were sampled for lipid and stable isotopes analyses and stomach content (data not included in this study). At the Alfred Wegener Institute, frozen fish were first thawed, and then blotted dry before further analysis. Total length (TL) and standard length (SL) were measured to the lowest full mm. Total wet weight (WW) and eviscerated wet weight (EWW) were recorded to the nearest 0.1 mg. Liver and gonads weight were determined to the nearest 0.01 mg. Otoliths (sagittae) were extracted. Otolith length (OL) was determined using a Leica 21.5M stereomicroscope equipped with a camera and image analysis software.

Table 1. Environmental and biological variables characterising sea-ice habitats selected for statistical modelling; abbreviations used in the text and figures are indicated in parentheses: sampled ice coverage during SUIT hauls (Coverage), modal ice thickness (Thickness), roughness of ice thickness (Roughness), surface water temperature (Temperature), surface water salinity (Salinity), chlorophyll *a* concentration at the surface (Chlorophyll *a*), combined nitrate + nitrite concentration at the depth of the chlorophyll *a* maximum (NO_x), mixed layer depth (MLD)

Station code	**216**	**223**	**248**	**258**	**276**	**285**	**321**	**331**	**333**	**345**	**358**	**376**	**397**
Basin	Nansen	Nansen	Nansen	Nansen	Amundsen	Amundsen	Amundsen	Amundsen	Amundsen	Amundsen	Amundsen	Amundsen	Nansen
Coverage (%)	98.3	81.5	56.4	100	78.7	100	63.8	0.0	4.0	62.3	85.8	100	96.2
Thickness (m)	0.45	1.15	1.14	0.75	0.85	0.85	0.55	0.00	0.00	1.05	1.38	1.40	0.70
Roughness	0.15	0.34	0.34	0.06	0.18	0.15	0.48	0.00	0.00	0.24	0.14	0.49	0.39
Temperature (°C)	-1.06	-1.51	-1.55	-1.61	-1.42	-1.56	-1.61	-1.58	-1.22	-1.60	-1.81	-1.82	-1.76
Salinity	30.9	31.8	32.2	32.6	30.2	30.6	29.4	30.4	30.1	30.1	33.1	33.1	32.6
MLD (m)	9	15	18	15	22	22	20	20	20	25	30	25	22
Chlorophyll *a* (mg m^{-3})	0.29	0.20	0.27	0.15	0.26	0.32	0.35	0.36	0.19	0.44	0.32	0.28	0.24
NOx (µmol l^{-1})	6.21	4.63	6.84	1.56	2.42	2.42	0.12	0.12	1.10	0.50	1.26	3.01	3.46
Apherusa glacialis (ind. 1000 m^{-2})	195.10	2218.44	152.67	502.24	823.16	1906.75	349.86	136.84	44.12	342.66	na	na	162.97
Themisto libellula (ind.1000 m^{-2})	9.46	7.11	3.80	30.38	87.10	853.57	512.33	310.07	345.23	260.05	na	na	6.11
Calanus glacialis (ind. 1000 m^{-2})	37.85	1911.27	30528.14	4146.93	1177.70	2216.59	184.62	154.31	498. 49	178.16	na	na	1124.51
Calanus hyperboreus (ind. 1000 m^{-2})	41.45	3697.39	4946.13	555.57	471.08	309.85	29.54	11.65	74.31	0.00	na	na	65.19

Table 2. Summary of sampled sea-ice area drift characteristics and polar cod abundance at each corresponding SUIT station

Station code	SUIT				Sea-ice drift		Sea-ice origin				
	Latitude (ºN)	Longitude (ºE)	Trawled distance (m)	Fish abundance (10^3 ind. km^{-2})	Drift duration (days)	Drift distance (km)	Latitude (ºN)	Longitude (ºE)	Depth (m)	Formation date	Area
216	82.50	30.00	2219	5.85	240	2113	81.68	60.72	200	11 Dec	Kara Sea
223	84.07	30.12	703	4.97	261	2056	80.83	79.71	100	22 Nov	Kara Sea
248	83.97	75.80	1578	0.63	249	1795	80.87	93.20	0	11 Dec	Kara Sea
258	82.71	109.53	1613	2.48	269	1985	77.62	103.66	0	25 Nov	Kara Sea
276	83.06	129.76	1630	7.36	269	1998	76.81	111.22	100	30 Nov	Laptev Sea
285	82.91	129.76	1342	10.05	271	2004	76.64	110.57	0	29 Nov	Laptev Sea
321	81.68	129.79	1083	11.54	255	1868	76.62	111.97	0	24 Dec	Laptev Sea
331	81.90	130.59	1374	0.36	276	1975	76.81	110.99	100	4 Dec	Laptev Sea
333	83.03	127.05	1292	0.77	na	na	na	na	na	na	na
345	85.16	122.59	1392	8.98	321	2358	78.05	108.66	100	24 Oct	Laptev Sea
358	87.86	60.67	1476	0.67	343	2546	81.06	113.36	2000	12 Oct	Laptev Sea
376	87.42	52.90	125	15.92	618	4248	78.58	105.08	0	16 Jan	Laptev Sea
397	84.19	17.41	982	0	333	2594	80.57	82.33	200	1 Nov	Kara Sea

Among the measured (TL, SL) and weighted (WW) fish, a random selection of ten fish (from three stations with the highest catches) were processed for energy content estimation. These fish were freeze-dried until complete desiccation (constant mass). After drying, they were re-weighed to determine the total dry weight (DW). Water content was calculated as the difference between WW and DW, expressed as %WW. Then, fish were homogenized with a blender. A subsample of each fish of approximately 0.5 g was used for calorimetry. Individual energy content, expressed as kJ g^{-1}, was determined at the Royal Netherlands Institute for Sea Research (NIOZ) with an isoperibol bomb calorimeter (IKA C2000 basic) calibrated with benzoic acid.

Data analysis

Pairwise linear regressions were applied between TL, SL, WW, EWW and OL. To describe the condition of fish a set of indices were estimated: Fulton's condition index ($K = 100*WW/TL^3$), condition index (CI = 100*EWW/WW), Hepatosomatic index (100*liver weight/WW) and Gonadosomatic index (100*gonads weight/WW). To assess the statistical difference between basins and areas of sea ice formation, the Wilcoxon signed-rank test was performed on fish abundance data and condition indices (Wilcoxon 1945).

Generalised Linear Models (GLM) (McCullagh and Nelder 1989) were used to analyse the relationship of polar cod abundance with sea-ice habitat properties. Eight environmental variables were selected a priori, from a suite of 30 variables obtained during sampling (Online resource 1), by Spearman's rank correlation coefficient, used to identify redundant variables. In pairs with correlation higher than 0.7, only one variable was chosen for subsequent analysis based on the ecological relevance to the objectives of this study, and model requirements, e.g. normality of data. In a second approach, four biological variables (zooplankton species densities, representing potential prey of polar cod, caught during the same trawls) were additionally used for statistical modelling (Table 1). Zooplankton data collection is described in David et al. (2015). Data were checked for normality by histograms, Shapiro tests and qqplots. To obtain an even distribution of residuals, two environmental variables were transformed: proportional ice coverage during SUIT hauls ('coverage') by square-power transformation and nitrate + nitrite (NOx) by square-root transformation. The biological variables were log transformed. The response variable, polar cod abundance was square-root transformed.

Two full models were submitted to model selection: 1) a model containing all physical and biological variables and 2) a model contained only physical variables (Table 1). Two stations from which no quantitative prey abundance data was available were excluded from model 1). An automatic backwards selection using the Akaike Information Criterion (AIC) was applied for selection of the most parsimonious model. Since this method can result in over-fitted models (Vaz et al. 2008), alternatively simple models containing just one variable, one variable and its quadratic term, combinations of two and three variables, simple or with interactions, were fitted. The resulting models were further compared based on AIC, adjusted R-squared and dispersion. The significance of model improvement by AIC was confirmed with ANOVA statistics.

For all analyses, R software version 3.2.0 (R Core Team 2015) was used with the libraries vegan, FactoMineR, plyr, MASS, mixtools and modEvA.

RESULTS

Sea-ice habitat properties and sea ice back-tracking

Across the Eurasian Basin 13 stations were sampled (Fig. 1). Five stations were located in the Nansen Basin, and eight stations in the Amundsen Basin. Four of the Nansen Basin stations were sampled during the first half of August, and the Amundsen Basin stations during late-August to mid-September. The last station (Stn 397) was sampled in the Nansen Basin on 29 September 2012 at the onset of winter. Two of the Amundsen Basin stations were nearly ice-free. At all other stations sea ice was present, with concentrations ranging from 56 to 100 % (Table 1). Modal ice thickness ranged from 0.45 to 1.40 m. Surface water temperatures ranged between -1.8 and -1.0°C. Surface water salinity was significantly higher in the Nansen Basin (30 – 33) than in the Amundsen Basin (29 – 31) ($W = 0$, p-value < 0.01). A detailed description of the above mentioned physical properties of the study region was provided in David et al. (2015).

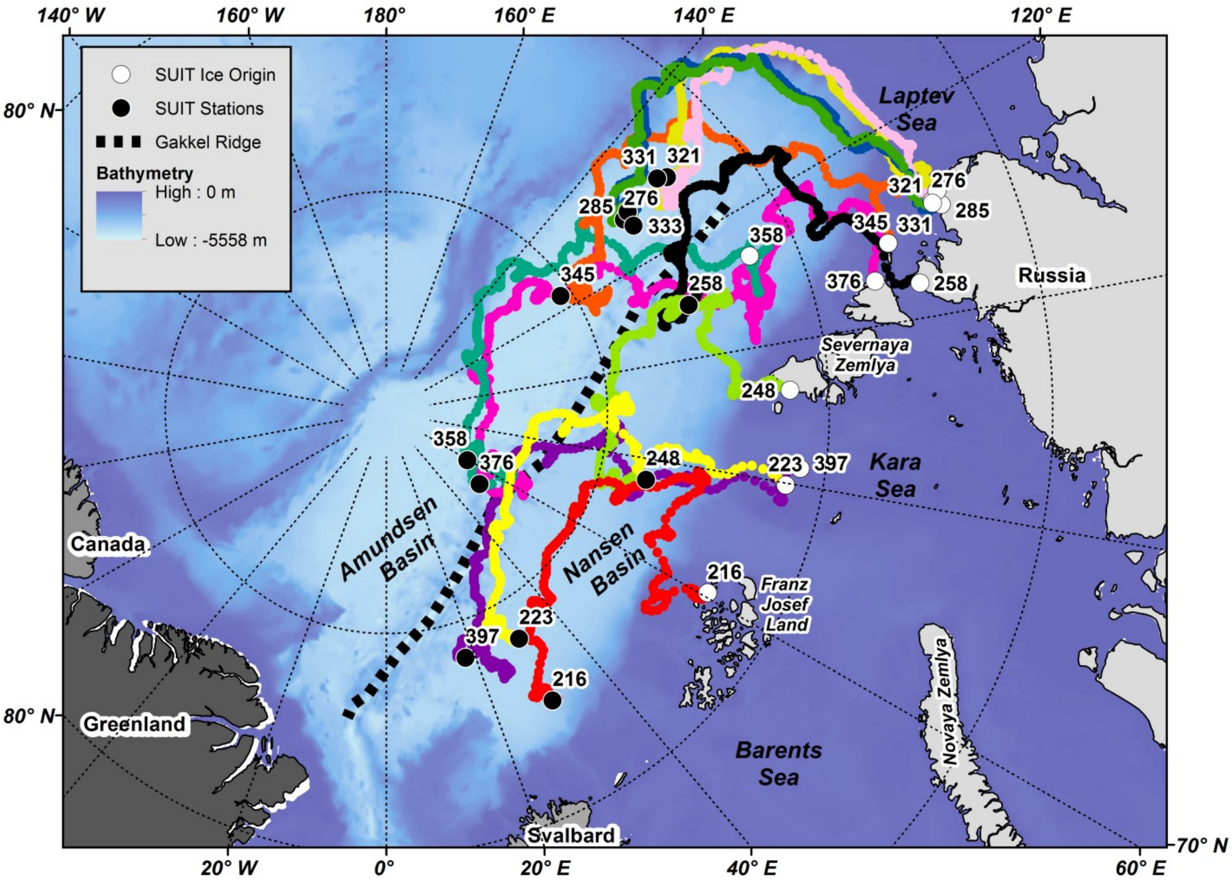

Figure 2. Back-tracked drift pathways of sea ice at SUIT sampling locations during RV Polarstern expedition IceARC (ARK XXVII/3). Black circles represent the SUIT station locations. White circles represent the likely formation areas of sampled sea ice. Number codes next to formation areas and sampling locations indicate corresponding SUIT station numbers.

Thirteen areas of sea ice, corresponding to the ice sampled during each SUIT station, were back-tracked to their area of ice formation (Fig. 2, Table 2). We found that most of the ice originated from shallow coastal areas where ice is formed in polynyas situated along the fast ice edge. A minor part was formed during freeze-up and in deeper waters (> 200 m). Sea ice from all stations sampled in the Nansen Basin originated from the Kara Sea sector (Fig. 2). At Stn 216, the ice originated from the coast of Franz Josef Land. At the Gackel ridge station (Stn 258), the ice originated from the coast of Severnaya Zemlya, bordering the Kara Sea sector. At all of the Amundsen Basin stations, the sampled sea ice originated from the Laptev Sea coast east of Severnaya Zemlya (Fig. 2). The mean drift duration of the sampled sea ice was 308 days, with a range of 240 to 618 days (Table 2). Shorter drift durations (240 and 249 days) were determined for the sampled sea-ice areas at Stn 216 and 248 in the Nansen Basin. The longest drift duration was determined for the sampled sea-ice area at Stn 376 in the Amundsen Basin.

Abundance, population structure and biomass distribution of polar cod

Polar cod abundance in the 0-2 m surface layer ranged between 0 and 15920 ind. km^{-2} (median = 4977, sd = 5130) (Fig. 1, Table 2). The highest abundance was encountered at Stn 376 in the Amundsen Basin. The total number of fish caught at each station ranged between 0 and 28. Only at the early winter Stn 397, no fish were caught. One and two fish were caught at the open water stations, Stn 331 and 333, respectively.

The median polar cod abundance was higher in the Amundsen Basin than in the Nansen Basin (Fig. 1), coinciding with a tendency to higher abundances under sea ice originating from the Laptev Sea compared to sea ice formed in the Kara Sea (Fig. 2). When the two open water stations in the Amundsen Basin were excluded from analysis, this pattern was statistically significant ($W = 27$; $p < 0.05$) (Fig. 3).

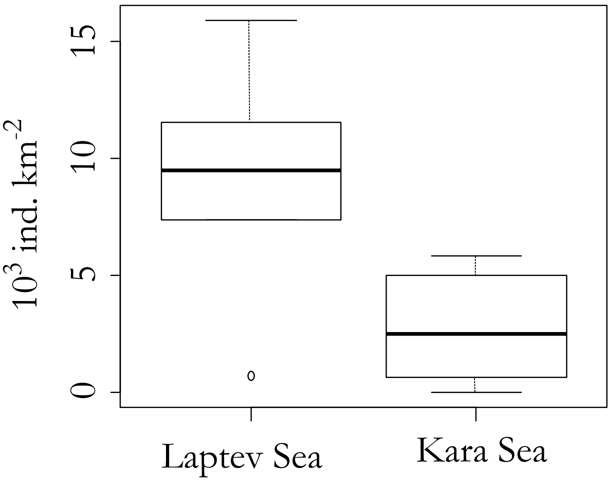

Figure 3. Boxplot of polar cod abundance at sampling stations grouped according to two main areas of sea ice formation: Laptev Sea and Kara Sea. The horizontal bar indicates median abundance. The upper and the lower edges of the 'box' (hinges) denote the approximate 1st and 3rd quantiles, respectively. The two open water sampling stations (Stn 331 and 333) were excluded.

The most parsimonious model using polar cod abundance as a response variable showed a strong positive relationship of fish abundance with surface salinity (p < 0.01) and the abundance of the ice-amphipod *A. glacialis* ($p < 0.01$) (Adj.$R^2 = 0.72$, AIC = 25) (Table 3). When only physical variables were included as predictors, the most parsimonious model showed a negative effect of surface salinity ($p < 0.01$) and a positive effect of sea-ice thickness ($p < 0.05$) and coverage ($p < 0.1$) on modelled fish abundance (Adj.$R^2 = 0.56$, AIC = 37) (Table 3).

Table 3. Summary results of the most parsimonious models testing the association of polar cod abundance (Ab) with sea-ice habitat properties resulting from model selection. Adj.R^2, adjusted R-squared; AIC, Akaike's Information Criterion

			Model terms		
Response variable	**Overall model statistics**		**Variables**	**Linear estimate**	***p*-value**
Ab	Dispersion	0.70	Salinity	-0.9570	0.00413
	Adj.R^2	0.56	Thickness	1.8270	0.02848
	AIC	37	Coverage	$1.789*10^{-4}$	0.05617
Ab	Dispersion	0.38	Salinity	-0.6717	0.00511
	Adj.R^2	0.72	*A. glacialis*	0.6788	0.00400
	AIC	25			

The total length (TL) of polar cod caught ranged between 52 and 140 mm (Fig. 4). Fish in the Nansen Basin were significantly larger than fish in the Amundsen Basin ($W = 911$, $p < 0.001$). This pattern was driven by the dominance of larger fish at two stations, Stn 216 and 223, having a mean TL per station of 86 and 100 mm, respectively. Two exceptionally large fish were caught, one at Stn 216 (TL = 137 mm) and one at Stn 285 (TL = 140 mm). The Nansen fish comprised only 28 % of the total catch, with a TL mode of 89 mm and a range of 56 to 137 mm. The Amundsen fish had a TL mode of 72 mm and a range of 52 to 140 mm. The mean individual fish wet weight (WW) was 4.96 g (range: 1.1 to 18.8 g) in the Nansen Basin and 2.16 g (range: 0.8 to 8.5 g) in the Amundsen Basin.

The total biomass per station ranged between 0 and 66 kg km^{-2} (median = 19.34 kg km^{-2}, sd = 18.79). The highest biomass was encountered at Stn 376 in the Nansen Basin. Except Stn 397 where no fish were caught, the lowest biomass was found at the open water Stn 331, closely followed by Stn 248 and 333. Average biomass was somewhat higher in the Nansen Basin than in the Amundsen Basin, due to the influence of larger fish caught at Stn 216 and 223, but this pattern was not statistically significant ($W = 22$; $p > 0.1$).

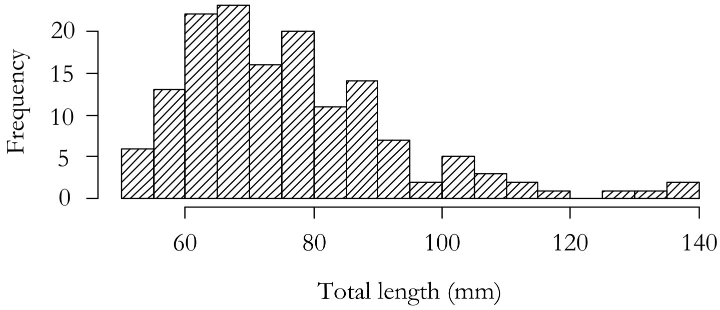

Figure 4. Histogram of the size distribution for polar cod sampled with the Surface and Under Ice Trawl during RV Polarstern expedition IceARC (ARK XXVII/3).

Allometrics and energy content

A summary of various allometric regression analyses was provided in Table 4. Significant positive linear relationships existed between TL and otolith length (OL) (n = 130, Adj.R^2 = 0.94; $p < 0.001$) and between TL and standard length (SL) (n = 130, Adj.R^2 = 0.99, $p < 0.001$). Wet weight (WW) and eviscerated wet weight (EWW) were exponentially related with TL (n = 127, Adj.R^2 = 0.96, $p < 0.001$). The exponential regression coefficient *b* for fish of size 52 to 120 mm was 2.13 for WW estimates and 2.10 for EW estimates (Table 4).

The condition indices were analysed in 130 fish having a mean length (TL) of 76 mm and mean weight (WW) of 3.2 ± 2.5 g (Table 5). The condition index CI had a mean of 78.8 % ± 3.3. Fish from the Nansen Basin had a significantly higher CI (80 % ± 3.3) compared with fish from the Amundsen Basin (78 % ± 3.2) (W = 10793, $p < 0.001$). Fulton's index (K) had a mean of 62.8 % ± 7.2 (Table 5). Fish from the Nansen Basin had an averaged similar K (62 % ± 6) compared with fish from the Amundsen Basin (64 % ± 7) (W =1688, $p > 0.1$). The hepatosomatic index (HSI) was significantly higher and was more variable in the Amundsen Basin (1.4 % ± 0.8) compared to the Nansen basin (1.0 % ± 0.6) (W= 1257, $p < 0.05$).

Table 4. Relationships between total body length [mm] (TL), wet weight [mg] (WW), eviscerated wet weight [mg] (EWW), otolith length [mm] (OL), and standard length [mm] (SL) for fish with a TL range of 52 – 120 mm. The lowermost row shows the regression model of a similar study by Matley et al. (2013) in which FL is fork length

Response variable	Regression model with coefficients	Adj. R^2	*p*-value
L	$20.6631 + OL* 24.2791$	$R^2 = 0.943$	$p < 0.001$
SL	$-0.2736 + 0.9187 * TL$	$R^2 = 0.996$	$p < 0.001$
WW	$0.0004 * TL^{2.1305} -1$	$R^2 = 0.963$	$p < 0.001$
EWW	$0.0004 * TL^{2.1073} -1$	$R^2 = 0.965$	$p < 0.001$
WW	$1.72E-05 * FL^{2.8}$ 1)	na	na

1)(Matley et al. 2013)

Table 5. Summary of body condition indices of all fish caught in our samples; CI – condition index; K – Fulton's condition index; HSI – hepatosomatic index; GSI – gonadosomatic index; Standard deviations are provided in parentheses

Total length [mm]	Wet weight [g]	CI [%]	K [%]	HSI [%]	GSI [%]
76.8 (16.6)	3.27 (2.5)	78.8 (3.5)	62.8 (7.2)	1.3 (0.8)	3.8 (1.8)
n=130	n=127	n=127	n=127	n=96	n=114

The ten fish from three stations (Stn 216, 285 and 321) analysed for water and energy content had a mean TL of 77.7 mm (range: 60 to 133 mm), mean WW of 3.5 g, thus well representing the sampled population. Their mean water content was 73.2 % ± 3.1 (Table 6). The fish had a mean individual dry weight (DW) of 0.9 ± 0.8 g and a mean dry energy density of 27.25 ± 1.3 kj g^{-1} DW (Table 6).

Table 6. Mean total body length, wet weight, dry weight and energy content of polar cod (n=10); Standard deviations are provided in parentheses

Total length [mm]	Wet weight [g]	Water content [%]	Dry weight [g]	Calorie content [Cal/g]	Energy content [kJ g^{-1}]
77.7 (20.8)	3.5 (3.8)	73.2 (3.1)	0.9 (0.8)	6511 (316)	27.2 (1.3)

DISCUSSION

Under-ice distribution and association with sea-ice habitats

We used a Surface and Under Ice Trawl (SUIT) for the first time in the Arctic Ocean, enabling us to provide the first large-scale estimate of polar cod (*Boreogadus saida*) abundance under sea ice throughout the Eurasian Basin. When absolute fish numbers were considered per haul, our stations' catches, between 0 and 28 individuals, corresponded well with previous under-ice observations of small schools described by Gradinger and Bluhm (2004). At a median 5000 ind. km^{-2} over the sampling area, our abundances were low compared to coastal areas, where school densities up to 614*10^{6} ind. km^{-2} were reported from Allen Bay (Matley et al. 2012), or benthic population abundance of 23800 ind. km^{-2} near Svalbard (Nahrgang et al. 2014). In previous studies, mainly pelagic and demersal trawls were used in open water areas (Matley et al. 2013; Nahrgang et al. 2014; Ponomarenko 2000), while under-ice abundance estimates were made based on hand net sampling (Melnikov and Chernova 2013) and observations by divers (Gradinger and Bluhm 2004). Using the SUIT enabled us to representatively capture the variability of the under-ice environment and facilitate large-scale abundance estimates of under-ice polar cod, assuming other error sources were minimal. Such error sources may be the low efficiency of the SUIT to sample animals from crevices and wedges in the ice, or the ability of polar cod to avoid or escape the net. Videos from the SUIT camera showed no indication of escape or avoidance of the net by polar cod. The mere omnipresence of polar cod in under-ice catches rather indicated that the sluggish lifestyle of polar cod (Gradinger and Bluhm 2004) may have worked in favour of sampling this species with a net that is relatively small for catching fast-swimming fish. Due to the uncertainties regarding the potential sampling of animals protected by the under-ice topography, however, the abundance estimates presented here should be regarded rather as a minimum estimate of the true abundance.

Our statistical model using purely physical variables showed that higher fish abundances were associated with lower surface salinity, thicker sea ice, and higher sea-ice coverage during sampling. Surface salinities were significantly higher in the Nansen Basin than in the Amundsen Basin due to the larger influence of Atlantic Water (David et al. 2015; Rudels et al. 2013). Besides regional differences in water mass distribution, reduced surface salinity may be caused by freshwater release of melting sea ice. Like most stations in the Amundsen Basin, station 216 in the Nansen Basin had a relatively low surface salinity and sea ice in an advanced state of melting (David et al. 2015), associated with comparably high abundances of polar cod (Fig. 1). Besides lower surface salinities, and probably melting conditions, modal sea-ice thicknesses and sea-ice coverage during sampling had a positive effect on modelled polar cod abundance. This is not a contradiction, since it implies that in areas of decaying sea ice polar cod most likely concentrated under the remaining thicker ice. Deterioration of the sea-ice habitat and melting of ice wedges, which serve as protection for the fish, have been proposed to explain higher polar cod densities found under the remaining sea ice during late-summer (Hop and Pavlova 2008). Clearly, the under-ice habitat was preferred to the open water surface layer, as is evident from the positive effect of sea-ice coverage during sampling on modelled polar cod abundance.

A significant influence of melting conditions on the distribution of polar cod was confirmed by the negative effect of surface salinity in the model including prey density. The positive effect of the under-ice density of the ice-amphipod *A. glacialis* on modelled polar cod abundance indicates that under-ice prey availability was probably a key factor influencing the under-ice distribution of polar cod (Table 3). Release of ice amphipods into the pelagic habitat has been reported to occur during advanced stages of ice melt and break-up, offering a pulse of high-energy prey at the ice-water interface (Hop et al. 2011; Scott et al. 1999). The diet of polar cod under sea ice, however, is not well documented, because the inaccessibility of this habitat has so far only allowed a small number of living fish to be analysed, leaving little evidence of polar cod feeding on sea ice resources (Renaud et al. 2012). Polar cod collected north of the Svalbard archipelago by under-ice divers were mainly one-year old fish and had a diet containing *A. glacialis* and other ice amphipods among various pelagic resources (Lønne and Gulliksen 1989). Preliminary data from an analysis of 13 stomachs of polar cod collected during the present study, from seven stations, indicated that ice-associated copepods (*Tisbe* spp.) and the under-ice amphipod *A. glacialis* were important food items (H. Flores, unpublished data).

While statistical relationships do not necessarily imply cause-effect relationships, the factors selected by the two statistical models represent plausible ecological interactions: Our models results could imply that polar cod were concentrating under remaining sea ice during advancing melt and preferred thicker sea ice that survived longest and was most likely to host sufficient under-ice prey.

Population structure and allometrics

We found fish with total lengths ranging between 52 and 140 mm. Their mean size was 76 mm, which corresponded to the first-year age class according to Ponomarenko (2000). This mean size is lower than previously reported mean size values for first-year fish from coastal Arctic ice-covered regions (Lønne and Gulliksen 1989), but similar to observations from the central Arctic deep-sea basins (Melnikov and Chernova 2013). The length of the first-year polar cod is related to the time of hatching, and depends on the growth rate of juveniles. According to the length-age relationship $SL_{mm} = 4.357 + 0.196\ age_{days}$ described in Bouchard and Fortier (2011), these 52 to 140 mm TL polar cod were between 201 and 652 days old (mean = 336 days) in August-September. Since hatching period was recorded from January to July in the Laptev Sea (Bouchard and Fortier 2011), this suggests either the under-ice fish represented the latest hatchers or the growth rate of under-ice fish was much slower than the pelagic ones.

The growth rate of juveniles depends on the temperature and the food availability in the environment (Ponomarenko 2000). The under-ice water temperature was below -1ºC in the Eurasian Basin, probably inducing a slower growth rate for fish associated with the sea-ice habitat compared to coastal habitats (Falk-Petersen et al. (1986). In our study, the regression coefficient *b* describing the weight-length relationship was 2.13. This value is not in line with the cubic law presumed for this relationship (Craig et al. 1982; Matley et al. 2013). This was probably due to the dominance of young fish in our samples, as in our size range the weight-length relationship of the entire population found by Matley et al. (2013) fits still well with our data (Pearson correlation coefficient = 0.97, $p < 0.001$). Our low values of regression coefficient *b* could mean that the young fish from our study were investing more energy in growth, and less in lipid storage, as is common in juvenile fish (Anthony et al. 2000).

The under-ice fish from our samples had very low hepatosomatic index (HSI) values compared with polar cod from the Canadian Arctic or Svalbard, which included a higher proportion of large fish (Matley et al. 2013; Nahrgang et al. 2010). The lower HSI and higher condition index (CI) values in the Nansen Basin compared to samples from the Amundsen Basin could indicate that local feeding conditions prior to the sampling were more favourable in the Amundsen Basin.

Somewhat contrasting with generally low HSI values, the energy content in our fish was at the high end of the range previously reported for polar cod (Elliott and Gaston 2008; Harter et al. 2013;

Hop et al. 1997a), suggesting a high lipid content in tissue other than liver. In polar cod from the present study, gonads were the most lipid-rich tissue, DW lipid content averaging 87% (D. Kohlbach, unpublished data). At the end of summer, polar cod start allocating energy to gonadal development (Hop et al. 1995). Hence, carbon resources were probably routed to gonads development rather than to storage lipids in the liver. At the end of summer GSI values are below 5% (Hop et al. 1995) and increase in mature polar cod to about 30% by the spawning period in January (Hop et al. 1995, Nahrgang et al. 2014). The gonadosomatic index (GSI) values in our study (Table 5) were comparable with GSI in larger polar cod in July – August, as reported in Hop et al. (1995), indicating that fish from our study could have only begun to develop from the juvenile state towards reproductive maturity. The high energy content found in this study for polar cod exceeds those reported by Elliott and Gaston (2008) for Canadian Arctic (21.9 kJ/g dry weight) and by Weslawski et al. (1994) for the Svalbard region (24.2 kJ/g dry weight) and are similar with those reported by Cairns (1987) for the western Hudson Strait (26.5 kJ/g dry weight). For polar cod in the present study, accumulation of energy could have been facilitated by feeding on lipid-rich under-ice amphipods, such as *A. glacialis* and *Onisimus glacialis* (Scott et al. 1999). This highlights the potential of polar sea-ice habitats to nourish and maintain highly energy-efficient food webs.

'Sea-ice drift' hypothesis

Assuming that young polar cod drift passively with sea ice, we hypothesised that the observed under-ice fish distribution in the central Arctic could be related to populations in the area of ice formation. The actual timing or mechanism determining fish to associate with sea ice is not known. According to age estimates of fish in the present study, we consider that the latest hatchers are more likely to remain associated with the underside of sea ice. Instead of migrating to deeper layers like other young of the year fish (Geoffroy et al. 2015), this behaviour would allow them to avoid competition with older, hence bigger, individuals from the same year, or to avoid predation. During the sea-ice drift, limited mobility of the fish outside their under-ice habitat was reported (Gradinger and Bluhm 2004; Lønne and Gulliksen 1989). Only during storm events fish were observed swimming at some distance from the ice (Melnikov and Chernova 2013).When calm conditions were restored, fish seemed to seek shelter in their under-ice refuge again (Melnikov and Chernova 2013), indicating only short interruptions of their fidelity to the sea-ice underside.

To investigate pathways and formation areas of sampled sea ice, back-tracking of sea ice at the sampling locations was performed using a combination of NSIDC/CERSAT sea ice drift and concentration information. We found that ice forming near Franz Josef Land and in the Kara Sea drifted into the Nansen Basin, whereas ice that formed along the western Laptev Sea coast, east of Severnaya Zemlya, drifted into the Amundsen Basin. We found higher fish abundances in the Amundsen Basin, which was linked to sea ice originating from the Laptev Sea - Severnaya Zemlya area. If the under-ice population of polar cod in the high Arctic reflects coastal population dynamics where the sampled sea ice was formed, then the Laptev Sea shelf, particularly in the vicinity of Severnaya Zemlya, likely served as an important recruitment ground for under-ice polar cod. Higher recruitment in that area could have been enhanced by the presence of early polynyas (Bouchard & Fortier 2008).

The accuracy of ice drift pathway estimates is, however, difficult to assess, since buoy observations of ice drift in the eastern Arctic Ocean are rare. In addition, the uncertainties associated to ice drift products are not spatially uniform (Sumata et al. 2014). For back-tracking, we therefore applied a drift data set that shows good performance on the Siberian shelf (Krumpen et al. 2013; Rozman et al. 2011). Because CERSAT motion data is only available during winter months, the summer period (June – August) was bridged with NSIDC drift data. During summer months, however, high temperatures and strong surface melt of sea ice make sea ice drift determination more challenging, which may introduce additional uncertainty to our estimates of sea ice origin and pathways.

A good agreement of the size/age structure of under-ice fish with drift times from their potential recruitment regions provides strong indication of a continuous sea ice-driven advection of polar cod from specific coastal hatching areas across the Arctic Ocean. Spawning takes place in January and February in the Kara Sea (Ponomarenko 2000), followed by hatching usually during May and June (Ponomarenko 2000). In the Laptev Sea hatching already starts by the end of winter and extends to July (Bouchard and Fortier 2011). According to Bouchard and Fortier (2011) larvae length in late summer can vary form 10 mm in July hatchers to 50 mm in January hatchers. By the time new sea ice forms, generally October to December in the case of our back-tracked sea ice, the metamorphosis is completed, but the post-larvae are typically not yet fully active swimmers. Post-larvae remaining in the surface water (Graham and Hop 1995) might seek refuge under the sea ice and can get carried along with the sea ice drift. Assuming a larval growth rate of 0.188 mm d^{-1} for a mean under-ice temperature of -1.5ºC (growth = 0.032* temperature + 0.236) (Bouchard and

Fortier 2011) and considering that larvae spent 120 days from summer until ice formed near coastal areas, plus around 300 days mean drift of the sampled sea ice (Table 2), we would expect mainly first-year polar cod with total lengths between about 88 and 128 mm in our under-ice catches, which agrees well with our observations. Hence, it appears realistic that young polar cod recruited to the sea ice in the Kara and Laptev Seas, and subsequently drifted into the central Arctic Ocean.

In spite of such strong circumstantial evidence, however, polar cod distribution in the central Arctic Ocean may alternatively or in combination with sea ice drift be driven by other vectors, such as ocean currents and migration of fish that associate with the sea ice underside at an older age.

The ecological importance of under-ice polar cod in the central Arctic Ocean

The central role of polar cod in the Arctic marine food web is mainly related to their high standing biomass on the Arctic shelves (Hop and Gjøsæter 2013). Huge aggregations of polar cod estimated from coastal areas were found to be a sufficient energy resource to support the high abundance of top predators reported for the same regions (Crawford and Jorgenson 1996; Matley et al. 2012; Welch et al. 1992; Welch et al. 1993). However, no large-scale polar cod stock estimates exist from the ice-covered central Arctic Ocean.

The mere omnipresence of polar cod we found over such vast area, even considering minimum abundances, indicates the potential of central Arctic under-ice habitats to host a significant fish stock. This stock could be indicative of a substantial trophic carbon flux in a central Arctic Ocean assumed to deliver relatively low primary productivity compared to the Arctic shelves (Fernández-Méndez et al. 2015). Spatial and seasonal heterogeneity of primary production and consumers connecting algal biomass to fish might influence fish sparse distribution.

The outcome of statistical models and high energy content of the fish suggest that during the drift phase, polar cod were indeed closely associated with the underside of sea ice, where they found ample high-energy food to survive the drift, until they begin their first spawning cycle. By advection with the Transpolar Sea Ice Drift, juvenile polar cod hatched on the Siberian shelf could potentially recruit to populations in the Svalvard archipelago, Barents Sea, and Greenland Sea, enhancing genetic exchange among polar cod populations around the Arctic Ocean. In spite of relatively low fish abundance, their omnipresence over the entire Eurasian Basin indicates that the central Arctic under-ice habitats may constitute a favourable environment for polar cod survival and a potential source of genetic exchange and recruitment for coastal populations. As the central Arctic will be exposed to further shortening of the ice-covered season and reduced sea ice extent, it remains unclear how the under-ice subpopulation will be affected and to which extent this will impact the pan-Arctic population of polar cod.

Compliance with Ethical Standards

This article does not contain any studies with human participants performed by any of the authors or any experimental studies with animals performed by any of the authors. All work were performed according to and within the regulations enforced by the German Animal Welfare Organisation and no specific permissions were required. The R/V Polarstern is operated by Alfred Wegener Institute and has all necessary authorization to use trawls to collect animals for scientific purposes. The organisms collected are neither protected nor endangered in the central Arctic waters.

Acknowledgements

We thank Captain Uwe Pahl and the crew of RV Polarstern expedition IceArc (ARK XXVII/3) for their excellent support with work at sea. We thank Michiel van Dorssen for operational and technical support with the Surface and Under Ice Trawl (SUIT). SUIT was developed by IMARES with support from the Netherlands Ministry of EZ (project WOT-04-009-036) and the Netherlands Polar Program (projects ALW 851.20.011 and 866.13.009). We thank Felipe Oliveira Ribas and Sander Holthuijsen from the Royal Netherlands Institute for Sea Research (NIOZ) for their support in energy content measurements in fish samples. This study is part of the Helmholtz Association Young Investigators Group *Iceflux*: Ice-ecosystem carbon flux in polar oceans (VH-NG-800). We thank the three anonymous reviewers for their helpful suggestions and comments that contributed significantly to the improvement of the manuscript.

References

Anthony JA, Roby DD, Turco KR (2000) Lipid content and energy density of forage fishes from the northern Gulf of Alaska. J Exp Mar Biol Ecol 248:53-78. doi:10.1016/S0022-0981(00)00159-3

Barbosa AM, Brown JA, Jimenez-Valverde A, Real R (2015) modEvA: Model Evaluation and Analysis. URL: http://R-Forge.R-project.org/projects/modeva/

Benoit D, Simard Y, Fortier L (2008) Hydroacoustic detection of large winter aggregations of Arctic cod (*Boreogadus saida*) at depth in ice-covered Franklin Bay (Beaufort Sea). J Geophys Res Oceans 113. doi:10.1029/2007JC004276

Benoit D, Simard Y, Fortier L (2014) Pre-winter distribution and habitat characteristics of polar cod (*Boreogadus saida*) in southeastern Beaufort Sea. Polar Biol 37:149-163. doi:10.1007/s00300-013-1419-0

Boetius A et al. (2013) Export of Algal Biomass from the Melting Arctic Sea Ice. Science 339:1430-1432. doi:10.1126/science.1231346

Bouchard C, Fortier L (2008) Effects of polynyas on the hatching season, early growth and survival of polar cod *Boreogadus saida* in the Laptev Sea. Mar Ecol Prog Ser 355:247-256. doi:10.3354/Meps07335

Bouchard C, Fortier L (2011) Circum-arctic comparison of the hatching season of polar cod *Boreogadus saida*: A test of the freshwater winter refuge hypothesis. Progr Oceanogr 90:105-116. doi:10.1016/j.pocean.2011.02.008

Bradstreet MSW, Cross WE (1982) Trophic Relationships At High Arctic Ice Edges. Arctic 35:1-12

Brekke B, Gabrielsen G (1994) Assimilation efficiency of adult Kittiwakes and Brünnich's Guillemots fed Capelin and Arctic Cod. Polar Biol 14:279-284. doi:10.1007/bf00239177

Cairns D (1987) Diet and foraging ecology of Black guillemots in Northeastern Hudson Bay. Can J Zool 65:1257-1263

Craig PC, Griffiths WB, Haldorson L, McElderry H (1982) Ecological Studies of Arctic Cod (*Boreogadus saida*) in Beaufort Sea Coastal Waters, Alaska. Can J Fish Aquat Sci 39:395-406. doi:10.1139/f82-057

Crawford R, Jorgenson J (1996) Quantitative studies of Arctic cod (*Boreogadus saida*) schools: important energy stores in the Arctic food web. Arctic 49:181-193

David C, Lange B, Rabe B, Flores H (2015) Community structure of under-ice fauna in the Eurasian central Arctic Ocean in relation to environmental properties of sea ice habitats. Mar Ecol Prog Ser 522:15-32. doi:10.3354/meps11156

Elliott KH, Gaston AJ (2008) Mass–length relationships and energy content of fishes and invertebrates delivered to nestling thick-billed murres *Uria lomvia* in the Canadian Arctic, 1981–2007. Mar Ornithol 36:25-34

Falk-Petersen I-B, Frivoll V, Gulliksen B, Haug T (1986) Occurrence and size/age relations of polar cod, *Boreogadus Saida* (Lepechin), in Spitsbergen coastal waters. Sarsia 71:235-245. doi:10.1080/00364827.1986.10419693

Fernández-Méndez M, Rabe B, Katlein C, Nicolaus M, Peeken I, Flores H, Boetius A (2015) Photosynthetic production in the Central Arctic during the record sea ice minimum in 2012. Biogeosciences discussions 12:2897–2945. doi:10.5194/bgd-12-2897-2015

Fetterer F, Knowles K, Meier W, Savoie M (2002, updated daily) Sea Ice Index. Monthly Mean Sea Ice Extent. Boulder, Colorado USA: National Snow and Ice Data Center. doi:10.7265/N5QJ7F7W

Flores H et al. (2012) The Association of Antarctic Krill *Euphausia superba* with the Under-Ice Habitat. PLoS ONE 7. doi:10.1371/journal.pone.0031775

Fortier L, Sirois P, Michaud J, Barber D (2006) Survival of Arctic cod larvae (*Boreogadus saida*) in relation to sea ice and temperature in the Northeast Water Polynya (Greenland Sea). Can J Fish Aquat Sci 63:1608-1616. doi:10.1139/f06-064

Fowler C, Emery W, Tschudi M (2013) Polar Pathfinder Daily 25 km EASE-Grid Sea Ice Motion Vectors. Version 2. (daily and mean gridded field). Boulder, Colorado USA: NASA National Snow and Ice Data Center Distributed Active Archive Center. doi:10.5067/LHAKY495NL2T

Geoffroy M, Majewski A, LeBlanc M, Gauthier S, Walkusz W, Reist JD, Fortier L (2015) Vertical segregation of age-0 and age-1+ polar cod (*Boreogadus saida*) over the annual cycle in the Canadian Beaufort Sea. S.I. Arctic Gadids of Polar Biol

Geoffroy M, Robert D, Darnis G, Fortier L (2011) The aggregation of polar cod (*Boreogadus saida*) in the deep Atlantic layer of ice-covered Amundsen Gulf (Beaufort Sea) in winter. Polar Biol 34:1959-1971. doi:10.1007/s00300-011-1019-9

Gjøsæter H, Prozorkevich D (2012) In: Eriksen E (Ed.) Survey report from the joint Norwegian/Russian ecosystem survey in the Barents Sea August-October 2012. IMR/PINRO Joint Report Series, No. 2/2012. ISSN 1502-8828, pages 50-56.

Gradinger RR, Bluhm BA (2004) In-situ observations on the distribution and behavior of amphipods and Arctic cod (*Boreogadus saida*) under the sea ice of the High Arctic Canada Basin. Polar Biol 27:595-603. doi:10.1007/s00300-004-0630-4

Graham M, Hop H (1995) Aspects of reproduction and larval biology of Arctic cod (*Boreogadus saida*). Arctic 48:130-135

Harter BB, Elliott KH, Divoky GJ, Davoren GK (2013) Arctic Cod (*Boreogadus saida*) as Prey: Fish Length-Energetics Relationships in the Beaufort Sea and Hudson Bay. Arctic 66:191–196

Haug T, Tormod Nilssen K, Lindblom L, Lindstrøm U (2007) Diets of hooded seals (*Cystophora cristata*) in coastal waters and drift ice waters along the east coast of Greenland. Mar Biol Res 3:123-133. doi:10.1080/17451000701358531

Hop H, Gjøsæter H (2013) Polar cod (*Boreogadus saida*) and capelin (*Mallotus villosus*) as key species in marine food webs of the Arctic and the Barents Sea. Mar Biol Res 9:878-894. doi:10.1080/17451000.2013.775458

Hop H, Mundy C, Gosselin M, Rossnagel A, Barber D (2011) Zooplankton boom and ice amphipod bust below melting sea ice in the Amundsen Gulf, Arctic Canada. Polar Biol 34:1947-1958. doi:10.1007/s00300-011-0991-4

Hop H, Pavlova O (2008) Distribution and biomass transport of ice amphipods in drifting sea ice around Svalbard. Deep Sea Res Part II Top Stud Oceanogr 55:2292-2307. doi:10.1016/j.dsr2.2008.05.023

Hop H, Tonn WM, Welch HE (1997a) Bioenergetics of Arctic cod (*Boreogadus saida*) at low temperatures. Can J Fish Aquat Sci 54:1772-1784

Hop H, Trudeau VL, Graham M (1995) Spawning energetics of Arctic cod (*Boreogadus saida*) in relation to seasonal development of the ovary and plasma sex steroid levels. Can J Fish Aquat Sci 52:541-550. doi:10.1139/f95-055

Hop H, Welch HE, Crawford RE (1997b) Population structure and feeding ecology of Arctic cod schools in the Canadian High Arctic. In: Reynolds J (ed) Fish Ecology in Arctic North America, Fairbanks, Alaska, 19–21 May 1992. Am Fish Soc Symp 19, Bethesda, Maryland, pp 68-80

IPCC (2014) Climate Change 2014: Impacts, Adaptation, and Vulnerability. Part A: Global and Sectoral Aspects. Contribution of Working Group II to the Fifth Assessment Report of the Intergovernmental Panel on Climate Change [Field, C.B., V.R. Barros, D.J. Dokken, K.J. Mach, M.D. Mastrandrea, T.E. Bilir, M. Chatterjee, K.L. Ebi, Y.O. Estrada, R.C. Genova, B. Girma, E.S. Kissel, A.N. Levy, S. MacCracken, P.R. Mastrandrea, and L.L. White (eds.)]. Cambridge University Press, Cambridge, United Kingdom and New York, NY, USA

Krumpen T, Janout M, Hodges KI, Gerdes R, Girard-Ardhuin F, Holemann JA, Willmes S (2013) Variability and trends in Laptev Sea ice outflow between 1992-2011. Cryosphere 7:349-363. doi:10.5194/tc-7-349-2013

Kwok R, Rothrock DA (2009) Decline in Arctic sea ice thickness from submarine and ICESat records: 1958-2008. Geophys Res Lett 36:L15501. doi:10.1029/2009gl039035

Lønne O, Gabrielsen G (1992) Summer diet of seabirds feeding in sea-ice-covered waters near Svalbard. Polar Biol 12:685-692

Lønne O, Gulliksen B (1989) Size, age and diet of polar cod, *Boreogadus saida* (Lepechin 1773), in ice covered waters. Polar Biol 9:187-191

Markus T, Stroeve JC, Miller J (2009) Recent changes in Arctic sea ice melt onset, freezeup, and melt season length. J Geophys Res Oceans 114:C12024. doi:10.1029/2009jc005436

Matley J, Fisk A, Dick T (2013) The foraging ecology of Arctic cod (*Boreogadus saida*) during open water (July–August) in Allen Bay, Arctic Canada. Mar Biol 160:2993-3004. doi:10.1007/s00227-013-2289-2

Matley JK, Crawford RE, Dick TA (2012) Summer foraging behaviour of shallow-diving seabirds and distribution of their prey, Arctic cod (*Boreogadus saida*), in the Canadian Arctic. Polar Res 31. doi:10.3402/polar.v31i0.15894

McCullagh P, Nelder JA (1989) Generalized linear models. vol 2. Chapman and Hall London, United Kingdom

Melnikov IA, Chernova NV (2013) Characteristics of under-ice swarming of polar cod *Boreogadus saida* (Gadidae) in the Central Arctic Ocean. J Ichthyol 53:7-15. doi:10.1134/s0032945213010086

Nahrgang J, Camus L, Broms F, Christiansen JS, Hop H (2010) Seasonal baseline levels of physiological and biochemical parameters in polar cod (*Boreogadus saida*): Implications for environmental monitoring. Mar Pollut Bull 60:1336-1345. doi:10.1016/j.marpolbul.2010.03.004

Nahrgang J, Varpe O, Korshunova E, Murzina S, Hallanger IG, Vieweg I, Berge J (2014) Gender specific reproductive strategies of an arctic key species (*Boreogadus saida*) and implications of climate change. PLoS ONE 9:e98452. doi:10.1371/journal.pone.0098452

Ponomarenko V (2000) Eggs, larvae, and juveniles of polar cod *Boreogadus saida* in the Barents, Kara, and White Seas. J Ichthyol 40:165-173

R Core Team (2015) R: A language and environment for statistical computing. R Foundation for Statistical Computing, Vienna, Austria. URL http://www.R-project.org/

Rabe B, Wisotzki A, Rettig S, Somavilla Cabrillo R, Sander H (2012) Physical oceanography during POLARSTERN cruise ARK-XXVII/3 (IceArc). *Alfred Wegener Institute, Helmholtz Center for Polar and Marine Research, Bremerhaven*. doi:10.1594/PANGAEA.802904

Rigor IG, Wallace JM (2004) Variations in the age of Arctic sea-ice and summer sea-ice extent. Geophys Res Lett 31. doi:10.1029/2004gl019492

Rozman P et al. (2011) Validating satellite derived and modelled sea-ice drift in the Laptev Sea with in situ measurements from the winter of 2007/08. Polar Res 30. doi:10.3402/Polar.V30i0.7218

Rudels B, Schauer U, Björk G, Korhonen M, Pisarev S, Rabe B, Wisotzki A (2013) Observations of water masses and circulation in the Eurasian Basin of the Arctic Ocean from the 1990s to the late 2000s. Ocean Science Discussions 9:147-169. doi:10.5194/os-9-147-2013

Scott CL, Falk-Petersen S, Sargent JR, Hop H, Lønne OJ, Poltermann M (1999) Lipids and trophic interactions of ice fauna and pelagic zooplankton in the marginal ice zone of the Barents Sea. Polar Biol 21:65-70. doi:10.1007/s003000050335

Shaw W, Stanton T, McPhee M, Morison J, Martinson D (2009) Role of the upper ocean in the energy budget of Arctic sea ice during SHEBA. J Geophys Res Oceans 114. doi:10.1029/2008JC004991

Shimada K et al. (2006) Pacific Ocean inflow: Influence on catastrophic reduction of sea ice cover in the Arctic Ocean. Geophys Res Lett 33. doi:10.1029/2005gl025624

Snyder JP (1992) An Equal-Area Map Projection For Polyhedral Globes. Cartographica: The International Journal for Geographic Information and Geovisualization 29:10-21. doi:10.3138/27h7-8k88-4882-1752

Søreide JE, Hop H, Carroll ML, Falk-Petersen S, Hegseth EN (2006) Seasonal food web structures and sympagic–pelagic coupling in the European Arctic revealed by stable isotopes and a two-source food web model. Progr Oceanogr 71:59-87. doi:10.1016/j.pocean.2006.06.001

Stroeve J, Serreze M, Holland M, Kay J, Malanik J, Barrett A (2012) The Arctic's rapidly shrinking sea ice cover: a research synthesis. Climatic Change 110:1005-1027. doi:10.1007/s10584-011-0101-1

Sumata H et al. (2014) An intercomparison of Arctic ice drift products to deduce uncertainty estimates. J Geophys Res Oceans 119:4887-4921. doi:10.1002/2013jc009724

Van de Putte A, Flores H, Volckaert F, van Franeker J (2006) Energy Content of Antarctic Mesopelagic Fishes: Implications for the Marine Food Web. Polar Biol 29:1045-1051. doi:10.1007/s00300-006-0148-z

Van de Putte AP, Jackson GD, Pakhomov E, Flores H, Volckaert FAM (2010) Distribution of squid and fish in the pelagic zone of the Cosmonaut Sea and Prydz Bay region during the BROKE-West campaign. Deep-Sea Res Pt II 57:956-967

van Franeker JA, Flores H, Van Dorssen M (2009) Surface and Under Ice Trawl (SUIT). In: Flores H (author) Frozen Desert Alive -The role of sea ice for pelagic macrofauna and its predators: implications for the Antarctic pack-ice food web. Dissertation, University of Groningen, Groningen, Netherlands

Vaz S, Martin CS, Eastwood PD, Ernande B, Carpentier A, Meaden GJ, Coppin F (2008) Modelling species distributions using regression quantiles. J Appl Ecol 45:204-217. doi:10.1111/j.1365-2664.2007.01392.x

Welch HE et al. (1992) Energy Flow through the Marine Ecosystem of the Lancaster Sound Region, Arctic Canada. Arctic 45:343-357

Welch HE, Crawford RE, Hop H (1993) Occurrence of Arctic cod (*Boreogadus saida*) schools and their vulnerability to predation in the Canadian High Arctic. Arctic 46:331-339

Wilcoxon F (1945) Individual comparisons by ranking methods. Biometrics Bulletin 1:80-83

Weslawski JM, Ryg M, Smith TG, Oritsland NA (1994) Diet of ringed seals (*Phoca hispida*) in a fjord of West Svalbard. Arctic 47:109-114

2.3. *Chapter III*

Community structure of under-ice fauna in relation to winter sea-ice habitat properties from the Weddell Sea

Carmen David[1,2*], Fokje Schaafsma[3], Jan Andries van Franeker[3],
Benjamin Lange[1,2], Angelika Brandt[2], Hauke Flores[1,2]

[1] Alfred Wegener Institut Helmholtz-Zentrum für Polar- und Meeresforschung (AWI), Am Handelshafen 12, 27570, Bremerhaven, Germany; [2] University Hamburg, Centre for Natural History (CeNak), Zoological Museum, Martin-Luther-King Platz 3, 20146, Hamburg, Germany; [3] Institute for Marine Research and Ecosystem Studies Wageningen UR (IMARES), PO Box 57, 1781 AG Den Helder, The Netherlands

under review in Polar Biology
Manuscript number: POBI-D-15-00239

ABSTRACT

Climate change-related alterations of Antarctic sea-ice habitats are expected to significantly impact the interaction of ice-associated organisms with the environment, with repercussions on ecosystem functioning. The nature of this interaction is poorly understood, particularly during the critical period of winter-spring transition. The aim of this study was to investigate the role of sea-ice and underlying water-column properties in structuring the under-ice communities during late winter/early spring. We used a Surface and Under Ice Trawl to sample the community in the ice-water interface layer in the northern Weddell Sea from August to October 2013. The under-ice community was numerically dominated by the copepods *Stephos longipes*, *Ctenocalanus* spp. and *Calanus propinquus* (67%) and furcilia larvae of Antarctic krill *Euphausia superba* (30%). Abundance and biomass distributions at our sampling stations indicated the presence of three community types, following a geographical gradient in the investigation area: (1) high biomass, krill-dominated in the west, (2) high abundance, copepod-dominated in the east, and (3) low abundance, low biomass at the ice edge. Combined analysis with environmental data indicated that community structure was correlated with sea-ice coverage, salinity and bottom depth. With the sample size of this study, strong relationships between community composition and sea-ice habitat properties could not be detected. The results of this study show that the Antarctic under-ice community is rather heterogeneous, probably driven by biogeographic distribution patterns, sea ice habitat properties, and seasonal progression. The response of under-ice communities to changing sea-ice habitats may thus considerably vary seasonally and regionally.

INTRODUCTION

The most prominent environmental feature of the Southern Ocean is a seasonal pack-ice cover varying in extent from four million km^2 in summer to twenty million km^2 in winter (Gloersen and Campbell 1991; Turner et al. 2013; Zwally et al. 2002). Phytoplankton primary production can exceed 2 g C m^{-2} d^{-1} during summer and drops to nearly zero in winter (Arrigo et al. 2008). During winter, the main primary production occurs within sea ice, making sea-ice habitats an important seasonal refuge for many species (Lizotte 2001; Quetin et al. 2013; Siegel and Loeb 1995; Thomas and Dieckmann 2002).

Sea ice hosts a specific algal community that can serve as a critical carbon source for young Antarctic krill *Euphausia superba* (hereafter referred to as krill) (Atkinson et al. 2002; O'Brien 1987; Schmidt et al. 2014) and a variety of other species (Gannefors et al. 2005; Hopkins and Torres 1989; Hopkins et al. 1993). Besides ice algae, other resources provided by sea-ice habitats such as protozoans, small copepods and detritus may offer an alternative food source for ice-associated species during winter (Daly 1990; Gannefors et al. 2005; Meyer 2012; Schmidt et al. 2014). Substantial top predator communities foraging in ice-covered regions (Ainley et al. 2007, 2012; Loeb et al. 1997; van Franeker et al. 1997) indicates the potential of the under-ice habitat to sustain large productivity.

The Weddell Sea is one of the most productive sectors of the Southern Ocean (Arrigo et al. 1997, 2008). Its main feature is the Weddell Gyre, which is shaped by the influence of bathymetry and northern islands, enclosing this area as a distinct biogeographical region, entirely sea ice covered during winter (De Broyer et al. 2014). Only few winter studies exist from this area, since logistic difficulties in extreme environmental winter conditions impede field work (Flores et al. 2011; Hunt et al. 2011).

Many studies in the Southern Ocean focused on krill (Atkinson et al. 2008; Flores et al. 2012; Meyer 2012), on sea-ice meiofauna (Schnack-Schiel et al. 2001a, 2001b, 2008a), or on the pelagic community structure (Hunt et al. 2011; Pakhomov and Froneman 2004; Schnack-Schiel et al. 2008b; Yang et al. 2011), but not much is known about meso- and macrofauna communities living at the sea-ice water interface layer. Typically, the surface community is integrated into the epipelagic community (Fisher et al. 2004; Giesecke and González 2012; Hunt et al. 2011; White and Piatkowski 1993), even though the surface layer is known to host a distinct community (Flores et al. 2014; Krakatitsa 1993). In the Lazarev Sea, Flores et al. (2014) found a marked difference in macrofauna community structure between the 0-2 m surface layer and the 0-200 m epipelagic layer. In addition, Flores et al. (2014) demonstrated a significant response of surface macrofauna communities to sea-ice properties in the Lazarev Sea.

Sampling under pack-ice, however, is particularly challenging. Most commonly, ice-associated macrofauna have been sampled by scuba divers. This method is excellent in describing the small-scale structure of sea-ice habitats during sampling, yet the larger scale spatial distribution and variability of the organisms, and species diversity may not be representatively sampled. Furthermore, there is a need to record habitat properties simultaneously with species sampling on larger spatial scales in order to realistically relate species distribution with their habitat variability and dynamics.

Using the Surface and Under Ice Trawl (SUIT), we studied the community composition of under-ice fauna during late winter 2013 in the Weddell Sea. With an attached sensors array, the SUIT recorded environmental parameters while sampling over profiles of approximately 1-3 km in length. This study aims to describe the association of faunal communities in the under-ice water layer (0-2 m) with the sea-ice habitat properties during winter. In particular we address the following objectives: 1) to provide an inventory of winter under-ice fauna in the northern Weddell Sea, and to highlight dominant species defining the under-ice communities and 2) to investigate the role of sea-ice habitat properties in structuring the under-ice community.

MATERIALS AND METHODS

Sampling technique and data collection

Sampling was performed during RV *Polarstern* expedition PS 81 (ANT XXIX/7), between 31 August and 2 October 2013, across the ice-covered Weddell Sea, between 61°S, 42°W and 58°S, 25°W (Fig. 1). Eleven stations were sampled, four during daytime and seven during nighttime (Table 1). The first seven stations (Stns 551-567) were sampled from west to east approximately along the 60ºS parallel, and the last four stations (Stns 570-579) northward along the 26ºW meridian (Fig.1). These last four stations were positioned at the eastern side of South Sandwich Islands, in shallower waters than the earlier stations (Fig.1, Table 1). Stations 567-579 were sampled almost two weeks after stations 551-565.

Horizontal hauls were performed with the Surface and Under Ice Trawl (SUIT) (Flores et al. 2012; van Franeker et al. 2009). The SUIT consisted of a steel frame with a 2 m x 2 m opening and two parallel 15 m long nets attached: 1) a 7 mm half-mesh commercial shrimp net, which covered 1.5 m of the opening width and was lined with 0.3 mm mesh at the rearmost 3 m of the net; and 2) a 0.3 mm mesh zooplankton net, which covered 0.5 m of the opening width. Floats attached to the top of the frame kept the net at the surface or the sea ice underside. To enable sampling under undisturbed ice, an asymmetric bridle forces the net to shear away from the ship, towing at an angle of approximately 60° to starboard of the ship's track, at a cable length of 150 m. A detailed description of the SUIT sampling technique and performance was provided as supplementary material in Flores et al. (2012). Depending on the sea-ice conditions, SUIT haul durations varied between 17 and 42 min (mean = 29 min) over an average distance of 1.5 km (Table 1).

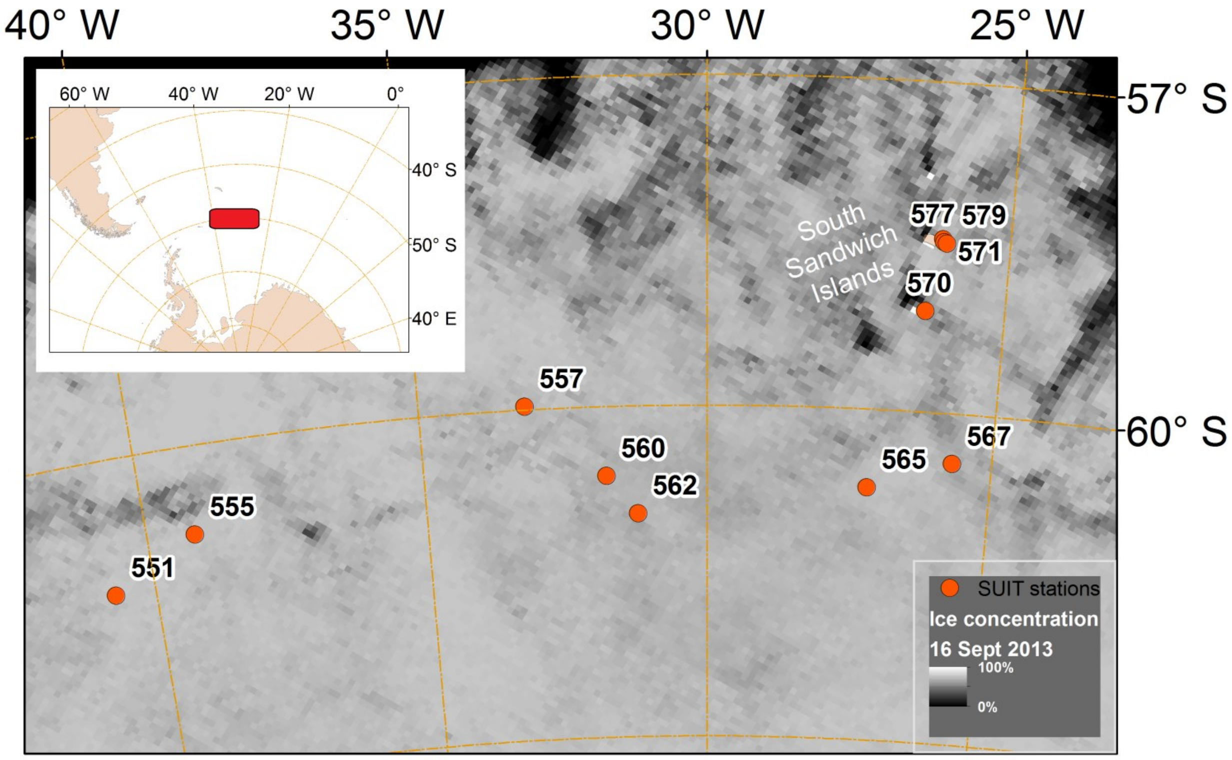

Figure 1. SUIT station map during RV *Polarstern* expedition ANT XXIX/7. Sea-ice concentration acquired from Bremen of University (http://www.iup.uni-bremen.de: 8084/amsr/); sampling was performed from west to east, from August to October 2013. Number codes next to sampling locations indicate station numbers

Table 1. Station table with the environmental variables characterising sea-ice habitats; abbreviations used in the text as indicated in the parentheses: Bottom depth (Depth), Satellite sea-ice coverage averaged over 6.25 km grid cell (Coverage), Modal sea-ice thickness (Thickness), Snow layer thickness (Snow), Roughness of sea ice thickness (Roughness), Surface water temperature (Temperature), Surface water salinity (Salinity), Chlorophyll *a* concentration at the surface (Chlorophyll *a*)

Station code	Date	Sampling time	Latitude (°S)	Longitude (°W)	Depth (m)	Trawling distance (m)	Coverage (%)	Thickness (m)	Snow (m)	Roughness	Temperature (°C)	Salinity	Chlorophyll *a* (mg m^{-3})
551	8/31/2013	Night	61.22	40.72	2525	834	87.5	0.300	0.2-0.5	NA	-1.84	34.4	0.110
555	9/9/2013	Day	60.80	39.15	3308	1761	99.5	0.475	0.2-0.5	3.734	-1.85	34.3	0.104
557	9/10/2013	Night	59.96	33.17	3427	1429	94.0	0.700	0.075	0.833	-1.86	33.9	0.134
560	9/11/2013	Night	60.63	31.78	1841	1290	96.0	0.525	0.1	1.030	-1.86	33.8	0.108
562	9/12/2013	Night	60.97	31.24	2409	946	92.5	0.525	0.25	0.969	-1.86	33.8	0.097
565	9/16/2013	Day	60.71	27.17	3399	928	96.5	0.525	0.25	2.297	-1.87	34.2	0.103
567	9/28/2013	Night	60.45	25.70	6158	558	86.5	0.675	0.6	1.148	-1.88	33.6	0.204
570	9/29/2013	Night	59.08	26.34	940	1524	96.0	0.425	0.15	0.853	-1.86	33.9	0.223
571	9/30/2013	Day	58.42	26.11	1024	1987	84.0	0.225	0.05	0.829	-1.84	34.1	0.165
577	10/2/2013	Day	58.44	26.10	1006	3178	51.5	0.475	0.2-0.5	1.207	-1.84	33.7	0.164
579	10/2/2013	Night	58.46	26.05	1195	2731	46.0	0.575	NA	1.504	-1.83	34.1	0.275

Environmental data

A sensor array was mounted in the SUIT frame, including a Conductivity Temperature Depth probe (CTD) with built-in fluorometer, two spectral radiometers, and a video camera. Water inflow speed and direction were estimated using a Nortek Aquadopp® Acoustic Doppler Current Profiler (ADCP). Temperature and salinity profiles were obtained with a Sea and Sun CTD75M probe. Calibration of fluorometric chlorophyll *a* concentrations was done from water samples obtained during stationary work. The calibration coefficients were derived from the linear relationship between chlorophyll *a* concentrations of water samples (measured with a Turner 10-AU fluorometer) with fluorometric chlorophyll *a* concentrations of the corresponding 10 m depth range. Data gaps in the CTD measurements caused by low battery voltage were filled using complementary datasets from the shipboard sensors (temperature, salinity and chlorophyll *a* at Stns 557, 560 and at Stn 562 only for chlorophyll *a*), using correction factors determined by linear regression. An altimeter Tritech PA500/6-E connected to the CTD measured the distance between the net and the sea-ice underside. Sea-ice draft was calculated as the difference between the depth of the net relative to the water level, measured by the CTD pressure sensor, and the distance to the sea-ice underside, measured by the altimeter, and corrected for pitch and roll angles. Draft was then converted into sea-ice thickness by using a sea-ice density value of 900 kg m^{-3}. Sea-ice roughness was calculated after the formula:

$$roughness = \sqrt{\frac{1}{n}(x_1^2 + x_2^2 + \cdots + x_n^2)}.$$

where (x_1, $x_{2, \ldots,}$ x_n) is the set of n values of sea-ice thickness along one sampling profile.

The trawled area was calculated by multiplying the distance sampled in water, estimated from ADCP data, with the net width (0.5 m for the zooplankton net, and 1.5 m for the shrimp net respectively).

During each haul, sea-ice concentration [%], sea-ice thickness and snow depth, changes in ship speed and irregularities were estimated visually by an observer on deck. A detailed description of environmental data acquisition was provided in David et al. (2015).

Gridded daily sea-ice concentrations for the Southern Ocean derived from AMSR2 satellite data, using the algorithm specified by Spreen et al. (2008), were downloaded from the sea-ice portal hosted by University Bremen and Alfred Wegener Institute (www.meereisportal.de).

Biological data

The catch was partially sorted on board. Ctenophores were immediately extracted from samples, identified and their volume was measured. Several species were sampled for lipid and stable isotope analyses (data not included in this study). The remaining material was then preserved in 4% formaldehyde/seawater solution for quantitative analysis. After the cruise, the quantitative samples were analysed for species composition and abundance at the Alfred Wegener Institute. Macrofauna (> 0.5 cm) abundances were derived from the analysis of the shrimp net samples. Mesozooplankton abundances were derived from analysis of the zooplankton net samples. High abundance zooplankton samples were fractionated with a plankton splitter (Motoda 1959), and only a sub-sample (1/2 to 1/8 depending on the sample size) of the original sample was counted and subsequently scaled to the full sample size by multiplication with the subsampling factor. With few exceptions, all animals were identified to the species level, and to developmental stage and sex in krill and copepod species. The adult copepods and their juvenile stages were both considered in abundance calculations. Areal abundances were calculated dividing the total number of animals per haul by the trawled area. In all macrofauna species, total body length was measured to the nearest 1 mm, and a mean size per species was used for biomass calculations. Zooplankton biomass was calculated using known species length to weight relationships and was expressed as mg dry weight m^{-2} (Mizdalski 1988). For copepod species, separated into developmental stages, and ostracods a mean dry weight was theoretically assumed (Mizdalski 1988). A list of all species including names of authors and years of description is presented in Table 2.

Data analysis

The patterns of diversity over the sampling area were investigated by three diversity indices, calculated for the whole biological dataset: (1) species richness (the number of species observed at each station) [S]; (2) the Shannon index [H] (Shannon 1948); and (3) Pielou's evenness index [J].

Species abundance data were analysed using Non-Metric Multidimensional Scaling (NMDS) (Kruskal 1964) based on a Bray-Curtis dissimilarity matrix (Bray and Curtis 1957). The NMDS is commonly regarded as the most robust unconstrained ordination method in community ecology (Minchin 1987). The performance of the NMDS was assessed with Shepard plots and stress values (Clarke and Warwick 2001). A hierarchical clustering of the sampling stations was performed using the Bray-Curtis dissimilarity matrix of the species abundance data (Legendre and Legendre 2012).

Table 2. List of species with their mean abundances and frequency of occurrence over the sampling area

Taxon	Mean abundance (ind. 100 m^{-2})	Standard deviation	Range	Frequency of occurrence
CTENOPHORA				
Beroe spp. Fabricius, 1780	0.02	0.05	0-0.18	0.09
Callianira antarctica Chun, 1897	0.02	0.04	0-0.11	0.27
Siphonophora				
Diphyes antarctica Moser, 1925	0.14	0.18	0-0.60	0.63
Marrus sp.	<0.01	0.01	0-0.04	0.09
Unidentified siphonophore	1.25	1.73	0-5.29	0.82
MOLLUSCA				
Pteropoda				
Clione limacina Phipps, 1774	0.06	0.08	0-0.23	0.45
Clio pyramidata Linnaeus, 1767	0.01	0.03	0-0.11	0.18
Limacina helicina Phipps, 1774	0.14	0.31	0-1.02	0.36
Spongiobranchaea australis d'Orbigny, 1834	0.06	0.08	0-0.27	0.64
Unidentified gastropod	0.23	0.41	0-1.08	0.64
ANNELIDA				
Polychaeta				
Tomopteris carpenteri Quatrefages, 1866	0.11	0.21	0-0.70	0.36
Unidentified polychaete 1	1.00	1.23	0-4.12	0.91
Unidentified polychaete 2	0.04	0.08	0-0.26	0.36
ARTHROPODA				
Crustacea				
Cyllopus lucasii Bate, 1862	0.15	0.21	0-0.63	0.55
Eusirus laticarpus Chevreux, 1906	1.48	1.50	0.06-5.02	1
Eusirus microps Walker, 1906	0.02	0.05	0-0.16	0.27
Hyperoche medusarum Krøyer, 1838	0.03	0.05	0-0.12	0.27
Primno macropa Guérin-Méneville, 1836	0.10	0.13	0-0.45	0.82
Themisto gaudichaudii Guérin, 1825	<0.01	0.01	0-0.04	0.09
Vibilia antarctica Stebbing, 1888	0.02	0.05	0-0.14	0.27
Unidentified gammarid amphipod	0.03	0.04	0-0.11	0.45
Euphausiacea				
Euphausia superba Dana, 1850	83.04	103.62	9.44-359.79	1
Euphausia frigida Hansen, 1911	0.01	0.02	0-0.08	0.09
Thysanoessa macrura Sars, 1883	0.11	0.12	0-0.36	0.64
Thysanoessa vicina Hansen, 1911	0.02	0.07	0-0.23	0.09
Decapoda				
Unidentified decapod	<0.01	0.01	0-0.04	0.09
Copepoda				
Calanus propinquus Brady, 1883	51.19	70.38	2.33-237.59	1
Ctenocalanus spp.	160.13	282.71	0.44-931.73	1
Euchirella rostromagna Wolfenden, 1905	0.38	0.70	0-1.72	0.27
Heterorhabdus austrinus Giesbrecht, 1902	0.18	0.24	0-0.63	0.45

Taxon	Mean abundance (ind. 100 m^{-2})	Standard deviation	Range	Frequency of occurrence
Idomene spp.	0.60	1.11	0-2.88	0.45
Metridia spp.	1.98	3.07	0-9.32	0.82
Oithona similis Claus, 1866	0.79	1.03	0-3.58	0.91
Paraeuchaeta sp.	0.56	0.97	0-3.17	0.45
Pseudocylopina sp.	5.16	9.47	0-30.93	0.73
Stephos longipes Giesbrecht, 1902	249.82	405.50	1.26-1326.23	1
Tharybis sp.	0.52	1.29	0-4.32	0.36
Unidentified harpacticoid	0.03	0.08	0-0.23	0.18
Ostracoda				
Unidentified ostracods	7.09	10.88	0-31.72	0.73
CHAETOGNATHA				
Eukrohnia hamata Möbius, 1875	0.03	0.08	0-0.27	0.27
Sagitta spp.	0.26	0.44	0-1.43	0.54
Sagitta gazellae Ritter-Záhony, 1909	0.09	0.19	0-0.63	0.36
Sagitta maxima Conant, 1896	0.07	0.23	0-0.77	0.09
Unidentified chaetognaths (*Eukrohnia* type)	0.63	0.60	0-1.97	0.91
CHORDATA				
Salpida				
Salpa thompsoni Foxton, 1961	0.13	0.22	0-0.72	0.54
Ihlea racovitzai Van Beneden & Selys	<0.01	0.01	0-0.03	0.09
Unidentified salpes	0.05	0.16	0-0.54	0.27
Appendicularia				
Oikopleura spp.	1.30	1.77	0.02-5.02	1
VERTEBRATA				
Osteichthyes				
Aethotaxis mitopteryx DeWitt, 1962	<0.01	0.02	0-0.05	0.09

To assess the statistical differences between day and night sampling, and geographical location of sampling sites, i.e. proximity to islands, the nonparametric Mann-Whitney-Wilcoxon test was performed on species abundance data (Wilcoxon 1945).

The association of the under-ice community structure with all possible combinations of environmental variables was evaluated with the BioEnv analysis (Clarke and Ainsworth 1993). The BioEnv analysis estimates the subset of environmental variables that has the highest correlation with the biological data. The association of the community structure with the selected subsets of environmental variables was evaluated with a Mantel test (Mantel 1967). The Mantel test relates 2 distance matrices, one from the biological and one from the environmental dataset, using Spearman correlation. The significance of Mantel test correlations was assessed with a bootstrapping procedure with 999 iterations.

For all analyses, R version 3.2.0 was used with the libraries 'vegan', 'FactoMineR', 'plyr' and 'MASS' (R Core Team 2015).

RESULTS

Sea-ice habitats

All 11 stations were ice-covered. Satellite-derived sea-ice concentrations at sampling locations, ranged from almost 50 to 100 %, with the lowest values present at the two northernmost stations 577 and 579 (Table 1). Modal sea-ice thickness ranged from 0.2 to 0.7 m. Snow depth ranged between 0.05 and 0.60 m. The sea-ice roughness coefficient generally varied between 0.8 and 2.3, with a maximal value of 3.7 at station 555. Surface-water temperature was on average -1.85ºC (range from -1.83 to -1.87 ºC) at a mean salinity of 34 (range 33.6 to 34.4). Surface-water chlorophyll *a* concentrations ranged between 0.10 and 0.27 mg m^{-3}.

Variability in species diversity, abundance and biomass distribution

In total, 45 species belonging to 12 phyla were identified in our samples (Table 2). Species richness (S) at most of the stations ranged between 20 and 28. The maximum number of 28 species was encountered at station 557, and the minimum of 9 species at station 577 (Table 3). The highest Shannon diversity (H) was encountered at station 579, and the highest evenness (J) at station 577. The lowest Shannon and evenness indices were found at station 560 (Table 3). No spatial patterns were noticed in the distribution of diversity indices.

Table 3. Diversity indices calculated at each sampling station

Station	Richness	Shannon	Evenness
551	19	1.58	0.54
555	23	1.34	0.43
557	28	1.31	0.39
560	23	0.86	0.27
562	23	1.00	0.32
565	20	1.54	0.51
567	25	1.20	0.37
570	21	1.33	0.44
571	16	1.43	0.51
577	9	1.59	0.72
579	22	1.70	0.55

Among higher level taxa, copepods had the highest abundances, accounting for 67% of the mean relative abundance over all stations, followed by euphausiids with 30% (Fig. 2). The balance between copepods and euphausiids, however, was markedly different between stations: at most stations, copepods accounted for about 70 to 95% of the abundance, whereas at stations 571, 577 and 579 copepods contributed only about 30% of the mean abundance. At stations 571, 577 and 579, the euphausiids dominated the species composition, accounting on average 65% of the mean abundance (Fig. 2). The other taxonomic groups each accounted for less than 1% of the abundance, yet most groups had high frequencies of occurrence (Table 2). Exceptions were salps, which were present at only six stations, and ctenophores, which were present at only four stations with no apparent spatial patterns (Table 2).

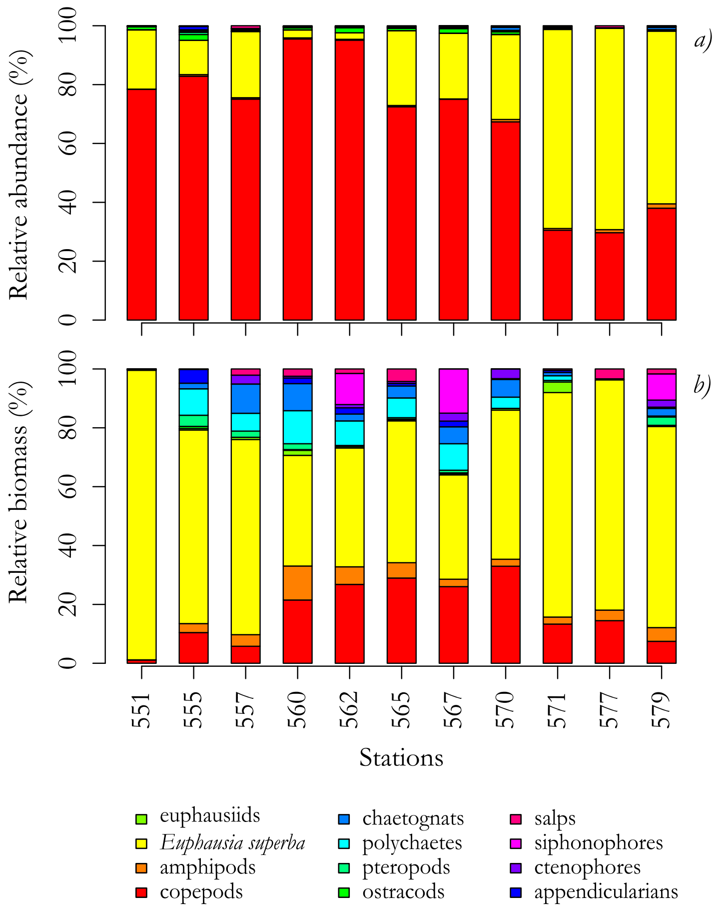

Figure 2. Relative a) abundance and b) biomass (dry weight) of taxonomic groups at the sampling stations (numbers on the *x*-axis).

Krill had the highest biomass as a single species, accounting for 60% of the mean biomass over all stations, while the other euphausiids together contributed less than 1% (Fig.2). Notably, krill heavily dominated total biomass at the first three and the last three stations. The second most important biomass-rich taxonomic group was copepods with 17% of the mean biomass over all stations. Four of the taxonomic groups had a noteworthy contribution to the total biomass: amphipods (4.1%), polychaetes (5.1%), chaetognaths (3.9%) and ctenophores (3.1%), while the contribution of the remaining taxonomic groups was approximately 1%.

Cumulative abundances of all species ranged from 0.1 ind. m^{-2} at station 577 to 18.7 ind. m^{-2} at station 562 (Fig. 3). The most abundant species were the small calanoid copepods *Stephos longipes* and *Ctenocalanus* spp., followed by the larger species *Calanus propinquus* (Table 2). The ice-associated cyclopoid *Pseudocyclopina* sp. occurred in higher numbers at stations 551, 555 and 567. The copepods were followed numerically by euphausiids, mainly Antarctic krill larvae and first-year juveniles. Sub-adult krill were only encountered in significant abundance at station 551. A detailed description of the population structure of first-year krill in the investigation area was provided by Schaafsma et al. (2016). Among the amphipods, the ice-associated species *Eusirus laticarpus* was numerically dominant at all stations.

The chaetognaths *Eukrohnia hamata* and *Sagitta* spp. were widely distributed over the sampled area with somewhat increased abundances at the stations with higher copepod abundances (Online Resource 1). *E. hamata* was highly correlated with the abundances of *C. propinquus* ($r = 0.91$), *Ctenocalanus* spp. ($r = 0.68$), and to a lesser extent krill larvae ($r = 48$). *Sagitta* spp. was correlated with krill larvae ($r = 0.56$) and *Ctenocalanus* spp. ($r = 0.66$) (Online Resource 2).

Cumulative dry-weight biomass of all species (except one fish *Aethotaxis mitopteryx* caught at station 562) at each station ranged from 0.1 mg DW m^{-2} at station 577 to 14.5 mg DW m^{-2} at station 551 (Fig. 3). Higher biomass encountered at the first three stations was largely driven by the contribution of krill and at stations 562 and 567 by a shared contribution of krill, copepods and ctenophores.

Community structure and association with sea-ice habitat properties

Based on the composition of zooplankton abundance and biomass at sampling stations, three community types were visually identified, namely: (1) *krill-dominated*, (2) *copepod-dominated,* and (3) *low biomass/abundance* (Fig. 3). The *'krill-dominated'* community was characterized by the high biomass contribution of larval, juvenile and adult krill, yet by relatively low cumulative abundances. The *krill-*

dominated community was present at the westernmost stations 551, 555 and 557 (Fig. 3). The *copepod-dominated* community had the highest cumulative abundances and was numerically dominated by copepods. It had variable to high biomass values, with a higher contribution from copepods and krill and moderate contribution of amphipods, polychaetes, chaetognaths and ctenophores. This *copepod-dominated* community was present at stations 560, 562, 565 and 567. The *low biomass/abundances* community was characterized by low cumulative abundances and biomass values. It was dominated by krill larvae in abundance and biomass. This community characterized the northernmost four stations 570, 571, 577 and 579, in close proximity to the marginal ice zone.

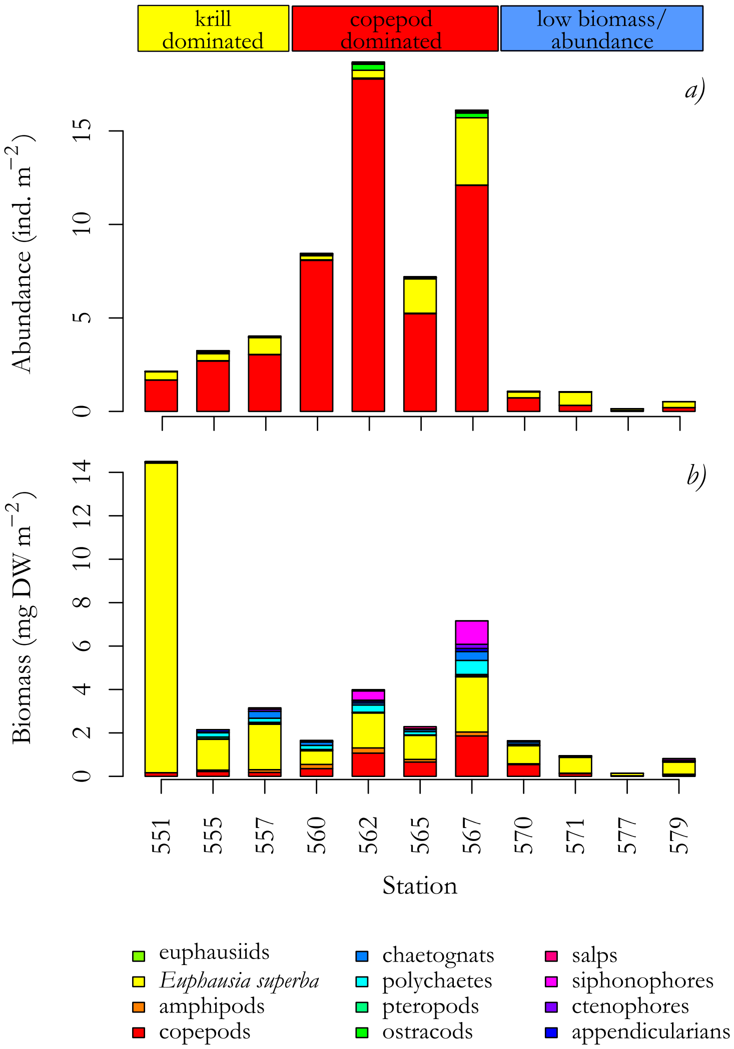

Figure 3. Cumulative a) abundance and b) biomass (dry weight) of taxonomic groups at the sampling stations (numbers on the *x*-axis).

The three community types were confirmed by the NMDS ordination and cluster analysis (Fig. 4). The first NMDS axis separated the '*copepod-dominated*' community type (stations 560-567), which was associated with amphipods, ostracods, *Sagitta* spp., and the copepods *Stephos longipes* and *Ctenocalanus* spp., from the '*low biomass/abundances*' community type (stations 570-579), which was associated with *Thysanoessa macrura* and *Salpa thompsoni*. The second axis of the NMDS ordination was mainly influenced by station 567 at the upper part of the ordination plot, which was associated with the copepods *C. propinquus* and *Ctenocalanus* spp., and krill furcilia. The '*krill-dominated*' community stations 551 and 555 were positioned at the lower part of the ordination plot and were associated with sub-adult and juvenile krill, ice-copepods *Pseudocylopina* sp., and the pteropods *Limacina helicina* and *Clione limacina*. Station 557 had an intermediate position between the '*krill-dominated*' and the '*copepod-dominated*' community stations, but was grouped with the '*krill-dominated*' stations in the cluster analysis.

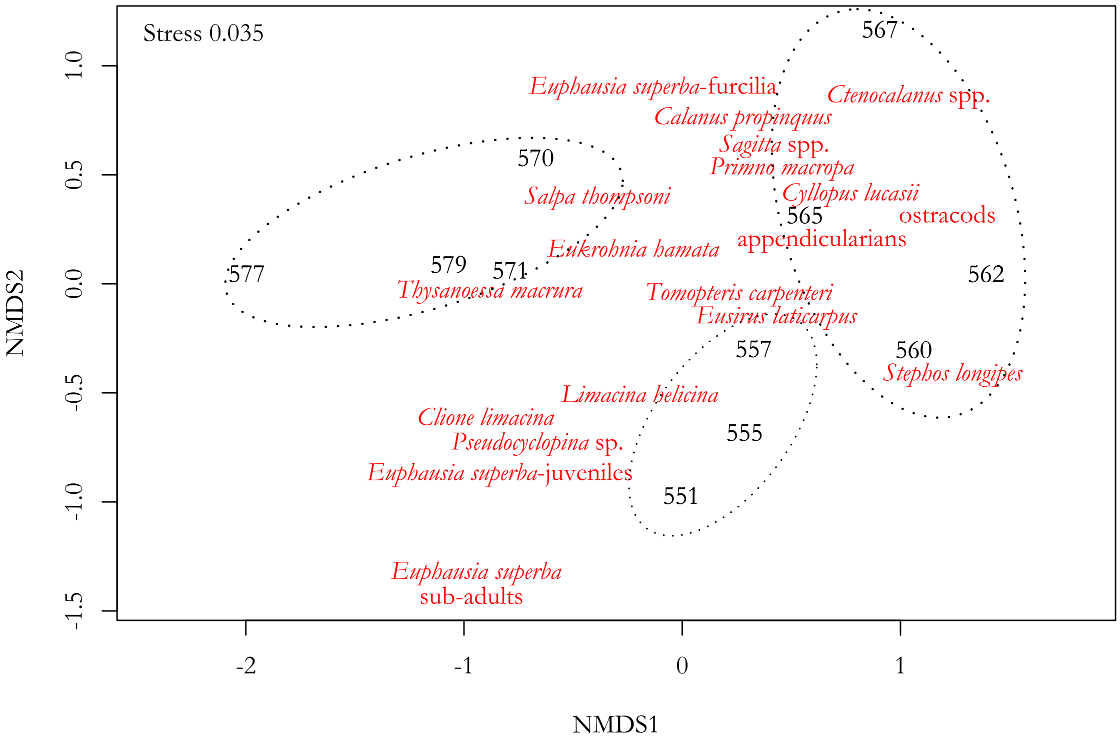

Figure 4. NMDS plot on SUIT stations and dominant species abundance. The ellipsoids represent grouping of stations determined with hierarchical clustering using the Bray-Curtis dissimilarity matrix of species abundance at sampling stations.

Water depth alone had the highest correlation, of any single environmental variable, with the variability of species abundances (*r* = 0.42; Mantel test *p* = 0.004; Table 4). The highest correlation between species abundance and environmental variables was achieved by a combination of snow depth, sea-ice coverage, temperature, chlorophyll *a* concentration and water depth (*r* = 0.47; Mantel test *p* = 0.008; Table 4).

Table 4. Combinations of environmental variables selected by BioEnv analysis. Combinations were ranked according to their correlation coefficients with the biological datasets tested with Mantel test: Abundance (species abundance as selected in NMDS). NP: number of variables; *r*: Spearman correlation coefficient; Variables names as defined in Table 1

	NP	Environmental variables	*r*	*p*
Abundance				
	1	depth	0.42	0.010
	2	coverage + depth	0.42	0.011
	3	coverage + depth + temperature	0.42	0.015
	4	coverage + depth + temperature + chlorophyll a	0.42	0.013
	5	coverage + depth + temperature + chlorophyll a + snow	0.47	0.008
	6	coverage + depth + temperature + chlorophyll a + snow + salinity	0.46	0.013
	7	snow coverage + depth + temperature + chlorophyll a + snow + salinity + thickness	0.47	0.008
	8	snow coverage + depth + temperature + chlorophyll a + snow + salinity + thickness + roughness	0.46	0.010

DISCUSSION

Sea-ice habitats

During winter 2013 the Southern Ocean had a sea-ice extent of approximately 19 million km^2 (Data source: www.meereisportal.de, University of Bremen and Alfred Wegener Institute). During this time, RV *Polarstern* expedition ARK XXIX/7 sampled in the pack-ice of the Weddell Sea from west to east approximately along the 60°S parallel. Daily sea-ice concentration data, from passive microwave-satellite measurements, were over 90% during August-September along our cruise track, and decreased to approximately 50% when sampling northward during the beginning of October. These values were in good agreement with the range of sea-ice coverage determined from SUIT sensors. Only at the last two stations (577 and 579), the SUIT sensor-derived ice coverage was about 95%, whereas satellite-derived ice coverage, averaged over a 39 km^2 area, was 50%, placing these stations into the marginal ice zone. In our ice-thickness profiles, modal ice thicknesses ranged from 0.2 to 0.7 m, while on-board visual observations of snow depth during profiles ranged from 0.05 to 0.6 m. Snow depth and modal ice thickness values from our SUIT hauls were consistent with the general pattern observed during airborne-electromagnetic ice thickness surveys, and ground-based snow and ice surveys conducted in the vicinity of the sampling area during our cruise (R. Ricker & T. Krumpen, unpublished data). Our snow depth and ice thickness values are also in agreement with previous measurements carried out in the Weddell Sea (Worby et al. 2008). Therefore, our local sampling profiles were representative of the regional-scale snow and sea-ice conditions.

The seasonal progression towards the end of winter was obvious at the last sampling locations, which was characterized by lower sea-ice coverage, a decrease in surface salinity and an increase in surface-water chlorophyll *a* concentration. Under-ice chlorophyll *a* concentrations were relatively low over the sampled area, and were consistent with previous winter values reported for the Weddell Sea (Nöthig et al. 1991). We did, however, observe a steady increase in surface chlorophyll *a* concentrations at the last five sampling locations, reaching a maximum concentration of 0.27 mg m^{-3} at the last station 579 (Table 1), indicating that the productive season, in the northern part of the research area, had commenced by the end of September. At the last two stations 577 and 579, the lower satellite-derived ice coverage observations indicated an advanced state of melting, which was also evident by our observed lower surface salinities. Besides advanced melting and a deteriorating sea-ice habitat with seasonal progression, the observed variability of the sea-ice habitat properties remains difficult to explain on a rather small dataset covering such a vast area. The stations sampled during the first half of our cruise did not show any seasonal or regional patterns in sea-ice properties. Local differences in sea-ice properties may have a background in atmospheric anomalies, wind patterns and occasional storm events (Holland and Kwok 2012; Kohout et al. 2014). Changes in surface-water temperature and salinity were rather small, likely due to the influence a quasi-homogeneous Winter Water layer circulated within the Weddell Gyre (Nöthig et al. 1991).

Species diversity and sampling performance

We identified at least 45 species in the upper 2 m of the ice-covered water column. In terms of species richness, copepods dominated the community with 12 species, followed by amphipods with 7 species (Table 2). Our diversity was lower than in epipelagic fauna from the Weddell Sea (Fisher et al. 2004; Hopkins and Torres 1988; Siegel et al. 1992), however, a comparison to previous sampling of the epipelagic layer is complicated by differences in net type, mesh sizes, sampling depth interval, season and sample size. Most Antarctic zooplankton studies integrated the epipelagic community over at least the upper 50 meters (Hopkins and Torres 1988; Lancraft et al. 1991; Siegel et al. 1992). The species composition from those studies is thus much more influenced by pelagic fauna, often dominated by the deeper-dwelling copepods (Razouls et al. 2000; Schnack-Schiel et al. 2008b). Moreover, larger sample size in previous studies could have accounted for higher diversity due to increased sampling effort. Siegel et al. (1992), with a sampling size double the size compared to our study, found that richness and diversity were highly variable horizontally, and were lower directly under the pack-ice than in the underlying water column. In the Weddell Sea, diversity was shown to increase with depth (Hopkins and Torres 1988). When the sampled depth range is taken into account (1% of the 200 m epipelagic depth stratum), however, our species richness is surprisingly high. This agrees with previous studies from the Lazarev Sea that found the diversity in the under-ice surface layer does not decrease much during winter because only few species migrate to greater depths and some even exhibit a hibernal upward migration (Flores et al. 2011, 2014). Our overall species richness was slightly higher, with 8 species more than reported in these winter studies from the Lazarev Sea, even when excluding the copepods and ostracods, which were not quantitatively sampled by Flores et al. (2011, 2014). A notable difference in the under-ice community of the two regions, however, was the extremely low numbers of post-larval krill and the absence of fish larvae and cephalopods under the pack-ice in the northern Weddell Sea compared to the Lazarev Sea. This difference could be due to regional differences or because of the much more southern sampling location within the Lazarev Sea, but inter-annual variability cannot be excluded.

Sampling the sea-ice underside with the SUIT, over an average profile distance of 1.5 km, results in an increased sampling effort per station compared to other methods such as under-ice pumps, hand nets or remotely operated vehicles (Brierley and Thomas 2002). This allowed us to capture the larger spatial variability of fauna with a patchy distribution (Schnack-Schiel 2003). Behavioural avoidance of the net by macrofauna cannot be excluded, but footage from the video camera mounted in the SUIT frame showed no visible avoidance. A potential underestimation of species, which are protected by the sea-ice underside topography, however, is difficult to assess with certainty. Due to known diel patterns (Flores et al. 2012; Siegel et al. 2005), the abundance of some species, e.g. *E. superba*, *C. propinquus*, may have been under-estimated at our daytime stations 555, 565, 571, and 577. At these stations, however, the abundances of *E. superba* and *C. propinquus* were well within the range of the other night time stations, and no significant diel effect was found (Wilcoxon test: *E. superba* $p = 0.92$; *C. propinquus* $p = 0.79$). This indicates that the general variability of species abundances was similar or larger compared to diel variability within our small dataset.

Under-ice community structure

In terms of species presence, we found a similar under-ice community composition over the sampling area, largely resembling the Weddell Sea ice-covered surface community dominated by sympagic and pelagic copepods, and larger grazers, such as euphausiids and amphipods (Schnack-Schiel 2003). Similar to other under pack-ice studies on both epipelagic and surface layers (Schnack-Schiel et al. 2008b; Siegel et al. 1992), we found no basis for the separation into distinct species assemblages. Differences in community structure between sampling locations were largely determined by the variability in species abundances and biomass, rather than in the variability of species composition.

a) Copepods

Copepods numerically dominated (67 %) the under-ice community. The dominant species in our samples, *S. longipes*, is ubiquitous under the Weddell Sea pack-ice (Kiko et al. 2008; Schnack-Schiel et al. 2001b, 2008a) and has a life cycle strongly associated with the seasonal fluctuations of sea-ice (Kurbjeweit et al. 1993). Our abundances were lower than those found in the western Weddell Sea, during spring and summer (Kiko et al. 2008; Schnack-Schiel et al. 2001b), likely due to the inclusion of smaller stages in the abundance calculations by these authors. *Ctenocalanus* spp. was the second most abundant species in our samples. This small calanoid is abundant in the epipelagic layer

(Schnack-Schiel et al. 2008b). Its population structure in the surface layer is female-dominated during late winter/early spring (Schnack-Schiel and Mizdalski 1994), which agrees with our findings. The cyclopoid *Pseudocyclopina sp.* and the harpacticoid *Idomene sp.* are inhabitants of sea ice, ubiquitous in the western Weddell Sea (Menshenina and Melnikov 1995; Schnack-Schiel et al. 2008a) and eastern Weddell Sea (Schnack-Schiel et al. 1995). These species appeared frequently in our catches, yet with generally low under-ice abundances, except at the two most western stations 551 and 555. Due to their small size compared to the mesh size used, however, an underestimation of our sampling was likely. One of the dominant pelagic copepods in the Weddell Sea, *C. propinquus,* had much lower abundances under ice than previously reported in epipelagic studies (Hopkins and Torres 1988; Schnack-Schiel and Hagen 1994; Siegel et al. 1992). This species was described to remain in the upper 200 m during winter (Hopkins and Torres 1988; Schnack-Schiel and Hagen 1995) and actively feed (Pasternak and Schnack-Schiel 2001), and demonstrated the ability to switch to an omnivorous diet (Metz and Schnack-Schiel 1995).

b) Antarctic krill

Antarctic krill numerically dominated the species composition at the three northernmost stations 571, 577 and 579 (Fig. 2). First-year krill dominated the population structure in this study (Schaafsma et al. 2016). Adult krill numbers were very low, while dominance of sub-adult krill within the krill population was restricted to the westernmost station 551, where krill heavily dominated the cumulative biomass composition (95%). Our results agree with previous late winter/early spring studies from the Scotia/Weddell Sea and Antarctic Peninsula regions, which also found furcilia VI to be the dominant stage in the under-ice layer (Daly 1990, 2004). A winter study from the Lazarev Sea often found higher abundances of sub-adult krill under ice than in the epipelagic layer (0-200 m depth layer), highlighting the pivotal role of sea ice in the functional ecology of other development stages of this species, besides larvae (Flores et al. 2012). In addition, Rectangular Midwater Trawls (RMT) conducted in the 0-500 m depth layer near the SUIT locations showed that abundances of (sub-) adult krill were very low (Schaafsma et al. 2016). This indicates that (sub-) adult krill in the study region were in general low in abundance or too patchily distributed to be representatively sampled with the small sample size of this study. In larval and juvenile krill, a comparison of our catches with the RMT krill catches from the 0-500 m layer, showed that volumetric densities were higher in the under-ice layer than in the 0-500 m depth layer, but areal densities indicated that large parts of the juvenile population dwelled at a lower depth (Schaafsma et al. 2016).

c) Amphipods, chaetognaths and pteropods

Other taxonomic groups, e.g. amphipods, chaetognaths, pteropods, occurred in lower abundances but nevertheless contributed significantly to the total biomass, mainly at stations 560, 562, 565 and 567. The ice-associated amphipod *E. laticarpus* occurred at stations with higher ice coverage and thicker ice (Table 1, Online Resource 1). *E. laticarpus* was distributed everywhere over the sampling area and was the most abundant amphipod in our samples. Their mean abundance of 1.48 ind. 100 m^{-2}, however, was about half the winter under-ice abundance found in the Lazarev Sea (Flores et al. 2011).

The chaetognaths *E. hamata* and *Sagitta gazellae* are known predators of copepods and krill larvae (Giesecke and González 2012). *E. hamata* feeds year-round, mainly on copepods (Kruse et al. 2010), while *Sagitta* spp. feeds on krill larvae during winter (Lancraft et al. 1991), which agrees well with our species distributions. Higher chaetognaths abundances observed at the stations with higher copepod abundances and krill larvae, indicates a potential behavioral predator response of chaetognaths, such that they may have followed the prey distribution. When copepods were attracted to the under-ice resources during winter, chaetognaths were likely attracted by increased prey abundance under the ice. Similarly, the simultaneous migration of chaetognaths and copepods to deep water at the beginning of the productive season, was suggested by our data and also confirms predatory behaviour by the chaetognaths.

Pteropods have been reported to numerically account for up to 35% of the Southern Ocean zooplankton community (Hunt et al. 2008). Two of the major contributors, the thecosome *L. helicina*, and its allegedly monophagous predator, the gymnosome *C. limacina* (Hunt et al. 2008), were observed at less than half of our sampling locations. The low abundances found during our study (Table 2) agree with the winter under-ice abundances reported from the Lazarev Sea (Flores et al. 2011). Flores et al. (2011) suggested an association of *C. limacina* with the ice-water interface during winter, which were likely attracted to the under-ice environment by a predatory response to the presence of their prey *L. helicina*, at the sea-ice underside. The abundances of *L. helicina* in this study, however, were probably too low to serve as a sufficient food source for *C. limacina*.

Community structure associated with sea-ice habitat properties

When overall abundance and biomass distribution at our stations were considered, gradual changes were observed according to three community types (Fig. 3 and 4). The *krill-dominated* community was characterised by higher overall biomass with krill being the major contributor. There were, however, notable differences in the krill composition at these stations (Online resource 3). At the westernmost station 551 the biomass was dominated by sub-adults, and stations 555 and 557 were dominated by first-year juveniles. Excluding post-larval krill, krill larvae-dominated and copepod-dominated communities had similar biomass over the sampling area.

The *copepod-dominated* community was characterized by higher abundances dominated by copepods. On the NMDS plot the *copepod-dominated* community was associated with the dominant species of the under-ice community, e.g. *S. longipes*, *C. propinquus,* and krill larvae. One evident characteristic of this community was not only the dominance of copepods (in abundance), but also the high contribution of other taxonomic groups, e.g., amphipods, pteropods, chaetognaths and ctenophores (in biomass), which is an indication of a heterotrophic food web with filter-feeders (*L. helicina*, appendicularians) as herbivores. Ammonium concentrations at the surface were higher at the *copepod-dominated* community sampling locations (0.4 – 1.1 µmol l^{-1}) than the rest of our locations (C. Klaas, unpublished data.), supporting the assumption of extensive heterotrophic activity. The decrease in surface salinities below typical Winter Water values (< 34.4; Krell et al. (2005) suggests melting had already started at the time of our sampling.

At the last four stations, which were characterised as *low biomass/abundances* communities, the sea ice was in an advanced state of melt. Copepod abundances were low, while some other species, e.g. *L. helicina*, *C. limacina*, were absent from our samples (Online resource 1). This was the strongest signal detected within the under-ice community composition. This could be due to a combined effect of the seasonal evolution of sea-ice habitats by the end of winter, inducing a behavioural response of some species performing vertical migration (Schnack-Schiel and Hagen 1995; Schnack-Schiel et al. 1995), closeness to the marginal ice zone (MIZ) and the geographic location of these stations at the eastern side of the South Sandwich Islands. At the time of our sampling, the satellite-derived sea-ice coverage decreased to about 50%, and only the thicker and rougher ice remained. The MIZ is typically more productive than other ice-covered areas (Brierley and Thomas 2002), which is in part a contradiction to our low biomass under-ice catches at the MIZ stations. On the NMDS map, the cluster of *low biomass/abundances* community stations was associated with a more pelagic assemblage, e.g. *S. thompsoni*, *T. macrura*, *T. carpenteri*, indicating a potential transition away from an ice-associated community. Moreover, the shallower bathymetry surrounding the islands, where these stations were located, would have also been expected to provide the increased productivity that is typical of shelf and slope areas. Increased productivity in the water column could have caused pelagic species to migrate into more productive deeper water layers. With such small sample size, it remains difficult to differentiate the seasonal effect, i.e. retreat of sea ice, from local effects, i.e. proximity of islands at smaller scales. Nonetheless, the above mentioned contradictions would rather indicate that reduction of the sea-ice coverage induced an immediate response in the surface community structure.

In the BioEnv analysis, the combinations of environmental variables, which resulted in the three best correlations with the species abundance matrix, contained satellite-derived sea ice coverage and snow depth, indicating that the community composition responds to both regional and local properties of sea-ice habitats. Broad scale hydrography and bathymetry played an equally important role, as was evident from the occurrence of temperature, salinity and water depth as selected variables among the eight best BioEnv model combinations. Using only coarse descriptors of sea-ice properties such as visually observed sea-ice coverage and floe size, Flores et al. (2014) could not identify a correlation between community structure and sea-ice properties during winter. Using sensor-derived data, our study gives a first insight, albeit limited by a small sample size, on the relationships between sea-ice properties and under-ice community structure. This demonstrates the potential of this approach for larger sample sizes.

CONCLUSION

Our study provides new findings for a better understanding of under-ice faunal distribution during late winter/early spring. It emphasise the fact that under-ice fauna distribution is very heterogeneous in space and time, making generalizations difficult and demanding more complex modelling. To understand which species will be the winners and which will be losers in a changing ice-covered environment, extended observations are needed for future predictions of such a complicated system. As the climate continues to warm, it is prudent to understand the ecological relationships between sea-ice dependent krill and krill predators, as well as the interactions among sea-ice dependent species that may be forced into competition for a shared food resource. Therefore, besides species distribution our focus should extend to quantifying food web energy fluxes, which would provide a broader view of the changing system, ultimately reflected in carbon cycle alterations.

Acknowledgments

We thank Captain Stephan Schwarze and the crew of RV Polarstern expedition ANT XXIX/7 for their excellent support with work at sea. We thank Michiel van Dorssen for operational and technical support with the Surface and Under-Ice Trawl (SUIT). SUIT was developed by IMARES with support from the Netherlands Ministry of EZ (project WOT-04-009-036) and the Netherlands Polar Program (projects ALW 851.20.011 and 866.13.009). This study is part of the Helmholtz Association Young Investigators Group *Iceflux*: Ice-ecosystem carbon flux in polar oceans (VH-NG-800). We thank Dr. Astrid Cornils for help with copepod species identification. We thank Dr. Christine Klaas for providing chlorophyll *a* measurements of water samples used for calibration.

References

Ainley D, Jongsomjit D, Ballard G, Thiele D, Fraser W, Tynan C (2012) Modeling the relationship of Antarctic minke whales to major ocean boundaries. Polar Biol 35:281-290. doi:10.1007/s00300-011-1075-1

Ainley DG, Dugger KM, Toniolo V, Gaffney I (2007) Cetacean occurrence patterns in the Amundsen and southern Bellingshausen Sea sector, Southern Ocean. Mar Mammal Sci 23:287-305

Arrigo KR, van Dijken GL, Bushinsky S (2008) Primary production in the Southern Ocean, 1997-2006. J Geophys Res-Oceans 113. doi:10.1029/2007jc004551

Arrigo KR, Worthen DL, Lizotte MP, Dixon P, Dieckmann G (1997) Primary Production in Antarctic Sea Ice. Science 276:394-397. doi:10.1126/science.276.5311.394

Atkinson A, Meyer B, Bathmann U, Stübing D, Hagen W, Schmidt K (2002) Feeding and energy budget of Antarctic krill *Euphausia superba* at the onset of winter-II. Juveniles and adults. Limnol Oceanogr 47:953-966

Atkinson A et al. (2008) Oceanic circumpolar habitats of Antarctic krill. Marine Ecology Progress Series 362:1-23

Bray JR, Curtis JT (1957) An ordination of the upland forest communities of southern Wisconsin. Ecol Monogr 27:325-349

Brierley AS, Thomas DN (2002) Ecology of Southern Ocean pack ice. In: Advances in Marine Biology, vol 43. Academic Press, pp 171-276. doi:10.1016/S0065-2881(02)43005-2

Clarke K, Ainsworth M (1993) A method of linking multivariate community structure to environmental variables. Mar Ecol Progr Ser 92:205-205

Clarke KR, Warwick RM (2001) Change in marine communities: an approach to statistical analysis and interpretation, 2nd edition. PRIMER-E Limited, Plymouth Marine Laboratory, UK

Daly KL (1990) Overwintering development, growth, and feeding of larval *Euphausia superb*a in the Antarctic marginal ice zone. Limnol Oceanogr 35:1564-1576

Daly KL (2004) Overwintering growth and development of larval *Euphausia superba*: an interannual comparison under varying environmental conditions west of the Antarctic Peninsula. Deep-Sea Res Pt II 51:2139-2168

De Broyer C, Koubbi P, Griffiths H, Raymond B, Udekem d'Acoz C d', Van de Putte A, Danis B, David B, Grant S, Gutt J, Held C, Hosie G, Huettmann F, Post A, Ropert-Coudert (2014) Biogeographic Atlas of the Southern Ocean. Scientific Committee on Antarctic Research, Cambridge, UK

Fisher EC, Kaufmann RS, Smith KL (2004) Variability of epipelagic macrozooplankton/micronekton community structure in the NW Weddell Sea, Antarctica (1995-1996). Mar Biol 144:345-360

Flores H et al. (2014) Seasonal changes in the vertical distribution and community structure of Antarctic macrozooplankton and micronekton. Deep-Sea Res Pt I 84:127-141. doi:DOI 10.1016/j.dsr.2013.11.001

Flores H et al. (2011) Macrofauna under sea ice and in the open surface layer of the Lazarev Sea, Southern Ocean. Deep-Sea Res Pt II 58:1948-1961

Flores H et al. (2012) The Association of Antarctic Krill *Euphausia superba* with the Under-Ice Habitat. PLoS ONE 7. doi:10.1371/journal.pone.0031775

Gannefors C et al. (2005) The Arctic sea butterfly *Limacina helicina*: lipids and life strategy. Mar Biol 147:169-177

Giesecke R, González HE (2012) Distribution and feeding of chaetognaths in the epipelagic zone of the Lazarev Sea (Antarctica) during austral summer. Polar Biol 35:689-703. doi:10.1007/s00300-011-1114-y

Gloersen P, Campbell WJ (1991) Recent variations in Arctic and Antarctic sea-ice covers. Nature 352:33-36

Holland PR, Kwok R (2012) Wind-driven trends in Antarctic sea-ice drift. Nature Geosci 5:872-875. doi:10.1038/ngeo1627

Hopkins T, Torres J (1988) The zooplankton community in the vicinity of the ice edge, western Weddell Sea, March 1986. Polar Biol 9:79-87

Hopkins T, Torres J (1989) Midwater food web in the vicinity of a marginal ice zone in the western Weddell Sea. Deep Sea Res Pt I 36:543-560

Hopkins TL, Lancraft TM, Torres JJ, Donnelly J (1993) Community structure and trophic ecology of zooplankton in the scotia sea marginal ice zone in winter (1988). Deep Sea Res Pt I 40:81-105. doi:10.1016/0967-0637(93)90054-7

Hunt B, Pakhomov E, Hosie G, Siegel V, Ward P, Bernard K (2008) Pteropods in southern Ocean ecosystems. Prog Oceanogr 78:193-221

Hunt BPV, Pakhomov EA, Siegel V, Strass V, Cisewski B, Bathmann U (2011) The seasonal cycle of the Lazarev Sea macrozooplankton community and a potential shift to top-down trophic control in winter. Deep-Sea Res Pt II 58:1662-1676. doi:10.1016/j.dsr2.2010.11.016

Kiko R, Michels J, Mizdalski E, Schnack-Schiel SB, Werner I (2008) Living conditions, abundance and composition of the metazoan fauna in surface and sub-ice layers in pack ice of the western Weddell Sea during late spring. Deep-Sea Res Pt II 55:1000-1014. doi:10.1016/j.dsr2.2007.12.012

Kohout AL, Williams MJM, Dean SM, Meylan MH (2014) Storm-induced sea-ice breakup and the implications for ice extent. Nature 509:604-607. doi:10.1038/nature13262

Krell A, Schnack-Schiel SB, Thomas DN, Kattner G, Zipan W, Dieckmann GS (2005) Phytoplankton dynamics in relation to hydrography, nutrients and zooplankton at the onset of sea ice formation in the eastern Weddell Sea (Antarctica). Polar Biol 28:700-713

Kruse S, Hagen W, Bathmann U (2010) Feeding ecology and energetics of the Antarctic chaetognaths *Eukrohnia hamata*, *E. bathypelagica* and *E. bathyantarctica*. Mar Biol 157:2289-2302

Kruskal JB (1964) Nonmetric multidimensional scaling: A numerical method. Psychometrika 29:115-129. doi:10.1007/bf02289694

Kurbjeweit F, Gradinger R, Weissenberger J (1993) The life cycle of *Stephos longipes*-an example for cryopelagic coupling in the Weddell Sea (Antarctica). Mar Ecol Prog Ser 98:255-262

Lancraft TM, Hopkins TL, Torres JJ, Donnelly J (1991) Oceanic micronektonic/macrozooplanktonic community structure and feeding in ice covered Antarctic waters during the winter (AMERIEZ 1988). Polar Biol 11:157-167

Legendre P, Legendre L (2012) Numerical ecology. vol 24. Third edition edn. Elsevier, Oxford, UK

Lizotte MP (2001) The Contributions of Sea Ice Algae to Antarctic Marine Primary Production. Am Zool 41:57-73. doi:10.1093/icb/41.1.57

Loeb V, Siegel V, Holm-Hansen O, Hewitt R, Fraser W, Trivelpiece W, Trivelpiece S (1997) Effects of sea-ice extent and krill or salp dominance on the Antarctic food web. Nature 387:897-900

Mantel N (1967) The detection of disease clustering and a generalized regression approach. Cancer research 27:209-220

Menshenina LL, Melnikov IA (1995) Under-ice zooplankton of the western Weddell Sea. In: Proceedings of the NIPR Symposium on Polar Biology, 8:126-138

Metz C, Schnack-Schiel S (1995) Observations on carnivorous feeding in Antarctic calanoid copepods. Mar Ecol Progr Ser 129:71-75

Meyer B (2012) The overwintering of Antarctic krill, *Euphausia superba*, from an ecophysiological perspective. Polar Biol 35:15-37. doi:10.1007/s00300-011-1120-0

Minchin PR (1987) An evaluation of the relative robustness of techniques for ecological ordination. In: Prentice IC, van der Maarel E (eds) Theory and models in vegetation science. Springer, pp 89-107

Mizdalski E (1988) Weight and length data of zooplankton in the Weddell Sea in austral spring 1986 (ANT V/3). Berichte zur Polarforschung (Reports on Polar Research) 55

Motoda S (1959) Devices of simple plankton apparatus. Memoirs of the Faculty of Fisheries, Hokkaido University 7:73-94

Nöthig EM, Bathmann U, Jennings Jr JC, Fahrbach E, Gradinger R, Gordon LI, Makarov R (1991) Regional relationships between biological and hydrographical properties in the Weddell Gyre in late austral winter 1989. Mar Chem 35:325-336. doi:10.1016/S0304-4203(09)90025-1

O'Brien D (1987) Direct observations of the behavior of *Euphausia superba* and *Euphausia crystallorophias* (Crustacea: Euphausiacea) under pack ice during the Antarctic spring of 1985. J Crustacean Biol 7:437-448

Pakhomov EA, Froneman PW (2004) Zooplankton dynamics in the eastern Atlantic sector of the Southern Ocean during the austral summer 1997/1998 - Part 1: Community structure. Deep-Sea Res Pt II 51:2599-2616. doi:10.1016/j.dsr2.2000.11.001

Pasternak AF, Schnack-Schiel SB (2001) Seasonal feeding patterns of the dominant Antarctic copepods *Calanus propinquus* and *Calanoides acutus* in the Weddell Sea. Polar Biol 24:771-784

Quetin LB, Ross RM, Frazer TK, Haberman KL (2013) Factors affecting distribution and abundance of zooplankton, with an emphasis on Antarctic krill, *Euphausia superba*. Antarctic Research Series 70:357-371. doi:10.1029/AR070p0357

R Core Team (2015) R: A language and environment for statistical computing. R Foundation for Statistical Computing, Vienna, Austria URL http://www.R-project.org/

Schaafsma FL, David C, Pakhomov EA, Hunt BPV, Lange BA, Flores H, van Franeker JA (2016) Size and stage composition of age class 0 Antarctic krill (*Euphausia superba*) in the ice-water interface layer during winter/early spring. Polar Biology doi:10.1007/s00300-015-1877-7

Schmidt K, Atkinson A, Pond DW, Ireland LC (2014) Feeding and overwintering of Antarctic krill across its major habitats: The role of sea ice cover, water depth, and phytoplankton abundance. Limnol Oceanogr 59:17-36

Schnack-Schiel S, Mizdalski E (1994) Seasonal variations in distribution and population structure of *Microcalanus pygmaeus* and *Ctenocalanus citer* (Copepoda: Calanoida) in the eastern Weddell Sea, Antarctica. Mar Biol 119:357-366

Schnack-Schiel SB (2003) The macrobiology of sea ice. In: Thomas DN, Dieckmann GS (eds) Sea ice: an introduction to its physics, chemistry, biology and geology. Blackwell Science Ltd., Oxford, UK

Schnack-Schiel SB, Dieckmann GS, Gradinger R, Melnikov I, Spindler M, Thomas DN (2001a) Meiofauna in sea ice of the Weddell Sea (Antarctica). Polar Biol 24:724-728

Schnack-Schiel SB, Haas C, Michels J, Mizdalski E, Schünemann H, Steffens M, Thomas DN (2008a) Copepods in sea ice of the western Weddell Sea during austral spring 2004. Deep-Sea Res Pt II 55:1056-1067

Schnack-Schiel SB, Hagen W (1994) Life cycle strategies and seasonal variations in distribution and population structure of four dominant calanoid copepod species in the eastern Weddell Sea, Antarctica. J Plankton Res 16:1543-1566. doi:10.1093/plankt/16.11.1543

Schnack-Schiel SB, Hagen W (1995) Life-cycle strategies of *Calanoides acutus*, *Calanus propinquus*, and *Metridia gerlachei* (Copepoda: Calanoida) in the eastern Weddell Sea, Antarctica. Ices J Mar Sci 52:541-548. doi:10.1016/1054-3139(95)80068-9

Schnack-Schiel SB, Michels J, Mizdalski E, Schodlok MP, Schröder M (2008b) Composition and community structure of zooplankton in the sea ice-covered western Weddell Sea in spring 2004—with emphasis on calanoid copepods. Deep-Sea Res Pt II 55:1040-1055

Schnack-Schiel SB et al. (1995) Life cycle strategy of the Antarctic calanoid copepod *Stephos longipes*. Prog Oceanogr 36:45-75. doi:10.1016/0079-6611(95)00014-3

Schnack-Schiel SB, Thomas DN, Haas C, Dieckmann GS, Alheit R (2001b) The occurrence of the copepods *Stephos longipes* (Calanoida) and *Drescheriella glacialis* (Harpacticoida) in summer sea ice in the Weddell Sea, Antarctica. Antarct Sci 13:150-157

Shannon C (1948) A mathematical theory of communication. Bell Sys Tech J 27:379-423

Siegel V, Loeb V (1995) Recruitment of Antarctic krill *Euphausia superba* and possible causes for its variability. Mar Ecol Progr Ser 123:45-56

Siegel V, Skibowski A, Harm U (1992) Community structure of the epipelagic zooplankton community under the sea-ice of the northern Weddell Sea. Polar Biol 12:15-24

Spreen G, Kaleschke L, Heygster G (2008) Sea ice remote sensing using AMSR-E 89-GHz channels. J Geophys Res-Oceans 113:C02S03. doi:10.1029/2005jc003384

Thomas D, Dieckmann G (2002) Antarctic sea ice-a habitat for extremophiles. Science 295:641-644

Turner J, Hosking JS, Phillips T, Marshall GJ (2013) Temporal and spatial evolution of the Antarctic sea ice prior to the September 2012 record maximum extent. Geophys Res Lett 40:5494-5498. doi:10.1002/2013gl058371

van Franeker JA, Bathmann UV, Mathot S (1997) Carbon fluxes to Antarctic top predators. Deep-Sea Res Pt Ii 44:435-455. doi:10.1016/S0967-0645(96)00078-1 van Franeker JA, Flores H, Van Dorssen M (2009) Surface and Under Ice Trawl (SUIT). In: Flores H (author) Frozen Desert Alive -The role of sea ice for pelagic macrofauna and its predators: implications for the Antarctic pack-ice food web. Dissertation, University of Groningen, Groningen, Netherlands

White MG, Piatkowski U (1993) Abundance, horizontal and vertical distribution of fish in eastern Weddell Sea micronekton. Polar Biol 13:41-53

Wilcoxon F (1945) Individual comparisons by ranking methods. Biometrics bulletin 1:80-83

Worby AP, Geiger CA, Paget MJ, Van Woert ML, Ackley SF, DeLiberty TL (2008) Thickness distribution of Antarctic sea ice. J Geophys Res-Oceans 113:C05S92. doi:10.1029/2007jc004254

Yang G, Li C, Sun S (2011) Inter-annual variation in summer zooplankton community structure in Prydz Bay, Antarctica, from 1999 to 2006. Polar Biology 34:921-932. doi:10.1007/s00300-010-0948-z

Zwally HJ, Comiso JC, Parkinson CL, Cavalieri DJ, Gloersen P (2002) Variability of Antarctic sea ice 1979–1998. J Geophys Res-Oceans 107:9-1-9-19. doi:10.1029/2000jc000733

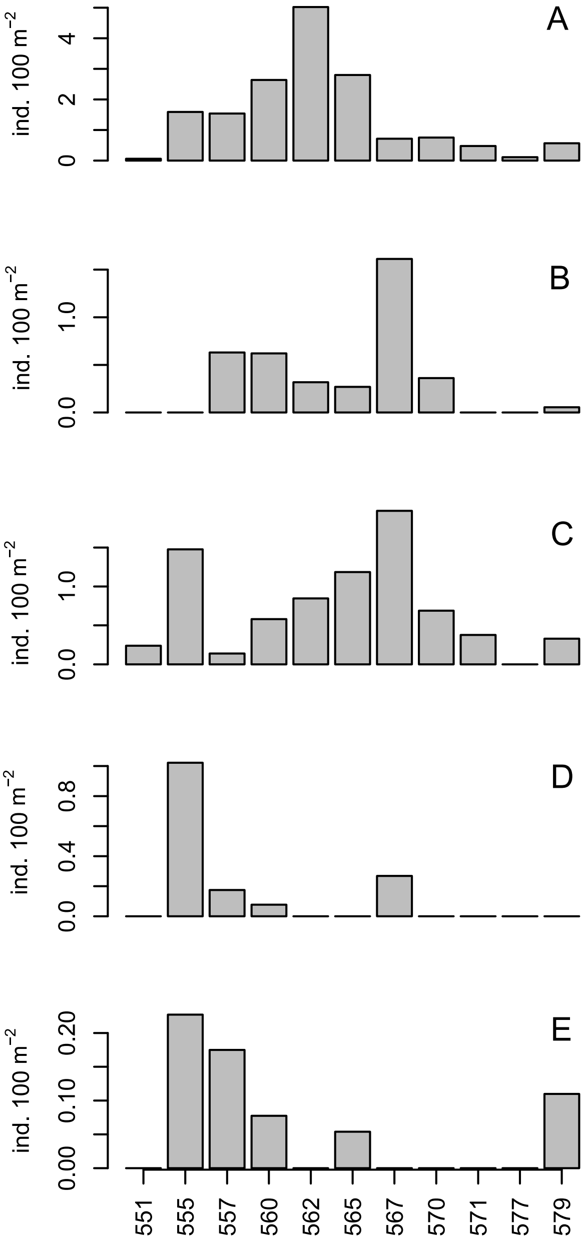

Online resource 1. Abundance of species (A: *Eusirus laticarpus*, B: *Sagitta* spp., C: *Eukrohnia hamata*, D: *Limacina helicina*, E: *Clione limacina*) at SUIT sampling stations (numbers indicated on *x*-axis)

Online resource 2

Table S1. Spearman correlation between abundances of representative species of under-ice community at sampling locations. Correlation coefficients higher <0.50 presented in bold

	Clione limacina	*Limacina helicina*	*Eusirus laticarpus*	*Euphausia superba* larvae	*Euphausia superba* juveniles	*Euphausia superba* sub-adults	*Thysanoessa macrura*	*Calanus propinquus*	*Ctenocalanus* spp.	*S. longipes*	*Pseudocyclopina* sp.	ostracods	*Sagitta* spp.	*Eukrohnia hamata*	*Salpa thompsoni*	appendicularians
Clione limacina	1															
Limacina helicina	**0.55**	1														
Eusirus laticarpus	0.38	0.26	1													
Euphausia superba larvae	-0.11	0.12	0.36	1												
Euphausia superba juveniles	**0.51**	**0.71**	-0.19	-0.21	1											
Euphausia superba sub-adults	-0.25	-0.38	-0.08	-0.15	0.01	1										
Thysanoessa macrura	0.00	0.46	-0.43	0.24	**0.74**	-0.01	1									
Calanus propinquus	-0.23	0.23	**0.61**	**0.57**	-0.15	0.06	0.03	1								
Ctenocalanus spp.	0.04	0.45	**0.69**	0.54	0.06	0.13	0.09	**0.81**	1							
Stephos longipes	0.39	0.35	**0.72**	0.10	0.22	0.34	-0.12	0.33	**0.65**	1						
Pseudocyclopina sp.	-0.21	0.26	-0.02	0.09	0.36	0.13	0.55	0.56	0.43	0.06	1					
ostracods	-0.02	0.35	**0.60**	0.13	0.06	0.11	-0.12	**0.81**	**0.78**	**0.50**	0.48	1				
Sagitta spp.	0.08	0.40	0.47	**0.56**	0.07	0.21	0.18	0.46	**0.66**	0.26	0.05	0.31	1			
Eukrohnia hamata	0.03	0.40	**0.57**	0.48	0.01	-0.21	0.04	**0.91**	**0.68**	0.25	**0.51**	**0.81**	0.30	1		
Salpa thompsoni	0.02	0.18	0.29	**0.61**	0.08	0.18	0.34	0.34	0.42	0.02	0.18	0.10	**0.78**	0.19	1	
appendicularians	0.12	**0.54**	**0.63**	0.47	0.11	-0.21	0.03	**0.84**	**0.73**	0.44	0.31	**0.82**	0.37	**0.93**	0.14	1

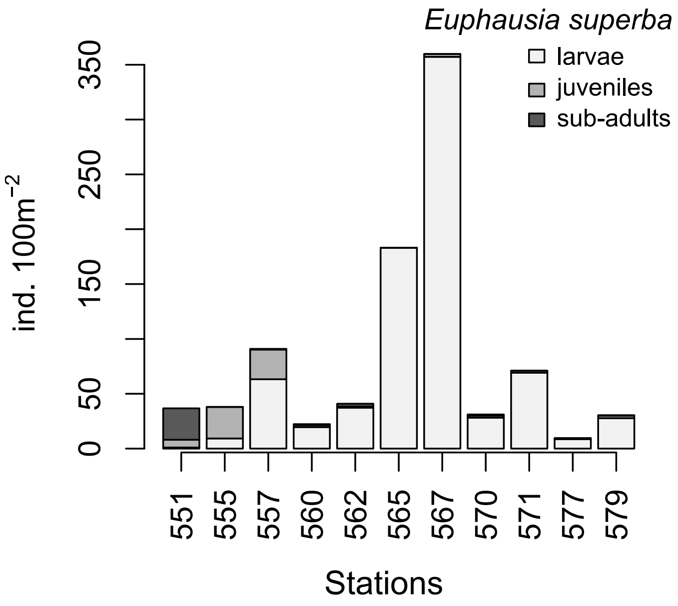

Online resource 3. Abundance of *Euphausia superba* (separated by developmental stage: larvae, juveniles and sub-adults) at SUIT sampling stations (numbers indicated on *x*-axis); the sub-adults group includes the adults

2.4. Chapter IV

What makes the under-ice habitat attractive during winter: carbon demand of Antarctic krill larvae and ice-associated copepods in relation to food availability and predation pressure in the northern Weddell Sea

Carmen David[1,2*], Fokje L. Schaafsma[3], Jan A. van Franeker[3], Evgeny A. Pakhomov[4], Brian P.V. Hunt[4],
Benjamin Lange[1,2], Angelika Brandt[2], Hauke Flores[1,2]

[1] Alfred-Wegener-Institut Helmholtz-Zentrum für Polar- und Meeresforschung (AWI), Am Handelshafen 12, 27570, Bremerhaven, Germany; [2] University Hamburg, Centre for Natural History (CeNak), Zoological Museum, Martin-Luther-King Platz 3, 20146, Hamburg, Germany; [3] Institute for Marine Research and Ecosystem Studies Wageningen UR (IMARES), PO Box 57, 1781 AG Den Helder, The Netherlands; [4] Department of Earth, Ocean and Atmospheric Sciences, 2020-2207 Main Mall, University of British Columbia, Vancouver, BC, V6T1Z4, Canada

Publication in preparation for submission

ABSTRACT

Recruitment of krill, *Euphausia superba* is believed to largely depend on sea-ice conditions during winter, but little is known about the species' interactions competing for the limited winter resources. The distribution of carbon demand of dominant under sea ice and in the water column species during winter in response to food availability, grazing pressure and predation pressure has been studied. Dominant under-ice (ice-water interface 0 – 2 m) and pelagic species (0 – 500 m) were sampled during late winter/early spring 2013 in the northern Weddell Sea, Southern Ocean. Chlorophyll *a* concentrations in the surface water increased with seasonal progression from end of winter to early spring. The distribution of carbon demand of herbivorous species in the ice-water interface layer did not follow similar pattern, indicating that ice algae were likely important as a carbon source. A niche partitioning was evident between herbivorous ice-associated species, e.g. the copepod *Stephos longipes* and krill larvae, and dominant pelagic species, e.g. the copepods *Calanus propinquus*, *Metridia gerlachei* and *Ctenocalanus* spp.. Grazing pressure on phytoplankton standing stock was higher under ice than in the water column. Predation impact by chaetognaths, however, was largely restricted to the water column and minimal under ice, making the under-ice habitat an attractive environment and a winter refuge for species adapted to survive in the sea-ice habitat. The value of the under-ice environment as a winter habitat for certain zooplankton species seemed to be given primarily by a) ice algae as an additional abundant carbon source, and b) low predation pressure. In a future Antarctic system, reduced sea-ice algal production as a result of sea ice decline, may be compensated by increased water column phytoplankton productivity, but the sheltered environment for the krill larvae and other ice-associated species would still break away with unknown consequences for the affected populations.

INTRODUCTION

Antarctic krill *Euphausia superba* is a keystone species of the Southern Ocean, supporting large populations of top predators and a growing fishery (Krafft et al. 2015; McBride et al. 2014). Antarctic krill occur in regions undergoing rapid environmental change, particularly loss of winter sea-ice (Atkinson et al. 2008). Recruitment success of krill largely relies on larval survival during their first winter (Atkinson et al. 2004; Meyer et al. 2009). Current knowledge of larval krill ecology in winter is, however, based on a small number of studies due to logistical and practical difficulties of working in winter sea ice (Daly 2004; Ross et al. 2004). Unlike adults, larval krill have low lipid reserves (Hagen et al. 2001) and can survive only a few weeks without food (Meyer et al. 2002). Sea ice is considered to be a key overwintering habitat for krill (Daly 2004; Meyer et al. 2009), as ice algae provide an important source of energy (e.g. Daly and Macaulay 1991; Meyer et al. 2002a). Moreover, sea-ice structures act as a potential refugee from predators (Meyer et al. 2009).

Other pelagic species also associate with the under-ice environment, especially during winter (Ainley et al. 1986; Flores et al. 2011), when primary production in the water column decreases to nearly zero (Arrigo et al. 2008). Besides ice algae, other resources provided by sea-ice habitats such as protozoans, small copepods and detritus may offer an alternative food source for the species dwelling at the ice-water interface (Daly 1990; Meyer 2012; Schmidt et al. 2014). Many copepods species were described to remain in the upper epipelagic layer and actively feed during winter (Pasternak and Schnack-Schiel 2001, 2007), and some demonstrated the ability to switch to an omnivorous diet (Atkinson 1995; Metz and Schnack-Schiel 1995). Chaetognaths are the most voracious and abundant predators of copepods (Froneman et al. 1998; Giesecke and González 2012; Öresland 1990; Pakhomov et al. 1999). In the Southern Ocean, they can achieve up to 50% of total predation impact of the carnivorous zooplankton (Pakhomov et al. 1999). They feed year-round, mainly on copepods and krill larvae (Kruse et al. 2010; Lancraft et al. 1991; Oresland 1995). Within the zooplankton community, the copepods are regarded as the most conspicuous grazers (Atkinson et al. 1996; Bernard and Froneman 2003; Pakhomov and Froneman 2004) and are believed to have the ability to largely control the phytoplankton standing stock in some regions (Froneman et al. 2000; Urban-Rich et al. 2001). Most grazing impact studies are, however, based on observations during spring, summer or autumn blooms (Atkinson et al. 1996; Bernard et al. 2012; Lee et al. 2013; Pakhomov and Froneman 2004; Swadling et al. 1997). In resource-limited environments, like winter ice-covered regions, little is known about how species interact and their ability to meet the food requirement.

Here we focus on the intermediate trophic levels in an Antarctic sea-ice associated food web during winter, considering dominant grazers, copepods and krill larvae, and their main predators, the chaetognaths. The distribution of carbon demand of these dominant under sea ice and in the water column species in response to food availability, grazing pressure and predation pressure has been studied. Dominant species were sampled in the ice-water interface layer (0 – 2 m) and in the water column (0 – 500 m) during late winter/early spring 2013 in the northern Weddell Sea. We compared the carbon demand of dominant grazing species and predator pressure between the ice-water interface layer and the water column.

MATERIAL AND METHODS

Sampling technique and data collection

Sampling was performed during RV *Polarstern* expedition PS81 (ANT XXIX/7), between 31 August and 2 October 2013, across the ice-covered Weddell Sea, from 58° to 61°S, and from 42° to 25°W (Fig. 1). At 11 stations, the ice-water interface layer (0-2 m) was sampled with a Surface and Under Ice Trawl (SUIT; van Franeker et al. 2009). Four of these stations were completed during daytime, and seven during nighttime (Table 1). Seven SUIT stations were sampled from west to east approximately along the 60 ºS parallel, and four stations northward along the 26ºW meridian (Fig.1).

The SUIT consisted of a steel frame with a 2 m x 2 m opening and two parallel 15 m long nets attached: 1) a 7 mm half-mesh commercial shrimp net, lined with 0.3 mm mesh in the rear 3 m of the net, covered 1.5 m of the opening width and 2) a 0.3 mm mesh mesozooplankton net covered 0.5 m of the opening width. Floats attached to the top of the frame kept the net at the sea-ice underside. An asymmetric bridle forces the net to tow at an angle of approximately 60º starboard of the ship's track, at a cable length of 150 m. A detailed description of the SUIT sampling technique and performance was provided as supplementary material in (Flores et al. 2012). Depending on the sea-ice conditions, SUIT haul durations varied between 17 and 42 min (mean = 29 min) over an average distance of 1.5 km (Table 1). A detailed description of SUIT operations during PS81 expedition was provided in the Chapter III of this thesis.

Nine oblique (0-500 m layer) sampling stations were positioned in the proximity of the horizontal SUIT hauls. Among the oblique hauls, five were conducted during the night, two at dusk and two during the day (Table 1). The 0-500 m layer was sampled with double oblique hauls using a Rectangular Midwater Trawl (RMT). The trawl consisted of two nets: 1) a RMT-8 with a mesh size of 4.5 mm at the opening and 0.85 mm at the codend with a mouth opening of 8 m^2, and 2) a RMT-1 with a 0.33 mm mesh and an opening of 1 m^2. A mechanical impeller flowmeter (Hydro Bios, Kiel) was mounted in the mouth of the RMT-8 to measure the volume of filtered water. The volume of water filtered by the RMT-1 ranged between 1055 and 4280 m^3. Further details of RMT sampling are given in Schaafsma et al. (2016).

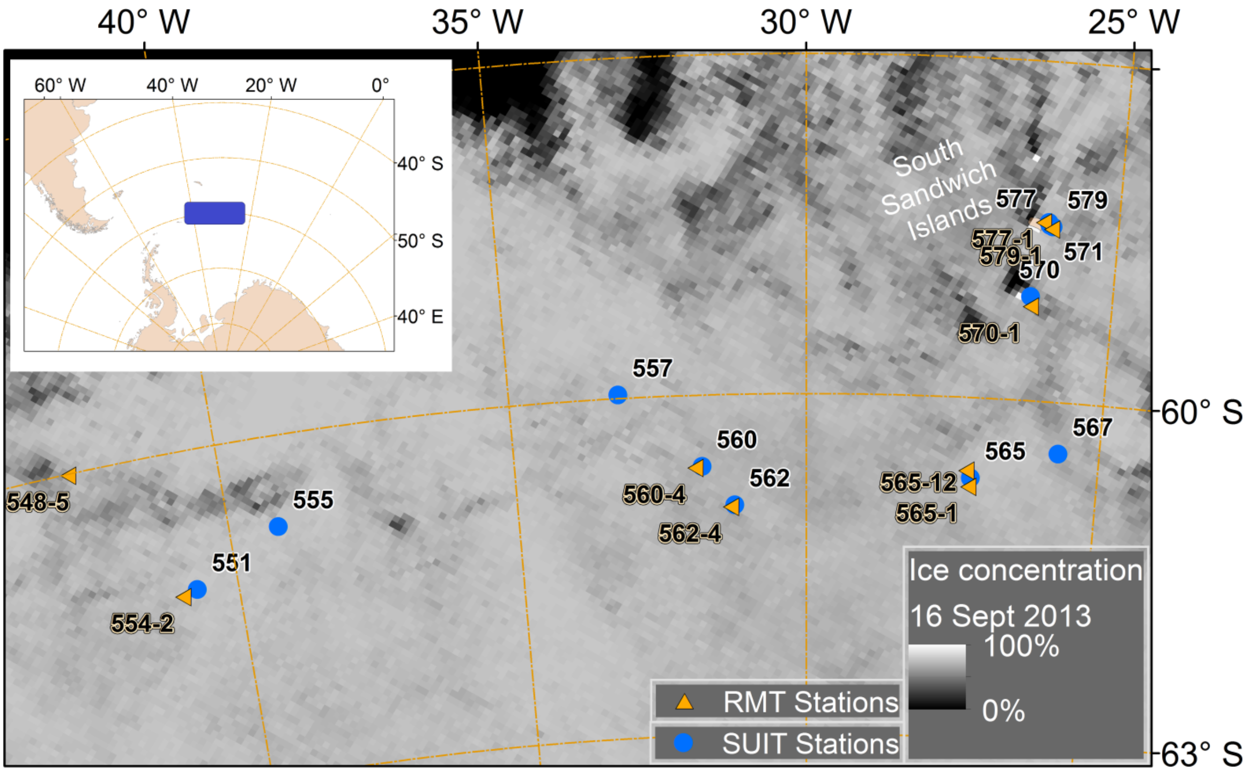

Figure 1. SUIT and RMT stations map during RV *Polarstern* expedition PS81 ANT XXIX/7. Sea-ice concentration acquired from University of Bremen (http://www.iup.uni-bremen.de: 8084/amsr/); sampling was performed from west to east, from August to October 2013; number codes next to sampling locations indicate station numbers.

Table 1. Station table of SUITs and corresponding RMTs sampling scheme

SUIT				RMT				
Station code	Date	Latitude °S	Longitude °W	Station code	Date	Latitude °S	Longitude °W	Sampling depth
551_1	31-08-2013	61.22	40.73	548_5	29-8-2013	60.00	42.43	500
555_47	09-09-2013	60.80	39.15	554_2	1-9-2013	61.25	40.92	500
557_2	10-09-2013	59.97	30.16	-	-	-	-	-
560_2	11-09-2013	60.63	31.78	560_4	12-9-2013	60.62	31.83	500
562_5	12-09-2013	60.97	31.24	562_4	12-9-2013	60.97	31.23	200
565_5	16-09-2013	60.71	27.17	565_1	16-9-2013	60.76	27.14	500
567_2	28-09-2013	60.45	25.70	565_12	17-9-2013	60.62	27.18	500
570_5	29-09-2013	59.08	26.34	570_1	29-9-2013	59.15	26.26	600
571_2	30-09-2013	58.42	26.12	-	-	-	-	-
577_2	02-10-2013	58.44	26.10	577_1	2-10-2013	58.40	26.14	500
579_2	02-10-2013	58.46	26.05	579_1	2-10-2013	58.45	26.00	600

Environmental data

An array of sensors was mounted in the SUIT frame, including a Conductivity Temperature Depth probe (CTD; Sea and Sun CTD75M) with built-in fluorometer, two spectral radiometers, and a video camera. Water inflow speed was estimated using a Nortek Aquadopp® Acoustic Doppler Current Profiler (ADCP). The trawled area was calculated by multiplying the distance sampled in water, estimated from ADCP data, with the net width (0.5 m for the zooplankton net, and 1.5 m for the shrimp net respectively). An altimeter (Tritech PA500/6-E) connected to the CTD probe measured the distance between the net and the sea-ice underside. Sea ice draft was calculated as the difference between the depth of the net relative to the water level, measured by the CTD pressure sensor, and the distance to the sea-ice underside, measured by the altimeter, and corrected for pitch and roll angles. Draft was then converted into sea-ice thickness by using a sea-ice density value of 900 kg m^{-3}. During each haul, sea-ice concentration [%], sea-ice and snow thicknesses, changes in ship speed and irregularities were estimated visually by an observer on deck. A detailed description of environmental data collection was provided in Chapter III of this thesis.

Gridded daily sea-ice concentrations for the Southern Ocean, derived from AMSR2 satellite data, using the algorithm specified by Spreen et al. (2008), were downloaded from the sea-ice portal hosted at University Bremen (www.meereisportal.de).

A CTD-probe with a carousel water sampler was used to collect environmental parameters from the water column. The CTD (Seabird SBE911+) was equipped with a fluorometer (Wetlabs FLRTD) and a transmissiometer (Wetlabs C-Star). Among all CTD stations, the closest in time and space to the SUIT stations were chosen. Chlorophyll *a* (Chl *a*) concentrations of water samples, measured with a Turner 10-AU fluorometer, were kindly provided by Christine Klaas (Alfred Wegener Institute). Calibration of the fluorometer with a range of concentrations of a Chl *a* standard (from Anacystis nidulans, Sigma-Aldrich) was carried out at the beginning and at the end of the cruise.

Conversion to carbon units was performed applying a carbon:Chl *a* equivalent ratio of 50 (Atkinson et al. 1996).

Biological data

The zooplankton catch was partially sorted on board. Few animals were immediately extracted and frozen at -20°C for further analysis. A quantitative subsample of the material was preserved in 4% formaldehyde/seawater solution. After the expedition, the preserved samples from SUIT hauls were analysed for species composition and abundance at the Alfred Wegener Institute. Samples from RMT hauls were analysed at the University of British Columbia. Here we present the data only from the SUIT mesozooplankton net and from the RMT1. Adult copepods and their copepodite stages were integrated per species in abundance calculations. Areal abundances from horizontal hauls were calculated by dividing the total number of animals per haul by the trawled area. For oblique hauls, volumetric abundances were calculated by dividing the total number of animals per haul by the volume of water filtered. Conversion to areal abundances was done by multiplying volumetric abundances by the sampling depth of 500 m.

In macrofauna species, total body length was measured to the nearest 0.1 mm and a mean size per species was used for biomass calculations. Zooplankton biomass was calculated using known species length – weight relationships and was expressed as mg dry weight m^{-2} (Mizdalski 1988). For copepod species, a mean dry weight was theoretically assumed for each developmental stage (Mizdalski 1988) and scaled to biomass using the stage abundance of each species.

Krill from the SUIT catches were staged according to Makorov and Denys (1981). An analysis of length – stage indicated that the group of individuals with a body length (BL) of 14 mm, was 75% composed of furcilia VI, while the group with a BL of 15 mm was 75% composed of juveniles. According to this analysis, krill from RMT were considered furcilia for body lengths < 15 mm.

Morphometrics, dry weight and proportional digestive gland size

Freshly caught krill from four SUIT stations (557, 562, 567 and 571) were staged according to Makorov and Denys (1981) and frozen at -20°C. At the Alfred Wegener Institute's laboratory, BLs were measured from the tip of the rostrum to the tip of the telson under the stereomicroscope with a digital camera attached, using the Leica LAS V4.1 image analyser software. Additionally, the length of the digestive gland and the carapace length were measured. The proportional digestive gland size expressed in the ratio of the carapace length is here used as a suitable measurement of an indicator of recent feeding (O'Brien et al. 2011; Virtue et al. 2010).

After measurements, krill samples were placed in pre-weighted vials as individuals, or pooled between 2 to 4 individuals per vial for smaller organisms. Vials containing fresh krill were first weighted on a microbalance, then freeze-dried and weighted again after the drying process.

Data analysis

SUIT sampling stations and associated RMT stations were grouped according to three community types identified based on the under-ice faunal abundance and biomass composition: Type I *krill-dominated* – stations 551, 555 and 557; Type II *copepod-dominated* – stations 560, 562, 565 and 567; Type III *low biomass/abundance* – stations 570, 571, 577 and 579 (Chapter III of this thesis). Carbon demand under sea ice and in the water column was calculated for abundant ice-associated species (Antarctic krill furcilia, *Stephos longipes* Giesbrecht, 1902), and for abundant pelagic species (*Calanus propinquus* Brady, 1883, *Ctenocalanus* spp., and *Metridia gerlachei* Giesbrecht, 1902). The carbon demand was calculated by multiplying each species' areal abundance with individual ingestion rates: *Ctenocalanus* spp. 3 μg C ind^{-1} d^{-1} (Pakhomov and Froneman 2004); *C. propinquus* 10 μg C ind^{-1} d^{-1} and *M. gerlachei* 5 μg C ind^{-1} d^{-1} (Drits et al. 1993; Pakhomov and Froneman 2004; Schnack 1983); furcilia 23 μg C ind^{-1} d^{-1} (Pakhomov et al. 2004). Due to the high variability of reported ingestion rates, generally the values at the lower end of the reported range were chosen. For *Ctenocalanus* spp., *M. gerlachei* and *S. longipes,* individual ingestion rates were chosen based on a sensitivity analysis performed to determine the rate of change in total community carbon demand with various ingestion rates.

Predation by chaetognaths was estimated using ingestion rates of 0.22 prey items ind^{-1} d^{-1} for *Sagitta* spp., and 0.07 prey items ind^{-1} d^{-1} for *Eukrohnia hamata* Möbius, 1875 (Giesecke and González 2012). The experiments on which these feeding rates were based used copepods as prey items.

Statistical differences in carbon demand and body condition of animals between all three under-ice community types were assessed with the Kruskal Wallis test (Kruskal 1952). To assess the statistical differences in grazing impact and predation pressure between the three under-ice community types, all possible combinations of two were tested using the nonparametric Mann-Whitney-Wilcoxon test (Wilcoxon 1945).

RESULTS

Environmental conditions

All sampled stations were ice-covered. Satellite-derived sea-ice coverage at the sampling locations, averaged over a grid cell of 6.25 km, was in general between 86 and 100 %. Only at two stations (570 and 579) sampled north of 60˚S at the end of September/beginning of October (Fig. 1) sea-ice coverage was about 50 %. Sea-ice thickness was still within the range (0.43 to 0.70 m) of the preceding stations, with one exception (station 571, 0.23 m). Snow cover was present at all stations, ranging from 0.05 to 0.6 m. Under-ice water temperatures and salinities were on average -1.83 ± 0.012 ˚C and 34.14 ± 0.11, respectively. Further details of sea-ice and water parameters and snow cover are given in Table 1 of Chapter III.

Chlorophyll a distribution

Under-ice (0 – 2 m layer) chlorophyll *a* concentrations ranged from 0.097 to 0.134 mg Chl *a* m^{-3} south of 60°S during August/early-September and showed higher values ranging from 0.164 to 0.275 mg Chl *a* m^{-3} north of 60°S during late-September/beginning of October (Chapter III - Table 1). Within the mixed layer depth, chlorophyll *a* concentrations at most of sampling stations were within the same range as the under-ice chlorophyll *a* concentrations. Under-ice chlorophyll *a* distribution at sampling stations gradually increased from type I to type III stations (Fig. 2).

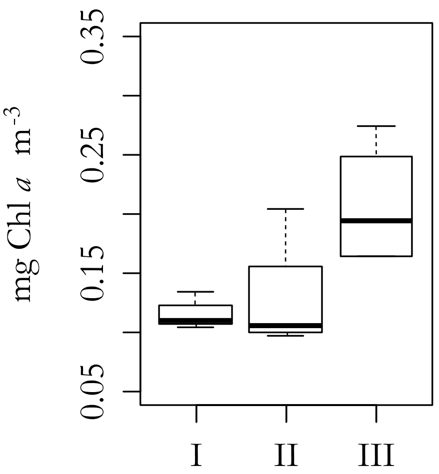

Figure 2. Distribution of available chlorophyll *a* under ice (0 – 2 m depth) in 3 types of stations (on the x axis), grouped according to the under-ice community types identified in Chapter III; the horizontal bar indicates median concentrations; the upper and the lower edges of the 'box' (hinges) denote the approximate 1st and 3rd quantiles, respectively

Zooplankton structure

Detailed description of the zooplankton species composition, abundance and biomass under ice is presented in Chapter III. Preliminary description of zooplankton from the water column (0 - 500 m layer) was presented in Pakhomov and Hunt (2014).

Under-ice dominant copepods species *Calanus propinquus*, *Ctenocalanus* spp. and *Stephos longipes* numerically accounted for 64% of total community, while krill larvae represented another 25%, thus together contributing for the majority of the under-ice community. The chaetognaths represented only 0.33% of the under-ice community. In biomass terms, the selected copepod species represented 15% of total under-ice community, krill larvae 25%, while juveniles and (sub-)adult krill represented another 35% together. The chaetognaths represented about 4% of the total biomass under ice. Krill larvae abundance in the 0 – 2 m layer varied between 0.01 ind. m^{-2} and 3.57 ind. m^{-2}, with a median abundance of 0.28 ind. m^{-2} (Table 2) and a median biomass (dry weight) of 0.55 mg DW m^{-2}. The abundance of *C. propinquus* under ice was 0.16 ind. m^{-2}, and accounted for about 20% of the biomass of krill larvae. Higher abundances had *S. longipes* and *Ctenocalanus* spp. of 1.04 and 0.23 ind. m^{-2} respectively, but both species accounted for much less biomass of only 0.04 and 0.03 mg DW m^{-2} respectively (Table 2).

Table 2. Summary of *Euphausia superba* larvae, copepods and chaetognaths areal abundances (ind. m^{-2}) and biomass (mg DW m^{-2}) in the 0 - 2 m surface layer and the 0 - 500 m layer in ice-covered waters; standard deviation follows the values and the range of abundance is given in parenthesis; PRA is percentage abundance of total zooplankton community and PRB is percentage biomass of total zooplankton community

	Under ice (0 – 2 m)				**Water column (0 – 500 m)**		
Species	Median abundance	PRA %	Median biomass	PRB %	Median abundance	PRA %	Median biomass (mg DW m^{-2})
Euphausia superba	0.28±1.07 (0.01 – 3.57)	25.27	0.55±2.14	24.54	2.48±11.08 (0 – 30.68)	0.40	4.97±22.15
Stephos longipes	1.04±4.05 (0.01 – 13.26)	35.89	0.04±0.14	3.38	-	-	-
Calanus propinquus	0.16±0.70 (0.02 – 2.37)	13.31	0.11±0.49	12.59	518.40±1200.96 (0 – 3677)	7.07	362.90±840.67
Ctenocalanus spp.	0.23±2.83 (0.004 – 9.32)	14.81	0.03±0.04	0.60	1415.93±1238.13 (54 – 4205)	13.38	21.24±18.57
Metridia gerlachei	<0.01	0.62	<0.01	0.07	1039.20±894.72 (306.3 – 3077.3)	13.44	727.42±626.30
Eukrohnia hamata	0.0058±0.006 (0 – 0.02)	0.24	0.01±0.02	0.84	649.20±401.29 (123.9 – 1438.9)	6.41	1803.47±1114.80
Sagitta spp.	0.0027±0.005 (0 – 0.01)	0.09	0.05±0.11	3.05	55.85±33.82 (8.7 – 115.1)	0.41	1120.39±678.37

In the water column (0 – 500 m layer) copepod species selected for grazing impact estimates contributed with 33.9% to the zooplankton community, while krill, all stages together, represented only 0.4%. The chaetognaths accounted for about 7 % of the zooplankton community, largely dominated by *E. hamata*.

In the 0 – 500 m layer, areal abundance of krill larvae varied between 0.00 and 30.68 ind. m^{-2}, with a median areal abundance of 2.48 ind. m^{-2}. Their median areal biomass was about one order of magnitude higher than under ice, 4.97 mg DW m^{-2} respectively (Table 2). Both *Ctenocalanus* spp. and *Metridia gerlachei* had high areal abundances in the water column of 1415 ind. m^{-2} and 1039 ind. m^{-2}, respectively. In terms of biomass, *M. gerlachei* clearly dominated (727 mg DW m^{-2}) followed by *C. propinquus* (352.9 mg DW m^{-2}; Table 2).

Eukrohnia hamata was the most abundant chaetognath in the ice-water interface layer (0.006 ind. m^{-2}). *Sagitta* spp. accounted for only half the median abundance of *E. hamata* (0.003 ind. m^{-2}). In terms of biomass, however, the larger *Sagitta* spp. accounted for the five-fold value (0.05 mg m^{-2}) compared to *E. hamata* (0.01 mg m^{-2}; Table 2). In the water column, *E. hamata* dominated both in abundance and biomass (649.200 ind. m^{-2}; 1803.47 mg DW m^{-2}) compared to *Sagitta* spp. (55.85 ind. m^{-2}; 1120.39 mg DW m^{-2}).

Based on median values, 10 % of the total sampled krill furcilia population and biomass were caught in the ice-water interface layer, which only represented 0.4 % of the water-column sampled depth, indicating concentration in the under-ice habitat. In contrast, abundances of the pelagic copepods in the ice-water interface layer were below 0.1% of their integrated water-column abundances.

Under ice, *C. propinquus* and *Ctenocalanus* spp. abundances were highly correlated ($r = 0.81$; Chapter III - Table S1). Among the chaetognaths, the abundance of *E. hamata* under-ice had the highest correlation with *C. propinquus* ($r = 0.91$) and *Ctenocalanus* spp. ($r = 0.68$) abundances. *Sagitta* spp. was highly correlated with *Ctenocalanus* spp. ($r = 0.66$) and to a lesser degree to krill larvae ($r = 0.56$). In the water column, notably *M. gerlachei* had a strong negative correlation with *C. propinquus* ($r = -0.73$; Table 3). Among the chaetognaths, *Sagitta* spp. was highly correlated with *Ctenocalanus* spp. ($r = 0.60$).

Table 3. Correlation table between the areal abundance of krill larvae, copepods and chaetognaths in the water column (0 – 500 m); correlation coefficients >0.50 are presented in bold

	Calanus propinquus	*Ctenocalanus* spp.	*Metridia gerlachei*	*Euphausia superba*	*Eukrohnia hamata*	*Sagitta*.spp.
Calanus propinquus	1					
Ctenocalanus spp.	**0.58**	1				
Metridia gerlachei	**-0.73**	-0.15	1			
Euphausia superba	0.20	0.15	-0.32	1		
Eukrohnia hamata	0.13	0.27	-0.05	0.19	1	
Sagitta.spp.	0.25	**0.60**	0.22	0.42	**0.50**	1

Krill larvae proportional digestive gland size

Krill furcilia VI (measured from frozen samples collected at four stations) had an average length of 10.9 mm (range 7.7 to 15.4 mm) with a dry weight of 1.65 mg (range 0.63 to 2.86 mg) (Table 4). There were significant differences among stations in both larval length (Kruskal Wallis $Chi^2 = 10.2$; $p = 0.016$) and individual dry weight (Kruskal Wallis $Chi^2 = 9.3$; $p = 0.025$). Smaller larvae were found at station 567, intermediate size larvae at stations 562 and 571, and bigger larvae at station 557 (Table 4). This is in agreement with the spatial variability in length distribution found by Schaafsma et al. (2016). The digestive gland (expressed as % carapace) varied from 26 % to 53 % (Fig. 3). Krill larvae at station 557 had the largest digestive gland (median = 0.43% carapace). This was significantly higher than in larvae at station 571, which had the smallest digestive gland (median = 0.34% carapace; Wilcox test: $W = 87$, $p < 0.01$). Larvae at station 567 had intermediate values, with the highest variability (median = 0.39% carapace; Wilcox test with Stn 557: $W = 43$, $p = 0.38$; Wilcox test with Stn 571: $W = 145$, $p = 0.059$).

Table 4. Summary of body condition of krill furcilia VI presenting averaged values per sampling station and standard deviations

Station code	n	Body length [mm]	Wet weight [mg]	Dry weight [mg]	Carapace length [mm]	Digestive gland length [mm]
557	7	13.33±0.92	11.25±0.72	2.64±0.32	3.98±0.44	1.66±0.30
562	11	11.08±0.59	7.01±2.31	1.74±0.48	na	na
567	12	9.08±0.04	4.87±0.72	0.74±0.15	2.76±0.36	1.11±0.23
571	19	11.35±1.23	9.71±3.15	1.69±0.54	3.69±0.52	1.29±0.33

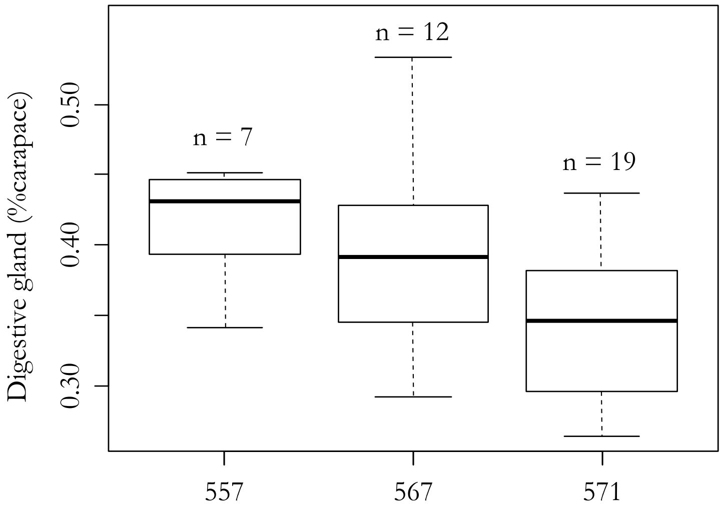

Figure 3. Digestive gland (expressed as percentage of the carapace length) of krill furcilia VI collected at three SUIT sampling stations (station codes indicated on the x-axis); the horizontal bar indicates median values; the upper and the lower edges of the 'box' (hinges) denote the approximate 1st and 3rd quantiles, respectively

Carbon demand of dominant herbivores

Abundance data of each dominant herbivorous species combined with their individual ingestion rates are summarised in Table 5 for the under-ice surface community and in Table 6 for the water-column community (0 – 500 m layer). In the under-ice surface layer, furcilia had the highest carbon demand ranging from 0.24 to 82.15 µg C m^{-2} d^{-1}, with a median of 6.42 µg C m^{-2} d^{-1} (Table 5). *C. propinquus* and *S. longipes* had second and third highest carbon demand with a median of 1.04 and 1.61 µg C m^{-2} d^{-1} respectively. In general the carbon demand of all species was highest at type II stations, compared to type I and III stations.

In the 0 – 500 m layer, *C. propinquus* and *M. gerlachei* had the highest median carbon demands of 5184 and 5196 µg C m^{-2} d^{-1} respectively (Table 6). *Ctenocalanus* spp. had a slightly lower carbon demand of 4248 µg C m-2 d-1. Krill furcilia had the lowest carbon demand ranging between 0 and 759 µg C m^{-2} d^{-1}, with a median of 272 µg C m^{-2} d^{-1}. In general, the carbon demand in the 0-500 m stratum showed a similar trend as in the under-ice surface, with the highest overall carbon demand found at type II stations.

Grazing impact

Using data on integrated chlorophyll *a* biomass in the water, daily grazing impact under ice of all species considered here combined varied between 0.7% (station 577) and 32.9% (station 567) of the phytoplankton standing stock. Within the three community types identified in Chapter III, type II stations had higher grazing impact of 25% compared to 3.2% at type I stations (Wilcox test: $W = 0$, $p = 0.057$) and 2.1% at type III stations (Wilcox test: $W = 16$, $p = 0.028$; Fig. 4).

In the 0 – 500 m layer, daily grazing impact of all species considered here varied between 0.4% (station 548-5) and 10.2% (station 565-12) of the phytoplankton standing stock. Type II stations had the highest grazing impact of 5.2% compared to the grazing impact at type I stations (2.7%; Wilcox test: $W = 2$, $p = 0.533$) and at type III stations (1.2%; Wilcox test: $W = 12$, $p = 0.057$; Fig. 4).

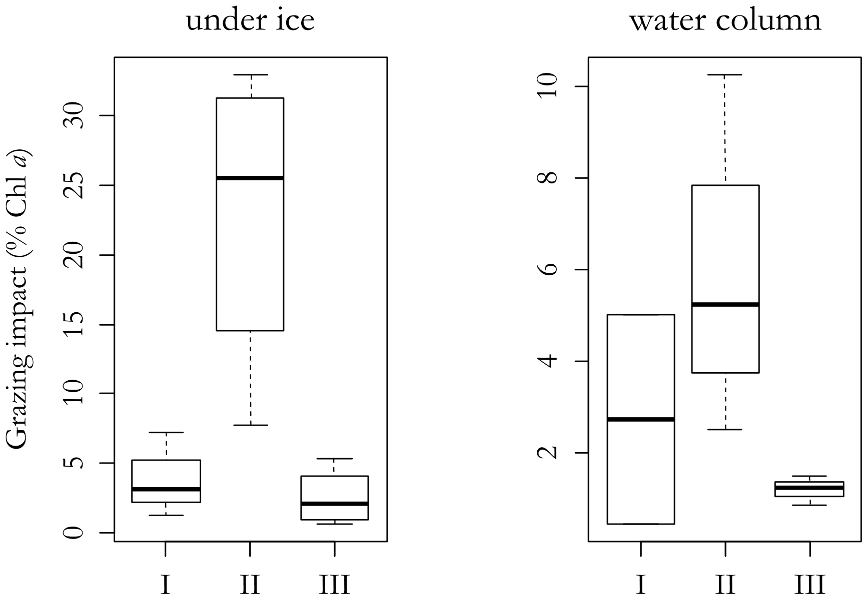

Figure 4. Grazing impact of dominant herbivorous species expressed as percentage of chlorophyll *a* biomass under ice (0 – 2 m depth) and in the water column (0 – 500 m depth) in 3 types of stations (on the x axis), grouped according to the under-ice community types identified in Chapter III; the horizontal bar indicates median values; the upper and the lower edges of the 'box' (hinges) denote the approximate 1st and 3rd quantiles, respectively

Table 5 Carbon demand of dominant herbivorous species and chaetognaths predation rates under ice (0 – 2 m layer)

	Station code	Ingestion rates (μg C m^{-2} d^{-1})				Chaetognaths predation (prey item m^{-2} d^{-1})	
		Euphausia superba	*Stephos longipes*	*Calanus propinquus*	*Ctenocalanus* spp.	*Eukrohnia.hamata*	*Sagitta* spp.
Type I	551	0.239	1.043	1.295	0.216	0.0002	0.0000
	555	2.110	2.090	1.715	0.688	0.0010	0.0000
	557	14.468	2.502	1.134	1.176	0.0001	0.0031
Type II	560	4.502	6.551	1.613	4.020	0.0004	0.0014
	562	8.563	13.262	9.304	10.505	0.0006	0.0007
	565	42.117	1.586	9.264	7.963	0.0008	0.0006
	567	82.154	0.140	23.759	27.952	0.0014	0.0035
Type III	570	6.424	0.034	5.983	0.197	0.0005	0.0008
	571	15.902	0.143	1.389	0.097	0.0003	0.0000
	577	1.971	0.013	0.233	0.013	0.0000	0.0000
	579	6.375	0.118	0.623	0.018	0.0002	0.0001
	median	6.424	1.042	1.613	0.115	0.0004	0.0006

Table 6 Carbon demand of dominant herbivorous species and chaetognaths predation rates in the water column (0 – 500 m layer)

		Ingestion rates (µg C m^{-2} d^{-1})				Chaetognaths predation (prey item m^{-2} d^{-1})	
	Station code	*Euphausia superba*	*Calanus propinquus*	*Ctenocalanus* spp.	*Metridia gerlachei*	*Eukrohnia.hamata*	*Sagitta* spp.
Type I	548-5	286.43	595.01	163.55	3258.05	8.67	1.92
	554-2	0.00	0.00	2502.37	8151.66	100.72	9.18
Type II	560-4	401.67	19114.15	6317.39	1822.32	68.78	4.84
	562-4	0.00	6676.56	2670.62	2596.44	24.20	2.45
	565-1	13.25	5184.33	12615.21	5195.85	51.13	14.83
	565-12	422.92	36775.82	7405.54	1531.49	78.71	25.32
Type III	570-1	39.27	5748.84	7470.65	6047.67	38.45	12.29
	577-1	759.88	1533.92	4247.79	15386.43	43.36	13.69
	579-1	272.19	2434.49	3155.82	9204.47	45.44	15.16
	median	272.19	5184.33	4247.79	5195.85	45.44	12.29

Predation pressure

Predation pressure by chaetognaths was expressed as percentage of the areal abundances of dominant herbivorous species selected in this study, hereafter named mesozooplankton. Under ice (0 – 2 m depth stratum), daily predation pressure varied between 0% and 0.13% of the mesozooplankton stock. Lowest daily predation pressure was encountered at type II stations (0.02%), and somewhat higher at type I (0.04%) and type III stations (0.05%; Fig. 5).

In the 0 – 500 m layer, daily predation pressure varied between 1.14% and 4.46% of the mesozooplankton stock (Fig. 5). Daily predation pressure was similar at all stations, except at station 554-2, where maximum predation rate was found. Predation pressure in the water column was in general one order of magnitude higher than in the ice-water interface.

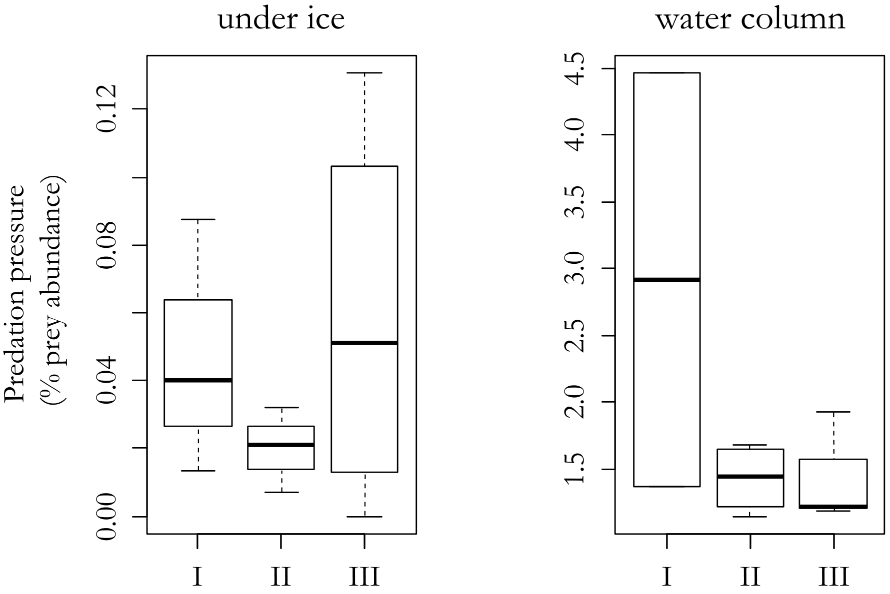

Figure 5. Predation impact by chaetognaths expressed as percentage of dominant prey abundance (krill larvae and copepod species *S. longipes*, *C. propinquus*, *Ctenocalanus* spp., and *M. gerlachei*); under ice (0 – 2 m depth) and in the water column (0 – 500 m depth); x-axis labels correspond to 3 types of stations following three community types identified in Chapter III; the horizontal bar indicates median values; the upper and the lower edges of the 'box' (hinges) denote the approximate 1st and 3rd quantiles, respectively

DISCUSSION

Under-ice food availability and carbon demand

In the ice-water interface layer, Antarctic krill furcilia accounted for over 60% of the cumulative carbon demand of the dominant herbivorous species. This can largely be attributed to the relatively high carbon demand of Antarctic krill (Pakhomov et al. 2004), even at the lower ingestion rates assumed for winter time (Meyer and Auerswald 2014), in combination with a dominance in abundance (Chapter III, Schaafsma et al. 2016). During austral winter, krill furcilia were mostly associated with the sea-ice underside during daytime, and dispersed in the water column, not deeper than 20 m, during the night (Pakhomov & Hunt 2014). In our night-time-dominated sampling scheme, integrated per-area abundance of krill furcilia in RMT samples was 10-fold higher than in SUIT samples. This corresponds well with the 10-fold difference between the 20 m dispersal range of the krill larvae in the water column and the 0 – 2 m depth layer sampled by SUIT (Table 2). Because krill larvae were observed to aggregate in crevices and in horizontal gaps between stacked ice floes (U. Freier, K. Meiners pers. comm.), where they may not have been caught quantitatively with a SUIT, our estimates of krill larvae total carbon demand at the sea-ice underside may have been underestimated.

It appears that due to low chlorophyll *a* (Chl *a*) concentrations during our survey, krill larvae likely not have encountered sufficient autotrophic resources in the water column. Previous studies shows that at Chl *a* concentrations of 0.3-0.5 mg m^{-3} only half-saturated daily growth rates in *E. superba* were possible (Atkinson et al. 2006; Ross et al. 2000). Accordingly, our average proportional digestive gland sizes of 38% may indicate sub-optimal feeding conditions (O'Brien et al. 2011; Virtue et al. 2010). The range of proportional digestive gland sizes observed in our study is in good agreement with measurements of krill larvae sampled under the pack ice by divers during PS81 expedition, who reported similar values in the inner pack ice, but significantly higher proportional digestive gland sizes in the Marginal Ice Zone (MIZ), where phytoplankton biomass was higher (MIZ; B. Meyer, pers. comm.). In our study the lowest proportional digestive gland sizes were recorded at Stn 571 in the MIZ, indicating a potential local effect compared to the spatially much wider extending sampling by divers in the MIZ during PS81 expedition.

The three different under-ice community types at the ice-water interface layer (Chapter III) differed in their total carbon demand. This pattern, however, did not mirror the distribution of Chl *a* in the surface water: the community with the lowest total carbon demand was associated with the stations having the highest Chl *a* concentrations in the upper two meters under ice (Fig. 2, Table 5). This decoupling of grazer carbon demand from pelagic food availability in surface waters implies that ice-associated grazers could have covered a considerable part of their food demand with sea-ice algae and other sea-ice derived resources (Daly 1990; O'Brien et al. 2011; Pakhomov et al. 2004). During Antarctic winter, primary production occurs mainly in sea ice (Arrigo et al. 1997). Hyperspectral measurements along our SUIT profiles at three stations (555, 567 and 577) demonstrated that the chlorophyll *a* concentration in sea ice was about an order of magnitude higher than in the surface 0–2 m water layer (B. Lange unpublished data). Lower Chl *a* concentration in sea ice was observed at station 577, where the carbon demand of krill furcilia was also minimal (Table 5). Low availability of ice algae in this area could also explain the low feeding intensity of krill larvae observed at the nearby station 571. At this station, the lowest sea-ice thickness observed during the expedition could indicate loss of ice algae caused by advanced melting.

In the 0-500 m layer, *C. propinquus* and *M. gerlachei* equally contributed for the bulk of the carbon demand at most stations. During winter, *C. propinquus* is distributed in the upper 200 m of the water column and concentrate in the 200 -500 m layer by early spring (Schnack-Schiel and Hagen 1995). During our expedition, their adults were distributed between 175 m depth and the surface (Pakhomov and Hunt 2014), and became less abundant in the ice-water interface layer by the end of September (Chapter III). *M. gerlachei* has a winter distribution spread through mid-water layers (Schnack-Schiel 2001) and was barely present in our under-ice samples suggesting little or no association with sea-ice habitats. Both *C. propinquus* and *M. gerlachei* have been found to preferentially ingest ciliates and dinoflagelates even during diatom-dominated spring blooms (Atkinson 1995; Atkinson et al. 1996), indicating the potential of these species to rely on heterotrophic resources, thus to overcome winters with low phytoplankton resources. Almost exclusive presence of triacylglycerols and not wax esters in *C. propinquus* and *Stephos longipes*, and the equal presence of these two lipid classes in *M. gerlachei* (Schnack-Schiel 2001) indicate active feeding during the dark season (Hagen and Auel 2001; Sargent et al. 1981). The explanation is that triacylglycerols are usually considered short-term energy reserves, while wax esters may serve as long-term deposits (Sargent and Henderson 1986).

In terms of total carbon demand of dominant grazers, values for copepods from the 0-500 m water column were more than 3 orders of magnitude higher than those of krill larvae and copepods in the ice-water interface layer (Table 5). This indicates that the bulk of the mesozooplankton carbon flux was passed through the abundant pelagic copepod species in our study area during winter 2013, and under-ice fauna only accounted for a small portion. In the light of low phytoplankton biomass in the water column, this food web was most likely fuelled by detritus and microbial secondary production.

O'Brien et al. (2011) revealed two main feeding strategies in postlarval krill: individuals below the ice feed mostly on sea-ice diatoms, while those in open water ingest copepods and detritus. This implies that not only krill larvae, but the postlarval krill as well, graze ice algae in winter (O'Brien et al. 2011), and can largely dominate under-ice community biomass and hence the carbon demand (Flores et al. 2012; Hunt et al. 2011). This would reflect in increased competition with the less efficiently feeding krill larvae. However, krill size ranges or maturity stages are often found to be relatively restricted in schools or swarms of krill (Kawaguchi et al. 2010; Quetin and Ross 1984; Watkins 2000) which is probably due to a combination of behavioural and physical factors (Quetin and Ross 1984; Siegel 2012). This separation of younger and mature krill reduces the competition for food and the risk of adults preying upon the younger stages.

During our survey, postlarval krill significantly contributed to the under-ice community only at two stations. The community biomass of station 551 was dominated by sub-adult krill, which together with a low number of first-year juveniles, second-year juveniles and adults accounted for 98%. At station 555, the community biomass was dominated by first-year juveniles (62%; Chapter III – Fig.S2; Schaafsma et al. 2016). By a tentative estimate of minimal krill adults, sub-adults and juveniles carbon demand at stations 551 and 555, an increase in under-ice grazing impact with 77% and 50% respectively could be inferred. Nevertheless, the limited presence of postlarval krill from northern Weddell Sea during winter 2013 remains difficult to explain. If only a modest number of postlarval krill would have be present, such as at station 551, the overall autotrophic food sources within the under-ice zooplankton community would have been differently partitioned.

Grazing pressure

In the ice-water interface layer, grazing pressure in relation to chlorophyll *a* concentration of planktonic algae was higher by a factor of 2 compared to the water column. This indicates that, without accounting for the surplus of resources potentially available from ice algae, competition for autotrophic resources was higher in the under-ice habitat.

Grazing impact on autotrophic carbon standing stock by dominant copepods in the water column was similar with values found near South Georgia in late summer, which actually considered the entire zooplankton community demand (Pakhomov et al. 1997). If other herbivorous species would have been considered here, such as salps, some pteropods and other euphausiids than Antarctic krill, which had an increased contribution to the pelagic zooplankton community at few stations (Pakhomov and Hunt 2014), grazing impact in the water column would have been higher. Under ice, these species had a much lower contribution to the total community biomass (Chapter III). A potential overestimation in our grazing impact might have been partially attributed to a low chlorophyll *a* concentration in the water during winter, a time when majority of grazers compensate their food demand with heterotrophic resources. Despite these limitations, our comparative analysis provides an indication that krill larvae and other ice-associated grazers generally encountered a higher competition for pelagic autotrophic carbon sources at the ice-water interface, if sea-ice autotrophic carbon sources were ignored.

From chlorophyll *a* biomass in the sea ice, however, only a small fraction placed at underside of sea ice is directly accessible for grazers scraping at the ice surface. If we would assume that at least 10% of ice algae biomass would effectively be available for grazers at the underside of ice, this fraction would still be by a factor of 7 higher than the highest Chl *a* concentration found in the ice-water interface layer. Therefore even in higher grazing impact area, such as identified at under-ice community type II stations, krill larvae under ice would still have faced lower competition for autotrophic food resources than in the water column. Exceptionally, the low proportional digestive gland sizes of krill larvae at station 567 could have been resulted from the combined effect of lower Chl *a* in the sea ice in this area and higher intra-species competition, as the highest larvae under-ice abundance was found here.

The high carbon demand of the midwater copepods, however, implies that at the low Chl *a* concentrations present during our study, the competition for autotrophic resources may not be a key factor driving their vertical distribution, as potentially sufficient heterotrophic resources were available in deeper layers. Therefore, the competition for food was probably not the only factor driving the association of krill larvae and other species with the under-ice habitat.

Predation pressure

Our daily predation pressure by chaetognaths in the under-ice surface layer correspond with the meso- and bathypelagic chaetognaths predation rates on the midwater copepods standing stock in the Lazarev Sea (Kruse et al. 2010a). In the epipelagic waters near Marion Island, however, the predation impact by chaetognaths was much higher (Froneman et al. 1998), and similar to our water-column daily predation rates.

The predation impact by chaetognaths was minimal in the upper 2 m under ice and largely restricted to the water column. One explanation would be that chaetognaths were attracted by the distribution of copepods (Froneman et al. 1998), as shown by high correlations between the copepods and chaetognaths' abundances in our samples (Table 3; Chapter III). Conversely, the higher predation pressure under ice at type II stations concurred with elevated copepod abundances, and to a lesser degree with krill larvae (Table 5). The correlations of *E. hamata* and to a lesser degree of *Sagitta* spp. with copepods and krill larvae distribution in the ice-water interface layer indicate that those few chaetognaths foraging under ice were indeed following their potential prey.

Stomach content analysis revealed that various species, such as pteropods and other chaetognaths, besides copepods and euphausiids, contribute to chaetognaths' diet (Froneman et al. 1998; Giesecke and González 2012). Hence, predation impact on copepods and krill larvae in our under-ice estimates might actually have been even lower. Conversely, the water column community had high abundances of carnivorous gelatinous organisms (jellyfish *Periphylla periphylla* Péron & Lesueur, 1810, siphonophores *Diphyes antarctica* Moser, 1925 and ctenophores *Callianira* sp.) which collectively accounted for >50 % of the total biomass (Pakhomov and Hunt 2014). These species would therefore increase even more the predation pressure on mesozooplankton in the water column. At the ice-water interface, these species were absent or rarely occur in our samples with low biomass, gelatinous species altogether accounting for < 5% of community biomass. Lower predation pressure could thus be a key advantage of species dwelling in the ice-water interface layer.

CONCLUSION

In the northern Weddell Sea, a niche partitioning was evident during winter 2013 between a) krill furcilia and ice-associated copepods in the ice-water interface layer, and b) dominant pelagic copepods deeper in the water column. The value of the under-ice environment as a winter habitat for certain zooplankton species seemed to be given primarily by a) ice algae as an additional abundant carbon source, and b) low predation pressure. The high carbon flux in the water column at low chlorophyll *a* concentrations suggests that heterotrophic carbon sources were well available. Phytoplankton was not as critical as ice algae availability for krill larvae and other ice-associated species, which would additionally benefit from predator avoidance by seeking the under-ice habitat.

The potential contribution of ice algal production to the heterotrophic carbon flux in the midwater is not well known. Changes in structural composition and extent of sea-ice will affect ice algae production and will disproportionally impact krill larvae and juveniles and ice-associated species. Despite its presumed importance to Antarctic krill-dependent food webs, little is known about the total magnitude or spatial and temporal variability of ice algal production. This variability, combined with constant evolution of the pack ice, demands new approaches to estimate the spatio-temporal variability of ice algal production in relation to sea-ice properties. In a future Antarctic system, reduced ice algal production as a result of sea-ice decline, may be compensated by increased water column phytoplankton productivity, but the sheltered environment for the krill larvae and other ice-associated species would still break away with unknown consequences for the affected populations.

Acknowledgments

We thank Captain Stephan Schwarze and the crew of RV Polarstern expedition ANT XXIX/7 for their excellent support with work at sea. We thank Michiel van Dorssen for operational and technical support with the Surface and Under Ice Trawl (SUIT). SUIT was developed by IMARES with support from the Netherlands Ministry of EZ (project WOT-04-009-036) and the Netherlands Polar Program (projects ALW 851.20.011 and 866.13.009). This study is part of the Helmholtz Association Young Investigators Group Iceflux: Ice-ecosystem carbon flux in polar oceans (VH-NG-800).

References

Ainley D, Fraser W, Sullivan C, Torres J, Hopkins T, Smith W (1986) Antarctic mesopelagic micronekton: evidence from seabirds that pack ice affects community structure. Science 232:847-849

Arrigo KR, Worthen DL, Lizotte MP, Dixon P, Dieckmann G (1997) Primary Production in Antarctic Sea Ice. Science 276:394-397. doi:10.1126/science.276.5311.394

Atkinson A (1995) Omnivory and feeding selectivity in five copepod species during spring in the Bellingshausen Sea, Antarctica. Ices J Mar Sci 52:385-396. doi:10.1016/1054-3139(95)80054-9

Atkinson A et al. (2006) Natural growth rates in Antarctic krill (*Euphausia superba*): II. Predictive models based on food, temperature, body length, sex, and maturity stage. Limnol Oceanogr 51:973-987. doi:10.4319/lo.2006.51.2.0973

Atkinson A, Shreeve RS, Pakhomov EA, Priddle J, Blight SP, Ward P (1996) Zooplankton response to a phytoplankton bloom near South Georgia, Antarctica. Mar Ecol Progr Ser 14:195-210

Atkinson A, Siegel V, Pakhomov E, Rothery P (2004) Long-term decline in krill stock and increase in salps within the Southern Ocean. Nature 432:100-103

Atkinson A et al. (2008) Oceanic circumpolar habitats of Antarctic krill. Mar Ecol Progr Ser 362:1-23. doi:10.3354/Meps07498

Bernard K, Froneman P (2003) Mesozooplankton community structure and grazing impact in the Polar Frontal Zone of the south Indian Ocean during austral autumn 2002. Polar Biol 26:268-275

Bernard KS, Steinberg DK, Schofield OM (2012) Summertime grazing impact of the dominant macrozooplankton off the Western Antarctic Peninsula. Deep-Sea Res Pt I 62:111-122

Daly KL (1990) Overwintering development, growth, and feeding of larval *Euphausia superb*a in the Antarctic marginal ice zone. Limnol Oceanogr 35:1564-1576

Daly KL (2004) Overwintering growth and development of larval *Euphausia superba*: an interannual comparison under varying environmental conditions west of the Antarctic Peninsula. Deep-Sea Res Pt II 51:2139-2168

Drits A, Pasternak A, Kosobokova K (1993) Feeding, metabolism and body composition of the Antarctic copepod *Calanus propinquus* Brady with special reference to its life cycle. Polar Biol 13:13-21

Flores H et al. (2011) Macrofauna under sea ice and in the open surface layer of the Lazarev Sea, Southern Ocean. Deep-Sea Res Pt II 58:1948-1961

Flores H et al. (2012) The Association of Antarctic Krill *Euphausia superba* with the Under-Ice Habitat. PLoS ONE 7. doi:10.1371/journal.pone.0031775

Froneman P, Pakhomov E, Perissinotto R, McQuaid C (2000) Zooplankton structure and grazing in the Atlantic sector of the Southern Ocean in late austral summer 1993: Part 2. Biochemical zonation. Deep-Sea Res Pt I 47:1687-1702

Froneman P, Pakhomov E, Perissinotto R, Meaton V (1998) Feeding and predation impact of two chaetognath species, *Eukrohnia hamata* and *Sagitta gazellae*, in the vicinity of Marion Island (Southern Ocean). Mar Biol 131:95-101

Giesecke R, González HE (2012) Distribution and feeding of chaetognaths in the epipelagic zone of the Lazarev Sea (Antarctica) during austral summer. Polar Biol 35:689-703. doi:10.1007/s00300-011-1114-y

Hagen W, Auel H (2001) Seasonal adaptations and the role of lipids in oceanic zooplankton. Zoology 104:313-326. doi:10.1078/0944-2006-00037

Hunt BPV, Pakhomov EA, Siegel V, Strass V, Cisewski B, Bathmann U (2011) The seasonal cycle of the Lazarev Sea macrozooplankton community and a potential shift to top-down trophic control in winter. Deep-Sea Res Pt II 58:1662-1676. doi:10.1016/j.dsr2.2010.11.016

Kawaguchi S, King R, Meijers R, Osborn JE, Swadling KM, Ritz DA, Nicol S (2010) An experimental aquarium for observing the schooling behaviour of Antarctic krill (*Euphausia superba*). Deep-Sea Res Pt II 57:683-692

Krafft BA, Skaret G, Knutsen T (2015) An Antarctic krill (Euphausia superba) hotspot: population characteristics, abundance and vertical structure explored from a krill fishing vessel. Polar Biol:1-14. doi:10.1007/s00300-015-1735-7

Kruse S, Hagen W, Bathmann U (2010) Feeding ecology and energetics of the Antarctic chaetognaths *Eukrohnia hamata*, *E. bathypelagica* and *E. bathyantarctica*. Mar Biol Res 157:2289-2302. doi:10.1007/s00227-010-1496-3

Kruskal WH (1952) A nonparametric test for the several sample problem. The Annals of Mathematical Statistics:525-540

Lancraft TM, Hopkins TL, Torres JJ, Donnelly J (1991) Oceanic micronektonic/macrozooplanktonic community structure and feeding in ice covered Antarctic waters during the winter (AMERIEZ 1988). Polar Biol 11:157-167

Lee DB, Choi KH, Ha HK, Yang EJ, Lee SH, Lee S, Shin HC (2013) Mesozooplankton distribution patterns and grazing impacts of copepods and *Euphausia crystallorophias* in the Amundsen Sea, West Antarctica, during austral summer. Polar Biol 36:1215-1230

Makorov R, Denys C (1981) Stages of sexual maturity of *Euphausia superba*. BIOMASS Handbook 11:1-13

McBride MM et al. (2014) Krill, climate, and contrasting future scenarios for Arctic and Antarctic fisheries. Ices J Mar Sci. doi:10.1093/icesjms/fsu002

Metz C, Schnack-Schiel S (1995) Observations on carnivorous feeding in Antarctic calanoid copepods. Mar Ecol Progr Ser 129:71-75

Meyer B (2012) The overwintering of Antarctic krill, *Euphausia superba*, from an ecophysiological perspective. Polar Biol 35:15-37. doi:10.1007/s00300-011-1120-0

Meyer B, Atkinson A, Stöbing D, Oettl B, Hagen W, Bathmann U (2002) Feeding and energy budgets of Antarctic krill *Euphausia superba* at the onset of winter—I. Furcilia III larvae. Limnol Oceanogr 47:943-952

Meyer B, Auerswald L (2014) The expedition of the research vessel" Polarstern" to the Antarctic in 2013 (ANT-XXIX/7). Berichte zur Polar-und Meeresforschung (Reports on polar and marine research) 674

Meyer B et al. (2009) Physiology, growth, and development of larval krill *Euphausia superba* in autumn and winter in the Lazarev Sea, Antarctica. Limnol Oceanogr 54:1595-1614. doi:10.4319/lo.2009.54.5.1595

Mizdalski E (1988) Weight and length data of zooplankton in the Weddell Sea in austral spring 1986 (ANT V/3). Berichte zur Polarforschung (Reports on Polar Research) 55

O'Brien C, Virtue P, Kawaguchi S, Nichols P (2011) Aspects of krill growth and condition during late winter-early spring off East Antarctica (110–130 E). Deep-Sea Res Pt II 58:1211-1221

Oresland V (1995) Winter population structure and feeding of the chaetognath *Eukrohnia hamata* and the copepod *Euchaeta antarctica* in Gerlache Strait, Antarctic Peninsula. Mar Ecol Progr Ser 119:77-86

Öresland V (1990) Feeding and predation impact of the chaetognath *Eukrohnia hamata* in Gerlache Strait, Antarctic Peninsuula. Mar Ecol Progr Ser 63:201-209

Pakhomov E, Hunt B (2014) Pelagic Food Webs. In: Meyer B, Auerswald L (eds) The expedition of the research vessel" Polarstern" to the Antarctic in 2013 (ANT-XXIX/7), vol 674. Alfred Wegener Institute, Berichte zur Polar-und Meeresforschung (Reports on polar and marine research), pp 31-48

Pakhomov E, Verheye H, Atkinson A, Laubscher R, Taunton-Clark J (1997) Structure and grazing impact of the mesozooplankton community during late summer 1994 near South Georgia, Antarctica. Polar Biol 18:180-192

Pakhomov EA, Atkinson A, Meyer B, Oettl B, Bathmann U (2004) Daily rations and growth of larval krill *Euphausia superba* in the Eastern Bellingshausen Sea during austral autumn. Deep-Sea Res Pt II 51:2185-2198

Pakhomov EA, Froneman PW (2004) Zooplankton dynamics in the eastern Atlantic sector of the Southern Ocean during the austral summer 1997/1998 - Part 2: Grazing impact. Deep-Sea Res Pt II 51:2617-2631. doi:10.1016/j.dsr2.2000.11.002

Pakhomov EA, Perissinotto R, Froneman PW (1999) Predation impact of carnivorous macrozooplankton and micronekton in the Atlantic sector of the Southern Ocean. J Marine Syst 19:47-64. doi:10.1016/S0924-7963(98)00023-2

Pasternak AF, Schnack-Schiel SB (2001) Seasonal feeding patterns of the dominant Antarctic copepods *Calanus propinquus* and *Calanoides acutus* in the Weddell Sea. Polar Biol 24:771-784

Pasternak AF, Schnack-Schiel SB (2007) Feeding of *Ctenocalanus citer* in the eastern Weddell Sea: low in summer and spring, high in autumn and winter. Polar Biol 30:493-501

Quetin LB, Ross RM (1984) School composition of the Antarctic krill *Euphausia superba* in the waters west of the Antarctic Peninsula in the austral summer of 1982. J Crustacean Biol 4:96-106

Ross RM, Quetin LB, Baker KS, Vernet M, Smith RC (2000) Growth limitation in young *Euphausia superba* under field conditions. Limnol Oceanogr 45:31-43

Ross RM, Quetin LB, Newberger T, Oakes SA (2004) Growth and behavior of larval krill (*Euphausia superba*) under the ice in late winter 2001 west of the Antarctic Peninsula. Deep-Sea Res Pt II 51:2169-2184. doi:10.1016/j.dsr2.2004.07.001

Sargent J, Gatten R, Henderson R (1981) Lipid biochemistry of zooplankton from high latitudes. Oceanis 7:623-632

Sargent JR, Henderson RJ (1986) Lipids. In: Corner EDS, O'Hara S (eds) Biological chemistry of marine copepods Univ. Press, Oxford, UK

Schaafsma FL, David C, Pakhomov EA, Hunt BPV, Lange BA, Flores H, van Franeker JA (2016) Size and stage composition of age class 0 Antarctic krill (*Euphausia superba*) in the ice-water interface layer during winter/early spring. Polar Biology. doi:10.1007/s00300-015-1877-7

Schmidt K, Atkinson A, Pond DW, Ireland LC (2014) Feeding and overwintering of Antarctic krill across its major habitats: The role of sea ice cover, water depth, and phytoplankton abundance. Limnol Oceanogr 59:17-36

Schnack-Schiel SB (2001) Aspects of the study of the life cycles of Antarctic copepods. In: Copepoda: Developments in Ecology, Biology and Systematics. Springer, pp 9-24

Schnack-Schiel SB, Hagen W (1995) Life-cycle strategies of *Calanoides acutus*, *Calanus propinquus*, and *Metridia gerlachei* (Copepoda: Calanoida) in the eastern Weddell Sea, Antarctica. Ices J Mar Sci 52:541-548. doi:10.1016/1054-3139(95)80068-9

Schnack SB (1983) Feeding of two Antarctic copepod species (*Calanus propinquus* and *Metridia gerlachei*) on a mixture of centric diatoms. Polar Biol 2:63-68. doi:10.1007/BF00303171

Siegel V (2012) Krill stocks in high latitudes of the Antarctic Lazarev Sea: seasonal and interannual variation in distribution, abundance and demography. Polar Biol 35:1151-1177

Spreen G, Kaleschke L, Heygster G (2008) Sea ice remote sensing using AMSR-E 89-GHz channels. J Geophys Res-Oceans 113:C02S03. doi:10.1029/2005jc003384

Swadling K, Gibson J, Ritz D, Nichols P, Hughes D (1997) Grazing of phytoplankton by copepods in eastern Antarctic coastal waters. Mar Biol 128:39-48

van Franeker JA, Flores H, Van Dorssen M (2009). The Surface and Under Ice Trawl (SUIT). In: Flores H (2009) Frozen Desert Alive-The role of sea ice for pelagic macrofauna and its predators: implications for the Antarctic pack-ice food web.. Dissertation, University of Groningen, pp. 181–188.

Urban-Rich J, Dagg M, Peterson J (2001) Copepod grazing on phytoplankton in the Pacific sector of the Antarctic Polar Front. Deep-Sea Res Pt II 48:4223-4246. doi:10.1016/S0967-0645(01)00087-X

Virtue P et al. (2010) Krill growth and condition in Western Indian Ocean sector of the Southern Ocean 30-80° E in austral summer 2006. Deep-Sea Res Pt II 57:948-955

Watkins J (2000) Aggregation and vertical migration. In: Everson I (ed) Krill: Biology, Ecology and Fisheries. pp 80-102

Wilcoxon F (1945) Individual comparisons by ranking methods. Biometrics bulletin 1:80-83

3. Discussion

Over the past decades, growing evidence of changes in both ice cover and the water column have been documented in the Arctic and Southern Ocean (IPCC 2014), raising questions about the potential biological consequences. The scientific community has only just begun to unravel the repercussions these changes incur for organisms and ecosystems of the polar sea-ice zones. For example, the relationships between environmental properties, ice-algae production and associated communities remain difficult to evaluate due to lack of quantitative data on the spatial variability of all these parameters. Recently, increased efforts were made to estimate total primary production at the basin scale, despite large error margins caused by the patchiness of ice-algal biomass remaining unresolved (Arrigo et al. 2008; Fernández-Méndez et al. 2015). Many studies documented the importance of ice-associated fauna, showing that species feeding on ice algae, at the underside of sea-ice, have higher energy density and a lipid composition with great value to the higher trophic levels (Budge et al. 2008; Søreide et al. 2006). For an assessment of ecosystem change, the cryo-pelagic carbon flux needs to be better incorporated into global climate and sea-ice-ocean models. To achieve this goal, however, fundamental questions still remain unanswered such as: "how are the species distributed under ice and what environmental factors drive their distribution?"; "which are the dominating species and how relevant are they for the ecosystem dynamics?"; "how do the environmental factors relate to these species?". In assessing this climate-driven alteration to the system, it is, therefore, imperative to quantify the under-ice fauna distribution at the basin scale, as it represents the missing link in the polar food web and, consequently, the carbon flux estimations.

In the following sections, I will first discuss the similarities and differences between sea-ice habitats of the Arctic and Southern Ocean, and explain how these reflect on the distribution of the under-ice communities. I will continue by addressing the role of sea-ice in structuring the ice-associated communities in the central Arctic Ocean and the northern Weddell Sea. I will conclude by integrating new findings on ice-associated faunal diversity and food web functionality in a climate change context and show the potential to learn from one polar system about the other, through an integrated global significance of sea-ice fauna.

3.1. Improving understanding of under-ice faunal distribution in the Arctic and Southern Ocean

Both polar oceans are largely ice-covered, and yet, due to limited access, little is known about the ecological processes occurring below sea ice. The high spatial variability in sea-ice and associated fauna remains difficult to explain when only small scales are sampled, such as ice cores or the underside of individual ice floes. Sampling the underside of sea-ice with the Surface and Under Ice Trawl (SUIT) over an average 1.5 km profile, allowed us to cover a larger spatial variability of a patchily distributed fauna (Schnack-Schiel 2003) with an increased sampling effort compared to other methods, e.g. under-ice pumps, hand nets or remotely operated vehicles (Brierley and Thomas 2002).

This thesis provides the first large-scale records of under-ice fauna distribution from the central Arctic Ocean and the northern Weddell Sea. Environmental parameters, like sea-ice thickness and coverage, surface-water temperature and salinity, chlorophyll *a* concentration, were continuously recorded while collecting fauna. For now, the small sample size (13 Arctic stations and 11 Antarctic stations) limits a better evaluation of potential associated sampling biases, large scales extrapolation or disentangling the regional from seasonal effects on species distribution. Nevertheless, this dataset creates a baseline with the potential to increase our understanding of ecological processes under the sea-ice.

In the central Arctic, besides differences in sea ice due to latitudinal extent and seasonal progression, two environmental regimes were identified, broadly coherent with the two ocean basins sampled: the Nansen Basin regime and the Amundsen Basin regime (Chapter I). The main distinction was noticed in nutrient concentration and salinity distribution, corroborating with Atlantic Water circulation in the Eurasian Basin (Rudels et al. 2013). During early August, the Nansen Basin had a more compact sea-ice cover. At the end of August, while sampling in the Amundsen Basin, the pack-ice began to reduce and ice was thinning, leaving locally large open-water areas. Break-up of sea ice by early September likely allowed more light to penetrate into the water column. This favoured the increased chlorophyll *a* concentration that we observed in the Amundsen Basin regime, depleting nutrients in the surface layer. The under-ice community structure clearly responded to the patterns in sea-ice and water-column properties, reflecting the two environmental regimes: (1) copepod-dominated in the Nansen Basin and (2) amphipod-dominated in the Amundsen Basin. Overall, biomass was dominated by the polar cod, *Boreogadus saida*, present throughout the sampled area, and with the high contribution of ctenophores, mainly *Beroe* spp., at few sampling locations.

In the northern Weddell Sea, oceanographic features were largely dominated by the influence of the Weddell Gyre and the latitudinal extent of the surface Winter Water (Chapter III). We found surface-water temperature and salinity varying within a small range over the sampled area. Conversely, sea-ice and snow thicknesses and sea-ice roughness were highly variable with no distinctive spatial pattern. Similar to the central Arctic situation, an increase in surface chlorophyll *a* concentration was noticed at the last stations sampled, coinciding with the break-up of sea-ice at the end of winter. Community composition was rather heterogeneous, with structural differences following a geographical gradient in the investigation area. In the apparent absence of adult krill over the investigated area, krill larvae and copepods co-dominated the community composition, biomass and carbon flux (Chapter III, IV).

In both central Arctic and northern Weddell Sea, at the time of our sampling, a compact pack-ice was encountered at first, followed by the break-up and reduction of sea-ice by the end of sampling (Chapter I, III). The main difference between the two systems was the sampling season: it was summer at that time in the Arctic Ocean and winter in the Southern Ocean (Table 1). The seasonal difference further complicates the comparability of data. Whilst the sea ice was similarly melting during the sampling of both systems, seasonal differences might have been a key factor driving some species distribution. It does show that the seasonal change in sea-ice cover can have different consequences: a change in species composition and a change in species abundance in the under-ice surface layer.

In our regional-scale sampling of the two systems, the central Arctic and northern Weddell Sea, we found a diverse under-ice community, dominated by few ubiquitous species. The Arctic and Antarctic under-ice communities were numerically dominated by copepods, accounting for 69% and 67%, respectively, of the mean relative abundance at all stations of each sampled system (Table 2). The overall copepod dominance in the under-ice surface waters was due to the same abundant and ubiquitous species that has previously been reported to dominate the pelagic zooplankton community (Kosobokova and Hirche 2009; Kosobokova et al. 2011; Schnack-Schiel 2001), suggesting that pelagic species forage intensively under the sea ice. In our Arctic samples, higher densities of under-ice fauna were mainly driven by the large calanoid copepods, *Calanus glacialis* and

Calanus hyperboreus (Chapter I). In the northern Weddell Sea, their Antarctic counter-species, *Calanus propinquus,* and the smaller copepod species, *Stephos longipes* and *Ctenocalanus* spp., occurred in high numbers (Chapter III). The high abundances of these pelagic copepods at the underside of the sea-ice highlight the potential of a high energy transfer from the sea-ice production into the water column. This indicates that the ice-water interface layer is a major functional link within the sea-ice associated ecosystem (Flores et al. 2011).

Table 1. Summary of sea-ice habitat properties recorded in the central Arctic Ocean during the ARK XXVII/3 expedition (referred to as ARCTIC in the table) and in the Weddell Sea during the ANT XXIX/7 expedition (referred to as ANTARCTIC in the table); median values are presented.

ARCTIC	ANTARCTIC
Summer	**Late winter/early spring**
Mid-night sun	Reduced light
Sea ice	**Sea ice**
Seasonal and perennial ice zone	Seasonal ice zone
Pack-ice, mostly first-year ice (95%)	Pack-ice, only first-year ice
Coverage 0 – 100%	Coverage 46 – 99%
Modal ice thickness 0.8 m	Modal ice thickness 0.5 m
No snow	Snow highly variable 0.06 – 0.6 m
Water column	**Water column**
Temperature -1.5°C	Temperature -1.8°C
Salinity 31	Salinity 34
Chlorophyll *a* under-ice 0.28 mg m^{-3}	Chlorophyll *a* under-ice 0.13 mg m^{-3}
All stations with similar bottom depth ~4000 m	Most stations with bottom depth ~3000 m; four stations with ~1000 m

At the ice-water interface in the central Arctic and northern Weddell Sea, species composition presented a mixture of pelagic and ice-associated species (Table 2). Under-ice studies, in which sampling is usually performed with pumps, hand nets or by directly collecting organisms from the underside of ice by divers, fail to incorporate pelagic species. Epipelagic sampling, on the other hand, fails to incorporate ice-associated species, as these stay attached on the ice or swim at the ice-water interface. The mixture of species we found at the ice-water interface, having different levels of fidelity to the sea-ice habitat, indicates a highly dynamic food web with varying species interactions according to the season or local and regional sea-ice habitat variability. The combined effect of these factors complicates our perception and interpretation of the ecological processes taking place in relation to sea-ice dynamics.

Table 2. Summary of diversity and abundance of the under-ice community sampled in the central Arctic Ocean during the ARK XXVII/3 expedition in summer 2012 (referred to as ARCTIC in the table) and in the northern Weddell Sea during the ANT XXIX/7 expedition in winter 2013 (referred to as ANTARCTIC in the table).

ARCTIC	ANTARCTIC
Diversity Lower number of species (28) More ice-associated species, crustaceans dominated Amphipods: 6 ice-associated and 2 pelagic species Copepods: only 1 ice-associated species	**Diversity** Higher number of species (45) More pelagic species, crustaceans dominated Amphipods: 2 ice-associated and 6 pelagic species Copepods: 4 ice-associated species
Abundance 1st Copepods (69%), 2nd Amphipods (28%) Overall range: 0.3 - 69 ind. m^{-2} Median: 5.5 ind. m^{-2}	**Abundance** 1st Copepods (67%), 2nd Euphausiids (mainly *Euphausia superba*) (30%) Overall range: 0.1 - 18.4 ind. m^{-2} Median: 2.1 ind. m^{-2}

Rather than variation in species composition, the differences in community structure between sampling locations were largely determined by variation in species abundances and biomass. In the central Arctic Ocean, the balance was between the copepod-dominated and amphipod-dominated community; while in northern Weddell Sea, the balance was between the copepod-dominated and krill-dominated community. The progressive reduction of Arctic copepod numbers from the Nansen Basin to the Amundsen Basin suggests that seasonal emigration from the surface layer might have gradually started at the end of August. In northern Weddell Sea the heterogeneity of under-ice fauna was probably driven by biogeographic and seasonal distribution patterns. The identified communities did not correlate with the sea-ice properties over the sampling area and may indicate that additional parameters could play a role in structuring the under-ice community. Similar to the Arctic community, a sharp decrease in copepod abundance and community biomass, coinciding with the seasonal degradation of sea ice, was observed.

Looking at both systems analysed, it remains difficult to disentangle seasonal from the regional effects on the community composition. In the Arctic study, the decrease in copepod abundances coincided with known seasonal vertical migration patterns (Darnis and Fortier 2014). In the northern Weddell Sea, increased water-column productivity in early spring might have prompted the Antarctic copepods to migrate into the water column. An inter-seasonal comparison of under-ice fauna in the Lazarev Sea showed that community composition responds differently to the presence of sea ice, as some species were more abundant in open water than under ice (pelagic amphipods, *Cyllopus lucasii*, *Hyperiella dilatata,* Stebbing, 1888), only seasonally abundant under ice (*Clione antarctica*), or associated with sea ice year-round (*Eusirus laticarpus*) (Flores et al. 2011).

A comparison between the under-ice community during winter 2013 in the northern Weddell Sea and the under-ice community during winter 2006 in the Lazarev Sea indicated structural differences (Fig. 1). The under-ice community in the Weddell Sea was dominated by copepods and krill larvae (Chapter III), compared to the numerical dominance of postlarval krill (96%) in the Lazarev Sea (Flores et al. 2011). In the Weddell Sea study, however, the improved version of the SUIT had two sampling nets attached, a shrimp and a mesozooplankton net, compared to only one shrimp net used on the SUIT in the Lazarev Sea. This comparison highlights the importance of concomitantly studying size-fractionated fauna for a complete understanding of the carbon flux. As shown in the Weddell Sea, even small copepods can account for a large part of biomass and carbon flux (Chapter IV). Regrettably, in the Lazarev Sea study, their significance to the carbon flux remains unresolved, as they were not sampled with the same effort. A notable difference in the under-ice community between the two regions, however, was the extremely low numbers of post-larval krill and the absence of fish larvae and cephalopods under the pack-ice in the northern Weddell Sea compared to the Lazarev Sea (Fig. 1). Excluding the krill and the copepods from this regional comparison, the rest of under-ice macrofauna community in the Weddell Sea was higher in abundance than in the Lazarev Sea (Fig. 1). This difference could be due to regional variability in species distribution and environmental properties, but inter-annual variability can also not be excluded. The outcome of the seasonal comparison in the Lazarev Sea and the regional comparisons between the Weddell and Lazarev Sea indicate that future studies should be designed within an inter-seasonal and inter-regional comparability frame, as these aspects prove to be crucial in disentangling the confounding patterns in faunal distribution.

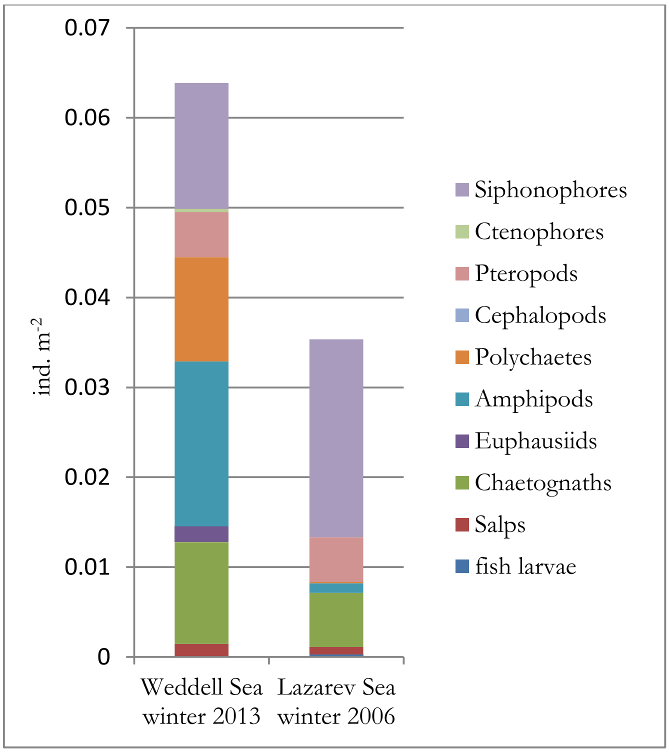

Figure 1. Macrofauna composition and averaged abundance by taxonomic group caught with the SUIT during the ANT XXIX/7 expedition in the Weddell Sea and during the ANT XXIII/6 expedition in the Lazarev Sea; *Euphausia superba* and copepods are excluded.

Combining the findings from both polar oceans, it can be concluded that the ice-water interface presents rather a heterogeneous mixture of ice-associated species and foraging pelagic species, but some structural differences in the under-ice community still emerged. The seasonal and geographical differences in community composition imply that ecosystem models incorporating cryo-pelagic processes have to reflect this variability. Until now, the low number of polar night studies in the high Arctic and Southern Oceans are the main limitation of our understanding of the year-round dynamics of the ice-associated community. While collecting data from the ice-covered areas remains a difficult task, a joint effort of the scientific community to combine various datasets into a common database would increase the understanding of faunal variability in ice-covered areas. Thus, assuring comparability of data among institutions and countries should be our first priority, alongside extended efforts for planning winter studies.

3.2. The role of sea-ice in structuring the under-ice community

The distribution of ice-associated fauna is assumed to be related to ice age, density and under-ice topography (Hop and Pavlova 2008; Hop et al. 2000). Ice-associated species may prefer a certain type of ice, e.g. multi-year ice or first-year ice (Hop et al. 2000). Some are found to be associated with ridges, which provide shelter during the melting season, such as the large amphipod *Gammarus wilkitzkii,* (Gradinger et al. 2010; Hop and Pavlova 2008), others prefer flat ice floes such as the amphipod *Apherusa glacialis,* (Hop and Pavlova 2008), and some prefer to remain near the ice edges (Beuchel and Lønne 2002; Hop et al. 2000). Narrow wedges of seawater along the edges of ice floes were shown to provide micro-habitats for polar cod inhabiting the sea ice over the Arctic deep-basins (Gradinger and Bluhm 2004) and rafted sea-ice structures were observed to be preferred by swarms of feeding Antarctic krill larvae (Meyer et al. 2009). Besides increased food resources provided by ice algae, by seeking the sea-ice habitat, krill larvae would additionally benefit from reduced predation pressure compared to the water column (Chapter IV). Most records describing the species' association with sea-ice habitats are, however, based on qualitative observations by divers which are only representative at small spatial scale. As the sea-ice structure can be highly variable from one floe to another, the distribution of ice-associated fauna can be patchily distributed reflecting the sea-ice structure variability. To understand the distribution of species at large scales, sampling needs to be large enough to cover this variability. Therefore, large scale sampling, as performed in the Lazarev Sea (Flores et al. 2014; Flores et al. 2011) and presented in this thesis, complement previous studies by adding fundamental information on species association with the sea-ice habitat.

In the central Arctic Ocean, nutrient concentration in the surface water was strongly related to the species distribution at the ice-water interface (Chapter I). Besides the water mass characteristics that largely define the two regimes identified, both ice thickness and its standard deviation (an expression of sea-ice underside roughness), were correlated with the under-ice community structure. The

Nansen Basin regime was characterised by heavier sea-ice, which can be considered as a compact, stable habitat. The Amundsen Basin regime presented a decline of sea-ice, representing the potential of a future warming state of an ice-covered system with looser ice and reduced cover. The Amundsen Basin regime was associated with increased abundances of ice-associated amphipods which are described to inhabit sea-ice structures, such as *Onisimun glacialis* and *Onisimus nanseni* (Hop et al. 2000). Release of ice amphipods into the pelagic habitat has been reported to occur during advanced stages of ice melt and break-up, offering a pulse of high-energy prey at the ice-water interface (Hop et al. 2011; Scott et al. 1999). A sharp sea-ice reduction was accurately mirrored by a change in dominance of ice-associated amphipod, *A. glacialis,* in ice-covered waters, with the pelagic amphipod, *T. libellula,* in the surface community of ice-free waters. This pattern suggests that habitat partitioning between ice-associated and pelagic species is abrupt, creating a small-scale pattern in the surface layer community according to sea-ice conditions.

The association of polar cod with sea-ice properties could imply that fish were concentrating under the remaining sea ice during advancing melt and preferred thicker sea ice that survived longest and was most likely to host sufficient under-ice prey such as the ice-amphipod, *A. glacialis* (Chapter II). The positive association of polar cod distribution with sea-ice thickness and ice-amphipod distribution, and the high energy content of the fish (Chapter II) suggest that during their drift with sea ice, polar cod are, indeed, closely associated with the underside of sea-ice, where they find ample high-energy food to survive the drift, until they begin their first spawning cycle. By advection with the Transpolar Drift, juvenile polar cod, hatched on the Siberian shelf, could potentially recruit to populations in the Svalvard archipelago, Barents Sea, and Greenland Sea. Besides acting as feeding and resting ground, sea ice also acts as a vector, potentially enhancing genetic exchange among polar cod populations around the Arctic Ocean.

In the northern Weddell Sea, the association of environmental variables with species distribution was less prominent than in the central Arctic Ocean. Weak correlations of under-ice fauna with sea-ice habitat properties in the northern Weddell Sea indicated rather a heterogeneous distribution of species at basin scale, with temporal dynamics of sea-ice, i.e. seasonal retreat of sea-ice, and local effects, e.g. proximity of islands; structuring the under-ice community at smaller scales (Chapter III). Reduced sea-ice coverage and lower bottom depth at stations placed in the proximity of the South Sandwich Islands reflected a different under-ice community from the rest of the sampled deep-basin area. Despite the limitations imposed by a small dataset, the correlation between the biological and environmental datasets supports the idea of sea-ice habitat properties impacting on under-ice community structure, thus demanding further investigation.

Antarctic krill larvae are known to remain associated with sea ice during austral winter as they depend on ice algae as an additional food source to survive the low primary production in the water column. During winter 2013 in the northern Weddell Sea, Antarctic krill larvae were mostly associated with the ice underside during daytime, and dispersed in the upper 20 m of the water column during the night (Pakhomov & Hunt 2014), thus showing fidelity to the sea-ice habitat. Antarctic krill larvae benefited from reduced competition under the ice and their feeding success increased in areas where higher chlorophyll *a* concentration was found in the sea-ice (Chapter IV). Besides Antarctic krill, other ice-associated species may also rely on sea-ice resources during winter, such as copepods, amphipods and herbivorous pteropods. The decoupling of grazer carbon demand from chlorophyll *a* distribution in the surface water implies that ice-associated grazers could have covered a considerable part of their food demand with sea-ice algae and other sea-ice derived resources. Improved estimates of ice algae production in sea ice at larger scales becomes of upmost importance in order to better relate and predict the distribution of ice-associated species and associated carbon flux from sea ice.

The role of ice-associated fauna remains crucial for the functioning of the polar ecosystems. Changes in composition, abundance, size and energy content of ice-associated communities will influence the energy flux through the Arctic and Antarctic marine ecosystems and, hence, growth and survival of top predators (Laidre and Heide-Jørgensen 2005; Mehlum and Gabrielsen 1993). The changes we observed in species dominance, e.g. Arctic copepods vs. amphipods or Antarctic krill vs. copepods, in response to changes in sea-ice conditions confirm the decisive role sea ice has on species distribution in surface water. Furthermore, these observed changes highlight the huge potential of this study to evaluate the dependency and interactions of certain species with the sea-ice habitat. Such a dataset will prove useful for applications in modelling, assessing ecological processes within food webs or investigating species interactions.

More data points are needed in order to capture the non-linearity of the system and to disentangle the combined effects of seasonal or regional differences. With a more extensive dataset, useful tools can be applied, such as General Additive Models, which can unravel the non-linearity; and mixed models, which can disentangle various, combined effects. When more under-ice data becomes available from future expeditions, more questions regarding faunal association with sea-ice habitats can be answered.

3.3. Under-ice diversity and resource partitioning

Research conducted over the past two decades has shown that the concept of short, low-diversity polar food chains is overly simplistic. Although comparatively few species do provide the bulk of food to polar marine top predators, the structure and functioning of marine food webs are nowadays believed to be broadly similar across all latitudes (Smetacek and Nicol 2005).

We found a rich and diverse under-ice community in both the central Arctic and the northern Weddell Sea, with crustaceans clearly dominating both communities. In the Arctic under-ice community, amphipods and copepods equally contributed to the species richness, with 8 species each of a total of 28 species (Chapter I). In the northern Weddell Sea, copepods were more diverse with 12 species recorded compared to only 7 amphipod species out of a total of 45 species (Chapter III). Diversity indices showed no spatial patterns over the vast sampled areas in both the central Arctic Ocean and the Weddell Sea. Small and apparently random variation in diversity was indicated by Shannon and evenness indices, across different regimes identified, i.e. the Nansen and Amundsen Basins in the Arctic and the krill and copepod-dominated regimes in the Antarctic. This suggests that sea-ice habitat variability does not significantly impact local diversity at the temporal and spatial scales over which the sampling was performed (Chapter I, III). In each of the systems, the species list was similar over the sampled areas indicating similar regional diversity. At larger temporal scales, it is not clear how local and regional diversity will adapt under the dramatic changes predicted to occur in the inter-annual fluctuations of the sea-ice conditions and water-mass circulation. Loss of sea-ice will probably diminish a number of ice-associated species whose life cycles are highly dependent on sea ice, such as *S. longipes* (Schnack-Schiel et al. 1995), while others such as the Arctic amphipod, *A. glacialis,* might adapt to a pelagic life (Berge et al. 2012).

Over the vast sampled area, the under-ice community composition was heterogeneous. Within the different identified community types, e.g. krill-, copepod- or amphipod-dominated, under-ice resource partitioning did not appear to be uniform, as suggested by generally low Shannon and evenness diversity indices. This indicates that we may have observed an ecological succession in which, the one or the other community type (dominated by few ubiquitous species) consumed the majority of primary production at the time. What differs is the efficiency of these dominant species, responsible for the large part of the carbon flux, to convert the available autotrophic food sources into high quality lipids, considered essential in polar food webs. The dominance of diatom fatty acid trophic markers in the lipids of calanoid copepods and ice-associated amphipods, for example, underpins the importance of sea-ice algae as a critical carbon source in the Arctic ice-associated ecosystem (Budge et al. 2008; Falk-Petersen et al. 2009).

During the productive season, sea ice can host locally high primary production (Arrigo 2008). During winter when autotrophic resources in the water column become limited, additional resources provided by sea-ice habitats such as protozoans, small copepods and detritus may offer an alternative food source for the species associated with sea ice (Daly 1990; Gannefors et al. 2005; Meyer 2012; Schmidt et al. 2014). Thus, the microbial component of the food web is believed to overcome the autotrophs' path in energy transfer (Wickham and Berninger 2007).

Using a tentative comparison of primary production versus food demand of the dominant grazers, we estimated a dominantly heterotrophic under-ice food web in the Amundsen Basin regime during our sampling period (Chapter I). In sea ice and water column combined, a nearly 1:1 ratio of primary production versus grazer food demand implies that the total algae production could have barely matched the food demand of under-ice grazers during the sampling period. Locally, however, grazers may have benefited from feeding on biomass-rich algal aggregates floating under the sea ice (Fernández-Méndez et al. 2014). At the end of winter in the northern Weddell Sea, a diversity of species, known to actively feed during winter, were found at a time when autotrophic resources in the water column were very low. Increased ammonium concentrations in the surface water in this area confirmed higher metabolic activity of the under-ice community, hence, indicating a heterotrophic food web (Chapter III). Limited water-column autotrophic resources, at the time when carbon demand of dominant pelagic grazers was high, suggests that heterotrophic resources would have been largely available in the water column (Chapter IV).

Since both of the observed heterotrophic systems, the Amundsen Basin and northern Weddell Sea, coincided with melting sea ice and, consequently, the availability of food resources other than ice algae expulsed from sea ice (e.g. detritus and in-ice meiofauna) might have triggered a switch to a heterotrophic-dominated food web. Our perception on many species' diet is changing, as many Arctic and Antarctic species, previously considered to be herbivorous, e.g. copepods, Antarctic krill larvae and juveniles, showed the ability to switch to an omnivorous diet (Atkinson 1995; Metz and

Schnack-Schiel 1995; Wickham and Berninger 2007). Winter investigations of Antarctic krill shed light on their overwintering strategies (Meyer 2012) and the use of heterotrophic resources as alternative source (O'Brien et al. 2011). Traditional hypotheses on polar night dormancy are currently being debated based on recent investigations in the Arctic Ocean; the relevance of the microbial food web in these systems also requires further investigation (Berge et al. 2009; Darnis et al. 2012).

Our findings indicate that the microbial component of the ice-associated food web could be prevailing when autotrophic resources are low. This coincides with the melting of sea-ice at the end of summer in the oligotrophic central Arctic Ocean and the end of winter in the northern Weddell Sea. In a future warming scenario, the relative contribution of the microbial component in the food web is expected to increase. This increase could lead to amplified recycling processes within the pelagic realm, consequently lowering the vertical export, thus weakening the cryo- and pelagic-benthic coupling.

To elucidate the carbon flux through a food web, a priority should be to disentangle the autotrophic vs. the microbial production and quantifying their relative contribution to the carbon fluxes. Stable isotopes and fatty acid tracers of carbon-derived from various sources, such as ice or pelagic algae have proved to be useful tools to achieve this goal (Budge et al. 2008; Pomerleau et al. 2014; Schmidt et al. 2006).

3.4. Climate change impact on food web functionality

Productivity, environmental stability and species interactions are considered to be fundamental factors determining an ecosystem's stability (Menge and Sutherland 1976). Productivity in ice-covered regions is spatially heterogeneous and temporally variable (Arrigo and Thomas 2004; Fernández-Méndez et al. 2015). Besides the regular high seasonal variability, the most dramatic changes in Polar Regions are expected to occur in sea ice due to the pronounced effects of global climate change. In general, there is little understanding of species' adaptation mechanisms to their environment facing extreme seasonal changes (e.g. food supply, ice cover and length of daylight), as well as long-term changes caused by global warming (e.g. decline in sea-ice cover, change in quantity and quality of food, rise in seawater temperature). Species respond to changes/perturbations in the physical environment by different adaptive strategies, such as altered timing of the reproductive events, diapause, and vertical migrations. Antarctic krill are probably one of the best investigated polar marine organisms, but their adaptability to climate change is largely speculative (Hill et al. 2013; Nicol 2006). Antarctic krill recruitment, driven largely by the winter survival of larval krill, is probably the population parameter most susceptible to climate change (Flores et al. 2012). The dominant Arctic species, *C. hyperboreus,* reproduces before February, showing a pre-bloom spawning strategy, their eggs representing an important food source for other zooplankton species at the beginning of the reproductive season (Melle and Skjoldal 1998). Conversely, *C. glacialis* has an after-bloom spawning strategy (Melle and Skjoldal 1998). A change in the timing of sea-ice break and freezing will likely induce a mismatch between the pulse of primary production and the start of feeding of the early developmental stages of these copepods. This will negatively impact the population size of species whose life cycles coordinate with sea-ice seasonal dynamics, with consequences in the entire food web. In contrast, increasing frequency of winter-spring polynyas on the Arctic shelves could improve early survival and population size in polar cod (Bouchard and Fortier 2008). An earlier ice break-up and more frequent winter polynyas, enhance the survival of juvenile 0+ polar cod by enabling a larger fraction of the annual cohort to hatch earlier and reach a larger size before winter (Bouchard and Fortier 2011).

The central role of polar cod in the Arctic marine food web is mainly related to their high standing stock around the Arctic shelves (Hop and Gjøsæter 2013) that serves as an important food supply for many top predators (Harter et al. 2013; Hop et al. 1997; Lønne and Gabrielsen 1992). As yet, there are no estimations on the under-ice stock of polar cod in the central Arctic Ocean. A tentative extrapolation from a median abundance of about 5000 fish km^{-2} estimated over the Eurasian Basin, with an average sea-ice cover of 1.8 million km^{2} in summer 2012, indicates that the under-ice fish stock could have been about 9 * 10^{9} fish (29000 t). This value corresponds to approximately 50% of the population size and 13.5% of the biomass reported for one- and two-year old polar cod from the Barents Sea in 2012 (18.2*109 fish, 217900 t) (Gjøsæter and Prozorkevich 2012). Caution is advisable with this extrapolation due to the limited number of fish and sampling locations it is based on. In the absence of comparable estimates on under-ice fish stocks from other sources, however, this value may be instructive for assessing the importance of the central Arctic under-ice habitat for polar cod populations and their ecological role. The sheer size of this stock is indicative of a substantial trophic carbon flux in a central Arctic Ocean assumed to deliver relatively low primary productivity (Fernández-Méndez et al. 2015). Decline of sea-ice coverage and thickness over the deep basins would result in reduced fish abundance in central Arctic Ocean (Chapter II). As polar cod are responsible for high energy transfer to top predators (Harter et al. 2013; Hop et al. 1997), any alterations in polar cod population are expected to have tremendous effects in the entire Arctic marine ecosystem. Increased efforts should be made to combine available information into a pan-Arctic polar cod database in order to make it possible to estimate the entire pan-Arctic fish stock. Important gaps remain in understanding the role the under-ice fish in central Arctic Ocean play in the pan-Arctic population, and their connectivity with different shelves' populations, as different migration patterns might actually represent important exchange of individuals among the pan-Arctic populations.

The importance of Antarctic krill in the Southern Ocean lies in the large populations of top predators it supports and a growing fishery (Krafft et al. 2015; McBride et al. 2014). In the Southern Ocean, sea ice provides multiple benefits for Antarctic krill, such as shelter, feeding ground and transport platform for larvae (Meyer et al. 2009). Reduction in duration, extent and geographical distribution of the winter habitat will have a cumulative negative impact on reproduction success and survival of Antarctic krill with cascading effects on the food web (Flores et al. 2012). The Antarctic krill-deficient situation, observed in the Weddell Sea during winter 2013, could be already a glimpse into a future warmer state of this ecosystem, with fewer krill and more copepods (Chapter IV).

Due to their similar trophic positions in the ice-associated food webs of the Arctic and Southern Oceans and their high standing stocks, the polar cod and Antarctic krill seem to share the same function as a key prey to endotherms. As a scientific community, we have barely started to understand the drivers of these population fluctuations, even though it is believed they depend, to a certain extent, on the sea-ice conditions. To predict the future, we need to better understand the mechanisms behind the present-day success of key species such as polar cod and Antarctic krill in maintaining such large stocks and their dependency on the sea ice.

3.5. Future perspectives

The polar marine ecosystems are likely to be more sensitive to climatic perturbations than those of temperate areas, as disproportionate warming is expected to occur here (Carmack and Wassmann 2006; Smetacek and Nicol 2005). Expected consequences involve changes in primary production, keystone predators and ecosystem regime shifts, i.e. from altered patterns of primary production, to changes in trophic structure and elemental cycling pathways.

Should sea-ice retreat farther north in the Arctic, flow polynyas and the barrier resulting from cool and dense water sinking may cease to exist, thus allowing northward immigration of sub-Arctic pelagic species (Carmack and Wassmann 2006). In contrast, the connectivity with selves through ice drift will cease to exist, to the detriment of some coastal and shelf species, e.g. polar cod, benthic amphipods, which will no longer have this transport platform to spread over the deeper basins. An increase in open water during summer in Arctic and Subarctic seas will result in increased primary and secondary production, hence biomass may increase for some important commercial fish stocks and new mixes of species may become targeted. In contrast, in the Southern Ocean, the potential for the existing species to adapt is mixed, and the potential for the invasion of large and highly productive pelagic fish species appears low. Thus, while a future Arctic Ocean fisheries might apparently benefit in the light of these changes, future Southern Ocean fisheries may remain largely dependent on existing species (McBride et al. 2014).

To face the climatic and environmental changes in the Arctic Ocean, Wassmann et al. (2011) identified four research categories in which immediate efforts are required: 1) time series, 2) adequate coverage in key regions, 3) new technologies and 4) making older Russian data internationally accessible. This thesis addresses the first three categories by providing a baseline for monitoring sea-ice-associated fauna and sea-ice habitats, providing better sampling coverage over vast areas of relatively inaccessible regions, and using a new innovative sampling device with modern sensor technology. These categories prove relevant for the Southern Ocean as well, as Flores et al. (2012) pointed out the immediate need for time series, better methodologies and better use of existing knowledge to improve our predictive abilities. Conservation of the Southern Ocean falls under the responsibility of the Convention for the Conservation of Antarctic Marine Living Resources (CCAMLR). CCAMLR has the responsibility to develop management procedures that specifically take into account climate change effects on ecosystems, as well as on the major harvested species, Antarctic krill. The Arctic Ocean is lacking such a framework; however, in 2015 a joint effort of international scientists developed the Future Directions of Arctic Sciences (Arctic Biodiversity: Majaneva et al. 2015) as a set of priorities to improve the overarching knowledge on the present and past Arctic Ocean, and, thus, better predict future scenarios in the high northern latitudes.

In the absence of appropriate baseline data, it is impossible to assess whether the past under-ice communities were more or less abundant, or differed in diversity and composition. In the future, the Arctic and Southern Ocean ice-associated community will be exposed to continuing changes, including a further shortening of the ice-covered season, the complete disappearance of Arctic multi-year ice, and changes in stratification and nutrient regimes. The subtle response of the ice-associated community to many of these changing parameters suggests that changes already have impacted Arctic and Southern Ocean under-ice communities, and will continue to do so in the future. Monitoring the course of changes in polar biodiversity and ecosystem structure will be key requirements for successful resource and conservation management for polar oceans in transition.

References

Ackley S, Sullivan C (1994) Physical controls on the development and characteristics of Antarctic sea ice biological communities—a review and synthesis. Deep-Sea Res Pt I 41:1583-1604

Arndt CE, Swadling KM (2006) Crustacea in Arctic and Antarctic Sea Ice: Distribution, Diet and Life History Strategies. In: Southward AJ, Sims DW (eds) Advances in Marine Biology, vol 51. Elsevier, San Diego, California 92101-4495, USA, p 119. doi:10.1016/S0065-2881(06)51004-1

Arrigo KA (2008) Chapter 5. Primary production in sea ice. In: Thomas DN, Dieckmann GS (eds) Sea ice: an introduction to its physics, chemistry, biology and geology. John Wiley & Sons, pp 143-183

Arrigo KR, Thomas DN (2004) Large scale importance of sea ice biology in the Southern Ocean. Antarct Sci 16:471-486

Arrigo KR, van Dijken G, Pabi S (2008) Impact of a shrinking Arctic ice cover on marine primary production. Geophys Res Lett 35. doi:10.1029/2008GL035028

Arrigo KR, van Dijken GL, Bushinsky S (2008) Primary production in the Southern Ocean, 1997-2006. J Geophys Res-Oceans 113. doi:10.1029/2007jc004551

Arrigo KR, van Dijken GL (2011) Secular trends in Arctic Ocean net primary production. J Geophys Res-Oceans 116. doi:10.1029/2011JC007151

Atkinson A (1995) Omnivory and feeding selectivity in five copepod species during spring in the Bellingshausen Sea, Antarctica. ICES J Mar Sci 52:385-396. doi:10.1016/1054-3139(95)80054-9

Atkinson A et al. (2008) Oceanic circumpolar habitats of Antarctic krill. Mar Ecol Progr Ser 362:1-23. doi:10.3354/Meps07498

Atkinson A, Siegel V, Pakhomov E, Jessopp M, Loeb V (2009) A re-appraisal of the total biomass and annual production of Antarctic krill. Deep-Sea Res Pt I 56:727-740

Atkinson A, Siegel V, Pakhomov E, Rothery P (2004) Long-term decline in krill stock and increase in salps within the Southern Ocean. Nature 432:100-103

Berge J et al. (2009) Diel vertical migration of Arctic zooplankton during the polar night. 5:69-72. doi:10.1098/rsbl.2008.0484

Berge J, Varpe O, Moline MA, Wold A, Renaud PE, Daase M, Falk-Petersen S (2012) Retention of ice-associated amphipods: possible consequences for an ice-free Arctic Ocean. Biol Lett 8:1012-1015. doi:10.1098/rsbl.2012.0517

Beuchel F, Lønne OJ (2002) Population dynamics of the sympagic amphipods *Gammarus wilkitzkii* and *Apherusa glacialis* in sea ice north of Svalbard. Polar Biol 25:241-250. doi:10.1007/s00300-001-0329-8

Bouchard C, Fortier L (2008) Effects of polynyas on the hatching season, early growth and survival of polar cod *Boreogadus saida* in the Laptev Sea. Mar Ecol Progr Ser 355:247-256. doi:Doi 10.3354/Meps07335

Bouchard C, Fortier L (2011) Circum-arctic comparison of the hatching season of polar cod *Boreogadus saida*: A test of the freshwater winter refuge hypothesis. Prog Oceanogr 90:105-116. doi:10.1016/j.pocean.2011.02.008

Brierley AS, Thomas DN (2002) Ecology of Southern Ocean pack ice. In: Advances in Marine Biology, vol 43. Academic Press, pp 171-276. doi:10.1016/S0065-2881(02)43005-2

Budge SM, Wooller MJ, Springer AM, Iverson SJ, McRoy CP, Divoky GJ (2008) Tracing carbon flow in an arctic marine food web using fatty acid-stable isotope analysis. Oecologia 157:117-129. doi:10.1007/s00442-008-1053-7

Carmack E, Wassmann P (2006) Food webs and physical–biological coupling on pan-Arctic shelves: Unifying concepts and comprehensive perspectives. Prog Oceanogr 71:446-477. doi:10.1016/j.pocean.2006.10.004

Comiso JC, Hall DK (2014) Climate trends in the Arctic as observed from space. Wiley Interdisciplinary Reviews: Climate Change 5:384-409. doi:10.1002/wcc.277

Daly KL (1990) Overwintering development, growth, and feeding of larval *Euphausia superb*a in the Antarctic marginal ice zone. Limnol Oceanogr 35:1564-1576

Darnis G, Fortier L (2014) Temperature, food and the seasonal vertical migration of key arctic copepods in the thermally stratified Amundsen Gulf (Beaufort Sea, Arctic Ocean). J Plankton Res 36:1092-1108. doi:10.1093/plankt/fbu035

Darnis G et al. (2012) Current state and trends in Canadian Arctic marine ecosystems: II. Heterotrophic food web, pelagic-benthic coupling, and biodiversity. Climatic Change 115:179-205. doi:10.1007/s10584-012-0483-8

De Broyer C, Koubbi P, Griffiths H, Grant S (2014) Biogeographic Atlas of the Southern Ocean. Scientific Committee on Antarctic Research, Cambridge, UK

Dong H, Zou X (2014) Variations of sea ice in the Antarctic and Arctic from 1997–2006. Front Earth Sci 8:384-392. doi:10.1007/s11707-014-0422-2

Falardeau M, Robert D, Fortier L (2014) Could the planktonic stages of polar cod and Pacific sand lance compete for food in the warming Beaufort Sea? ICES J Mar Sci. doi:10.1093/icesjms/fst221

Falk-Petersen S, Sargent J, Tande K (1987) Lipid composition of zooplankton in relation to the sub-arctic food web. Polar Biol 8:115-120. doi:10.1007/bf00297065

Falk-Petersen S, Mayzaud P, Kattner G, Sargent J (2009) Lipids and life strategy of Arctic Calanus. Mar Biol Res 5:18-39. doi:10.1080/17451000802512267

Fernández-Méndez M (2014) Primary productivity in Arctic sea ice and ocean. PhD dissertation. University of Bremen, Bremen, Germany

Fernández-Méndez M, Katlein C, Rabe B, Nicolaus M, Peeken I, Flores H, Boetius A (2015) Photosynthetic production in the Central Arctic during the record sea ice minimum in 2012 Biogeosciences discussions 12:2897–2945. doi:10.5194/bgd-12-2897-2015

Fernández-Méndez M, Wenzhöfer F, Peeken I, Sørensen HL, Glud RN, Boetius A (2014) Composition, Buoyancy Regulation and Fate of Ice Algal Aggregates in the Central Arctic Ocean. Plos One 9:e107452

Fisher EC, Kaufmann RS, Smith KL (2004) Variability of epipelagic macrozooplankton/micronekton community structure in the NW Weddell Sea, Antarctica (1995-1996). Mar Biol 144:345-360

Flores H et al. (2012) Impact of climate change on Antarctic krill. Mar Ecol Progr Ser 458:1-19. doi:10.3354/Meps09831

Flores H et al. (2014) Seasonal changes in the vertical distribution and community structure of Antarctic macrozooplankton and micronekton. Deep-Sea Res Pt I 84:127-141. doi:10.1016/j.dsr.2013.11.001

Flores H et al. (2011) Macrofauna under sea ice and in the open surface layer of the Lazarev Sea, Southern Ocean. Deep-Sea Res Pt II 58:1948-1961

Gannefors C et al. (2005) The Arctic sea butterfly *Limacina helicina*: lipids and life strategy. Mar Biol 147:169-177

Gjøsæter H, Prozorkevich D (2012) In: Eriksen, E (Ed.) Survey report from the joint Norwegian/Russian ecosystem survey in the Barents Sea August-October 2012. IMR/PINRO Joint Report Series, No. 2/2012. ISSN 1502-8828, pages 50-56.

Gosselin M, Levasseur M, Wheeler PA, Horner RA, Booth BC (1997) New measurements of phytoplankton and ice algal production in the Arctic Ocean. Deep-Sea Res Pt II 44:1623-1644. doi:10.1016/S0967-0645(97)00054-4

Gradinger R (1999) Vertical fine structure of the biomass and composition of algal communities in Arctic pack ice. Mar Biol 133:745-754

Gradinger RR, Bluhm BA (2004) In-situ observations on the distribution and behavior of amphipods and Arctic cod (*Boreogadus saida*) under the sea ice of the High Arctic Canada Basin. Polar Biol 27:595-603. doi:DOI 10.1007/s00300-004-0630-4

Gradinger R, Bluhm B, Iken K (2010) Arctic sea-ice ridges—Safe heavens for sea-ice fauna during periods of extreme ice melt? Deep-Sea Res Pt II 57:86-95. doi:10.1016/j.dsr2.2009.08.008

Grebmeier JM (2012) Shifting Patterns of Life in the Pacific Arctic and Sub-Arctic Seas. Annu Rev Mar Sci 4:63-78. doi:10.1146/annurev-marine-120710-100926

Griesel A, Mazloff M, Gille S (2012) Mean dynamic topography in the Southern Ocean: evaluating Antarctic Circumpolar Current transport. J Geophys Res-Oceans 117

Harter BB, Elliott KH, Divoky GJ, Davoren GK (2013) Arctic Cod (*Boreogadus saida*) as Prey: Fish Length-Energetics Relationships in the Beaufort Sea and Hudson Bay. Arctic 66:191–196

Haug T, Tormod Nilssen K, Lindblom L, Lindstrøm U (2007) Diets of hooded seals (*Cystophora cristata*) in coastal waters and drift ice waters along the east coast of Greenland. Mar Biol Res 3:123-133. doi:10.1080/17451000701358531

Hill SL, Phillips T, Atkinson A (2013) Potential Climate Change Effects on the Habitat of Antarctic Krill in the Weddell Quadrant of the Southern Ocean. Plos One 8:e72246. doi:10.1371/journal.pone.0072246

Hempel G (1985) Antarctic marine food webs. In: Antarctic nutrient cycles and food webs. Springer, pp 266-270

Hop H, Gjøsæter H (2013) Polar cod (*Boreogadus saida*) and capelin (*Mallotus villosus*) as key species in marine food webs of the Arctic and the Barents Sea. Mar Biol Res 9:878-894. doi:10.1080/17451000.2013.775458

Hop H, Mundy C, Gosselin M, Rossnagel A, Barber D (2011) Zooplankton boom and ice amphipod bust below melting sea ice in the Amundsen Gulf, Arctic Canada. Polar Biol 34:1947-1958. doi:10.1007/s00300-011-0991-4

Hop H, Pavlova O (2008) Distribution and biomass transport of ice amphipods in drifting sea ice around Svalbard. Deep-Sea Res Pt II 55:2292-2307. doi:10.1016/j.dsr2.2008.05.023

Hop H, Poltermann M, Lonne OJ, Falk-Petersen S, Korsnes R, Budgell WP (2000) Ice amphipod distribution relative to ice density and under-ice topography in the northern Barents Sea. Polar Biol 23:357-367. doi:10.1007/s003000050456

Hop H, Tonn WM, Welch HE (1997) Bioenergetics of Arctic cod (*Boreogadus saida*) at low temperatures. Can J Fish Aquat Sci 54:1772-1784. doi:10.1139/f97-086

Horner R et al. (1992) Ecology of sea ice biota. Polar Biol 12:417-427. doi:10.1007/bf00243113

Horner R, Schrader G (1982) Relative contributions of ice algae, phytoplankton, and benthic microalgae to primary production in nearshore regions of the Beaufort Sea. Arctic:485-503

IPCC (2014) Climate Change 2014: Impacts, Adaptation, and Vulnerability. Part A: Global and Sectoral Aspects. Contribution of Working Group II to the Fifth Assessment Report of the Intergovernmental Panel on Climate Change [Field, C.B., V.R. Barros, D.J. Dokken, K.J. Mach, M.D. Mastrandrea, T.E. Bilir, M. Chatterjee, K.L. Ebi, Y.O. Estrada, R.C. Genova, B. Girma, E.S. Kissel, A.N. Levy, S. MacCracken, P.R. Mastrandrea, and L.L. White (eds.)]. Cambridge University Press, Cambridge, United Kingdom and New York, NY, USA

Jakobsson M, Grantz A, Kristoffersen Y, Macnab R (2004) Bathymetry and physiography of the Arctic Ocean and its constituent seas. The organic carbon cycle in the Arctic Ocean Springer, Heidelberg:1-6

Kilias E, Kattner G, Wolf C, Frickenhaus S, Metfies K (2014) A molecular survey of protist diversity through the central Arctic Ocean. Polar Biol 37:1271-1287

King J (2014) Climate science: A resolution of the Antarctic paradox. Nature 505:491-492. doi:10.1038/505491a

Kosobokova K, Hirche H-J (2009) Biomass of zooplankton in the eastern Arctic Ocean – A base line study. Prog Oceanogr 82:265-280. doi:10.1016/j.pocean.2009.07.006

Kosobokova KN, Hopcroft RR (2010) Diversity and vertical distribution of mesozooplankton in the Arctic's Canada Basin. Deep-Sea Res Pt II 57:96-110. doi:10.1016/j.dsr2.2009.08.009

Kosobokova K, Hopcroft R, Hirche H-J (2011) Patterns of zooplankton diversity through the depths of the Arctic's central basins. Mar Biodiv 41:29-50. doi:10.1007/s12526-010-0057-9

Krafft BA, Skaret G, Knutsen T (2015) An Antarctic krill (*Euphausia superba*) hotspot: population characteristics, abundance and vertical structure explored from a krill fishing vessel. Polar Biol:1-14. doi:10.1007/s00300-015-1735-7

Krembs C, Tuschling K, Juterzenka Kv (2002) The topography of the ice-water interface–its influence on the colonization of sea ice by algae. Polar Biol 25:106-117

Kwok R, Cunningham GF, Pang SS (2004) Fram Strait sea ice outflow. J Geophys Res-Oceans 109:C01009. doi:10.1029/2003jc001785

Kwok R, Rothrock DA (2009) Decline in Arctic sea ice thickness from submarine and ICESat records: 1958-2008. Geophys Res Lett 36:L15501. doi:10.1029/2009gl039035

Laidre KL, Heide-Jørgensen MP (2005) Arctic sea ice trends and narwhal vulnerability. Biol Conserv 121:509-517

Lavoie D, Denman K, Michel C (2005) Modeling ice algal growth and decline in a seasonally ice-covered region of the Arctic (Resolute Passage, Canadian Archipelago). J Geophys Res 110:C11009

Leu E, Falk-Petersen S, Kwasniewski S, Wulff A, Edvardsen K, Hessen DO (2006) Fatty acid dynamics during the spring bloom in a High Arctic fjord: importance of abiotic factors versus community changes. Can J Fish Aquat Sci 63:2760-2779. doi:10.1139/F06-159

Lizotte MP (2001) The Contributions of Sea Ice Algae to Antarctic Marine Primary Production. Am Zool 41:57-73. doi:10.1093/icb/41.1.57

Loeb V, Siegel V, Holm-Hansen O, Hewitt R, Fraser W, Trivelpiece W, Trivelpiece S (1997) Effects of sea-ice extent and krill or salp dominance on the Antarctic food web. Nature 387:897-900

Lønne O, Gabrielsen G (1992) Summer diet of seabirds feeding in sea-ice-covered waters near Svalbard. Polar Biol 12:685-692

Lønne O, Gulliksen B (1989) Size, age and diet of polar cod, *Boreogadus saida* (Lepechin 1773), in ice covered waters. Polar Biol 9:187-191

Majaneva S, Peeken I, Choy E, David C, Degen R, Górska B, Jørgensen L, Kirievskaya D, Mazurkiewicz M, Narcy F, Richard J, Rastrick S, Kedra M, Berge J and Bluhm B (2015) Arctic Biodiversity - Marine Biodiversity: From Individuals to Pan-Arctic. Arctic in Rapid Transition 1-2, International Arctic Research Center, Fairbanks, Alaska. doi:10.2312/ART.0329.18148

Matley JK, Crawford RE, Dick TA (2012) Summer foraging behaviour of shallow-diving seabirds and distribution of their prey, Arctic cod (*Boreogadus saida*), in the Canadian Arctic. Polar Res 31. doi:10.3402/polar.v31i0.15894

McBride MM et al. (2014) Krill, climate, and contrasting future scenarios for Arctic and Antarctic fisheries. ICES J Mar Sci. doi:10.1093/icesjms/fsu002

McCann K, Hastings A, Huxel GR (1998) Weak trophic interactions and the balance of nature. Nature 395:794-798

McMinn A, Pankowskii A, Ashworth C, Bhagooli R, Ralph P, Ryan K (2010) In situ net primary productivity and photosynthesis of Antarctic sea ice algal, phytoplankton and benthic algal communities. Mar Biol 157:1345-1356. doi:10.1007/s00227-010-1414-8

Mehlum F, Gabrielsen GW (1993) The diet of high-arctic seabirds in coastal and ice-covered, pelagic areas near the Svalbard archipelago. Polar Res 12:1-20. doi:10.1111/j.1751-8369.1993.tb00417.x

Meiners K et al. (2012) Chlorophyll a in Antarctic sea ice from historical ice core data. Geophys Res Lett 39. doi:10.1029/2012GL053478

Melle W, Skjoldal HR (1998) Reproduction and development of *Calanus finmarchicus*, *C. glacialis* and *C. hyperboreus* in the Barents Sea. Mar Ecol Progr Ser 169:211-228. doi:10.3354/meps169211

Menge BA, Sutherland JP (1976) Species Diversity Gradients: Synthesis of the Roles of Predation, Competition, and Temporal Heterogeneity. The American Naturalist 110:351-369. doi:10.2307/2459759

Metz C, Schnack-Schiel S (1995) Observations on carnivorous feeding in Antarctic calanoid copepods. Mar Ecol Progr Ser 129:71-75

Meyer B (2012) The overwintering of Antarctic krill, *Euphausia superba*, from an ecophysiological perspective. Polar Biol 35:15-37. doi:10.1007/s00300-011-1120-0

Meyer B et al. (2009) Physiology, growth, and development of larval krill *Euphausia superba* in autumn and winter in the Lazarev Sea, Antarctica. Limnol Oceanogr 54:1595-1614. doi:10.4319/lo.2009.54.5.1595

Mysak LA (2001) Patterns of Arctic circulation. Science 293:1269-1270

Nicol S (2006) Krill, Currents, and Sea Ice: Euphausia superba and Its Changing Environment. BioScience 56:111-120. doi:10.1641/0006-3568(2006)056[0111:kcasie]2.0.co;2

Nicol S, Worby A, Leaper R (2008) Changes in the Antarctic sea ice ecosystem: potential effects on krill and baleen whales. Mar Freshwater Res 59:361-382

O'Brien C, Virtue P, Kawaguchi S, Nichols P (2011) Aspects of krill growth and condition during late winter-early spring off East Antarctica (110–130 °E). Deep-Sea Res Pt II 58:1211-1221

Pfirman SL, Colony R, Nürnberg D, Eicken H, Rigor I (1997) Reconstructing the origin and trajectory of drifting Arctic sea ice. J Geophys Res-Oceans 102:12575-12586. doi:10.1029/96jc03980

Poltermann M (2000) Growth, production and productivity of the Arctic sympagic amphipod *Gammarus wilkitzkii*. Mar Ecol Progr Ser 193:109-116

Poltermann M, Hop H, Falk-Petersen S (2000) Life under Arctic sea ice – reproduction strategies of two sympagic (ice-associated) amphipod species, *Gammarus wilkitzkii* and *Apherusa glacialis*. Mar Biol 136:913-920. doi:10.1007/s002270000307

Pomerleau C, Nelson RJ, Hunt BPV, Sastri AR, Williams WJ (2014) Spatial patterns in zooplankton communities and stable isotope ratios (δ13C and δ15N) in relation to oceanographic conditions in the sub-Arctic Pacific and western Arctic regions during the summer of 2008. J Plankton Res 36:757-775. doi:10.1093/plankt/fbt129

Post AL et al. (2014) Chapter 4. Environmental setting. In: De Broyer C, Koubbi P, Griffiths H, Raymond B, Udekem d'Acoz C (eds) Biogeographic Atlas of the Southern Ocean. Scientific Committee on Antarctic Research, Cambridge, UK,

Renner AHH et al. (2014) Evidence of Arctic sea ice thinning from direct observations. Geophys Res Lett 41:5029-5036. doi:10.1002/2014gl060369

Rigor IG, Wallace JM (2004) Variations in the age of Arctic sea-ice and summer sea-ice extent. Geophys Res Lett 31. doi:10.1029/2004gl019492

Rooney N, McCann K, Gellner G, Moore JC (2006) Structural asymmetry and the stability of diverse food webs. Nature 442:265-269

Rudels B, Schauer U, Björk G, Korhonen M, Pisarev S, Rabe B, Wisotzki A (2013) Observations of water masses and circulation in the Eurasian Basin of the Arctic Ocean from the 1990s to the late 2000s. Ocean Science Discussions 9:147-169. doi:10.5194/os-9-147-2013

Saenz BT, Arrigo KR (2014) Annual primary production in Antarctic sea ice during 2005–2006 from a sea ice state estimate. J Geophys Res-Oceans 119:3645-3678. doi:10.1002/2013jc009677

Sakshaug E (2004) Primary and Secondary Production in the Arctic Seas. In: Stein R, MacDonald R (eds) The Organic Carbon Cycle in the Arctic Ocean. Springer Berlin Heidelberg, pp 57-81. doi:10.1007/978-3-642-18912-8_3

Schmidt K, Atkinson A, Petzke K-J, Voss M, Pond DW (2006) Protozoans as a food source for Antarctic krill, Euphausia superba: Complementary insights from stomach content, fatty acids, and stable isotopes. Limnol Oceanogr 51:2409-2427

Schmidt K, Atkinson A, Pond DW, Ireland LC (2014) Feeding and overwintering of Antarctic krill across its major habitats: The role of sea ice cover, water depth, and phytoplankton abundance. Limnol Oceanogr 59:17-36

Schnack-Schiel SB (2001) Aspects of the study of the life cycles of Antarctic copepods. In: Copepoda: Developments in Ecology, Biology and Systematics. Springer, pp 9-24

Schnack-Schiel SB (2003) The macrobiology of sea ice. In: Thomas DN, Dieckmann GS (eds) Sea ice: an introduction to its physics, chemistry, biology and geology. Blackwell Science Ltd., Oxford, UK, pp 211-239

Schnack-Schiel SB et al. (1995) Life cycle strategy of the Antarctic calanoid copepod *Stephos longipes*. Prog Oceanogr 36:45-75

Scott CL, Falk-Petersen S, Sargent JR, Hop H, Lønne OJ, Poltermann M (1999) Lipids and trophic interactions of ice fauna and pelagic zooplankton in the marginal ice zone of the Barents Sea. Polar Biol 21:65-70. doi:10.1007/s003000050335

Shimada K et al. (2006) Pacific Ocean inflow: Influence on catastrophic reduction of sea ice cover in the Arctic Ocean. Geophys Res Lett 33. doi:10.1029/2005gl025624

Smetacek V, Nicol S (2005) Polar ocean ecosystems in a changing world. Nature 437:362-368

Smith WO, Ainley DG, Cattaneo-Vietti R (2007) Trophic interactions within the Ross Sea continental shelf ecosystem. 362:95-111. doi:10.1098/rstb.2006.1956

Søreide JE, Carroll ML, Hop H, Ambrose WG, Hegseth EN, Falk-Petersen S (2013) Sympagic-pelagic-benthic coupling in Arctic and Atlantic waters around Svalbard revealed by stable isotopic and fatty acid tracers. Mar Biol Res 9:831-850. doi:10.1080/17451000.2013.775457

Søreide JE, Hop H, Carroll ML, Falk-Petersen S, Hegseth EN (2006) Seasonal food web structures and sympagic–pelagic coupling in the European Arctic revealed by stable isotopes and a two-source food web model. Prog Oceanogr 71:59-87. doi:10.1016/j.pocean.2006.06.001

Spreen G, Kaleschke L, Heygster G (2008) Sea ice remote sensing using AMSR-E 89-GHz channels. J Geophys Res-Oceans 113:C02S03. doi:10.1029/2005jc003384

Stroeve J, Serreze M, Holland M, Kay J, Malanik J, Barrett A (2012) The Arctic's rapidly shrinking sea ice cover: a research synthesis. Climatic Change 110:1005-1027. doi:10.1007/s10584-011-0101-1

Tilling RL, Ridout A, Shepherd A, Wingham DJ (2015) Increased Arctic sea ice volume after anomalously low melting in 2013. Nature Geosci 8:643-646. doi:10.1038/ngeo2489

Tremblay J-É, Gagnon J (2009) The effects of irradiance and nutrient supply on the productivity of Arctic waters: a perspective on climate change. In: Nihoul JJ, Kostianoy A (eds) Influence of Climate Change on the Changing Arctic and Sub-Arctic Conditions. NATO Science for Peace and Security Series C: Environmental Security. Springer Netherlands, pp 73-93. doi:10.1007/978-1-4020-9460-6_7

Turner J, Hosking JS, Phillips T, Marshall GJ (2013) Temporal and spatial evolution of the Antarctic sea ice prior to the September 2012 record maximum extent. Geophys Res Lett 40:5494-5498. doi:10.1002/2013gl058371

van Franeker JA, Flores H, Van Dorssen M (2009) Surface and Under Ice Trawl (SUIT). In: Flores H (2009) Frozen Desert Alive -The role of sea ice for pelagic macrofauna and its predators: implications for the Antarctic pack-ice food web. Dissertation, University of Groningen, Groningen, Netherlands

Wassmann P, Duarte CM, AgustÍ S, Sejr MK (2011) Footprints of climate change in the Arctic marine ecosystem. Global Change Biology 17:1235-1249. doi:10.1111/j.1365-2486.2010.02311.x

Wassmann P, Reigstad M (2011) Future Arctic Ocean seasonal ice zones and implications for pelagic-benthic coupling. Oceanography 24:220-231. doi:10.5670/oceanog.2011.74

Welch HE et al. (1992) Energy Flow through the Marine Ecosystem of the Lancaster Sound Region, Arctic Canada. Arctic 45:343-357

Whitworth III T (1980) Zonation and geostrophic flow of the Antarctic circumpolar current at Drake Passage. Deep Sea Research Part A Oceanographic Research Papers 27:497-507. doi:10.1016/0198-0149(80)90036-9

Wickham SA, Berninger U-G (2007) Krill larvae, copepods and the microbial food web: interactions during the Antarctic fall. Aquat Microb Ecol 46:1

Worby AP, Geiger CA, Paget MJ, Van Woert ML, Ackley SF, DeLiberty TL (2008) Thickness distribution of Antarctic sea ice. J Geophys Res-Oceans 113:C05S92. doi:10.1029/2007jc004254

Acknowledgements

This thesis was written at the Alfred Wegener Institute Helmholtz Centre for Polar and Marine Research in Bremerhaven and would not have been possible without the support of numerous people.

First, I would like to thank my supervisor, Dr. Hauke Flores, for giving me the opportunity to work in the interesting field of polar oceans, for doing a fantastic job as supervisor, for being supportive and an inspiration for me over the past three years.

I would like to thank my supervisor, Prof. Dr. Angelika Brandt, for on-going support and commitment during my PhD, for guiding and reviewing my work.

I am also deeply grateful to Prof. Dr. Christian Möllmann for his willingness to be the chair of the oral evaluation committee.

I would also like to thank my PhD committee members, Dr. Barbara Niehoff and Dr. Eva-Maria Nöthig, for their support, guidance and encouragements.

I would like to express additional thanks to many members of our section for their advices, availability and support, especially to our technical assistants, Christiane Lorenzen, Susanne Spahic and Sandra Murawski.

Many thanks go to my friends Hanne, Johannes, Paul, Tobias for her help, loving support, coffee breaks and recreational beers.

Special thanks go to my dearest friends, colleagues and roommates Ella, Fokje, Giulia, Nelly, Doro for sharing the best and the worst moments over these years. Life would not have been the same without any of you.

In particular, I thank from my heart to me dear friends Oana and Mihai for their support in my hardest moments on the way to this PhD. I would not have made it here without you.

Finally, my warmest thoughts and thanks go to my mom Maria and my sister Simona for always believing in me and supporting me along the way.

Statutory Declaration

(According to § 7 (4) doctoral degree regulations of the MIN Faculty)

Eidesstattliche Erklärung

(Gem. § 7 (4) MIN – PromO)

I hereby declare, on oath, that I have written the present dissertation by my own and have not used other than the acknowledged resources and aids.

Hiermit erkläre ich an Eides statt, dass ich die vorliegende Dissertationsschrift selbst verfasst und keine anderen als die angegebenen Quellen und Hilfsmittel benutzt habe.

Hamburg,
Hamburg, den

Signature
Unterschrift

August 25th 2015